Cerebellar Contributions to Prediction Error Processing in Reinforcement Learning

Inaugural-Dissertation

zur Erlangung des Doktorgrades
der Mathematisch-Naturwissenschaftlichen Fakultät
der Heinrich-Heine-Universität Düsseldorf

vorgelegt von

Dana Maria Huvermann
aus Bottrop

Düsseldorf, October 2025

aus dem Institut für Experimentelle Psychologie
der Heinrich-Heine-Universität Düsseldorf

Gedruckt mit der Genehmigung der
Mathematisch-Naturwissenschaftlichen Fakultät der
Heinrich-Heine-Universität Düsseldorf

Berichterstatter:

1. Prof. Dr. Jutta Peterburs

2. Prof. Dr. Christian Bellebaum

Tag der mündlichen Prüfung: 01.10.2025

Contents

Summary

Reinforcement learning is an essential function for most higher organisms to survive and thrive in dynamic environments. Herein, reward prediction errors (RPEs) play a central role. RPEs signal if an action outcome deviated from expectations and help improve future predictions. Traditionally, RPE processing has been linked to midbrain and prefrontal regions, but more recent evidence indicates RPE processing in the cerebellum as well. This dissertation explored the role of the cerebellum in reinforcement learning using different models of cerebellar dysfunction (i.e., patients with cerebellar stroke, transcranial magnetic stimulation of the cerebellum in healthy individuals) while recording cerebral signals. The key question was whether cerebellar deficits would change cerebral processing of RPEs.

Manuscript 1 investigated whether cerebellar deficits in patients with chronic cerebellar strokes and in healthy young adults receiving single-pulse cerebellar transcranial magnetic stimulation (TMS) would result in deficient RPE processing in a reinforcement learning task. Electroencephalography (EEG) was employed to measure cerebral RPE processing, focussing on the feedback-related negativity (FRN). The FRN had previously been shown to not only distinguish between negative and positive feedback but to also covary with RPEs. Both experiments showed that a cerebellar dysfunction led to a blunted RPE reflection in the FRN, suggesting cerebellar contributions to cerebral RPE processing. No behavioural deficits in overall learning success were apparent, potentially indicating compensation by other brain areas.

Manuscript 2 investigated response error processing in reinforcement learning. While naïve learners rely on feedback, advanced learners are able to recognise errors already at the response execution. Previous studies performed in non-reinforcement learning contexts implied the cerebellum in error processing. Manuscript 2 investigated whether cerebellar TMS applied in healthy adults altered error processing in reinforcement learning. EEG analyses of the error-related negativity (ERN) and error positivity (Pe) in the response-locked event-related potential showed that cerebellar TMS blunted error processing in the ERN but enhanced it in the Pe, with the latter potentially indicating compensation.

Last, Manuscript 3 explored the timing aspect of cerebellar-cerebral communication in error processing. While for the motor domain, a clear time window for cerebellar-cerebral communication is known, this is less clear for the cognitive domain. Several TMS timings around individual ERN latencies were investigated in a Go/Nogo Flanker task, i.e., a response conflict and inhibition task. It could be shown that only stimulation near ERN latency was effective in reducing error processing in ERN.

Together, these findings further implicate the cerebellum in reinforcement learning and the more general area of performance monitoring. Cerebellar deficits altered cerebral processing, even though this did not directly translate to substantial behavioural impairments. Future research into the functional significance of these cerebellar deficits is required.

List of Abbreviations

ACC	anterior cingulate cortex
AICA	anterior inferior cerebellar artery
CCAS	cerebellar cognitive affective syndrome
CR	conditioned reaction
CS	conditioned stimulus
dlPFC	dorsolateral prefrontal cortex
EEG	electroencephalography
ERN	error-related negativity
ERP	event-related potential
FRN	feedback-related negativity
fMRI	functional magnetic resonance imaging
GABA	gamma-aminobutyric acid
hEOG	horizontal electrooculogram
LME	linear mixed effects
MPRAGE	magnetisation-prepared rapid acquisition gradient-echo
MSA-C	multiple system atrophy-cerebellar type
Ne	error negativity
NIBS	non-invasive brain stimulation
OFC	orbitofrontal cortex
Pe	error positivity
PFC	prefrontal cortex
PICA	posterior inferior cerebellar artery
PRO	prediction of response-outcome
RewP	reward positivity
RPE	reward prediction error

rTMS	repetitive transcranial magnetic stimulation
SCA	superior cerebellar artery
SN	substantia nigra
SNc	substantia nigra pars compacta
spTMS	single-pulse transcranial magnetic stimulation
SUIT	spatially unbiased atlas template of the cerebellum
TMS	transcranial magnetic stimulation
UR	unconditioned reaction
US	unconditioned stimulus
vbLSM	voxel-based lesion symptom mapping
vEOG	vertical electrooculogram
vmPFC	ventromedial prefrontal cortex
VTA	ventral tegmental area
WCST	Wisconsin card sorting test

Introduction

Reinforcement learning

Introduction

For most living beings, the ability to learn is not just critical for survival but also important for general well-being. In disease, learning can be impaired, potentially leading to a less successful or fulfilling life. While one might initially think of classical learning disabilities, such as reading disorders or math disorders, disordered learning extends beyond the school premises. Basic learning mechanisms shape the basis for many behaviours. One example is agoraphobia: A person with agoraphobia might be afraid for their life when they step out their door because of an alteration in their learning system. The perception of the outside environment can be altered after a singular threatening encounter causing a strengthening in the association between threat and avoidance behaviour. The difficulty to unlearn this response towards fear has a significant impact on this person's life which creates the conviction that it would be dangerous to go outside. Another person might show an overly large preference towards certain substances, making it challenging for them to stop using a specific substance, and instead spiralling into addiction. It is thus of high interest to understand the processes underlying these learning mechanisms.

An important distinction is to be made between non-associative and associative learning (Pereira & van der Kooy, 2013; Thorwart & Livesey, 2016) which constitute two major categories of basic learning mechanisms. Other – in parts more advanced – learning mechanisms go beyond this distinction. These include, for example, observational learning where the learner observes and imitates others (Bandura, 2008; Bandura et al., 1974), and higher cognitive learning processes including insight where the learner takes into account a broader context of the learning situation (Köhler, 1921). The current work will, however, focus on basic learning mechanisms, and in particular associative learning.

Non-associative learning mechanisms describe learning without making associations between stimuli, and instead describe changes in reaction towards the same stimuli (Kirchkamp et al., 2012). This primarily comprises habituation and sensitisation. Habituation describes a decrease in reaction towards a stimulus with repeated exposure, while sensitisation describes an increase in reaction with repeated exposure (Kirchkamp et al., 2012).

Associative learning mechanisms, on the other hand, describe learning via association of a stimulus with another stimulus or reaction (Hawkins & Byrne, 2015). This mainly comprises classical and operant conditioning. Even small organisms, such as nematodes, have been shown to be susceptible to classical condition (A. J. Yu & Rankin, 2022). In classical

conditioning, an organism learns to associate an unconditioned stimulus (US; e.g., food) with a conditioned stimulus (CS; e.g., a bell ring; Clark & Squire, 1998; Windholz, 1997). While previously, only an unconditioned reaction (UR; e.g., salivating) was shown in response to the US (food), the animal now also displays a conditioned reaction (CR, e.g., salivating, but does not need to be the same as the UR) towards the CS (bell). On the other hand, operant conditioning is available to animals with more complex nervous systems, including some insects (Kriete & Hollis, 2022). Instead of linking two stimuli with each other, an action is linked to a stimulus (Skinner, 1963; Thorndike, 1933). These stimuli are categorised into rewards which increase a certain behaviour and punishments which decrease the behaviour. This can be accomplished both by using appetitive and aversive stimuli: supplying an appetitive stimulus is rewarding (positive reward), while removing it is punishing (negative punishment); supplying an aversive stimulus is punishing (positive punishment), while removing it is rewarding (negative reward; Papageorgi, 2021).

Humans use these basic learning strategies in everyday life, especially in unfamiliar environments. An example from Schultz (2016) illustrates this nicely: Imagine standing in front of a vending machine in Japan. You would like to receive the hot coffee drink, but it is not clear from the images which button to press. You might try a button, and, surprisingly, the coffee is dispensed! The next time you encounter this vending machine, surely, you would press the same button. Yet, the next time, a milk tea is dispensed instead. Someone must have refilled the machine in a different way. Now you are back to trying out buttons. This example nicely illustrates how important operant conditioning is to find our way in unfamiliar environments.

However, these principles are not only useful to describe behaviour. In the computer science domain, instead of describing real behaviours, these frameworks are used to *optimise* behaviour of an actor (Sutton & Barto, 2018c), e.g., a drone that needs to move autonomously. Many of the ideas originate in the psychological research of the early 20th century previously described. They were, however, further developed to be applicable in computer science. Interestingly, algorithms that work better in computer science also seem to show a better fit for natural learning behaviour (Niv, 2009). It is thus extremely useful to understand these frameworks when modelling the behaviour of animals, humans, or neural populations.

One such framework is reinforcement learning. It describes learning in an interactive environment. Its origins largely go back to the “Law of Effect” proposed by Thorndike (1911), i.e., essentially operant conditioning. It describes the strengthening or weakening of a behaviour when an animal receives a stimulus or when a stimulus is withdrawn (reward/punishment) in relation to a behaviour. Alan Turing first described such a construct in a computer that goes along with the psychological “trial-and-error learning” and referred to it as a “pleasure-pain system” (Turing, 1969). In computer science, reinforcement learning is a

subcategory of machine learning. Machine learning is a collective term for algorithms that can learn from data and apply the knowledge to new data. For reinforcement learning to take place, three prerequisites must be fulfilled (Sutton & Barto, 2018a): 1) the agent must be able to sense its *state*, 2) it must be able to take *actions* to influence this state, and 3) it must have a *goal*. This goal is usually to maximise a reward signal. These prerequisites are fulfilled for all operant conditioning contexts. Note that the state refers to not only the environment of the agent but also internal states. For example, it might be more or less useful to eat a large meal depending on satiety. The basic components of a reinforcement learning algorithm involve at least three components (Sutton & Barto, 2018a): 1) a *policy*, describing how the actor behaves in a given situation, 2) a *reward signal*, and 3) a *value function*. In natural learning situations, the reward signal is oftentimes (but not necessarily) supplied externally. While the value function attaches subjective values to actions, states, and stimuli, the policy allows for optimisation of behaviour. An essential dilemma in reinforcement learning lies between exploration and exploitation. To increase reward, the agent must choose (exploit) actions which have proven to produce a reward in the past. However, to maximise rewards in the future, it must also explore actions not previously tried, as the gains might be larger than the known action-reward relations. Stochastic relations need to be considered, as reward might not only differ in size, but also in reliability, thus requiring a given action to be made more than once to gain sufficient information.

Other types of machine learning, such as supervised and unsupervised learning (Sutton & Barto, 2018c), have also been related to animal/human behaviour and neural activity. Supervised learning describes learning from a training set with pairs of inputs (e.g., a situation) and correct outputs (e.g., an action; Priddy & Keller, 2005). The goal is then to generalise responses from this training set, in order to then also provide correct outputs towards new inputs. The output may be categorical (classifier) or continuous (regressor; Sen et al., 2020). This framework has often been referenced to describe cerebellar function (see below). Unsupervised learning, in contrast, does not require a teaching signal. Instead, input may be provided unlabelled, and patterns and characteristic properties are discovered without requiring any additional input (Kyan et al., 2014). This functionality has been proposed for the cerebral cortex (Marblestone et al., 2016). Note that the learning frameworks do not necessarily work separate from each other. For example, a reinforcement learning algorithm may include other approaches as subroutines.

Reinforcement learning algorithms

Even though reinforcement learning models have been derived from psychological theories and have been relevant in computer science since the 80s, their application in psychological/neuroscientific research has only become more popular in recent years. While

there is a multitude of reinforcement learning models (confer Sutton & Barto, 2018c for an overview), I will focus on the model used within this doctoral thesis (i.e., a Rescorla Wagner model; Rescorla & Wagner, 1972; A. R. Wagner & Rescorla, 1972) together with the closely associated temporal difference learning.

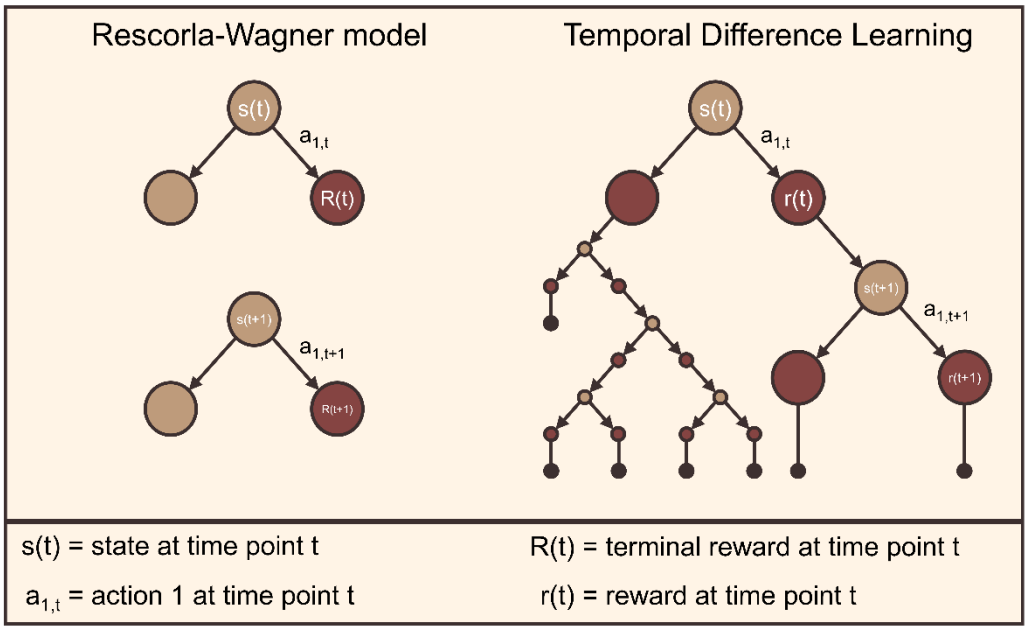

Figure 1. Graphical comparison of the Rescorla-Wagner model and temporal difference learning.

Rescorla-Wagner Model

The Rescorla-Wagner model originally described association strengths in the context of classical conditioning. It was developed in the 70s by the psychologists Robert Rescorla and Allan Wagner (Rescorla & Wagner, 1972; A. R. Wagner & Rescorla, 1972). The model equations describe associations between a CS and a US:

$$\Delta V_{X,t+1} = \alpha_X \beta (\lambda - V_{tot})$$

and

$$V_{X,t+1} = V_{X,t} + \Delta V_{X,t+1}$$

where $V_{X,t}$ is the associative strength of the CS X towards the US in trial t, λ is the maximal associative strength for the US, α_X is the learning parameter for stimulus X, and β is the learning parameter for the US. $\Delta V_{X,t+1}$ is thus the change in associative strength that is added to $V_{X,t}$ to form the updated association strength $V_{X,t+1}$.

For action value and reward prediction error (RPE) modelling, a simplified equation is oftentimes used (Dayan, 2004), with various terms to refer to it, e.g., Q-learning (Haruno & Kawato, 2006) or simple reinforcement learning (L. Zhang et al., 2020).

This derived equation describes the updating of action values and reads as follows:

$$V_{a,s+1} = V_{a,s} + \alpha(R_{a,t} - V_{a,s})$$

$V_{a,s}$ denotes the predicted action value for action a at state s while $R_{a,t}$ denotes the outcome received for action a in state s. $(R_{a,t} - V_{a,s})$ describes the error term, using the distance between the prediction for the outcome and the actually received outcome. α, often referred to as a learning parameter, is a parameter describing step size, i.e., how big of a change is applied to the prediction following an RPE. Note that the equation does not include a predictor for which actions would lead to which states; instead it is assumed that states are independent from each other in a trial-based fashion. If an environment would require the performance of several actions towards several states with a terminal outcome, the Rescorla-Wagner model would thus only update predictions after the receipt of the outcome. While this approach seems quite inefficient for organisms to perform in natural environments, the assumptions suffice in an experimental environment where one terminal outcome follows an action performed in a given environment, and where environments are independent from the performed action(s) (i.e., an action does not influence which environment is encountered next).

Temporal Difference Learning

Temporal Difference Learning also finds its origins in psychology, i.e., from the concept of secondary reinforcement (Sutton & Barto, 2018a). Secondary reinforcement describes that after a given CS is paired with an US, it can be further paired with a second CS, and the CS will trigger the UR as well (Myers, 1958). A good example for this might be money. While money itself cannot directly fulfil a primary need (e.g., it cannot be eaten), it can be used to fulfil them indirectly (e.g., by buying food).

Temporal difference learning enables updating without reaching the terminal outcome. It thus considers that one action might lead to a more profitable state than another, which in turn leads to a better total outcome. It is thus capable of describing more complex prediction processes.

While there are several temporal difference learning models, the simplest one is considered to be the TD(0) model. The corresponding equation reads as follows:

$$V(s_t) = V(s_t) + \alpha(r_{t+1} + \gamma V(s_{t+1}) - V(s_t))$$

where $V(s_t)$ denotes the value of the state s at time point t. At time point t+1, the update for $V(s_t)$ is then performed, using $V(s_{t+1})$, the value of the next state, and r_{t+1}, the observed outcome. Here, $r_{t+1} + \gamma V(s_{t+1}) - V(s_t)$ describes the RPE (also referred to as temporal

difference error), thus taking into consideration the next state in addition to the received reward and value of the state at time point t. Note that γ is added as a temporal discounting parameter, decreasing the value of states that lie further in the future. α again describes step size, in parallel to its function in the Rescorla-Wagner model.

Temporal difference learning describes natural behaviour better which is not divisible into trials, and where predictions can be updated at any time during the trial. An example for this would be driving back from work. We might estimate the time it takes based on previous drives home at the time of getting in the car. After driving for a few minutes, an announcement on the radio warns us against a traffic jam, prompting us to adjust our estimation. Notably, updating the estimate thus does not require to reach the terminal state (arrival at home).

Differentiation

To more clearly illustrate the differences between the Rescorla Wagner model and Temporal difference learning for a more experimental setting, one might consider a classical conditioning situation itself: the Rescorla Wagner model would assume that after CS-US associations have been learnt, no RPE occurs when the US is presented following the CS, as the contingency between CS and US is known, thus averting surprise at the US delivery. On the other hand, the temporal difference learning model would assume an RPE even in this scenario, however, at the time of CS delivery. Before the CS, no reward is expected, but after the CS, reward is expected (Niv & Schoenbaum, 2008). A graphical comparison of the two approaches is also given in Figure 1.

For the paradigm at hand of this doctoral thesis, a simple Rescorla-Wagner model suffices, as the interest of the studies at hand lies in RPEs at the time of outcome delivery in a trial-by-trial fashion.

Actor-critic model

Another notable model in neuroscience is the actor-critic model. The actor-critic model is a combination of policy-based and value-based reinforcement learning (Barto et al., 1983). In this algorithm, the actor, who chooses an action from several options (policy), is informed by a critic, who evaluates how good the action was and how to adjust (value). The critic thus uses a temporal-difference like evaluation function, while the actor determines the likelihood with which each action is chosen at a given state (Barto et al., 1983; Dayan & Balleine, 2002; Niv, 2009).

Differences in nomenclature between psychology and computer science

As described in the introduction, reinforcement learning originates from psychology, primarily relating to operant conditioning. Note that above, a classical conditioning scenario is being described using reinforcement learning algorithms. Following the use of the concept in

computer science, scenarios which are not operant conditioning have started to be referred to as reinforcement learning, as long as the behaviour of the agent can be described with a reinforcement learning algorithm (Averbeck & Costa, 2017; Gershman et al., 2015; Swain et al., 2011). This is mostly true for classical conditioning scenarios. Note that the application of reinforcement learning algorithms for classical conditioning has also been criticised as inappropriate (Dayan & Balleine, 2002). For the doctoral thesis at hand, the term *reinforcement learning* will be used with its meaning restricted to operant conditioning. However, evidence for reinforcement learning in the brain is oftentimes jointly drawn from the two types of conditioning, and studies investigating classical conditioning will be brought up accordingly.

Reinforcement learning in the brain

Beginnings

While this doctoral thesis focusses on studies in humans, many ground-breaking discoveries have been made through research in animals, and in particular in rodents and other primates. One such study which paved the way for reinforcement learning as a concept outside of computer science was performed by Wolfram Schultz and colleagues in 1993 and in further follow-up studies (Schultz et al., 1993, 1997; Silvetti & Verguts, 2012). In a simple classical conditioning setup, they recorded dopaminergic neurons of macaques. A CS (a tone) was followed by a US (a drop of juice). Initially, dopaminergic activity increased following delivery of the US. However, after learning throughout the task, dopaminergic activity increased already at the time of the CS. When the rewarding US was then unexpectedly not dispensed, dopaminergic activity decreased below the baseline level. In this way, the dopaminergic activity followed predictions made by temporal difference learning models, and displayed an RPE: before learning, the CS did not trigger an RPE, but the rewarding US triggered a positive RPE. The rewarding US was not previously expected and was a better outcome than expected, thus violating predictions in a positive direction. After learning, the CS triggered a positive RPE, giving notice to the soon occurring rewarding US. If then, the US was delivered as predicted, no RPE occurred, and the dopaminergic activity consequentially stayed at baseline level. However, if the US was not dispensed even though the CS was previously provided, a negative RPE occurred, as the received outcome was now worse than expected. These findings provided good evidence that dopamine neurons do not simply signal the reward (as assumed previously), but instead signal an RPE (Niv, 2009). Since the 90s, reinforcement learning has been explored more deeply in neuroscience.

Reinforcement learning in EEG

Many studies investigating reinforcement learning have been conducted using electroencephalography (EEG) as it offers a high temporal precision. In EEG, a measure for feedback processing was first proposed by Miltner and colleagues (1997), i.e., the feedback-

related negativity (FRN). The FRN is a frontocentral component in the feedback-locked event-related potential (ERP). It usually peaks within 200-350 ms after feedback onset with a relative negative peak. In its origins and also nowadays, it was closely associated with the error-related negativity (ERN) in terms of performance monitoring (Gehring et al., 2018; Holroyd & Coles, 2002; Potts et al., 2011). Performance monitoring encompasses a wide range of cognitive and emotional functions required for adaptive behaviour which includes feedback processing and error detection (see below for a more detailed overview; Peterburs & Desmond, 2016).

The ERN, originally termed error negativity (Ne), was first presented in 1989 by Michael Falkenstein and colleagues (Falkenstein et al., 1991; Gehring et al., 2018). The term “ERN” was introduced by Gehring and colleagues (1993), who found further evidence for this error-related activity soon after. The ERN is a frontocentral negativity in the response-locked ERP. It peaks within 100 ms post-response, and studies aligning its latency with the onset of electromyographic activity of the relevant muscle (to press a response button) have shown that the ERN onset starts at the same time (Gehring et al., 1993; Krigolson, 2018). The ERN is increased (i.e., more negative) for response errors as opposed to correct responses (Falkenstein et al., 1991; Gehring et al., 1993, 2018). It could also be shown that the ERN is larger for bigger over smaller errors (Albrecht & Bellebaum, 2023; Bernstein et al., 1995). The ERN has been proposed to reflect a fast-paced mismatch detection (Coles et al., 2001; Nieuwenhuis et al., 2001). Source analyses have indicated the anterior cingulate cortex (ACC) as a generator of the ERN (Herrmann et al., 2004; Hochman et al., 2009; Ladouceur et al., 2006; Roger et al., 2010; for a review see Wessel, 2012). This is also consistent with activations of ACC towards errors in functional magnetic resonance imaging (fMRI) studies (Kiehl et al., 2000; Lütcke & Frahm, 2008; van Veen & Carter, 2002) as well as lesion studies indicating reduced ERNs following damage to the medial prefrontal cortex (PFC) including the rostral ACC (Maier et al., 2015; Stemmer et al., 2004).

Studies investigating the ERN oftentimes used tasks where errors are caused by impulsive reactions rather than participants not knowing the correct response (Davies et al., 2001). Miltner et al. (1997) investigated the idea that if the information on the correctness of a response was not immediately known but provided through a feedback following the response, would the ERN occur at this later time point? They indeed found an ERN-like component following feedback presentation which was larger (i.e., more negative) for incorrect responses (negative feedback) than correct (positive feedback). Follow-up dipole analysis found that this component seemed to have the same neural generator as the ERN (i.e., ACC; Miltner et al., 1997). They concluded that there must be a general underlying system for error detection. In the following years, this ERN-like component was termed FRN, and treated as a separate but related ERP component. Following studies have further supported the ACC as a neural

generator for the FRN, via source localisation in EEG (Balconi & Scioli, 2012; Bellebaum & Daum, 2008; Hauser et al., 2014; R. Yu et al., 2011; for a review see San Martín, 2012), similar activation in fMRI studies (Amiez et al., 2012; Mies et al., 2011; Volz et al., 2005), and electrophysiological recordings in rodent, macaque and most recently also human ACC showing similar signals (Emeric et al., 2008; Oerlemans et al., 2025; Warren et al., 2015). A very recent study performed in humans found that lesions to the ACC did indeed result in a reduced differentiation between negative and positive feedback in FRN (Oerlemans et al., 2024), providing further support for the ACC as a neural generator. This similarity in neural generator thus further links FRN to ERN. The valence effect in the FRN is also well-evidenced and has been continuously confirmed in a wide range of studies (Paul et al., 2025; for a review see San Martín, 2012; see Figure 2 for a conceptual plot of the valence effect in FRN).

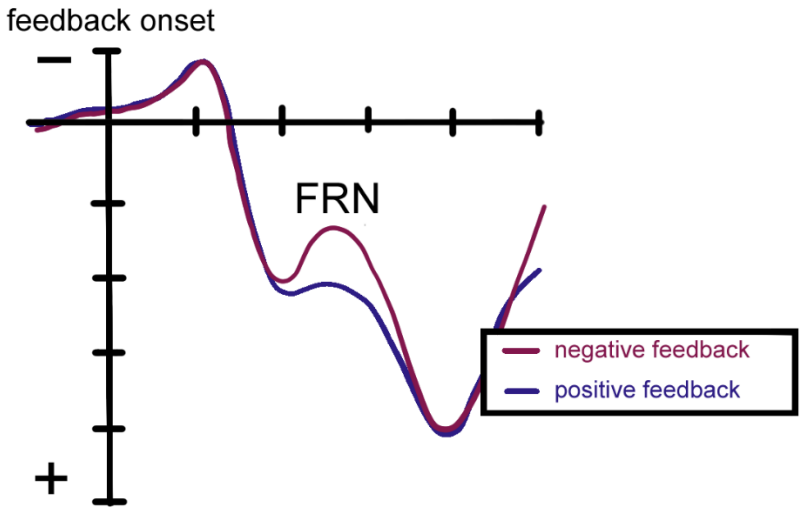

Figure 2. Conceptual plot showing the Feedback-related Negativity (FRN) in the feedback-locked grand-average event-related potential for positive and negative feedback.

Following the findings on the sensitivity on the FRN to feedback valence, separate accounts have been made for the underlying mechanism. Two major theories emerged: the reinforcement learning account proposed by Holroyd & Coles (2002; presented in more detail below), and the prediction of response-outcome (PRO) account by Alexander and Brown (2011). While the former account assumes a true reflection of outcome valence in FRN, the second account attributes the higher FRN amplitude in response to negative feedback towards a lower frequency of negative feedback. They consider that after learning, negative feedback will occur much less frequently, as participants would generally make more correct than incorrect choices. This would mean that the valence effect in the FRN amplitude could similarly be explained as a general salience signal, as rarer stimuli have a higher salience. This can be observed in so-called oddball tasks. In these tasks, participants need to identify an infrequent

target stimulus in a series of frequent standard stimuli (Picton, 1992). Alexander and Brown could provide evidence for their account by keeping the amount of negative and positive feedback on similar levels, thus mostly eliminating oddball effects. They did this within a time estimation task. Participants needed to press a button after a certain amount of time had passed. The task thus does not have clearly distinct correct or false reactions. The amount of positive and negative feedback can instead be manipulated by choosing the size of the "correct" response time window. Alexander and Brown were able to adapt this time window depending on individual task performances in a way that positive and negative feedback occurred similarly often, thus preventing any confounding effects of feedback frequency. They could show that valence effects disappeared. The PRO model thus reconciles different proposed functionalities of ACC, in particular conflict monitoring and reinforcement learning (Alexander & Brown, 2019).

However, several lines of evidence speak again the PRO model as the sole explanatory model for ACC and FRN: 1), only very few neurons in the ACC show valence-independent activations (Monosov, 2017). 2), in fMRI meta analyses, ACC was more strongly activated for signed over unsigned RPE (Corlett et al., 2022; Fouragnan et al., 2018; although these findings might yet be explainable by differences in feedback frequency). 3), the finding could not be consistently replicated, and other groups could still find a valence effect even after keeping feedback frequencies consistent among feedback valences (Becker et al., 2014; Schulreich et al., 2013). Nevertheless, even though the feedback valence effect might not be fully explainable by feedback frequency, feedback frequency is still an important variable to consider, especially when certain feedback types occur more frequently than others, such as positive feedback in later stages of learning tasks.

Another important aspect that overlaps in parts with frequency is expectancy, i.e., how expected the feedback was. In many studies, the concept of expectancy has been determined by the experimental manipulation, such as feedback probability (e.g., Bellebaum & Daum, 2008; M. X. Cohen et al., 2007; Pfabigan et al., 2011; for a review see Sambrook & Goslin, 2015). For example, in a probabilistic feedback learning task, a correct/incorrect choice does not lead deterministically to a positive/negative feedback, but rather with a certain probability. Here, a rare *negative* feedback (e.g., with a probability of 10 %) towards a *correct* choice might be considered *unexpected*, while a frequent *negative* feedback (e.g., with a probability of 90 %) towards an *incorrect* choice might be considered *expected*. However, subjective predictions might differ from objective probabilities. To explore this possibility, studies have been conducted where participants are asked for their expectation during the experimental course (Hajcak et al., 2007; Ichikawa et al., 2010). In these cases, participants are asked about their prediction after making a choice and before receiving feedback. It could be shown that

subjective predictions differed substantially from objective probability (Hajcak et al., 2005, 2007). While this could be considered the gold standard of assessing the expectations and consequently the expectancy of a feedback, it requires significantly more time and effort on the participants' part. In recent years, instead, reinforcement learning approaches used in computer science have been employed more and more to model the expectancy of a feedback and the resulting RPE. It could be shown that the accuracy of these approaches is comparable to the direct assessment of feedback expectancy (Ichikawa et al., 2010). Analyses relating the FRN to modelled RPEs could consistently show that the FRN tracks RPEs, with a more negative FRN towards negative RPEs and a more positive FRN towards more positive RPEs (Burnside et al., 2019; Chase et al., 2011; Fischer & Ullsperger, 2013; Frömer et al., 2021; Hoy et al., 2021; Humann et al., 2020; Kirschner et al., 2022; Rawls & Lamm, 2021). A conceptual plot of this finding is given in Figure 3.

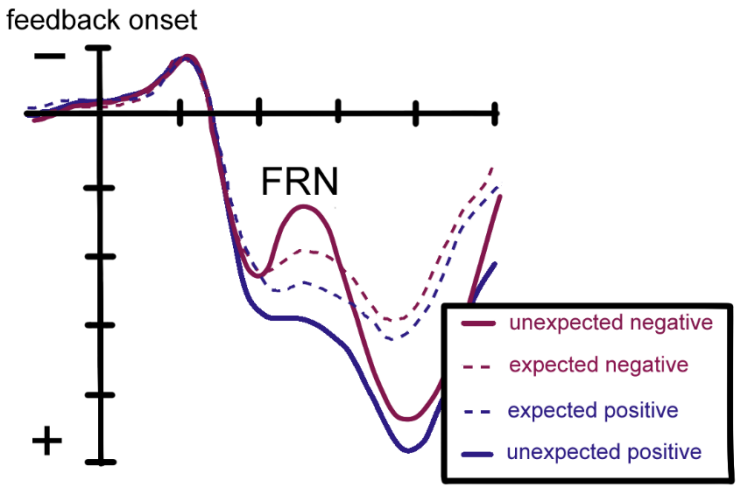

Figure 3. Conceptual plot showing the Feedback-related Negativity (FRN) as a function of valence (positive, negative) and expectancy (expected, unexpected).

As proposed originally by Miltner et al. (1997), the FRN was assumed to be a relative negativity, driven rather by negative than positive feedback. However, it was more recently proposed that the actual effect stems from a positivity towards positive feedback concurrent with an absence/reduction of this positivity towards negative feedback. This was in particular evidenced by principal component analysis (Proudfit, 2015; Yin et al., 2018). It was suggested to refer to the FRN more correctly as reward positivity (RewP; Holroyd et al., 2008; Proudfit, 2015). Notably, the term RewP was proposed as a more correct way to describe the FRN, i.e., limiting the term towards a matter of nomenclature. FRN/RewP have been oftentimes quantified within the difference signal between positive and negative feedback, thus yielding the same latency/amplitude in peak detection irrespective of whether the ERP for positive feedback is subtracted from that for negative feedback or the other way around. However, the

FRN and RewP have also been discussed as different components with differing sensitivities towards negative and positive valence and different quantifications (e.g., Cavanagh, 2015; Cavanagh et al., 2019; Meadows et al., 2016). Source localisation shows differences for FRN and RewP in neural generators: While literature supports the ACC as a generator of the FRN (Krigolson, 2018; also see above), results for the RewP differ: the basal ganglia, and especially the ventral striatum have been proposed as a neural generator (Proudfit, 2015). It was also shown that the RewP reflects the neural activity towards positive RPEs better (Cavanagh, 2015; Hoy et al., 2021), similar to the differing sensitivity of dopaminergic neurons towards positive and negative RPEs (see below). For the FRN, on the other hand, effects have been in some studies clearer for negative RPEs and in other studies clearer for positive RPEs (Chase et al., 2011; Hoy et al., 2021; Rawls & Lamm, 2021; Weber & Bellebaum, 2024). Future studies might uncover these potential differences in more detail. For this doctoral thesis, the term *FRN* will be used.

Reinforcement learning theory

A unified account of findings in EEG, (f)MRI, and the temporal difference learning principles was proposed in 2002 by Holroyd & Coles. The FRN was previously already closely linked to performance monitoring in terms of error monitoring, due to its close relation with ERN. Holroyd and Coles provided a unifying approach, linking this performance monitoring system to the reinforcement learning system in terms of a temporal difference learning signal. They proposed that the ACC receives a temporal difference signal from the basal ganglia, which acts as a critic, i.e., provides and updates a value-based signal. It also receives input from motor controllers, such as amygdala, orbitofrontal cortex (OFC), PFC, and others. These areas solve higher-level motor problems, and might weight different aspects, such as outcome value, outcome delay, effort, or also be more suitable to navigate different types of problems, e.g., social situations. According to the reinforcement learning theory, these also receive a temporal difference signal, in addition to sensory input. Holroyd and Coles proposed the ACC as a control filter, allowing and disallowing access of the motor controllers to the motor system. This thus offers an explanation why the FRN signal, likely generated by the ACC, can be observed in a large variety of situations (Faßbender et al., 2023; Peters et al., 2024).

Brain structures involved in reinforcement learning

A wide range of brain regions has been proposed to be involved in reinforcement learning. This is not surprising, as reinforcement learning is an important foundation for intact behaviour. Regions considered most central to reinforcement learning and in particular the processing of RPEs will be described below (also see Figure 4).

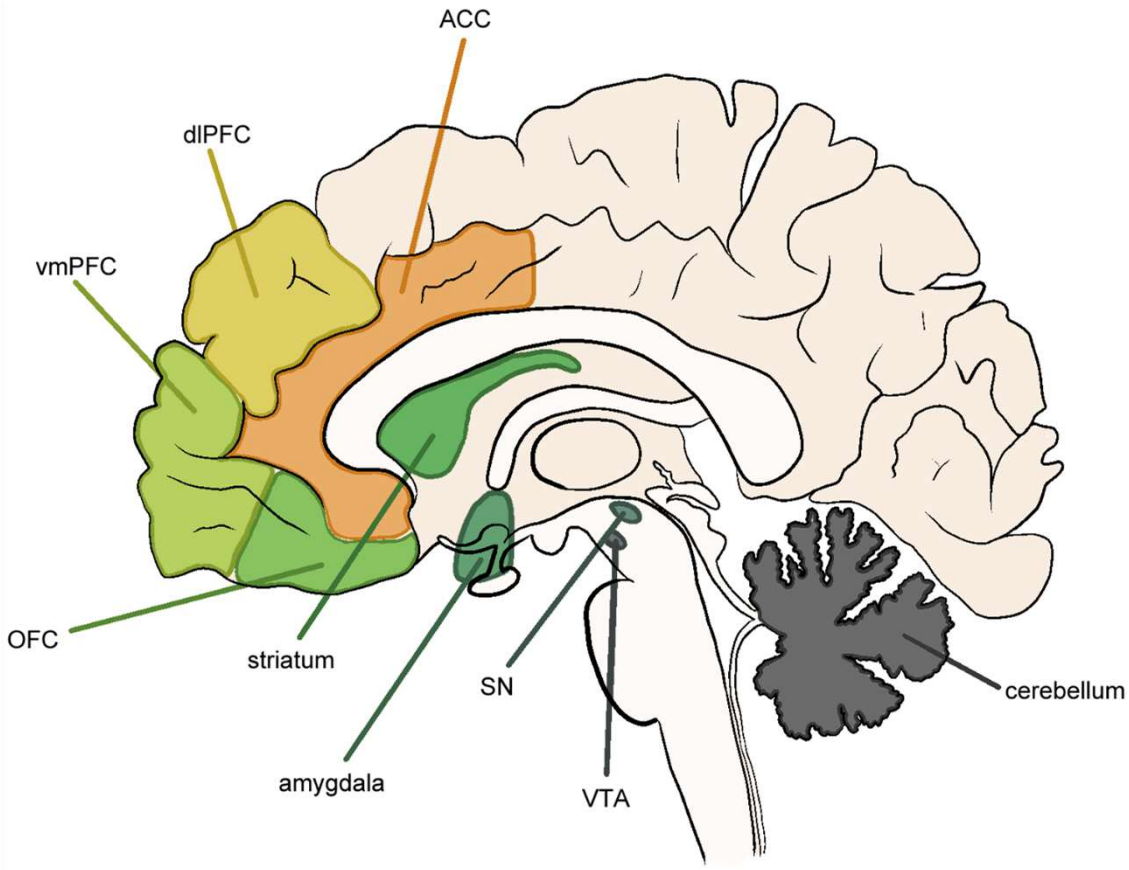

Figure 4. Overview of brain regions closely associated with reinforcement learning. ACC = anterior cingulate cortex, dlPFC = dorsolateral prefrontal cortex, vmPFC = ventromedial prefrontal cortex, OFC = orbitofrontal cortex, SN = substantia nigra, VTA = ventral tegmental area.

Substantia nigra

The substantia nigra pars compacta (SNc) has been consistently associated with reinforcement learning. The activity of dopamine cells follows predictions of temporal difference learning models quite closely, showing RPE signals (Nomoto et al., 2010; Zaghloul et al., 2009). There is good evidence that the SN is required for reinforcement learning. It was shown that people with disease affecting dopaminergic neurons in the SN, such as Parkinson's disease, show worse reinforcement learning (Shiner et al., 2012). Additionally, neurostimulation of the SN in Parkinson patients undergoing deep brain stimulation surgery also decreased reinforcement learning success (Ramayya et al., 2014). The SN is connected to a wide range of brain regions, including the thalamus, nucleus ruber, basal ganglia, cerebellum, primary motor cortex, primary sensory cortex, and others (Kwon & Jang, 2014). There also seems to be a distinction in functional connectivity for the motor, cognitive, and limbic domain (Y. Zhang et al., 2017): while the lateral SNc seems to mainly connect to sensorimotor regions, the medial SNc shows connections towards limbic regions, such as

OFC, hippocampus, and amygdala. The ventral SN connects to PFC, ACC, and anterior insula. It is thus conceivable that different parts of the SN process RPE depending on the domain.

Ventral tegmental area

The ventral tegmental area (VTA) is an area in the midbrain which contains dopaminergic cells and is also considered part of the reward circuitry (Morales & Margolis, 2017). Similar to dopaminergic neurons in the SNc, it could be shown that dopaminergic neurons in the VTA reflect RPEs (J. Y. Cohen et al., 2012; Takahashi et al., 2023). The VTA has reciprocal connections with a wide range of brain areas, including (medial) PFC, basal ganglia, amygdala, and several further subcortical structures related to reinforcement learning and reward (Coenen et al., 2018; Derdeyn et al., 2022; Kwon & Jang, 2014; Morales & Margolis, 2017). It also shows connectivity with sensorimotor areas (Hosp et al., 2019). There is evidence that the function of the VTA and SNc might differ, with the VTA relaying true value-based signals, while the SNc relays information that might better align with policy, in terms of an actor-critic model (Araújo et al., 2024; Fraser et al., 2023; Lerner et al., 2021; Ramayya et al., 2014). Besides the dopaminergic neurons and projections of the VTA, there has been considerable research on gamma-aminobutyric acid-ergic (GABAergic) and glutamatergic neurons in the VTA (Walsh & Han, 2014), also attributing a role in reinforcement learning to these neurons (J. H. Yoo et al., 2016).

Note that some studies do not differentiate between VTA and SNc, and instead only specify that they measured dopaminergic neurons (e.g., Bayer & Glimcher, 2005; Schultz et al., 1997) or jointly report results for the two structures (e.g., Chowdhury et al., 2013; S. Zhang et al., 2016). This is oftentimes due to difficulties in distinguishing the two areas (Trutti et al., 2019).

Striatum

The striatum, the largest part of the basal ganglia, has been recognised as one of the main processing stations for reinforcement learning. It receives dopaminergic input from the SN and the VTA, and is central to action selection (Bariselli et al., 2019; Silberberg & Bolam, 2015). Distinctions have been made into the ventral and dorsal striatum (and also the central striatum as a transitory zone; Basile et al., 2021). The ventral striatum contains the nucleus accumbens, while the dorsal striatum contains the nucleus caudatus and the putamen (Haber, 2011; Yates, 2023). Note that the ventral striatum also includes parts of the nucleus caudatus and putamen (Haber, 2011). The ventral and dorsal striatum differ in their connectivity to the PFC, with the ventral striatum receiving projections from the ventromedial PFC (vmPFC) while the dorsal striatum receives projections from the dorsolateral PFC (dlPFC; Averbeck & O'Doherty, 2022). Both areas have been implicated in reinforcement learning, mostly in terms of value functions (Fellows & Farah, 2007; Lee & Seo, 2007; O'Doherty, 2011; also see below). While the dorsal and ventral striatum do not directly project back to the PFC, they do so indirectly. The ventral

and dorsal striatum project towards the ventral and dorsal pallidum, respectively, which then projects towards the vmPFC and dlPFC, respectively, via the medial dorsal nucleus of the thalamus (Averbeck & O'Doherty, 2022).

Concerning function, there has been considerable support that the ventral and dorsal striatum act as critic and actor, respectively, in terms of an actor-critic model (Araújo et al., 2024; Balleine et al., 2007; O'Doherty et al., 2004). Consequently, the ventral striatum should reflect value-related information while the dorsal striatum should reflect policy-related information. The ventral striatum was shown to indeed reflect RPE and reward value (D'Ardenne et al., 2008; although there have been some inconsistencies dependent upon used measures; van der Meer & Redish, 2011). It is also connected to several brain areas associated with value-based functions. The vmPFC, with which the ventral striatum has reciprocal connections, is strongly associated with the tracking of outcome values (Hiser & Koenigs, 2018; Jocham et al., 2011). Considerable input to the ventral striatum comes from the VTA, which has consistently shown to reflect RPEs (D'Ardenne et al., 2008; Lerner et al., 2021). For the dorsal striatum, evidence points towards a role in action selection (Balleine et al., 2007; Nakano et al., 2000), further supported by its input broadly coming from, but not limited to, sensorimotor areas (Nakano et al., 2000; Postuma & Dagher, 2006). Findings thus seem consistent with an actor-critic distinction within the striatum.

Anterior cingulate cortex

The ACC has oftentimes been proposed to play a role in performance monitoring, an overarching framework for reinforcement learning (Botvinick et al., 1999; Clairis & Lopez-Persem, 2023; Holroyd et al., 2004). Important functional distinctions have been made according to topography: The ACC can be subdivided into a more anterior part, referred to as rostral/ventral ACC, and a more posterior part, referred to as caudal/dorsal ACC (Stevens et al., 2011). A functional distinction has been proposed in terms of hierarchy of action selection, with dorsal ACC monitoring performance of specific tasks and rostral ACC monitoring the execution of higher-level operations (Holroyd & Verguts, 2021). This is further supported by its connectivity towards other brain areas: the dorsal ACC has shown connectivity towards sensorimotor circuits, while the rostral ACC has shown connectivity towards prefrontal regions (Margulies et al., 2007). Similar has been proposed for prediction errors, with dorsal ACC suggested to compute prediction errors for specific events and rostral ACC to compute prediction errors concerning the context of the event (Holroyd & Verguts, 2021). Monosov (2017) conducted single cell recordings showing that ACC neurons reflected outcome uncertainty, with reward-related information more in the dorsal ACC and punishment-related information more in the rostral ACC. Only few neurons showed excitations towards uncertainty under both contexts. However, lesion studies have yielded less clear results considering the

role of the ACC, with the majority showing deficits in cognitive control and behavioural flexibility (e.g., Akam et al., 2021; Brockett et al., 2020; di Pellegrino et al., 2007; Maier et al., 2015; but also see Kennerley et al., 2006; Rushworth et al., 2003).

The connectivity of the ACC further supports a role in reinforcement learning. The pregenual ACC, a subdivision of the rostral ACC (Stevens et al., 2011), showed connectivity to the vmPFC and lateral OFC, areas which process outcome value information (Rolls, 2023). Connectivity with the VTA was also shown: the direction, however, depends on approach/avoidance behaviour (Elston et al., 2018, 2019), an important function for anxiety disorders (Aupperle & Paulus, 2010; Wong et al., 2022). Between the rostral and dorsal ACC, there seems to be a transitory zone which seems to integrate both sensorimotor and prefrontal networks, potentially with the function of conflict and error monitoring (Margulies et al., 2007).

Amygdala

The amygdala is most known for its function in fear (LeDoux, 2007). However, the amygdala has been found to be involved in a wide range of functions, such as aggression, maternal and sexual behaviours (LeDoux, 2007). The amygdala seems to also play a central role in reinforcement learning. A study performed in macaques could show that lesions in the amygdala resulted in deficits in both deterministic and stochastic reinforcement learning (Costa et al., 2016). The amygdala receives projections from the VTA (Tang et al., 2020) and it could be shown that inhibition of these projections can decrease learning of drug-seeking behaviour but did not affect reinstatement (D. M. Smith & Torregrossa, 2024).

Orbitofrontal cortex

Electrophysiological recordings and imaging studies have found a multitude of signals related to reinforcement learning within the OFC, including outcome value, choice representation, RPE, action-outcome history, and outcome expectation (for a review see Groman et al., 2021). The OFC might integrate these signals (Moneta et al., 2024). Indeed, it has been proposed that the OFC provides state representation, i.e., task-related information such as the mapping of state transitions (Schuck et al., 2018; Z. Zhang et al., 2018). This would naturally require the input of a lot of task-related information. Several lesion studies have indicated that the OFC is required for classical conditioning, the learning of stimulus-outcome associations, and meta reinforcement learning (Camille et al., 2011; Hattori et al., 2023; McDannald et al., 2011; Rudebeck et al., 2008).

Ventromedial prefrontal cortex

The vmPFC lies directly adjacent to the OFC and is functionally oftentimes closely associated with it, as both are part of the limbic loop (J. X. Wang et al., 2018). The vmPFC tracks expected outcome values, task state, and outcome values of irrelevant, alternative contexts, and seems

to integrate this information (Moneta et al., 2023, 2024). Patients with damage to the vmPFC show deficits in reinforcement learning within both maintenance and adaptation of outcome values (Schneider & Koenigs, 2017).

Dorsolateral prefrontal cortex

The dlPFC also tracks information closely related to reinforcement learning, such as outcome value and RPE (Lee & Seo, 2007). It seems to construct object value estimates from previous recent experiences, converting this information to choice signals (Tsutsui et al., 2016). This is further supported by the finding that the dlPFC modulates activity in the motor cortex (Morris et al., 2014), and studies using non-invasive brain stimulation (NIBS) showing that stimulation of the dlPFC influences reinforcement learning strategies (Ott et al., 2011; Overman et al., 2023). While stimulation of the left dlPFC increased reward-guided behaviour, stimulation of the right dlPFC increased avoidance-guided behaviour. As such, the role of the dlPFC has not fully been differentiated from the ACC (J. X. Wang et al., 2018).

Feedback valence

While the original article by Schultz and colleagues (1993) indicated that positive and negative RPEs are processed within the same system, this same finding has not been so clear in subsequent fMRI and EEG studies. The decrease of dopaminergic neuron firing rate below baseline observed by Schultz et al. (1993) was also rather small, as the baseline of dopaminergic neurons is rather low (3-8 spikes per second; Niv & Schoenbaum, 2008). It was shown that micro-stimulation of the SN only had an effect on behaviour related to positive, but not negative feedback (Ramayya et al., 2014). For EEG, there has been an ongoing debate on whether the valence effect within the FRN stems from a negativity towards negative feedback or rather a positivity towards positive feedback, resulting in the question whether different measures should be used (see above for a discussion of RewP). The FRN is more strongly associated with negative valence, while the RewP is more strongly associated with positive valence. The differentiation into valences has also been of topic in fMRI studies. Findings overlap, with the ventral striatum, i.e., the suggested generator of the RewP, rather coding positive prediction errors and the dorsal ACC, i.e., the suggested generator of the FRN, rather coding negative prediction errors (Meder et al., 2016). This effect was confirmed in a recent meta-analysis (Corlett et al., 2022).

Reward and punishment

While RPE valence is oftentimes considered before outcome valence, there might be differences in how prediction errors are processed for rewards and punishments. The findings by Schultz et al. (1993, 1997) were based on reward delivery and reward omission. One might assume that reinforcers can be grouped into rewarding ones (i.e., reward delivery, punishment omission) and punishing ones (i.e., reward omission, punishment delivery). Photostimulation

was able to elicit both approach behaviour by excitatory stimulation of the SNc and VTA, and avoidance behaviour by inhibitory stimulation of both SNc and VTA (Ilango et al., 2014). However, it could be argued that this did not require a distinction into reward-related and punishment-related stimuli. In practice, this assumption proves difficult. Studies in dopaminergic neurons examining aversive stimuli could not find a sensitivity towards punishment-related stimuli (punishment delivery and withdrawal; Fiorillo, 2013; Mirenowicz & Schultz, 1996). It is thus advisable to consider both appetitive and aversive contexts before generalising from one to the other.

Signed and unsigned reward prediction errors

While a true RPE is signed and thus contains valence information, the magnitude of the RPE can be regarded separately from valence, in the form of an unsigned RPE. Considering brain regions with more activity related to signed than unsigned RPE, a meta-analysis performed by Corlett et al. (2022) could find activation of the dorsal and ventral striatum, pallidum, medial PFC and anterior and posterior cingulate. As described above, these are regions associated with value-based functions or policy selection within reinforcement learning. In addition, neurons in the pallidum were shown to also reflect signed RPE activity, and correlate with learning rates in a classical conditioning setup (Kaplan et al., 2020). For the posterior cingulate, a multitude of functions has been proposed, including monitoring of subjective values and reward outcomes (Pearson et al., 2011). Considering brain regions that reflect an unsigned RPE more strongly than the signed RPE, Corlett et al. found the cerebellum, dlPFC, dorsomedial PFC, cingulate, SMA, supramarginal gyrus, parietal regions, middle temporal gyrus, claustrum, and a disparate region of insula. Several of these regions have been implicated in reinforcement learning: the cerebellum has been implicated in processing of RPEs in some initial studies (see below for an in-depth discussion). The dlPFC and parietal cortex have been found to track action values (Lee et al., 2012). The dorsomedial PFC including the SMA has been implicated in probabilistic reasoning concerning switching between exploitation and exploration (Domenech & Koechlin, 2015). The supramarginal gyrus and anterior insula have been associated with predictive functions (Siman-Tov et al., 2019). The middle temporal gyrus has been associated with the detection of general sensory mismatches, independent of actions (van Kemenade et al., 2019). Lastly, for the claustrum, a more general role in cognitive control and higher cognitive functions has been proposed (Madden et al., 2022; J. B. Smith et al., 2020). Taken together, there are considerable differences in brain regions processing signed and unsigned RPEs, which might be differentially related to valence and salience.

Classical and operant conditioning

As presented above, reinforcement learning encompasses only operant conditioning, as it requires an actor to influence its state through its actions. This is not the case for classical conditioning. Thus, while *brain activity* in both processes can be explained by reinforcement learning algorithms, this does not extend to behaviour. Brain activity might still differ depending on the type of conditioning. Corlett et al. (2022) found that there was an overlap in brain activations between classical and operant conditioning, especially in dorsal and ventral striatum, insula and midbrain. However, there were also differences in activation: operant conditioning engaged the dorsal and ventral striatum, anterior and posterior cingulate, and several other frontal and parietal regions more, while classical conditioning engaged the amygdala, parahippocampal gyrus, putamen, insula, and several other cortical and subcortical areas more. Note that this might be due to different use of positive/negative outcomes in classical and operant conditioning (Corlett et al., 2022). Notably, there yet seems to be a pattern where action-outcome association (which might only occur in operant conditioning) requires the ACC and not the OFC, but stimulus-outcome association (which can occur in both classical and operant conditioning) requires the OFC but not the ACC (Camille et al., 2011; Rudebeck et al., 2008). These findings are not explainable by valence effects. There might thus yet be a difference in the required brain areas for classical and operant conditioning, even though the overlap seems to be considerable.

Feedback delays

While feedback can be provided immediately upon action performance, it can also be provided after a delay. Feedback delay generally refers to the time passed between the response and feedback presentation. It could be shown by several groups that the FRN is more negative for negative over positive feedback only, or at least more strongly, for feedback delivered with only short delays compared to feedbacks delivered with longer delays post-response (Arbel et al., 2017; Höltje & Mecklinger, 2020; Weinberg et al., 2012; Weismüller & Bellebaum, 2016). At least one study (Peterburs et al., 2016) also showed a gradual decrease in valence differentiation with increasing feedback delay. This reflects fMRI findings showing that longer feedback delays result in less involvement of the striatum/dopaminergic structures and increased involvement of the medial temporal lobe, in particular the hippocampus (Foerde & Shohamy, 2011).

Evidence for a role of the cerebellum in reinforcement learning

While many neuroimaging studies have been conducted on the matter of reinforcement learning, focus has been put on dopaminergic structures. Descriptive models have further focussed on the cerebral cortex in relation to dopaminergic structures, as it is easy to measure with fMRI. Smaller structures, on the other side, are harder to measure with the resolution of

fMRI. In the past, it was general practice to not or not fully measure the cerebellum due to reasons of practicality. In fMRI, measuring the complete cerebellum in addition to the cerebrum oftentimes requires a larger field of view, increasing acquisition time. In addition, cerebellar activity is likely only partially captured by fMRI (Johnson et al., 2019). In EEG, the cerebellum lies in an impractical region at the lower back of the head, which is not covered by standard EEG caps and where impedances are usually higher. Additionally, muscle artefacts due to the proximity to the neck muscles are more present (Todd et al., 2018).

Considering recent studies in humans and rodents, this might have concealed a potential supportive role of the cerebellum in reinforcement learning (Berlijn et al., 2024; Kostadinov & Häusser, 2022; Kruithof et al., 2023). In rodents, several studies from different groups have found activity in the cerebellum and in projections originating from the cerebellum resembling RPEs (Hull, 2020; Kostadinov & Häusser, 2022; Manto et al., 2024). These studies offer good reason to look more closely at the cerebellum and its role in reinforcement learning. For humans, evidence is more correlative with only limited causal evidence (e.g., Nicholas et al., 2024; Rustemeier et al., 2016; Thoma et al., 2008). It is further not clear what the cerebellum contributes to the reinforcement learning processes, i.e., which role it plays. Within the doctoral thesis at hand, I attempted to contribute towards answering these questions.

The cerebellum and its functions

The human cerebellum is a brain structure located inferior and posterior to the cerebrum (Błaszczyk et al., 2024). It lies in the posterior cranial fossa, just below the occipital lobe. Even though its size is small (with its Latin name meaning *little brain*), its cortex is folded much more delicately. The cerebellum contains around 50 % of the total number of neurons in the brain and has around 80 % of the surface volume of the neocortex even though it makes up only around 10 % of the total brain mass (Azevedo et al., 2009; Sereno et al., 2020; van Essen et al., 2018). Concerning its composition, clear differences from the composition of the cerebrum must be considered. While these differences might enable the cerebellum to perform certain tasks that cannot be performed by the cerebrum (such as fine movements), they are also one of the reasons why cerebellar functionality beyond motor function has been historically underresearched. Its different composition requires potentially different ways of measuring, analysing, or interpreting data that require knowledge of these differences.

Anatomy

Macroscopic anatomy

The cerebellum consists of two hemispheres as well as the vermis in the middle (Colin et al., 2001; Voogd & Glickstein, 1998; Voogd & Marani, 2016). The cerebellar cortex can be distinguished into ten lobules which are separated by sulci running from left to right. Lobule I-

V are generally considered to be the anterior lobe of the cerebellum while lobule VI-IX are considered to lie in the posterior lobe of the cerebellum. The anterior and posterior lobe of the cerebellum are separated by the fissure prima (Moulton et al., 2014). Note that lobules VII and VIII are frequently separated into Lobule VIIa/VIIIa and VIIb/VIIIb, and Lobule VIIa is further separated into Crus I and II. The flocculonodular lobule (lobule X) is separated from the posterior cerebellum by the posterolateral fissure (Voogd & Glickstein, 1998). An anatomical overview of cerebellar lobes, lobules, and sulci is given in Figure 5. Broadly speaking, motor functions have been attributed to anterior parts and higher (non-motor) functions to the posterior part (e.g., cognition, emotion, social behaviour; Stoodley et al., 2016; Tedesco et al., 2011). The posterior cerebellar lobe, in particular Crus I and II, developed over-proportionately from an evolutionary standpoint, together with prefrontal cerebral areas, supporting the notion that it supports higher cognitive function (Balsters et al., 2010).

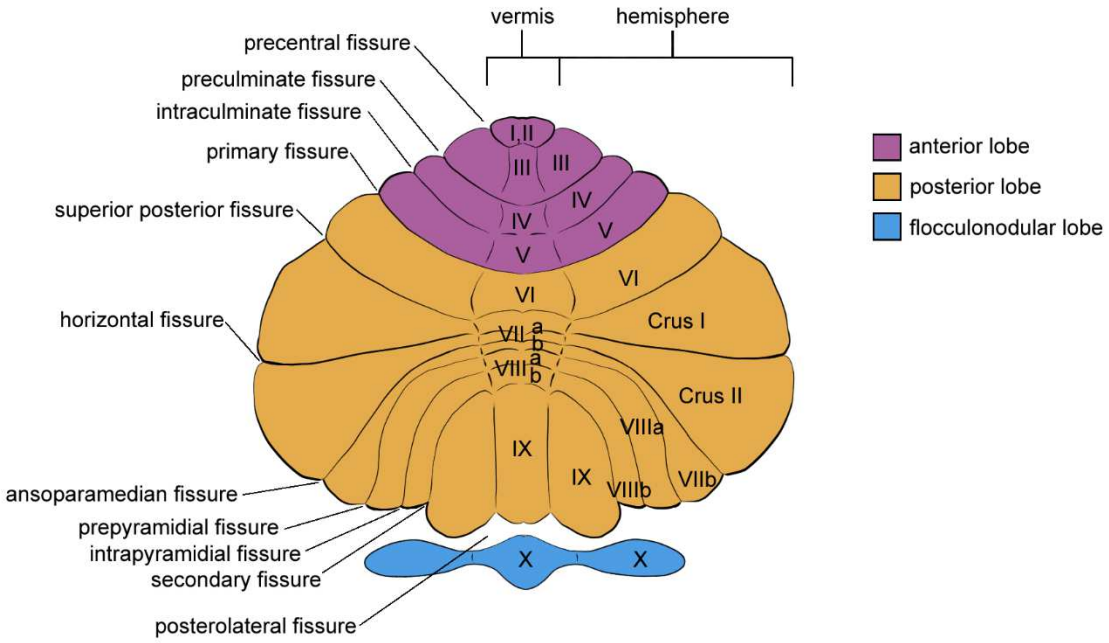

Figure 5. Schematic illustration of the cerebellar lobes, lobules, and sulci.

While anatomical parcellations of the cerebellum into lobules have been helpful to report findings, these do not reflect functionally distinct zones accurately, and activations often cross lobule borders. In recent years, attempts have been made to parcellate the cerebellum based on non-anatomical markers, such as resting state activity (Buckner et al., 2011) and task-based activations (King et al., 2019; Nettekoven et al., 2024). The most recent functional parcellation developed by Nettekoven et al. (2024) made use of several datasets which used different types of tasks, as to overcome inaccuracies due to lack of certain task types (e.g., motor tasks, working memory tasks, somatotopic tasks). The resulting parcellation distinguishes into four different functional regions on the coarsest level which are motor, action, demand, and social-

linguistic-spatial functions. Such functional parcellations have been shown to have higher predictability of functional boundaries (Nettekoven et al., 2024), and might be a useful addition to report (f)MRI findings.

Within the white matter in the middle of the cerebellum lie the cerebellar nuclei, the only output station of the cerebellum. There are four cerebellar nuclei: the dentate nucleus, the fastigial nucleus, the globose nucleus, and the emboliform nucleus (Colin et al., 2001; Prekop & Wingate, 2016). The globose nucleus and the emboliform nucleus are sometimes collectively referred to as interposed nucleus (Prekop & Wingate, 2016). The dentate nucleus is the largest of the four nuclei and contains 90 % of the cerebellar nuclei neurons (Colin et al., 2001). The output from the dentate nucleus seems to be segregated according to functionality, with dorsal parts sending projections towards cerebral motor areas, and ventral parts sending projections to cerebral non-motor areas (e.g., areas concerned with cognitive, emotional, executive, or linguistic functions; Ramnani, 2012).

The cerebellum is supplied with blood via three paired arteries. The posterior inferior cerebellar arteries (PICAs) originate directly from the intracranial vertebral arteries (Błaszczyk et al., 2024; Caplan, 2022; Delion et al., 2017). They supply posterior portions of the cerebellum, but in some cases also contribute to supply towards the cerebellar nuclei, in particular the fastigial nucleus and at times the ventral part of the dentate nucleus (Caplan, 2022; Delion et al., 2017). The intracranial vertebral arteries join at the medullo-pontine junction, forming the basilar artery. The anterior inferior cerebellar arteries (AICAs) then originate from the basilar artery (Delion et al., 2017), supplying a rather limited part of the anterior cerebellum and flocculus (Caplan, 2022). Lastly, the superior cerebellar arteries (SCAs) originate from the end of the basilar artery (Błaszczyk et al., 2024; Malicki et al., 2023), close to the location where it splits into the paired posterior cerebral arteries (Caplan, 2022). It supplies the upper areas of the cerebellum but also the cerebellar nuclei (Błaszczyk et al., 2024; Caplan, 2022; Delion et al., 2017; Malicki et al., 2023). The SCAs and PICAs can usually be distinguished in lateral and medial branches (Delion et al., 2017). Strokes in the cerebellum are often limited to these two major arteries, and oftentimes also to the medial or lateral branch (e.g., medial SCA; Caplan, 2022). Note that the supply of these three arteries is not limited to the cerebellum. For example, the AICAs largely supply the lateral pontine tegmentum, and the medial PICAs often also supply the dorsal medulla oblongata (Caplan, 2022). There is also evidence that the SCAs partially supply the lateral pontine tegmentum and the pontine and mesencephalic tectum (Caplan, 2022; Delion et al., 2017). Cerebellar strokes however do not always affect extracerebellar brain areas (Chaves et al., 1994).

Cytoarchitecture

Considering the seminal work of Korbinian Brodmann, who mapped the entire cerebral cortex based on the differences in cytoarchitectural organisation, one might expect that the same is true for the cerebellar cortex. However, very different from the cerebral cortex, the cerebellar cortex shows a uniform organisation, and consequently no differences in cytoarchitectural organisation between cerebellar areas with different functionality (Schmahmann, 2000). This peculiarity later resulted in the idea that the cerebellum might simply perform the same computations for different domains (see below). Note that more recent work did find more subtle differences in microscopic architecture and other areas, such as differences in dendritic bifurcation of Purkinje cells (Busch & Hansel, 2023), or Zebrin expression (Y.-C. Lin et al., 2020).

The cerebellar cortex consists of three layers (Voogd & Glickstein, 1998): The granule layer lies closest to the white matter and furthest from the cortical surface. The molecular layer is located on the surface of the cerebellar cortex, and in between the two lies the Purkinje layer.

Granule layer

The granule layer's main purpose is thought to separate patterns received from the input from mossy fibres and expand them (Dieudonné, 2016). It contains granule, Golgi, unipolar brush, and Lugaro cells (Ruigrok et al., 2015).

The small granule cells are the main type of cells in the human brain, with cerebellar granule cells making up more than half of all neurons in the human brain (Herculano-Houzel, 2010; M. J. Wagner et al., 2017). Granule cells receive their input mainly from mossy fibres which originate from several different brain regions (Shinoda & Sugihara, 2022; see below for a summary of input to the cerebellum via mossy fibres). While one granule cell receives input from 4-5 mossy fibres, one mossy fibre supplies 400-600 granule cells (Ito, 2009). The output of granule cells is excitatory, using glutamate as neurotransmitter (Hudson et al., 1976; Su et al., 1997). The axons reach into the molecular layer which is at the surface of the cerebellar cortex. There, the axons bifurcates, forming a 'T'-shape, and constituting the parallel fibres (D'Angelo, 2016). Besides granule cells, Golgi cells and unipolar brush cells can be found in the granular layer.

Golgi cells receive excitatory inputs from both mossy fibres and granule cells (Dieudonné, 2016). The input from granule cells originates both from ascending axons of neighbouring granule cells, as well as from more distant granule cells via parallel fibres. Golgi cells also receive inhibitory inputs from Lugaro cells (Lainé & Axelrad, 1998). Collaterals from climbing fibres also innervate Golgi cells (Castejon & Sims, 2000). While some Golgi cells are interconnected with each other, Golgi cells do not receive input from Purkinje cells or molecular

layer interneurons (Dieudonné, 2016). Golgi cell output is the only inhibitory input for granule cells. A role in spatio-temporal coordination of cerebellar responses has been proposed for the Golgi cells, consistent with their complex intracerebellar connectivity (Galliano et al., 2010).

Unipolar brush cells, which can be found in the cochlear nuclear complex in addition to the cerebellar cortex, receive their input, similarly to the granule cells, from mossy fibres (Martina, 2016). However, one unipolar brush cell receives input from only one mossy fibre, via its short dendrite with a brush-like ending (Martina, 2016). Their axons do not leave the granule layer, and instead terminate at several mossy fibres, forming a feedforward amplification of mossy fibre signal (Mugnaini et al., 2011).

Lastly, the Lugaro cells lie just beneath the Purkinje cell layer, but still in the granule layer (Hirono, 2016). They receive input from a multitude of fibres and cells, including climbing fibres, mossy fibres, granule cells, Purkinje cells and Golgi cells (Miyazaki et al., 2021). They are also well interconnected with neighbouring Lugaro cells (Miyazaki et al., 2021). While they do not innervate Purkinje cells, they exert an inhibitory output towards basket and stellate cells in the molecular layer as well as towards Golgi cells (Lainé & Axelrad, 1998; Miyazaki et al., 2021).

Molecular layer

The most superficial layer, i.e., the molecular layer, contains the parallel fibres as well as stellate and basket cells. Both of these cell types are inhibitory interneurons, and both receive excitatory input from parallel fibres and climbing fibres (S. J. Liu & Dubois, 2016; Watanabe, 2016). They are often collectively referred to as molecular layer interneurons. However, their function might differ, as they inhibitorily stimulate Purkinje cells at different points. Basket cells are located in the basal third of the molecular layer and stimulate the soma and axons of Purkinje cells (Watanabe, 2016). Thus, they can inhibit the spiking output of Purkinje cells (S. J. Liu & Dubois, 2016; Watanabe, 2016). Stellate cells on the other hand suppress Purkinje cell activity in a different way: they are located in the top 2/3 of the molecular layer and target the dendrites of Purkinje cells (Watanabe, 2016). As Purkinje cells also receive input from parallel fibres (Daniel & Crepel, 2022; Grangeray et al., 2016), stellate cells inhibit rather via counterbalancing the parallel fibre excitation without directly inhibiting the spiking output of Purkinje cells (Watanabe, 2016). This is often referred to as a feedforward inhibition.

Purkinje layer

Lastly, the much thinner Purkinje layer lies between the granule and molecular layer. It contains the Purkinje cells, but also the much smaller candelabrum cells (Grangeray et al., 2016; Lainé & Axelrad, 1994).

Purkinje cells are some of the most remarkable cells in the cerebellar cortex, having the largest dendritic tree out of all cells in the human brain (Busch & Hansel, 2024). They were first

described by Jan Evangeliska Purkyně in 1893 and famously characterised by Ramón y Cajal in 1899 (Grangeray et al., 2016). They receive excitatory input from the granule cells via the parallel fibres as well as from the climbing fibres. While one Purkinje cell receives input from an average of 200,000 parallel fibres, it is innervated by only one climbing fibre (Daniel & Crepel, 2022; Grangeray et al., 2016; Shinoda & Sugihara, 2022). Note that the latter information was strongly driven by findings in rodents, in which around 47.5 % of Purkinje cells have only one dendrite. Newer findings show that around 16.6 % of rodent Purkinje cells are polysynaptic, i.e., have several trunks emerge directly from the soma (Busch & Hansel, 2023). These numbers are strongly increased in humans, especially for the polysynaptic Purkinje cells (51.2 % instead of 16.6 %; Busch & Hansel, 2023), potentially hinting at inputs from more than one climbing fibre. Very recently it could be shown that indeed at least 1/10 of Purkinje cells receive input from more than one climbing fibre (Busch & Hansel, 2024). The Purkinje cells also receive inhibitory input from the molecular layer interneurons (see above). One single axons targeting the cerebellar nuclei constitutes the inhibitory, GABAergic output of the Purkinje cells (Grangeray et al., 2016). While stimulation of parallel fibres result in a simple spike output, stimulation of climbing fibres results in a complex spike output, which is a massive electrical output compared to the smaller and frequent simple spikes (Bauswein et al., 1983; Davie et al., 2008; Grangeray et al., 2016; Orozco et al., 2010).

The candelabrum cells form a part of an inhibitory loop between the molecular layer interneurons and Purkinje cells (Lainé & Axelrad, 1994; Osorno et al., 2022): They receive excitatory inputs from granule cells and mossy fibres, but also receive inhibitory inputs from Purkinje cells. Integrating these inputs, candelabrum cells project towards stellate and basket cells in the molecular layer. Nevertheless, their exact function is not yet well understood (Osorno et al., 2022).

Note that this unique neuroarchitecture of the cerebellum makes it a very suitable candidate for a supervised learner: the massive sensory input from the mossy fibres ensures sufficient input of information, while climbing fibre input has oftentimes been proposed as a teaching signal input, constituting the two main requirements for a supervised learner (Priddy & Keller, 2005; Raymond & Medina, 2018).

Cerebellar nuclei neurons

Lastly, the cerebellar nuclei consist of several distinct types of neurons. The two best known projecting neurons are the large glutamatergic projection neurons which project to several areas outside the cerebellum and the midsize GABAergic projection neurons which project to the inferior olive (Hoshino et al., 2022; Kebschull et al., 2024). Additionally, there are several other types of neurons described for the cerebellar nuclei, including glutamatergic, GABAergic, and glycinergic neurons (Bagnall et al., 2009; Uusisaari et al., 2007; Uusisaari &

De Schutter, 2011; Uusisaari & Knöpfel, 2010). Five types are found in all cerebellar nuclei, which are Class A and B glutamatergic projection neurons, GABAergic neurons projecting to the inferior olive, local GABAergic and glycinergic neurons, and GABA and glycinergic neurons projecting to the cerebellar cortex (Kebschull et al., 2024). However, so far, 14 types of excitatory cell types could be identified across all nuclei (Kebschull et al., 2024), showcasing a high complexity in cerebellar nuclei neurons. Knowledge on the neurons in the cerebellar nuclei and their function is however small in comparison to the cerebellar cortex (Kebschull et al., 2024; Uusisaari & De Schutter, 2011).

Connectivity with other brain areas

To understand the functionality of the cerebellum, it is helpful to know from which brain areas it receives projections and to which brain areas it projects (Strick et al., 2009). The cerebellum mostly connects with other brain areas in a closed-loop feedback system organised topologically (Chen et al., 2022), meaning that the areas towards which the cerebellum projects, project back to the same areas within the cerebellum. Thus, the function of brain areas with which a certain area of the cerebellum is connected might be indicative of the function of the cerebellar area.

Projections from and to the cerebellum pass via the three cerebellar peduncles, which are thick fibre bundles differentiated into the superior, middle, and inferior peduncle (Schmahmann, 2016).

The cerebellum receives all of its projections via either mossy fibres or climbing fibres (Ruigrok et al., 2015). The sources of mossy fibres are manyfold while the climbing fibres originate from the inferior olive. The sole output of the cerebellar cortex is the inhibitory output of the Purkinje cells. These project towards the cerebellar nuclei, which project towards a wide range of brain areas (Kebschull et al., 2024).

Cerebellar input via the mossy fibres mostly passes through four precerebellar nuclei: the pontine grey nucleus and reticulotegmental nucleus in the pons, the lateral reticular nucleus in the hindbrain, and the external cuneate nucleus in the medulla oblongata (Hoshino et al., 2022; Yamada & Hoshino, 2016). Input towards these nuclei stems from widespread areas within the frontal, parietal, temporal, and occipital lobe (Strick et al., 2009). Afferences from the pons mainly originate from the cerebral cortex, although the superior colliculus and other areas of the brain stem partially contribute (Glickstein, 2022). Some mossy fibre input also originates from the spinal trigeminal nucleus and Clark’s column in the spinal cord (Hoshino et al., 2022; Yamada & Hoshino, 2016) and mainly terminate in the anterior cerebellum, hinting at a primary motor function (Ruigrok et al., 2015). Historically, it was assumed that this large variety of inputs serves as a means of gaining as much sensory input as possible, to convey

sensorimotor information to the motor cortex (Strick et al., 2009). However, this view has changed since, following findings of outputs of the cerebellum to several other brain regions.

Initial problems arose from the circumstance that only monosynaptic projections could be traced. This problem could be overcome with the help of viral tracers, such as rabies virus (Kuypers & Ugolini, 1990). The group around Peter Strick could show via anterograde and retrograde tracing that the cerebellum is interconnected with both the primary motor cortex and prefrontal areas (R. M. Kelly & Strick, 2003; Middleton & Strick, 2001). The primary motor cortex projected mainly to cerebellar lobule IV-VI, which are primarily labelled as motor/pre-motor lobule. On the other hand, several prefrontal areas they examined were found to exclusively project back towards cerebellar Crus II which is located in the posterior cerebellum. A study using diffusion weighted imaging could confirm these results in humans (Palesi et al., 2017). They found that motor areas projected primarily to lobule I-VI (primarily the anterior lobe). However, projections from the cerebral cortex were primarily received by the largely non-motor Crus I, II, lobule VIIb and lobule VIII (Palesi et al., 2017). Areas in the cerebral cortex that projected to the cerebellum were mainly within the temporal and frontal lobe (Palesi et al., 2017). In total, around 70 % of the tracts seemed to involve cognitive cerebral and cerebellar areas, hinting towards non-motor functions of the cerebellum.

The cerebellum is widely interconnected with areas across all cerebral lobes. Tracing studies could show connections with the cerebellum via the pons from not only motor but also non-motor frontal areas, such as ACC, dlPFC and anterior PFC (Glickstein et al., 1985; Ramnani, 2012; Schmahmann & Pandya, 1997). Bidirectional connections between the cerebellum and parietal lobe, in particular the intraparietal sulcus and inferior parietal lobe, were shown in both tracing studies and functional connectivity in-vivo (Bostan & Strick, 2022; Clower et al., 2001; Habas, 2021; Prevosto et al., 2010; Ramnani, 2012). While Chen et al. (2022) found that a majority of projections into the cerebellum come from frontoparietal and subcortical networks, Palesi et al. (2017) found that the majority of projections originate from the temporal lobe. Within the temporal lobe, projections towards the cerebellum seems to mainly come from the superior temporal lobe via the pons (Schmahmann & Pandya, 1991, 1997). This connection could be shown to be functionally significant for auditory pattern discrimination (Stockert et al., 2021). Diffusion-weighted imaging in humans could however also show projections from the hippocampus and amygdala to the cerebellum (Palesi et al., 2017). Last, bidirectional connections between the cerebellum and occipital lobe have been demonstrated as well (Glickstein et al., 1994; Schmahmann & Pandya, 1992, 1993), although seemingly more strongly for higher visual areas (van Es et al., 2019; Xue et al., 2021). Note that the cerebellum also forms at least two closed loops with the contralateral inferior olive, which is the only source

of input towards the cerebellum via the climbing fibres (Bengtsson & Hesslow, 2006; De Zeeuw et al., 1998; Loyola et al., 2022).

Importantly, the cerebellum is also connected to areas involved in reinforcement learning. Studies in rodents and macaques showed that the cerebellum is connected with the striatum via the thalamus as a di-synaptic pathway (Hoshi et al., 2005; Ichinohe et al., 2000). This was further supported by resting state functional connectivity in humans (for a meta-analysis see Cauda et al., 2011). Further evidence comes from diffusion tensor imaging, diseases involving either the basal ganglia or the cerebellum, and task-based functional connectivity (for a review, see Bostan & Strick, 2018). Concerning the SN, studies in rodents and cats could show that stimulation of the cerebellum affected dopamine release in the SN (Nieoullon et al., 1978), and lesion of the SNc affected glutamate release in the cerebellum (Gołembiowska et al., 2013). The corresponding pathway likely also runs through the thalamus (Faull & Carman, 1968). However, a very recent study could also show a monosynaptic projection from the cerebellum towards the SNc (Washburn et al., 2024). On a similar note, projections from the dentate nucleus towards the VTA have also been shown (Beier et al., 2015; Watabe-Uchida et al., 2012). Lastly, the cerebellar lobule VI and Crus I have also been implicated in a salience network with the ACC (Habas et al., 2009). Resting-state functional connectivity between the ACC and cerebellum could further be shown in a recent meta-analysis (Kruithof et al., 2023). In sum, there is substantial evidence for a connectivity of the cerebellum with areas involved in reinforcement learning.

Cerebellar diseases

Cerebellar disorders (or ataxias) can be caused by focal cerebellar diseases (for example due to stroke) and cerebellar degeneration (which can have genetic, non-genetic or acquired causes). Cerebellar disorders differ based on their progression rate and age at onset (Palau & Arpa, 2016).

Cerebellar strokes

Focal cerebellar lesions are usually caused by ischemic or haemorrhagic stroke, tumour resections, abscesses, or demyelinating diseases such as multiple sclerosis (Palau & Arpa, 2016). Cerebellar strokes occur seldom and account only for around 2-3% of total annual strokes in the US (Edlow et al., 2008; P. J. Kelly et al., 2001; Tohgi et al., 1993). A majority is ischemic (Shenkin & Zavala, 1982). Prognosis concerning recovery of motor functions is quite good for ischemic cerebellar strokes, with 2/3 of patients reaching functional independence at the time of discharge; this was the case for only 40% of patients with haemorrhage (P. J. Kelly et al., 2001). Note that cognitive function does not recover as well (Erdlenbruch et al., 2024). Acute symptoms are oftentimes vertigo, dizziness, and unsteadiness (Sarikaya & Steinlin, 2018). Strokes in the anterior cerebellum up to lobule VI may lead to persistent motor deficits,

such as ataxia, while strokes in the posterior lobe do not seem to result in persistent motor deficits (Schmahmann et al., 2009; Stoodley et al., 2016). Instead, strokes in the posterior lobe have been associated with deficits in language, spatial and executive functions (Stoodley et al., 2016). Motor and non-motor symptoms have also been found after tumour resections in/near the cerebellum (De Smet et al., 2009; Konczak et al., 2005; Svaldi et al., 2024). Additionally, the connectivity to several cerebral areas is reduced acutely following cerebellar stroke (Fan et al., 2019), but differentially increased and decreased in chronic stroke, indicating reorganisational processes (Park et al., 2011).

Degenerative cerebellar disease

Degenerative cerebellar diseases can be acquired, sporadic, or due to genetic causes. Hereditary ataxias may be autosomal-dominant (e.g., spinocerebellar ataxias), autosomal-recessive (e.g., Friedreich's ataxia) or x-chromosomal (fragile X-associated tremor-ataxia syndrome) inheritance (Koeppen, 2001; Thieme & Timmann, 2022). Acquired ataxias may be infectious (such as cerebellitis, progressive multifocal leukoencephalopathy, Whipple's disease; Manto, 2001b), autoimmune (such as multiple sclerosis, Miller Fisher syndrome; Duquette, 2001), paraneoplastic (Afzal et al., 2015), toxic (alcohol, antiepileptic drugs, and others; Manto & Jacquy, 2001b; Pentney, 2001; for a systematic review see van Gaalen et al., 2014), or metabolic (hypothyroidism, hypomagnesemia, deficiency of vitamin E, and others; Koibuchi, 2001; Manto & Zulewski, 2001; Olmedo-Saura et al., 2023; Schuelke, 2005). Sporadic degenerative disorders include multiple system atrophy-cerebellar type (MSA-C) and sporadic adult onset ataxia of unknown aetiology (Berciano, 2001; Manto & Jacquy, 2001a). As such, there is a large variety in aetiology (Topka & Massaquoi, 2001) – however, symptoms are strongly influenced by the location of the damage rather than pathological characteristics (Manto, 2001a). An overview of genetics and phenotypes for different hereditary cerebellar ataxias is given at https://neuromuscular.wustl.edu/ataxia/aindex.html. A majority of these diseases also include involvement of extracerebellar areas (e.g., spinocerebellar ataxia types 1,2 and 3 or MSA-C), making interpretations of cerebellar contributions more difficult.

Currently, only a handful of cerebellar diseases are considered to primarily affect the cerebellum, most commonly spinocerebellar ataxia types 6, 14, and 27B (Rentiya et al., 2020; Satolli et al., 2024; Taron et al., 2022; Teive et al., 2011) as well as sporadic adult-onset ataxia of unknown aetiology (Abele et al., 2007). These disorders are thus especially suitable to investigate the effects of cerebellar degeneration on brain and behaviour.

Very rarely, cerebellar agenesis, i.e., the complete or partial absence of the cerebellum from birth, occurs (Romaniello & Borgatti, 2022). Realistically, even in patients with "no cerebellum", some amount of cerebellar tissue can be found post-mortem (Gardner et al., 2001). Importantly, living without a cerebellum is indeed possible for these patients, although with

considerable deficits in not only the motor domain but also the cognitive and emotional domain (Romaniello & Borgatti, 2022). This further strengthens the theoretical basis for a complementary rather than a holistic role of the cerebellum in these domains (see below).

Motor deficits

Motor symptoms associated with cerebellar diseases have been divided into four major categories: 1) postural and gait disturbances, 2) limb ataxia, 3) dysarthria, and 4) oculomotor disorders. These have been implemented in the International Cooperative Ataxia Ratings Scale (ICARS; Manto, 2001a; Trouillas et al., 1997).

1) Patients with cerebellar disorder may show an increased back-and-forth sway when standing still, known as titubation (Bodranghien et al., 2016). Their gait appears as “clumsy, staggering movements with a wide-based gait” (Bodranghien et al., 2016, p. 380).

2) Limb ataxia refers to a number of symptoms, including intention and other tremors, dysmetria, and diadochokinesis (Bodranghien et al., 2016; Holmes, 1917). Intention tremor is a tremor that increases when approaching a movement target (Bhatia et al., 2018). Note that other types of tremor, such as rest tremor (i.e., tremor occurring when at rest) and postural tremor (i.e., relating to tremor occurring when holding a body part, such as an arm, in a position against gravity) have also been described in connection with cerebellar disease (Holmes, 1917; Lenka & Louis, 2019). Dysmetria refers to the over- (hypermetria) or undershoot (hypometria) of a movement towards a target (Holmes, 1917; Hore et al., 1991). Together with tremor and oculomotor deficits, it might result in severe difficulties with grasping movements (Bodranghien et al., 2016).

3) Dysarthria describes symptoms related to deficits in speech production. These mainly relate to impairment of articulation and prosody (Darley et al., 1969a; Spencer & Slocomb, 2007). A slowness and slurring of speech is observed (Darley et al., 1969b; Manto, 2001a; Spencer & Slocomb, 2007), and, also noticeably, ‘scanning’ speech, which means excessive and equal stress of the syllables, disrupting the general rhythm (e.g., “won (pause) der (pause) ful”; Darley et al., 1969b; Kent et al., 2000). Further irregularities have been described for loudness, timing of breaks, and pitch (Spencer & Slocomb, 2007).

4) Oculomotor deficits comprise deficits in the slow eye movements, saccades, ocular alignment, gaze, and nystagmus (Bodranghien et al., 2016; Manto, 2001a; Salari et al., 2024). Concerning nystagmus, cerebellar disorders are often associated with a downbeat nystagmus (i.e., an upward drift of the eyes followed by a downward saccade; Hüfner et al., 2007; Yee, 1989), but also other forms of nystagmus, such as gaze-evoked nystagmus (i.e., a drift towards the centre when looking to the periphery), rebound nystagmus (i.e., a drift towards the prior gaze towards the periphery when looking towards the centre), and others (for an overview, see

Bodranghien et al., 2016). For the slow eye movements, smooth pursuit may be impaired, and instead, corrective saccades can be observed when following a moving object with the gaze (for a review, see Sharpe, 2008). The vestibulo-ocular reflex, i.e., the reflex to adjust the gaze when the head is moved while fixating an object, can also be impaired in cerebellar disorders (Ito, 1998; Szmulewicz et al., 2011). Saccades may be hyper- or hypometric depending on damage location (Barash et al., 1999; Bodranghien et al., 2016; Bötzel et al., 1993).

Note that non-specific symptoms, such as dizziness and vertigo as described above might also occur episodically or chronically (Bodranghien et al., 2016). Sensory function, such as pitch discrimination and proprioception may also be reduced (Frings et al., 2004; Parsons et al., 2009; Tinazzi et al., 2013; Weeks et al., 2017).

Cerebellar Cognitive Affective Syndrome

While researchers started to explore the role of the cerebellum in motor control more thoroughly in the 19th and 20th centuries, non-motor deficits in cerebellar disease have only been described sparsely in case reports. This might also have been the case because cognitive performance of adult patients with cerebellar damage lies in the lower normal range, with motor symptoms being more prominent (Leggio, 2016). The deficits are, in parallel to motor deficits, less in the fundamental inability to perform certain behaviours and more in the efficiency (Leggio, 2016). Notably, this still leads to relevant deficits in executive, language, and visuospatial function (Ahmadian et al., 2019). Previous evidence for a role of the cerebellum in non-motor function had mainly come from studies examining the connectivity of the cerebellum with cerebral non-motor areas (see above). In 1998, Schmahmann and colleagues described the “cerebellar cognitive affective syndrome” (CCAS; Schmahmann & Sherman, 1997, 1998) which they used as an umbrella term for several non-motor symptoms in patients with cerebellar damage. The syndrome was also closely connected to the proposed “Dysmetria of Thought” (Schmahmann, 1998): Schmahmann proposed that deficits in the non-motor domain relating to cerebellar damage might present similar in form to deficits in the motor domain. The meaning of dysmetria, i.e., an over- or undershooting of a movement, is thus transferred to mean an over- or undershooting of a non-motor process, such as an emotional reaction. Non-motor symptoms described for the CCAS include deficits in the executive function (e.g., planning, working memory), spatial cognition, personality changes, and linguistic difficulties that cannot be ascribed to motor function (Schmahmann & Sherman, 1998). While the initial study examined only 20 patients with mostly focal cerebellar damage (but also a number of cases with cerebellitis and cerebellar atrophy), the findings could be replicated in a much larger sample by Tedesco et al. (2011). Using a large subsample of 78 patients with only focal cerebellar damage (through ischemic or haemorrhagic stroke or surgical tumour resection), they could further show that non-motor deficits occur in particular

when the posterior lobe is affected, especially Crus I and II. This was mostly the case after damage within the PICA territory. This finding also fits with the above-described connectivity of the posterior cerebellar lobe with cerebral brain areas encompassing non-motor functions.

To characterise non-motor deficits specific to cerebellar function in a clinical setting, the CCAS scale was invented as a bedside test by the Schmahmann group (Hoche et al., 2018) and subsequently translated into several languages (Chirino-Pérez et al., 2022; Maas et al., 2021; Naeije et al., 2020; Rodríguez-Labrada et al., 2022; Thieme et al., 2020, 2022). The scale tests the core domains of CCAS, including executive, linguistic, visuospatial, and neuropsychiatric functions. An additional verbal memory test item is not part of CCAS, but considered an indicator item for extracerebellar involvement (Hoche et al., 2018). Later work performed by Thieme et al. (2021) could show that age and education, and to a lesser degree sex affected test scores and need to be considered when examining patients for a CCAS. Notably, the CCAS scale has a weakness in identifying patients with only mild forms of CCAS (Q. Liu et al., 2024). Nevertheless, the CCAS scale is as yet the only widely used assessment method to screen for CCAS which can be used to compare patient groups across studies and was proposed for clinical trials by an expert group (Klockgether et al., 2024).

Cerebellar involvement in other disorders

While there are diseases with predominantly cerebellar involvement (see above), these are oftentimes rather rare diseases. However, cerebellar involvement has also been described in more common disorders that had previously not been as closely associated with cerebellar function, such as anxiety disorders, autism spectrum disorder, schizophrenia/psychosis, and addiction (Andreasen & Pierson, 2008; Biswas et al., 2024; D'Mello & Stoodley, 2015; Miquel et al., 2016; Moulton et al., 2014; Schutter, 2021a; Y. Wang & Lan, 2023). For example, cerebellar activations towards threat and fear extinction have pointed towards a role of the cerebellum in fear and extinction learning, which is a form of reinforcement learning (Doubliez et al., 2023; Schutter, 2021a). Indeed, the connectivity between the cerebellum and amygdala as well as striatum is altered in several anxiety disorders, such as generalised and social anxiety disorder, post-traumatic stress disorder, and obsessive-compulsive disorder (Blithikioti et al., 2022; Etkin et al., 2009; Moreno-Rius, 2018; Roy et al., 2013; Shobeiri et al., 2024; Vaghi et al., 2017; H. Zhang et al., 2019; X. Zhang et al., 2022). Deficits in the non-motor domain were also related to cerebellar connectivity for autism spectrum disorder and psychosis, such as theory of mind, social cognition, executive function, and language in autism spectrum disorder (Biswas et al., 2024) and auditory hallucinations in psychosis (Pinheiro et al., 2021). Concerning addiction, findings have been less consistent but seem to relate the cerebellum to behavioural inhibition (Miquel et al., 2016). The involvement of the cerebellum in these

disorders highlights the need for further research concerning the cerebellum's role in non-motor processes.

Cerebellar function

Brief historical overview

Cerebellar function was characterised in several early works (Glickstein et al., 2009; Manto, 2001a; Schmahmann, 2016). In 1809, Luigi Rolanda could show that the ablation of the cerebellum resulted in difficulties in posture and movements (Schmahmann, 2016). He concluded that the cerebellum is responsible for movement initiation (Glickstein et al., 2009). A few years later, Flourens could show that it is rather the coordination than the initiation of movement (Schmahmann, 2016). Animals were not paralysed but he observed that their movements were irregular and uncoordinated (Glickstein et al., 2009). The coordination deficits were later described in more detail by Luciani (1891), using more advanced methods; he also made first descriptions of intention tremor (Glickstein et al., 2009).

In the late 19th century and early 20th century, several hallmark symptoms of cerebellar motor deficits were described, such as dysmetria and diadochokinesis by Babinksi (Clarac et al., 2009; Manto, 2001a), and ataxia by Gordon Holmes (1917). Holmes' work was especially noteworthy, with terminology in many cases still used today (Bodranghien et al., 2016; Haines, 2016; Manto, 2001a). To his avail was a large population of soldiers with gunshot or shrapnel wounds to the cerebellum due to poor helmet design in the first world war (Haines, 2016).

Descriptive models of cerebellar motor functions

While it is widely accepted that the cerebellum computes internal models for motor functions (Ishikawa et al., 2016), the exact nature of these models has been a matter of debate. Several proposals have been made to describe the function of the cerebellum in a way that generates predictions that can be tested. Internal models can be described as either forward or inverse models (Kawato et al., 2021).

According to the forward model, the cerebellum receives a copy of the motor command that is being sent to the muscle (Miall & Wolpert, 1996; Wolpert et al., 1998). From this command, it generates a prediction of the sensory outcome. For example, when grabbing a cup of coffee, the commands with the succession of movements is sent to the arm and hand. At the same time, it is being sent to the cerebellum. The cerebellum then predicts whether the cup of coffee will be grabbed or how far off we will be. When the movement has been executed, the actual sensory consequence will be sent back. For example, we might have been distracted due to speaking to another person and missed the cup slightly. This information can be compared to the predicted sensory consequences ("successfully grabbed the cup"), and an error signal can

be generated. This error signal can then be used as a learning signal to improve future predictions.

In contrast, the inverse model assumes the opposite: instead of the motor signal, the planned sensory outcome is sent to the cerebellum. In turn, the cerebellum generates the necessary motor commands to reach this outcome (Popa & Ebner, 2022; Schweighofer et al., 1998; Shidara et al., 1993). Both models have the advantage that the movement is independent from subsequent (delayed) sensory information (Tanaka et al., 2021).

Note that combinations of both models have been proposed (Wolpert & Kawato, 1998), oftentimes with the proposition that the forward model is more dominant early in the learning process and that the inverse model is more dominant late in the learning process (e.g., Olson et al., 2023). While there is good evidence that the cerebellum functions as a forward model, whether it also functions as an inverse model still requires evaluation (Popa & Ebner, 2022).

Several other models have been proposed as a basis for cerebellar function (see Manto, 2009 for an overview). One of the most prominent ones is the Marr-Albus theory, proposed in close temporal proximity by Marr (1969) and Albus (1971). They proposed that mossy fibre input serves as the motor/sensory input. This input is then expanded by granule cells into orthogonal representations provided at the parallel fibres (Sanger et al., 2020). These representations can subsequently be thresholded by the Purkinje cells. Climbing fibre input from the inferior olive, on the other hand, serves as a teaching/error signal, by modulating the synapses between parallel fibres and Purkinje cells through long-term potentiation and depression (Albus, 1971; Kawato et al., 2021; Manto, 2009; Marr, 1969; Sanger et al., 2020). Importantly, while Masao Ito proposed a complementary role for the cerebellum, Marr and Albus attributed a holistic role to the cerebellum in motor control, meaning that the cerebellum can control movements by itself (Kawato et al., 2021).

Universal Transform Theory

As detailed above, cerebellar damage does not only result in deficits in the motor but also several non-motor domains. Jeremy Schmahmann (1998) had proposed that non-motor deficits might present similar to motor deficits, relating the motor symptom *dysmetria* to the cognitive domain (‘Dysmetria of Thought’). In terms of functionality, this would mean that the cerebellum generates and updates internal models for motor and non-motor functions in a similar way (Guell et al., 2018; Popa & Ebner, 2022). Several findings have supported this assumption. One main line of support for universal cerebellar transform comes from the relatively homogeneous cytoarchitecture: despite the finding that cerebellar areas show distinct functionality pertaining to modality (e.g., anterior cerebellum with more sensorimotor functions, posterior lobe with more cognitive functions), the cytoarchitecture in the cerebellum

proves relatively unchanging across these areas (Ashida et al., 2018; Guell et al., 2018; Popa & Ebner, 2022; Schutter, 2021b). Additionally, deficits resulting from damage to the cerebellum appear relatively similar across domains, as they do not hamper the execution of movements/cognitive processes themselves but instead make them less precise (Guell et al., 2018; Schmahmann, 1998).

Multiple Functionality Theory

However, Orban de Xivry & Diedrichsen (2024) could show that the input to the cerebellum via both mossy and climbing fibres as well as the cerebellar output could change based on task demands. They proposed that it might not be possible to relate the cerebellar function to a single model of computation. This further built on the hypothesis of multiple functionality of the cerebellum, proposed by Diedrichsen et al. (2019). Diedrichsen and colleagues proposed that while the cerebellum may have uniform circuits, the underlying computations might differ. They note important differences between domains in task-based activity and functional connectivity to the cerebrum and propose that instead of looking at non-motor functions through the lens of sensorimotor computations, it might be more productive to examine these functions separately. They thus do not exclude a universal transform (Diedrichsen et al., 2019).

Reinforcement Learning

Behavioural patterns in cerebellar disease/disruption

Not many studies have been conducted on the potential deficits of patients with cerebellar damage in reinforcement learning. As outlined in a recent review by Berlijn et al. (2024), some initial studies showed no deficits in patients with cerebellar damage (Berlijn et al., in press; Dirnberger et al., 2010; Rustemeier et al., 2016; Turner et al., 2007) while others did (Mak et al., 2016; Mukhopadhyay et al., 2007; Nicholas et al., 2024; Thoma et al., 2008). There is thus yet no sufficient evidence for a clear behavioural correlate of cerebellar damage/disruption in reinforcement learning.

Neuroimaging findings

A recent meta-analysis conducted by Kruithof et al. (2023) examined cerebellar activations associated with reward anticipation and reward outcome. They reported activations in the anterior lobe, lobule VI, left Crus I and the vermis for reward anticipation, in conformity with the suspected role of the cerebellum in predictive processes. A recent systematic review by Berlijn et al. (2024) examined findings with a focus on studies employing feedback learning paradigms, independently of whether they examined reward anticipation or outcome. This allowed for examination of more specific effect patterns. Consistent with the meta-analysis by Kruithof et al., they found that feedback/outcome valence is related to activations in lobule VI (Peterburs et al., 2018; Tricomi & Fiez, 2008). Crus I and II seemed to be specifically related

to feedback learning (Balsters et al., 2013; Balsters & Ramnani, 2011). Crus I also seemed to play a role in switching behaviour within a study using reversal learning in addition to simple reinforcement learning (Peterburs et al., 2018). As noted above, cerebellar activations were also found for unsigned RPE processing in a large meta-analysis examining RPE activations (Corlett et al., 2022). Notably, several difficulties present when examining the cerebellum using fMRI: cerebellar blood flow changes are dominated by synaptic mossy fibre input to the granule cells, which is input-related activity (Diedrichsen et al., 2019). fMRI studies examining the cerebellar cortex thus show mainly the input rather than the output of the cerebellar cortex (Diedrichsen et al., 2019).

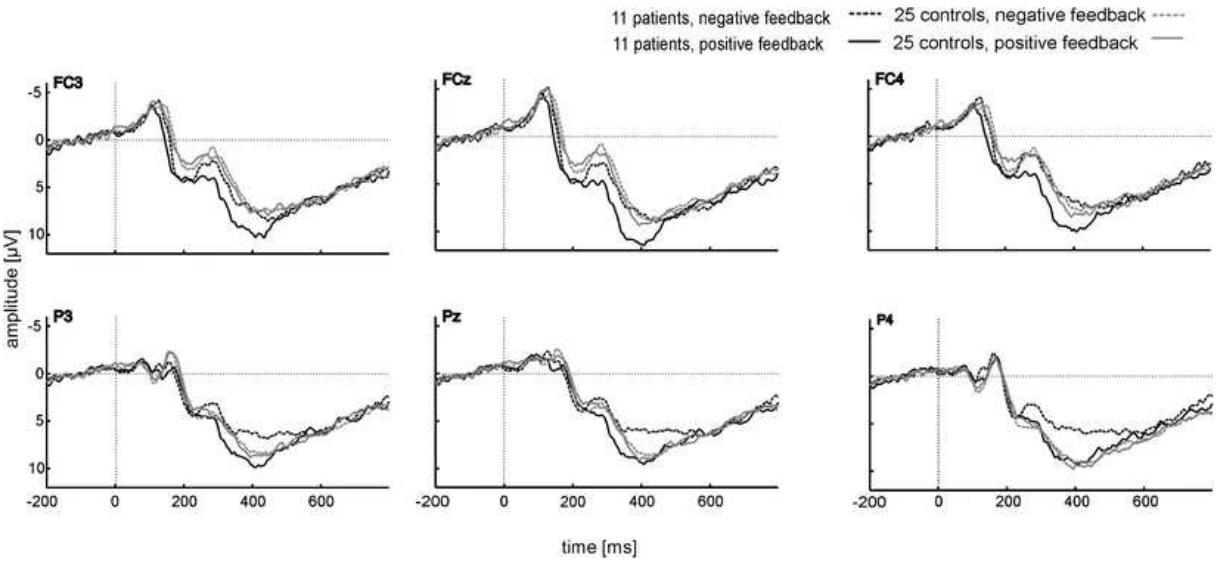

Figure 6. Feedback-locked grand-average ERPs for positive and negative feedback in the fractal task by Rustemeier et al. (2016). ERPs are given separately for patients with cerebellar stroke and healthy controls. Reproduced with permission from Springer Nature.

To my knowledge, there are yet no studies showing feedback processing in fMRI in patients with cerebellar damage. However, an initial study using EEG showed altered feedback processing in a small sample of patients with cerebellar stroke (Rustemeier et al., 2016). Rustemeier et al. (2016) employed a fractal task while measuring EEG in patients with cerebellar stroke and healthy controls. Within the fractal task, participants were able to choose between two fractals to receive a monetary reward or punishment. The chance to receive either feedback, was however at 50 % for all fractals, and learning was thus not possible. Examining the FRN, they found a differentiation between positive and negative feedback in the patients but not controls. The authors interpreted the effect as increased surprise in the patients: the differentiation between positive and negative feedback in FRN should be low as both feedback valences were of similar expectancy (following the hypothesis of Alexander & Brown, 2011). In the control group, this was likely the case, resulting in an overall non-significant difference in FRN. For the patients with cerebellar stroke, negative feedback resulted in a higher FRN than

positive feedback, indicating that the differentiation was stronger than in controls. The authors reasoned that feedback might have seemed more surprising for patients, resulting in an enhanced positive-negative differentiation in FRN. This argument is consistent with the dysmetria of thought hypothesis (Schmahmann, 1998), relating cerebellar dysfunction to an overshoot (hypermetria) of a cognitive action, i.e., in this case, salience/surprise. However, as no follow-up analyses or experiments regarding changes in feedback frequency/task progression were conducted, this conclusion remains unconfirmed.

Performance Monitoring Framework

The cerebellum has been implicated in reinforcement learning in terms of performance monitoring only rather recently, such as by Peterburs and Desmond (2016). Performance monitoring is an umbrella term capturing all processes necessary to enable flexible adjustments in constantly changing environments. This encompasses (1) feedback processing, (2) error detection, (3) inhibition of conflicting responses, (4) attentional control, and (5) emotional regulation (Peterburs & Desmond, 2016). Several lines of evidence support this argument: concerning (1), as detailed above, there have been several findings of cerebellar activation in feedback and RPE processing in fMRI, and initial studies showing deficits in reversal learning and feedback processing in patients with cerebellar stroke. Regarding (2), patients with cerebellar stroke and degeneration showed deficits in error processing in response conflict tasks (Peterburs et al., 2012, 2015). As for (3), patients with cerebellar lesions (stroke and surgical) showed deficits in response inhibition in Stroop and Go/Nogo tasks (Brunamonti et al., 2014; Neau et al., 2000). In regards to (4), patients with cerebellar lesions (stroke and surgical) also showed deficits in both attention and working memory tasks (Craig et al., 2021; Gottwald et al., 2003; Ilg et al., 2013; Ravizza et al., 2006). Concerning (5), patients with cerebellar lesions also showed mal-adjusted reactions towards (in particular *negative*) emotions, such as missing increases in flow velocity in the left middle cerebral artery towards negative stimuli (Adamaszek et al., 2017; Lupo et al., 2015), and deficits in the acquisition (in rats: Lopiano et al., 1990) and potentiation of startle response (Maschke et al., 2000). Taken together, there seems to be a strong basis for a role of the cerebellum in performance monitoring, including feedback processing/reinforcement learning (Peterburs & Desmond, 2016).

Recent findings in rodents

In recent years, rodent and primate studies have investigated reward-related information processing in granule cells, climbing fibres and Purkinje cells more in-depth. Findings consistent with a coding of RPEs were reported in several complementary studies. Wagner et al. (2017) investigated this in granule cells of rodents using calcium imaging. They found that separate granule cell populations code reward delivery, reward omission, and reward

anticipation. The findings were not explainable with licking behaviour (that also increases upon reward anticipation and delivery) or sensory input. The signals also showed dynamics across the task that one would expect from reinforcement learning signals: in the beginning, more activity related to reward delivery was found, while later in the task – when expectancies had formed – activity related to reward anticipation and omission was found. The findings could also be replicated across classical and operant conditioning (M. J. Wagner et al., 2017). Similarly, climbing fibre input into Purkinje cells as measured with complex spike activity was found to be consistent with unexpected reward delivery, omission, and anticipation (Heffley et al., 2018; Heffley & Hull, 2019; Kostadinov et al., 2019; Vignali et al., 2024). Interestingly, the signal increased toward both unexpected reward delivery (positive RPE) and omission (negative RPE), hinting at an unsigned RPE signal. However, a signed RPE in the cerebellum could be shown in at least one study using aversive instead of rewarding stimuli: Ohmae and Medina (2015) found that complex spike activity increased towards unexpected punishments (air puffs) but decreased below baseline towards unexpected punishment omission. This finding might indicate different RPE signalling in the cerebellum towards rewards and punishments.

These studies, however, all relate to the input of and internal processing within the cerebellum. What about the cerebellar output? Is the RPE input of the cerebellum used to drive RPE processing in cerebral areas? Initial studies in rodents showed that this might be indeed the case: projections from the cerebellum to the VTA and SN contain reward-related information (Carta et al., 2019; Washburn et al., 2024; J. Yoshida et al., 2022; T. Yoshida et al., 2024). Carta et al. (2019) could further show that stimulation of this (monosynaptic) pathway was suitable to induce short- and long-term place preference; optogenetic inhibition was, however, not aversive.

Regarding the wealth of new upcoming studies in rodents, the question emerges whether findings are indeed replicable in humans.

Research Objective

The aim of this dissertation was to further comprehend the role of the cerebellum in performance monitoring, and in particular error and feedback processing. Causal evidence was gathered investigating whether the cerebellum is required for performance monitoring. In all studies, a lesion approach was combined with EEG recordings of the cerebrum to derive whether damage/disruption of the cerebellum results in deficits in performance and changes in neural processing.

Feedback processing was investigated within a reinforcement learning task in Manuscript 1, using the FRN as an index of RPE processing within the cerebrum. Two parallel lesion

approaches were used: Experiment 1 used patients with chronic cerebellar stroke and matched controls; Experiment 2 applied cerebellar and control single-pulse transcranial magnetic stimulation (spTMS) in healthy young adults. TMS was used to induce 'virtual lesions': spTMS induces action potentials, and its effect has been characterised as excitatory or inhibitory depending on various factors, both on the neuron population and the single neuron level (Hannah et al., 2020; Romero et al., 2019). Its inhibitory effect on neuron populations is theoretically based on noise models, meaning that the TMS pulse induces noise in the target region (Harris et al., 2008). For the cerebellum, an inhibitory effect of spTMS has been assumed (Desmond et al., 2005; Schutter & van Honk, 2006; Viñas-Guasch et al., 2023; for a review see Fernandez et al., 2020).

Manuscript 2 investigated error processing within reinforcement learning contexts. Data from Experiment 2 in Manuscript 1 were re-analysed, focussing on error instead of feedback processing. The ERN was thus analysed, as well as the error positivity (Pe) which is an ERP component in the error-related signal that peaks later – at around 200-400 ms – and predominantly at parietal sites (Falkenstein et al., 1991; Wessel, 2012). The Pe is more strongly related to conscious error processing and error awareness (Nieuwenhuis et al., 2001; Ridderinkhof et al., 2009).

Last, Manuscript 3 dealt with the temporal aspect of disruption caused by cerebellar TMS in relation to cortical processing: spTMS was applied at a wider range of timings around individual ERN latencies in a response conflict paradigm (Go/Nogo Flanker task). The study aimed at finding differences in effectiveness of cortical disruption depending on TMS timing.

Overview of Studies

Manuscript 1 – The cerebellum contributes to prediction error coding in reinforcement learning in humans

Introduction and hypotheses

A cerebellar role in reinforcement learning has been initially investigated in patients with chronic cerebellar stroke (Rustemeier et al., 2016; Thoma et al., 2008). Recent studies in rodents found further evidence for cerebellar involvement in reinforcement learning, with signals related to reward anticipation, omission, and RPEs (Kostadinov & Häusser, 2022). Further animal studies indicated that these signals are conveyed to the cerebrum (Washburn et al., 2024; J. Yoshida et al., 2022; T. Yoshida et al., 2024). However, this has not yet been shown in humans, and there is an additional need for causal evidence to answer the question whether the cerebellum is required for RPE processing in extra-cerebellar (cerebral) regions traditionally associated with reinforcement learning. Two previous studies could show deficits in behavioural flexibility in patients with cerebellar damage (Nicholas et al., 2024; Thoma et al., 2008), and one study could show changes in neural processing of feedback in reinforcement learning in patients with chronic cerebellar stroke (Rustemeier et al., 2016).

Manuscript 1 aimed to contribute to the question whether the cerebellum is necessary for intact reinforcement learning and cortical RPE processing in humans. To this end, two separate experiments were conducted: in Experiment 1, patients with a chronic stroke restricted to the cerebellum and healthy controls performed a probabilistic feedback learning task while cerebral EEG was recorded. As detailed above, the frontocentral ERP component FRN can serve as a measure of cerebral RPE processing. In case the cerebellum contributes to cerebral RPE processing, RPE effects in FRN should be altered in patients with cerebellar damage (in this case, stroke) while it should be intact in the matched healthy controls. Experiment 2 was performed analogously in healthy young controls. In two separate sessions, they underwent single-pulse cerebellar TMS and control stimulation (i.e., TMS applied to the vertex) while performing the task. Following the same reasoning, participants should show deficits in RPE processing in FRN under cerebellar stimulation, while they should show intact RPE processing in FRN under control stimulation. In detail, the following was expected:

1) A general main effect in terms of increasing accuracy with task progression/ascending block number was expected (ME block).
    a. For Experiment 1, no differences between patients and controls were expected due to compensatory mechanisms available in chronic stroke, consistent with Rustemeier et al. (2016).

b. For Experiment 2, worse learning was expected when participants received cerebellar compared to vertex TMS. This was due to long-term compensatory processes – such as for chronic cerebellar stroke patients – not being available in spTMS, as stimulation is instantaneous. Instead, it was expected that behavioural performance might rather follow the pattern observed in patients with cerebellar degeneration (i.e., decreased performance), such as in response conflict paradigms (Peterburs et al., 2015; IE block x stimulation site).

2) A general effect of RPE on FRN was expected in terms of a main effect of feedback valence and RPE, respectively, as well as an interaction between feedback valence and unsigned RPE. FRN should be *enhanced* with increasing *negative* RPEs and *decreased* with increasing *positive* RPEs (ME feedback valence; ME RPE; IE feedback valence × RPE).
    a. For Experiment 1, it was expected that this effect is decreased in patients with cerebellar stroke, but intact in healthy controls (IE feedback valence × RPE × group).
    b. For Experiment 2, it was expected that this effect is decreased when healthy participants received cerebellar TMS but intact when they received vertex TMS (IE feedback valence × RPE × stimulation site).
3) In Experiment 1, lesion symptom mapping was performed in patients to investigate whether deficits in processing or behaviour in the reinforcement learning task can be related to certain lesion locations in the cerebellum. A relation between deficits and more posterolateral regions, in particular Crus I and II was expected, as these areas are more strongly related to higher cognitive processes.

Method

Participants

Experiment 1 was conducted in patients with chronic cerebellar stroke. Data from twenty-six patients entered the analyses. On average, experiments were conducted 8.4 years post-stroke (*SD* = 6.0 years; range from 1.5 months to 22 years). The majority of patients were men (20 men, 6 women) and middle-aged (*M* = 56.2 years, *SD* = 12.1 years). Patients with extracerebellar lesions, or who reported current psychiatric disease, current or past neurological disease, intake of medicine affecting the central nervous system, or alcohol or illicit drug abuse were excluded. Lesions were mostly in the posterolateral cerebellum, with most strokes within the PICA territory (PICA: 21 patients; SCA: 3 patients; PICA and SCA: 2 patients). Twenty-six healthy controls were matched to patients in age, sex, education, handedness, IQ, and depression indices. To match three patients with a diagnosis of major depression and intake of antidepressants, three controls with a clinical diagnosis of major

depression, antidepressant medication, and a roughly matched depression index entered the analysis.

Experiment 2 was conducted in healthy young adults. Data from twenty-four participants entered the analysis. Participants were mostly female (17 women, 7 men) young adults (*M* = 23.3 years, *SD* = 2.9 years), with an average IQ (*M* = 103.5, *SD* = 15.4) according to the Mehrfachwahl-Wortschatz-Test-B (Merz et al., 1975).

Procedure

Both Experiment 1 and 2 were conducted on two separate days. For Experiment 1, different task versions were tested in separate study sessions. For Experiment 2, different stimulation sites were targeted in separate study sessions.

In both experiments, a probabilistic feedback learning task was used (confer Bellebaum & Colosio, 2014; Eppinger et al., 2008). After a fixation cross, participants saw abstract stimuli and were instructed to press either the left or right button in response. The response time window in Experiment 1 was 3000 ms and 1000 ms in Experiment 2 (with the stimulus visible for half the duration). The higher response time window in Experiment 1 was due to the older age of the participants, as well as potential motor deficits in patients with cerebellar damage. The response was highlighted for 200 ms, followed by a feedback delay. The feedback was then presented for 1000 ms ('+20 ct' for positive feedback and '-10 ct' for negative feedback). For Experiment 1, two versions of the task were conducted: one version with a feedback delay of 500 ms, and another version with a delay of 6500 ms. Experiment 2 only used the 500 ms delay. Feedback was provided probabilistically. Two stimuli had contingent feedback that was thus learnable for participants (90-10 contingency for Experiment 1 and 80-20 contingency for Experiment 2). This meant that when pressing the correct one of the two buttons, positive feedback was given with a higher chance than negative feedback, but not in 100 % of the cases (and vice-versa for incorrect responses). Two other stimuli had random feedback that was thus not learnable (50-50 contingency). Participants were instructed to learn by trial and error how to gain more positive and less negative feedback.

For Experiment 2, spTMS was added to the procedure. The motor threshold was determined before the experiment and based on motor-evoked potentials measured at the hand using electromyography. Stimulation was conducted at 120 % of the motor threshold, and at the left cerebellum (1 cm below and 3 cm to the inion) and at the vertex (electrode position Cz) in separate sessions. Vertex is a common control site, particularly in experiments using cerebellar stimulation (Gatti et al., 2023). A Magstim double cone coil and a Magstim BiStim^2 unit (Magstim Co., Whitland, United Kingdom) were used for TMS.

EEG recording

EEG was recorded in both experiments. In Experiment 1, EEG was recorded at 1,000 Hz from 28 active Ag/AgCl electrodes (F7, F3, Fz, F4, F8, FC5, FC1, FC2, FC6, T7, C3, Cz, C4, T8, CP5, CP1, CP2, CP6, P7, P3, Pz, P4, P8, PO9, O1, Oz, O2, PO10) using the 10-20 system (Chatrian et al., 1985). AFz was used as a ground electrode, and FCz served as the online reference. Electrodes were placed on the mastoids to be used later as offline references. An additional electrode was placed to the left outer canthus of the left eye as the horizontal electrooculogram (hEOG), and Fp1 was used as the vertical electrooculogram (vEOG).

In Experiment 2, EEG was recorded at 1,000 Hz from 30 passive Multitrode electrodes (Fp1, Fp2, F7, F3, Fz, F4, F8, FC5, FC1, FC2, FC6, T7, C3, Cz, C4, T8, CP5, CP1, CPz, CP2, CP6, P7, P3, Pz, P4, P8, O1, Oz, O2, Iz) using the 10-20 system. AFz was used as a ground electrode, and FCz served as the online reference.

EEG preprocessing

Preprocessing for Experiment 1 was conducted within Brain Vision Analyzer software (version 2.2, Brain Products GmbH, Gilching, Germany). Data were first re-referenced to the mastoid electrodes, and FCz was restored as an active electrode. Next, a direct current drift correction was performed followed by a band-pass (high-pass: 1 Hz; low-pass: 30 Hz) and notch filter (50 Hz). Vertical and horizontal eye movement artefacts were removed based on the vEOG and hEOG using the semi-automatic Ocular Correction ICA implemented in the Brain Vision Analyzer. Data were then segmented around feedback markers, beginning from 200 ms before and ending 600 ms after the marker. A baseline correction was performed using the 200 ms directly before the feedback. An automated artefact rejection followed, excluding segments with a voltage step above 50 µV/ms, an amplitude exceeding 100 µV or below -100 µV, or activity not exceeding 0.1 µV. On average, 1.1 % of segments (*SD* = 2.5 %) were rejected. Single-trial ERPs were then exported via a generic data export.

Experiment 2 required a more extensive preprocessing due to artefacts from the TMS pulse. The ARTIST algorithm by Wu et al. (2018) was thus used. The algorithm included a direct current drift correction, removal of the TMS pulse artefact, removal of the pulse decay artefact via ICA, followed by a band-pass (high-pass: 1 Hz; low-pass: 30 Hz) and notch filter (50 Hz). After segmentation around the TMS pulse, ARTIST rejected segments containing movement artefacts (*M* = 2.8 % of segments, *SD* = 2.6 %) and interpolated bad channels (*M* = 0.96 channels, *SD* = 1.15 channels). A second ICA was used to remove bad independent components, and the signal was re-referenced to an average reference, restoring FCz as an active electrode. The time window between 300 and 100 ms preceding the TMS pulse was used for a baseline correction. Further preprocessing was conducted within the Brain Vision Analyzer. Data were then segmented around the feedback onset starting from 200 ms

preceding to 500 ms after the feedback marker. An additional baseline-correction was conducted using the time window from 200 ms before to feedback onset. Single-trial ERPs were exported via a generic data export.

Peak detection for the FRN was conducted using MATLAB and performed on the individual averages per condition (for Experiment 1: feedback valence [negative, positive] × feedback delay [short, long]; for Experiment 2: feedback valence [negative, positive] × stimulation site [cerebellum, vertex] × TMS timing [post-stimulus, pre-feedback]). FRN was quantified as the local maximal negative peak in the time window between 200 and 350 ms post-feedback at FCz (Sambrook & Goslin, 2015). Within the single-trial data, the mean amplitude in the time window of 40 ms around the corresponding FRN latency was then extracted and used in the analyses (Meadows et al., 2016).

Prediction error estimation

Concurrent with previous studies (Fischer & Ullsperger, 2013; Ichikawa et al., 2010; McDougle et al., 2019), RPE were estimated based on participants' responses and received feedback using a Rescorla-Wagner model (see general introduction for an in-depth explanation). Response probabilities were modelled using a softmax function (Boltzmann, 1868; Sutton & Barto, 2018c). The probability of the chosen action *p* was estimated using the estimated action value *Q* for action *a* and trial *t*:

$$p_{a_1,t} = \frac{e^{\beta * Q_{a_1,t}}}{e^{\beta * Q_{a_1,t}} + e^{\beta * Q_{a_2,t}}}$$

As parameters, a learning rate α per feedback valence, and an inverse temperature (exploration parameter) β were estimated using the function *fmincon* implemented in MATLAB.

Data analysis

Data were analysed in R (version 4.2.3). Only trials with learnable feedback (i.e., contingent feedback) were included in the analyses. Choice accuracy was analysed via ANOVAs with the within-subject factors feedback delay (short, long) and block (1-8) and the between-subject factor group (controls, patients) for Experiment 1 and the within-subject factors stimulation site (vertex, cerebellum), TMS timing (post-stimulus, pre-feedback), and block (1-6) for Experiment 2.

For all other choice switching and ERP analyses, linear mixed effects (LME) models were used via the packages lme4 (version 1.1-32; Bates et al., 2015) and lmertest (version 3.1-3; Kuznetsova et al., 2017). For choice switching in Experiment 1, the within-subject factors feedback valence (negative, positive), response type (false, correct), feedback delay (short, long), and block (1-8) as well as the between-subject factor group (controls, patients) were

included as fixed effects. For choice switching in Experiment 2, the within-subject factors feedback valence, response type, stimulation site (vertex, cerebellum), TMS timing (post-stimulus, pre-feedback) and block (1-6) were included as fixed effects.

For the FRN in Experiment 1, the within-subject factors feedback valence, feedback delay, and the unsigned RPE as well as the between-subject factor group were included as fixed effects. For the FRN in Experiment 2, the within-subject factors feedback valence, stimulation site, TMS timing, and the unsigned RPE were included as fixed effects.

For random effects, a maximal fit was attempted including all within-subject factors and an intercept per subject but in case of singular fit, lower interaction levels were removed stepwise (starting with main effects) until fit and convergence was ensured. Outliers were detected using Cook's distance (Cook, 1977) and subjects exceeding the criterion of $4/(n\text{-}p\text{-}1)$ were excluded. Interactions were resolved via simple slope analyses, using Bonferroni correction according to the number of slopes.

Lesion symptom mapping

For Experiment 1, an analysis of the additionally acquired structural MRI data was conducted. To this end, a 3D T1-weighted magnetisation-prepared rapid acquisition gradient-echo (MPRAGE) sequence was acquired on the first study session using a MAGNETOM Vida 3T system (Siemens Healthcare, Erlangen, Germany) and a 64-channel head coil (voxel size = 1 × 1 × 1 mm). For 5 patients for whom an MR scan was not possible, existing structural MR images were used.

After confirming no extracerebellar lesions, cerebellar lesions were manually traced on non-normalised T1 images previously aligned to the AC-PC line and saved as regions of interest within MRIcron (https://www.nitrc.org/projects/mricron). The cerebellum was subsequently isolated, and datasets were segmented using the function *suit_isolate_seg* provided by the spatially unbiased atlas template of the cerebellum (SUIT) toolbox (https://www.diedrichsenlab.org/imaging/suit.htm). Isolation masks were visually inspected and manually corrected if necessary. Next, datasets were normalised using the function *suit_isolate_mask* with the lesion mask as optional input, and lastly transformed into SUIT space using the function *suit_reslice* (Diedrichsen, 2006).

Voxel-based lesion symptom mapping (vbLSM) was performed via NPM which is implemented in MRIcron (Stoodley et al., 2016; Timmann et al., 2022). vbLSM tests for each voxel if there is a significant difference in a parameter of interest between patients with this voxel affected and patients with this voxel unaffected. As a parameter of interest, the difference FRN (high RPE – low RPE for negative valence) was chosen post-hoc, as differences between patients

and controls were found. The probabilistic atlas of the human cerebellum (Diedrichsen et al., 2009, 2011) was used to define affected lobule and nuclei.

Results and Discussion

As hypothesised, cerebellar lesions (Experiment 1) and cerebellar disruption (Experiment 2) decreased RPE coding in the FRN. While a significant effect of RPE for negative feedback could be found for the control group in Experiment 1 and the control stimulation in Experiment 2, this effect was non-significant for patients with chronic cerebellar stroke (Experiment 1) and when healthy participants received cerebellar stimulation (Experiment 2). Concerning behaviour, only minor changes were found, which was expected for Experiment 1 but not Experiment 2.

RPE coding was found in healthy controls (Experiment 1) and control stimulation (Experiment 2) only for negative feedback, consistent with previous studies that found RPE coding in FRN only or at least stronger for negative feedback (Chase et al., 2011; Hoy et al., 2021; Rawls & Lamm, 2021; but also see Cavanagh, 2015; Weber & Bellebaum, 2024). Importantly, RPE coding for patients (Experiment 1) and cerebellar stimulation (Experiment 2) was non-significant. This finding closely followed our hypotheses. Previous studies in healthy adults had also found an enhanced FRN with increasing negative RPE (Burnside et al., 2019; Chase et al., 2011; Fischer & Ullsperger, 2013; Frömer et al., 2021; Hoy et al., 2021; Humann et al., 2020; Kirschner et al., 2022; Rawls & Lamm, 2021). An absence of this RPE coding in FRN for cerebellar lesions/disruption indicates that the cerebellum is required for intact RPE coding. This is consistent with studies in animals that found signals appearing as RPE computation in the cerebellum as well as projections of such signals from the cerebellum to cerebral areas (Heffley et al., 2018; Heffley & Hull, 2019; Kostadinov et al., 2019; M. J. Wagner et al., 2017; Washburn et al., 2024).

Of note, the non-significant RPE effect in patients/cerebellar stimulation seemed to have resulted from an increase in FRN amplitude towards low RPEs instead of a decrease towards high RPEs. This points to an over-activation instead of an under-activation, potentially indicative of inappropriate surprise/salience towards expected feedback. This is consistent with a previous study (Rustemeier et al., 2016) that found increased negative-positive differentiation in the FRN in patients with cerebellar stroke, which was interpreted as an excessive surprise signal.

The vbLSM yielded that the decreased RPE differentiation in the FRN in Experiment 1 was connected to strokes within the posterolateral cerebellum, and in particular Crus I and II, lobule VIIb, and VIIIa. This is consistent with the hypothesis that deficits would be more strongly related to the posterolateral cerebellum and in particular Crus I and II. When comparing these

regions to functional atlases of the cerebellum, they overlap with working memory, default mode network, and spatial rotation (Nettekoven et al., 2024), which are all functions relevant for the performed task.

Considering the strong effect that cerebellar damage/disruption had on RPE processing in FRN, it seems unexpected that only minor changes were found in behaviour, with no deficits in learning performance and minor differences in choice switching that, however, did not affect overall learning success. First, deficits in reinforcement learning under cerebellar damage/disruption do not appear to be common, with most studies reporting no deficits in acquisition learning (Kruithof et al., 2025; Rustemeier et al., 2016; Thoma et al., 2008). Deficits seem to be rather related to behavioural flexibility (Kruithof et al., 2025; Nicholas et al., 2024; Thoma et al., 2008) which is also the domain where we found minor changes (choice switching). Second, the FRN does not have a strong behavioural correlate (Ullsperger, 2024). The likely generator of the FRN, the ACC, was shown to be essential for action-outcome learning but not stimulus-outcome learning (Camille et al., 2011; Rudebeck et al., 2008). The presentation of choices on screen in addition to selection of actions via button press might have sufficed to enable stimulus-outcome learning via other brain areas. A potential candidate for these compensatory processes might be the OFC which was shown to be essential for stimulus-outcome learning but not action-outcome learning (Camille et al., 2011; Rudebeck et al., 2008). However, since we did not measure indices of OFC, this notion cannot be confirmed conclusively. The FRN itself was connected to behavioural flexibility in studies with a more dynamic environment (M. X. Cohen & Ranganath, 2007; Fischer & Ullsperger, 2013; Kirschner et al., 2022; but also see Chase et al., 2011). However, in an exploratory analysis, we were able to relate only P3 but not FRN to choice switching (see Table 11); the task might not have been dynamic enough in the current study.

While the RPE effect in controls in Experiment 1 followed the expected direction, i.e., an enhanced FRN for high negative compared to low negative RPEs (Sambrook & Goslin, 2015), the direction of the effect was unexpectedly reversed for the control stimulation in Experiment 2. A likely explanation seems to be that vertex TMS affected processing, even though it is a common control site. At least one study (Jung et al., 2016) could show that vertex TMS reduced ACC activation. The control stimulation thus likely did not succeed as a control condition. Noteworthy, however, is that the findings in the cerebellar stimulation in Experiment 2 still replicated the findings in the patients in Experiment 1.

Conclusion

The findings point to a reliance of RPE processing in FRN on cerebellar output. Cerebellar damage and disruption led to non-significant RPE effects in FRN, while negative RPE was reflected in FRN for control participants and control stimulation. The pattern was consistent

across two studies with different lesion methods (stroke and spTMS). Behavioural performance was largely unaffected except for minor differences in behavioural flexibility. This study adds to a growing body of evidence indicating that the cerebellum processes RPEs and conveys these signals to other brain areas, further showing that this signal is required for RPE processing in FRN.

Manuscript 2 – Cerebellar single-pulse TMS differentially affects early and late error processing in reinforcement learning

Introduction and hypotheses

Feedback processing is an important aspect of reinforcement learning, and essential for the updating of action values to make better decisions. However, similar to response conflict tasks, response errors can be processed already at the stage of the response, when the feedback in the trial has not yet been provided. This requires an understanding of whether a specific response is correct or an error, which usually happens in later stages of reinforcement learning. Previous studies could show a shift in processing through the course of learning, with feedback-dominant processing in initial stages and error-dominant processing in later learning stages (Bellebaum & Colosio, 2014; Eppinger et al., 2008). Naturally, participants need to rely on feedback processing in initial stages as the correct response is unknown and needs to be found out via trial and error. Errors are committed because the correct answer is unknown, requiring participants to wait for the feedback to know whether their response was correct. In later stages, after several repetitions, however, an understanding of correct responses and errors should be acquired. Error rates should decrease, and errors are committed less commonly due to uncertainty and more commonly by accident/slips of attention. Participants at this stage know the correctness of responses at the time of response instead of needing to wait for the feedback. Concurrent with this, stronger processing can be found in error processing indices at later learning stages, such as the ERN (Bellebaum & Colosio, 2014; Eppinger et al., 2008).

Following the finding in Manuscript 1 that cerebellar disruption impacts RPE processing in the FRN in reinforcement learning, the question arose whether this is also the case for error processing in the ERN in reinforcement learning. Importantly, while feedback processing in FRN was disrupted, reinforcement learning was unaffected by cerebellar TMS, enabling error processing in later stages of the task. The ERN and FRN are closely connected in their function in performance monitoring as well as the neural generator (Hauser et al., 2014; Herrmann et al., 2004; Holroyd & Coles, 2002; Miltner et al., 1997; Roger et al., 2010; San Martín, 2012; Wessel, 2012), making a similar impact of cerebellar disruption more likely. While previously, Peterburs et al. (2012, 2015) could show that cerebellar deficits impact error processing in the ERN in response conflict tasks, it is unclear whether this is also the case for error processing in reinforcement learning contexts. The ERN is not often investigated in reinforcement learning task (see, e.g., Chase et al., 2011; Höltje & Mecklinger, 2020; Peterburs et al., 2016; Rustemeier et al., 2016; Weismüller & Bellebaum, 2016).

Manuscript 2 comprised a reanalysis of Experiment 2 of Manuscript 1: instead of feedback-related signals, the response-locked signals in the probabilistic feedback learning task were investigated. This re-analysis followed the findings by Peterburs et al. (2012, 2015) in *response conflict tasks*, which found impaired error processing in patients with cerebellar stroke or degeneration in the ERN. A later component, the Pe, which is more closely related to error awareness, was also investigated (Falkenstein et al., 1991; Nieuwenhuis et al., 2001; Ridderinkhof et al., 2009; Wessel, 2012). In Manuscript 2, we addressed the question whether error processing would also be impaired in *reinforcement learning tasks*. ERN and Pe were analysed. Effects were expected to follow the findings of Peterburs et al. (2015) in patients with cerebellar degeneration. In detail, the following was expected:

1) The ERN was expected to be increased for errors over correct responses (ME response type).
    a. We expected this effect to become larger with progressing learning, i.e., with increasing trial number, as participants do not have a representation of choice correctness at the beginning of the task (IE response type × trial number).
    b. We expected the interaction effect between response type and trial number to also be modulated by stimulation site: while the interaction effect should be intact for vertex TMS, the effect should be reduced for cerebellar TMS (IE response type × trial number × stimulation site).
2) The Pe was expected to be increased for errors over correct responses (ME response type).
    a. We expected this effect to become larger with progressive learning, i.e., with increasing trial number (IE response type × trial number)
    b. We did not expect any interactions between response type, trial type, and stimulation site. A change in Pe had previously been reported by Peterburs et al. (2012) for patients with chronic cerebellar stroke and interpreted as reflecting a compensatory mechanism. As spTMS only creates transient virtual lesion which should not allow for long-term compensatory mechanisms, we did not expect such a change under cerebellar TMS.

Method

As Manuscript 2 constituted a re-analysis of data from Experiment 2 in Manuscript 1, sample characteristics, procedure and EEG recording are given in the Methods section of Manuscript 1.

EEG preprocessing

EEG preprocessing closely followed the description for Experiment 2 in Manuscript 1 up to the segmentation around the feedback markers. Instead, segmentation was placed around the

response markers, starting 200 ms before and ending 500 ms post-response. A baseline correction was performed based on the interval from 200 to 100 ms before the response. Single-trial data were exported using a generic data export.

Peak detection for the ERN and Pe was performed based on the individual averages per condition (response type [error, correct] × stimulation site [vertex, cerebellum] × TMS timing [post-stimulus, pre-feedback]). The ERN was defined as the maximal negative peak within the time window from response onset to 100 ms post-response at electrode FCz (Hajcak & Foti, 2008). The Pe was defined as the maximal positive peak within the time window from 200 to 400 ms post-response at electrode Pz (Larson et al., 2010). For the analysis, the mean amplitude in a time window around the determined latency was extracted from the single-trial data (20 ms for the ERN; 40 ms for the Pe; Albrecht & Bellebaum, 2023; Meadows et al., 2016).

Data analysis

Data analysis was conducted in R (version 4.2.3). LME analyses were conducted for both ERN and Pe, using the within-subject factors response type (error, correct), stimulation site (vertex, cerebellum), TMS timing (post-stimulus, pre-feedback), trial type and all interactions between these factors as fixed effects.

For random effects, a maximal fit was attempted including all within-subject factors and an intercept per subject but in case of singular fit, lower interaction levels were removed stepwise (starting with main effects) until fit and convergence was ensured. No outliers were detected using Cook's distance (Cook, 1977) and a criterion of $4/(n\text{-}p\text{-}1)$. Interactions were resolved via simple slope analyses, using Bonferroni correction according to the number of slopes.

Results and Discussion

The expected effect of cerebellar TMS on ERN could be confirmed, with a non-significant error-correct differentiation for cerebellar TMS while it was intact for vertex TMS late in the task. For the Pe, an unexpectedly increased error-correct differentiation could be found for post-stimulus cerebellar TMS compared to vertex TMS.

The effect pattern found in the ERN conforms to findings previously reported in patients with cerebellar stroke and degeneration in a response conflict task (Peterburs et al., 2012, 2015). This could indicate that the role of the cerebellum in error processing presents similar in response conflict and reinforcement learning contexts, further supporting its proposed function in overall performance monitoring (Peterburs & Desmond, 2016).

Unexpectedly, the result pattern closely followed the pattern reported in chronic stroke patients (Peterburs et al., 2012): while the ERN showed a decreased error-correct differentiation, the Pe showed an increased error-correct differentiation, and behavioural performance was intact.

This pattern was previously interpreted by Peterburs et al. (2012) as long-term compensation available to patients following stroke recovery. However, in the study at hand, spTMS was used to induce temporary disruption. This technique applies instantaneous disruption present for only a short duration, and, naturally, long-term compensation should thus not be possible.

Instead, short-term compensation might seem plausible, as the learning performance was intact. Such compensation might come at the disadvantage of being more effortful or a problem in fast-paced environments. However, it cannot be established whether this was truly the case in the current study; compensation could have taken place at several other times within the task, such as the inter-trial interval. An alternative explanation for the increased error-correct differentiation in the Pe might be dysmetria (i.e., over- or undershooting of a goal-directed movement). Schmahmann (1998) proposed that dysmetria might not only occur in the motor domain but also the cognitive domain in terms of a *dysmetria of thought*. The Pe might thus display an exaggerated perception of errors or salience, in terms of a hypermetria/an overshoot. The differences in effects of cerebellar disruption on ERN and Pe might lie in the nature of their neural generators: while both components have shown to be generated by the ACC, additional generators seem to contribute to the Pe (Hester et al., 2005; Overbeek et al., 2005). The spTMS applied to the cerebellum might affect these regions differently.

Notably, this was a re-analysis of data from Manuscript 1. Feedback processing in terms of RPE processing was therefore already impacted, and the question arises whether the disrupted feedback processing might have impacted error processing, e.g., via a misadjusted update of action values, leading to deficits in error recognition. However, the effect in both ERN and Pe appeared to be stronger after post-stimulus (i.e., pre-response) TMS (although only on trend level for ERN). This indicates that the disruption of error processing took place more locally at the response stage.

Of note, the Pe appeared to show a less pronounced positive peak in the grand averages compared to studies using response conflict tasks. While the Pe has oftentimes not been analysed in studies that employed reinforcement learning (Bellebaum & Colosio, 2014; Eppinger et al., 2008; Herbert et al., 2011; Pietschmann et al., 2008), it appeared to be less pronounced in studies that did (Unger et al., 2012; Zhuang et al., 2021); this might thus simply be a property of Pe in feedback-based tasks, potentially due to errors being more ambiguous compared to errors in response conflict tasks. However, a posterior positivity is clearly visible within the topographical plots of the difference signal for cerebellar post-stimulus TMS (see Supplementary Figure S3).

In parallel to Manuscript 1, problems with the vertex stimulation as a control condition need to be considered. While no impact on error processing was apparent in the analyses performed in Manuscript 2, the analyses in Manuscript 1 pointed to an effect of vertex TMS on FRN. FRN

and ERN are closely connected, both in function and neural generator (Balconi & Scioli, 2012; Herrmann et al., 2004; Oerlemans et al., 2025; Roger et al., 2010; San Martín, 2012; Wessel, 2012). Further replication is thus necessary to make sure that the findings are valid, even though the findings in ERN and Pe under vertex stimulation appeared to be normal (Bellebaum & Colosio, 2014; Falkenstein et al., 1991; Miltner et al., 1997).

Conclusion

The expected deficits in error-correct differentiation in ERN when participants received cerebellar TMS could be confirmed, in accordance with previous studies using response conflict paradigms. The general result pattern with decreased error-correct differentiation in ERN, increased error-correct differentiation in Pe, and intact learning appeared to be consistent with a previous finding in chronic stroke patients. The study further supports that the cerebellum plays a role in performance monitoring and is required for error processing.

Manuscript 3 – The effect of cerebellar TMS on error processing: A combined single-pulse TMS and ERP study

Introduction and hypotheses

Last, in Manuscript 3, the question of timing of cerebellar involvement was investigated. While in the motor domain, there is an established time window concerning communication from the cerebellum to the motor cortex (Ugawa et al., 1991), this is not established for the cognitive domain. TMS in Manuscript 1 and 2 was applied at 100 ms post-stimulus and 100 ms pre-feedback. However, these stimulation time points are rather arbitrary, as they are not based on previous findings. To investigate this question, more timings need to be examined. Therefore, for the third study, instead of a reinforcement learning task, a Go/Nogo Flanker task was employed. The Flanker task required participants to press a left or right button in response to an arrow presented on screen. Shortly before the relevant arrow was presented, flanking arrows were presented which mostly pointed in the same direction but in a small number of trials in a different direction. This thus induced a response conflict, as the response towards the flanking arrow was prepared and needed to be suppressed when the relevant arrow pointed in the opposite direction. In Nogo trials, the response had to be inhibited altogether. The task thus did not require learning. This offered the advantage of a more flexible shift in stimulation timings while still avoiding an unnecessarily long task duration, as stimulation times did not need to be locked to certain stimuli in the task. Stimulation times were adjusted to the individual error latency which was the sum of the individual median error response times and mean ERN latencies (thus the estimated time point of the ERN peak). This was calculated based off data of a short version of the task previously conducted. Stimulation was then applied either 100 ms before, 50 ms before, at, or 50 ms after this individual error latency. We expected the following:

1) We expected increased error rates for cerebellar TMS compared to vertex TMS, but only when stimulation is applied before the response (IE stimulation site × TMS timing).
2) We expected an increased ERN towards errors compared to correct responses (ME response type).
    a. We expected this effect to be reduced when receiving cerebellar TMS before the ERN (-100 and -50 ms TMS timing; IE response type × stimulation site × TMS timing).
3) We expected an increased Pe towards errors compared to correct responses (ME response type).
    a. We did not expect this effect to be reduced when receiving cerebellar TMS compared to vertex TMS.

Method

Participants

Data from sixteen participants entered the analysis. Participants were predominantly female (13 women, 3 men) young adults (*M* = 24.0 years, *SD* = 3.7 years) with an average IQ (*M* = 98.75, *SD* = 10.88).

Procedure

The task analysed was part of a series of tasks performed within the same session. After EEG and TMS preparation (see Experiment 2 in Manuscript 1), a pre-task was performed to determine the individual ERN latency (see below for more details). Next, the probabilistic feedback learning task presented in Manuscript 1 (Experiment 2) was performed. Last, participants completed a Go/Nogo Flanker task while receiving spTMS, of which data was analysed for Manuscript 3. Go trials, in which participants needed to react to the presented stimuli made up 80 % of trials, while Nogo trials, in which participants needed to inhibit their response made up 20 % of trials, with a total of 600 trials. In the beginning of each Go trial, flanking arrows were presented above and below a fixation cross, both pointing either to the right or left. After 200 ms, the fixation cross was replaced by the target arrow which pointed in the same direction of the flanking arrows in 80 % of Go trials (congruent trials) or in the other direction in 20 % of Go trials (incongruent trials). Participants were instructed to react to the target arrow by indicating whether it pointed in the left or right direction by pressing one of two buttons on a response box within the response time window of 350 ms (alternatively 400 ms in case the miss rate was too high in the pre-task). In Nogo trials, the fixation cross was instead replaced by a circle, indicating that participants should not press a button using the same response time window as for Go trials. Afterwards, a fixation cross was presented for 500 ms. The inter-trial interval was jittered between 900 and 1300 ms.

The setup of the TMS is detailed in Manuscript 1. Stimulation timings were determined based on the individual error latency. To this end, a pre-task without TMS was performed that contained 120 trials using the same ratios of Go, Nogo, and congruent/incongruent trials. While participants subsequently performed the probabilistic feedback learning task, the median error response time and the mean ERN latency in this pre-task were calculated. The summary of these values was used to determine stimulation timings for the main Go/Nogo Flanker task. Stimulation took place at four different timings: 100 ms before, 50 ms before, at, or 50 ms after the individually calculated ERN latency. This strategy followed the approach of Verleger et al. (2009) who applied it for lateralised readiness potentials and TMS of the motor cortex.

EEG recording and preprocessing

EEG recording followed the procedure in Experiment 2 of Manuscript 1. Trials without a TMS pulse were manually removed before preprocessing. On average, 29.25 trials per subject and stimulation site were rejected due to missing TMS pulse (*SD* = 39.67 trials). Preprocessing then largely followed the explanations for Experiment 2 of Manuscript 1, using the ARTIST algorithm with the same settings. In artefact rejection, 14.88 trials per subject and stimulation site were rejected on average (*SD* = 14.72 trials). On average, 1.13 channels were interpolated (*SD* = 1.13 channels). Following preprocessing via ARTIST, data were exported to the BrainVision Analyzer and segmented around the response markers, starting 200 ms before and ending 600 ms after the marker. Data were averaged per condition (trial type [error, correct] × stimulation site [vertex, cerebellum] × TMS timing [early stimulation, late stimulation]) and the difference signal between the response types *error* and *correct* was formed (error – correct). Next, the peak detection was performed in the BrainVision Analyzer. ERN and Pe were quantified within the difference waveforms (error – correct responses). The ERN was extracted as the maximum negative peak at electrode FCz between response onset and 100 ms following response onset while the Pe was extracted as the maximum positive peak at Pz between 200 and 400 ms after response onset. The peak amplitudes were then exported for statistical data analysis using R.

Data analysis

LME analyses were performed for error rates, response times, difference ERN (error – correct trials), and difference Pe (error – correct trials). For the difference ERN, a follow-up analysis with the original waveforms (correct and error separately) was performed.

For error rates, the within-subject factors stimulation site (vertex, cerebellum) and TMS timing (early stimulation, late stimulation) were included as fixed effects. For response times, the within-subject factors stimulation site, TMS timing, and trial type (error, correct) were included as fixed effects. For the difference ERN and Pe, the within-subject factors stimulation site and TMS timing were included as fixed effects.

For random effects, a maximal fit was attempted including all within-subject factors and an intercept per subject but in case of singular fit, interaction terms and main effects were removed until fit and convergence was ensured. Subjects exceeding a Cook's distance (Cook, 1977) criterion of 4/n were excluded from the respective analysis. Interactions were resolved via simple slope analyses.

Results and Discussion

No effects of stimulation site could be found for accuracy or response time. The difference ERN (error – correct responses) was indeed reduced for cerebellar compared to vertex TMS,

as hypothesised. This pattern persisted only for the late stimulation (at calculated ERN latency or 50 ms post-ERN latency). Analyses of the original waveforms indicated that this effect was more strongly driven by the ERN for errors than correct responses. No significant effects arose for the difference Pe, consistent with the hypotheses.

The finding of a reduced difference ERN for cerebellar stimulation is consistent with previous findings in patients with chronic cerebellar stroke or degeneration (Peterburs et al., 2012, 2015). However, the overall pattern with a *reduced* error-correct differentiation in ERN, *unchanged* error-correct differentiation in Pe, and *unchanged* behavioural performance does not fit with either of the studies performed by Peterburs et al. (2012, 2015). Peterburs et al. (2015) found *reduced* error-correct differentiation in ERN with *unchanged* error-correct differentiation in Pe together with *decreased* performance in patients with degenerative cerebellar disorders. In the study in 2012, they found *reduced* error-correct differentiation in ERN with *increased* error-correct differentiation in Pe together with *unchanged* performance, potentially indicating a compensation of processing in ERN by Pe in patients with chronic cerebellar stroke. The pattern in the current study might have a better fit to results reported by Tunc et al. (2019) who used a Flanker task which might fit more closely to the Go/Nogo Flanker task used in this study (instead of the antisaccade task used in the studies performed by Peterburs et al., 2012, 2015). Tunc et al. found no differences in error rates between healthy controls and patients with cerebellar degeneration, but also a decreased difference ERN for patients compared to controls, although only on trend level. The Pe was, however, overall increased for healthy controls compared to patients.

Notably, cerebellar spTMS needs to be dissociated from investigations in cerebellar diseases, as effects might present differently. In this case, an interpretation in terms of facilitation cannot be excluded, potentially in terms of a decreased need of cognitive control that is reflected in the ERN amplitude. Unlike with cerebellar disease/damage, a disruption of the inhibitory output of the cerebellar cortex towards the deep cerebellar nuclei is a possibility with cerebellar TMS, potentially resulting in disinhibition of cerebellar output. However, this interpretation is limited to speculation. No differences in error rates and response times were found between cerebellar and vertex TMS, which might speak against facilitatory effects of cerebellar TMS.

An interesting pattern in Manuscript 3 was revealed via the manipulation of the TMS timing around the ERN latency: only late TMS reduced the difference ERN when stimulating the cerebellum, but not early TMS. This finding indicates that stimulation needs to occur in close temporal proximity to ERN to be effective. A necessity of such a close time point of stimulation might lie in the course of information exchange for the forward model computed within the cerebellum. Following the forward model, information on the performed action should reach the cerebellum in close temporal proximity to the execution of the action. It might be crucial to

stimulate closely to this time point, and earlier stimulation might leave enough time for cerebellar function to resume normal functionality.

Again, the potentially disruptive effect of vertex TMS on the ACC, the likely neural generator of the ERN, needs to be considered (Jung et al., 2016). Fortunately, recordings were made prior to the TMS, originally to compute the individual ERN latencies. These recordings were post-hoc analysed to compare whether cerebellar TMS truly led to a decrease in error-correct differentiation or whether possibly vertex TMS led to an increase in error-correct differentiation. When comparing the difference ERN from the recordings with no TMS to the ERN under cerebellar and vertex TMS, the effect in the main task seems to be truly driven by a decrease in error-correct differentiation when using the cerebellar TMS and not an increase towards vertex TMS. While this does not restore vertex as a valid control condition, it seems to indicate that its disruptive effects on the ACC do not prove as severe for error processing as for feedback processing. Considering that two participants dropped out following cerebellar TMS during the task, it is nevertheless highly recommended to use an active control site when investigating cerebellar TMS, despite reservations concerning the use of vertex TMS as a control.

Conclusion

Manuscript 3 adds to a growing body of research implicating the cerebellum in error processing and performance monitoring. It replicates findings that cerebellar damage and disruption reduce the error-correct differentiation in the ERN, and further shows that a close temporal proximity in stimulation to the ERN is required to be effective, following previous studies that showed this in the motor domain.

General Discussion

The aim of the studies presented within this dissertation was to better comprehend the role of the cerebellum within reinforcement learning, and performance monitoring in general. Previous work indicated that the cerebellum processes RPEs and is involved in performance monitoring, including both response inhibition and reinforcement learning (Berlijn et al., 2024; Kostadinov & Häusser, 2022). To investigate how this *cerebellar* computation interacts with *cerebral* performance monitoring, we conducted three studies using lesion methods to the cerebellum while recording EEG from the cerebrum. If cerebellar output is required for cerebral computations, cerebral computations should be altered when the cerebellum is damaged/disrupted. Manuscript 1 investigated RPE processing within a reinforcement learning paradigm in two parallel experiments: Experiment 1 involved patients with chronic cerebellar stroke, while Experiment 2 used cerebellar spTMS in healthy young adults. RPE processing was indeed found to be affected in FRN in both cerebellar groups/conditions but not in the control participants/under control stimulation. Reinforcement learning was unaffected. Manuscript 2 was a follow-up analysis of the data of Experiment 2 in Manuscript 1. Instead of feedback processing, error processing was investigated. Error processing was also affected under cerebellar TMS: while error processing in ERN was impaired, error processing in Pe was enhanced by cerebellar TMS compared to control stimulation to the vertex. Finally, in Manuscript 3, the cerebellar role in performance monitoring was investigated in a response conflict paradigm with a focus on TMS timing. Stimulation took place at four different timings, determined individually based on previously measured ERN latencies and response times. Similar to Manuscript 2, error processing in ERN was blunted, however, only when stimulation occurred close to the ERN latency. Behaviour was largely unaffected in all studies.

The cerebellum in reinforcement learning

Reward prediction error

In Manuscript 1, cerebellar lesions and disruption both led to an absent/decreased RPE coding in the FRN, indicating that cerebellar contribution is required for normal RPE coding in the FRN. This finding fits with previous studies in rodents and primates that found RPE-like signals and other signals consistent with reinforcement learning in the cerebellum (Heffley et al., 2018; Heffley & Hull, 2019; Kostadinov et al., 2019; Ohmae & Medina, 2015; Sendhilnathan et al., 2020, 2021; Vignali et al., 2024; M. J. Wagner et al., 2017). The results reported in Manuscript 1 indicate that the RPE signal found in the cerebellum in these studies is required for normal RPE coding in the forebrain; in particular in the neural generators of the FRN. This further converges with studies in rodents that found projections from the cerebellum to the VTA and SN conveying reward-related information (Carta et al., 2019; Washburn et al., 2024; J. Yoshida

et al., 2022; T. Yoshida et al., 2024). These two regions have been shown to be functionally connected to the ACC, one of the main neural generators of the FRN (Elston et al., 2018, 2019; Oerlemans et al., 2024, 2025; Y. Zhang et al., 2017). A connection via the SN or VTA might thus provide a potential pathway for RPE-related information from the cerebellum to the ACC.

RPE effect in patients (Experiment 1)

In Experiment 1, the direction of the effect in patients might be of interest: we found that the FRN amplitude did not appear to be reduced for high negative RPEs but instead increased for low negative RPEs, amounting to the non-significant RPE effect. This finding might be indicative of inappropriately increased perception of salience. This would converge with the "dysmetria of thought" hypothesis, i.e., that dysmetria, a symptom oftentimes found in the motor domain with cerebellar dysfunction, can also occur in the cognitive domain (Schmahmann, 1998). In the FRN, the salience signal towards feedback with low RPEs should result in low salience, as the outcome was expected. However, for cerebellar dysfunction (lesion/disruption), a cognitive hypermetria/overshoot of this salience signal might occur, making the FRN towards low RPEs inappropriate high. This interpretation would also be consistent with the interpretation of the findings reported by Rustemeier et al. (2016). They did not examine RPE coding but valence effects in FRN in a sample of patients with chronic cerebellar stroke within a fractal task. In this task, participants were able to choose between two different fractals (i.e., abstract and unfamiliar visual stimuli) to receive a monetary reward or punishment. However, the chance for either feedback type was 50 % for all fractals, and learning was thus not possible. Across the task, they found valence coding for patients. In controls, however, the valence effect did not reach significance. They interpreted this finding of increased valence coding for patients compared to controls in terms of surprise/salience. In controls, the FRN should differentiate less between positive and negative feedback as feedback stimuli were of similar expectancy (Alexander & Brown, 2011), as 50-50 contingencies were used. Rustemeier et al. speculated that the same effect did not occur for the patients, resulting in sustained surprise/salience towards feedback. RPE modelling was, however, not performed, making direct comparisons between the studies difficult.

The increased instead of decreased FRN in cerebellar damage points to a modulatory instead of a driving role of the cerebellum in RPE coding in the FRN. Many of the patients had lesions within the cerebellar cortex instead of the nuclei. Similarly, cerebellar TMS in Experiment 2 likely reached the cerebellar cortex more strongly than deeper structures. Considering that the output of the cerebellar cortex via the Purkinje cells is largely inhibitory (Ito et al., 1970; Zheng & Raman, 2010), it appears conceivable that the damage/disruption in the cerebellar cortex led to a disinhibition of the DCN, and then as a consequence to increased cerebellar output.

Considering the recent debate on RewP, an alternative explanation arises: if the valence and RPE effects we see within the time window of the FRN are in actuality not driven by a negativity but a positivity, the results concerning signal increase in the current study need to be interpreted differently. Namely, a more negative, thus less positive RewP would mean a decrease of signal towards low RPE, instead of an increase in signal, as interpreted above. In turn, this would be more fitting with a potentially driving role of the cerebellum within this process. However, this interpretation would result in an even stronger contradiction with behavioural findings, posing the question of how the signal can be strongly decreased when the behaviour is intact (see below for a discussion of the brain-behaviour disconnect). Considering recent observations and views, two deflections occur within the time window of the FRN: a negativity called N2 and a positivity referred to as RewP (Krigolson, 2018; Proudfit, 2015; Ullsperger, 2024). The N2 is sensitive towards frequency and surprise (Patel & Azzam, 2005; Ullsperger, 2024), while the RewP is more associated with RPE, in particular positive RPE (Ullsperger, 2024). However, it is difficult to separate the unsigned RPE from salience in the current study. The unsigned RPE represents surprise which involves salience. Thus, it cannot be excluded that the effect is more strongly driven by the negative component in the FRN time window, i.e., N2. Notably, it has been proposed that the negativity associated with FRN is in fact an N2 (Holroyd et al., 2008). However, without conducting an additional PCA to separate N2 and RewP in the data available, conclusions as to the contribution of N2 and RewP for the signal analysed cannot be drawn. Nevertheless, as one would expect a stronger signal for a highly relevant signal (high negative RPE) over one with lower relevance (low negative RPE), it might be more meaningful to interpret the signal as a negativity rather than positivity, although this interpretation remains speculative.

RPE in healthy participants (Experiment 1 and 2)

A further point of discussion concerns why RPE coding in FRN was found only for negative feedback in healthy controls (Experiment 1) and for control stimulation (Experiment 2). Not many previous studies have examined RPE coding in FRN separately for positive and negative feedback. Instead, a signed RPE was examined (e.g., Burnside et al., 2019; Fischer & Ullsperger, 2013; Frömer et al., 2021; Humann et al., 2020; Kirschner et al., 2022) which is, however, highly correlated with valence. Considering studies which examined RPE coding in FRN separately for positive and negative valence, some studies found effects stronger or only for negative valence (Chase et al., 2011; Hoy et al., 2021; Rawls & Lamm, 2021), and some only for positive valence (Cavanagh, 2015; Weber & Bellebaum, 2024). Recordings of single cells in the ACC show that some neurons only react to negative feedback, while others only react to positive feedback, and again others show excitation to both negative and positive feedback (Amemori et al., 2015; Kawai et al., 2015; Monosov, 2017). A potential reason for the differences in valence preference in the (suspectedly ACC-generated) signal in FRN might be

differences in paradigms which draw more attention towards either of the valence types and thus preferentially activate the respective neurons in ACC. For example, tasks in which participants can learn more easily will have less negative feedback in the later course of the task and negative feedback will consequently have more salience due to the lower frequency. The FRN is sensitive to salience (Hauser et al., 2014; Stewardson & Sambrook, 2020; Talmi et al., 2013). As proposed by Alexander and Brown (2011), frequency also explains parts of the valence effects found in FRN. It might be sensible to use tasks which show robust effects for RPEs under both positive and negative feedback to examine cerebellar influences on signed and unsigned RPEs. This might require online control of accuracy, such as achieved by Hoy et al. (2021) in a time estimation task. However, even though Hoy et al. were able to show RPE effects in FRN for both positive and negative feedback, further studies are necessary to show whether these effects are robust.

Valence

For Manuscript 1, a control analysis was performed to investigate whether processing was disrupted in general or whether this was specifically related to unsigned RPE. Interestingly, valence processing in FRN was indeed intact for both groups in Experiment 1 and both stimulation sites in Experiment 2. This is consistent with the robust valence effect in FRN (Sambrook & Goslin, 2015). Of note, the valence effect in Experiment 1, where feedback delay was varied, was only found for short feedback delays. This is consistent with a wide variety of literature showing that the valence effect in the FRN is dependent upon feedback timing: valence effects generally presented as decreased when feedback was more delayed (for a review see Hinneberg & Hegele, 2022). As detailed in the introduction, this might be due to a shift in involvement of different brain areas, with the striatum showing stronger activation for immediate feedback and the medial temporal lobe showing stronger activation for delayed feedback (Foerde & Shohamy, 2011).

It is also worth noting that the intact valence effect in the current study is different from the findings of Rustemeier et al. (2016) who also examined patients with chronic cerebellar stroke. Differences in paradigm should be considered: the fractal task that Rustemeier et al. used only included 50-50 contingencies. Learning was thus not possible, unlike in the task in the study at hand. Interestingly, Rustemeier et al. reported the findings of a probabilistic feedback learning task – which was conducted in the same patient sample – in their supplement: here, they did not find differences in valence coding in FRN between patients and controls. Notably, they also did not specify whether a general valence effect was found (although supplementary grand averages appear to show valence differences in the FRN time window). Learning success in this secondary probabilistic feedback learning task presented as parallel to our findings: no differences between patients and controls emerged. Intact valence coding and

acquisition learning in FRN in patients with chronic cerebellar stroke thus appears consistent across studies.

Brain-behaviour disconnect

While the abnormalities in RPE coding in FRN were quite pronounced, this was not the case for behavioural deficits. Only minor differences between patients and controls (Experiment 1) and between cerebellar and vertex stimulation (Experiment 2) were found. This finding prompts two questions: 1) what does the cerebellum contribute to reinforcement learning, and 2) how does the FRN relate to behaviour?

Cerebellar contribution to reinforcement learning

Concerning the first question, our findings did not indicate behavioural deficits concurrent with cerebellar damage or disruption besides minor changes in choice switching. While the main take-away of this finding could be that the cerebellum is not essential for the specific learning processes necessary for acquisition learning, several factors need to be considered. The task we used required participants to observe and understand patterns between stimuli, actions, and outcomes. They were not given information on how the task was to be performed except for that they would be able to influence the outcomes they received and the general course of the task. While the task did not include any other features making it more difficult besides the probabilistic contingencies (Experiment 1: 90-10 for two stimuli and 50-50 for the other two stimuli; Experiment 2: 80-20 for two stimuli and 50-50 for the other two stimuli), the task was not easy considering average accuracy. Accuracy for learnable stimuli in the last block was at around 70 % for Experiment 1 and at around 60 % for Experiment 2. The results can thus not be explained by a simple ceiling effect.

When considering other studies that examined reinforcement learning under cerebellar damage/disruption, a pattern seems to emerge with intact acquisition learning but deficient behavioural flexibility (i.e., an aspect for which we found minor changes): Rustemeier et al. (2016) and Berlijn et al. (in press) could not find deficits in patients with cerebellar stroke and degeneration, respectively. Thoma et al. (2008) could demonstrate that while patients with a cerebellar stroke showed normal acquisition in reinforcement learning, reversal learning was decreased. The same pattern with intact acquisition and deficient reversal learning was observed when Kruithof et al. (2025) applied theta-burst stimulation to the cerebellum. Nicholas et al. (2024) also found deficits in reinforcement learning in patients with cerebellar degeneration in a task that required behavioural flexibility throughout the whole task. They used shifting reward probabilities, thus requiring participants to constantly adjust action values. A decisive factor for deficits under cerebellar damage/disruption might thus be behavioural flexibility rather than acquisition learning. Notably, however, as Berlijn et al. (2024) outline in their systematic review, studies including the Wisconsin Card Sorting Test (WCST) or a

modified version of it did not yield as clear of a result pattern. The WCST requires participants to sort cards according to a pattern unknown to them that also changes throughout the task. This thus also requires behavioural flexibility. While some studies found deficits in patients with cerebellar damage (applying an old rule even though the rule shifted; Mak et al., 2016; Mukhopadhyay et al., 2007), others did not (Dirnberger et al., 2010; Turner et al., 2007). There is thus as yet no sufficient evidence for a clear behavioural correlate of cerebellar damage/disruption in reinforcement learning, although it seems more likely that flexibility rather than pure acquisition learning is affected in these patients.

Future studies are required to characterise the reinforcement learning deficits associated with cerebellar damage/disruption more in-depth. There might be differences both in terms of paradigm as well as in terms of clinical population/cerebellar stimulation. Concerning the paradigms, a wide range of paradigms with a focus on behavioural flexibility but differences in other requirements should be tested. Differences might be examined in task domain, required working memory load, risk behaviour, attention, and others. For example, reversal learning tasks might require the sensing of a sudden shift in stimulus-/action-outcome contingencies, which might pose higher demands to salience networks. This would be reconcilable with the deficits in unsigned RPE coding in FRN, which might also be interpreted as a deficient salience signal. Constantly shifting reward probabilities might require the involvement of other brain-areas involved in the computation of reward values, and should present as more difficult. In addition, more complex tasks such as two-step tasks requiring the performance of several actions instead of one have not yet been sufficiently explored within the framework of cerebellar dysfunction and might even require a different set of processes and brain areas. Balsters et al. (2013) could show initial evidence that the cerebellum, in particular Crus I and II, is active in higher-order rule learning (which is required for two-step tasks). In rodents, a deficit in the reversal but not acquisition stage concurrent with cerebellar Purkinje cell loss was also shown in a visual discrimination task and discussed in terms of higher- and lower-order rule learning (Dickson et al., 2017). Interestingly, while the task was framed as a visual discrimination task and results were mainly interpreted in terms of higher- and lower-order rule learning, mice were instrumentally conditioned to learn visual stimuli, thus constituting a reinforcement learning task. The study thus provides further evidence for a role of the cerebellum in behavioural flexibility. It might be beneficial to consider higher-order rule learning when investigating a cerebellar role in reinforcement learning in terms of behavioural flexibility.

Behavioural correlates of the FRN

Concerning the second question, previous studies indicated that the correlation between FRN and behaviour is not straightforward. An overview by Ullsperger (2024) shows that there is no strong basis for behavioural correlates for the FRN yet. A few studies showed a relation to

deficits within behavioural flexibility (Fischer & Ullsperger, 2013; Kirschner et al., 2022; but also see Chase et al., 2011) which is also the area where we found minor deficits in Experiment 1 and 2. However, the task we used in these experiments does not require a particularly high demand on behavioural flexibility; only acquisition learning was required. More severe deficits could potentially be found in tasks which require more behavioural flexibility, such as reversal learning tasks or tasks with continuously changing contingencies. The question on what the FRN reflects nevertheless persists. The signal clearly reflects RPEs, as many previous studies have shown (Burnside et al., 2019; Cavanagh, 2015; Chase et al., 2011; Fischer & Ullsperger, 2013; Frömer et al., 2021; Hoy et al., 2021; Humann et al., 2020; Kirschner et al., 2022; Rawls & Lamm, 2021; Weber & Bellebaum, 2024). Several explanations come to mind on why the deficient RPE processing represented in FRN does not result in a behavioural deficit in the present experiments.

First, it might be that the RPE signal in the FRN is simply not essential for acquisition learning. Instead, other regions besides the ACC, i.e., the likely neural generator of the FRN, might represent RPEs independently from ACC and are instead required for this type of learning. Several fMRI and electrophysiological studies in animals have shown that RPE is represented in SN, VTA, Striatum, OFC, and likely further other regions (J. Y. Cohen et al., 2012; D'Ardenne et al., 2008; Groman et al., 2021; Schultz et al., 1993, 1997; Takahashi et al., 2023). It thus seems that the RPE is widely represented in the brain, which seems adequate, as it is such a crucial value for the correct adjustment of action values, and consequently the reinforcement learning success in a wide variety of contexts. The RPE signal in the FRN seems to make up only a part of these representations. The FRN might not account for the complete distribution of RPE signals in the brain. Since the absent RPE coding in FRN in the cerebellar lesion patients and healthy participants under cerebellar TMS does not result in behavioural deficits, the RPE signal in FRN cannot be the only signal used for action value updating in acquisition learning in probabilistic feedback learning contexts. That would had to have resulted in behavioural deficits. Notably, this argumentation is not compatible with the reinforcement learning theory proposed by Holroyd and Coles (2002) which assumes that the ACC acts as a control filter for all reinforcement learning processes (and should thus represent all RPE signals). Following this theory, deficits in processing within ACC should have resulted in behavioural deficits, which was however not the case.

Second, RPE processing in FRN might be used for reinforcement learning in acquisition contexts but can be compensated by other brain areas. This could be, for example, a later, more effortful process. However, we examined later ERP components for Experiment 1 and 2, i.e., P3a and P3b, and could not find any effects consistent with such a conclusion. Several brain areas associated with RPE processing were, however, not captured, as there is no

straightforward ERP component reflecting their activity. It is very possible that these brain areas took over the function of the ACC. Importantly, these would have to be compensatory processes that are available on the short term, as the stimulation in Experiment 2 was instantaneous. Lesion studies could show that the ACC is necessary for action-outcome associations but not stimulus-outcome associations (Camille et al., 2011; Rudebeck et al., 2008). Of note, these findings demonstrate that the ACC cannot be the only final processing stage for all reinforcement learning processes. Instead, it seems that the ACC has a tendency towards action-based reinforcement learning. For stimulus-based reinforcement learning, areas such as OFC seem to be more relevant. Lesion studies could show that OFC is required for stimulus-outcome learning but not action-outcome learning, thus showing a double dissociation (Camille et al., 2011; Rudebeck et al., 2008). This insight is highly relevant to our findings. In the paradigm for Experiment 1 and 2, we assumed that action-outcome learning would take place, as choices were made by pressing one of two buttons on a response box. Stimuli were only used to represent the context of the choice, such that for a given stimulus, different contingencies between responses and outcomes applied. However, responses were additionally represented on screen via rectangles. In the previously mentioned studies, which showed a necessity of ACC for action-outcome learning, responses were made by moving a joystick, without representation on screen. The button presses and rectangle representation might have enabled learning via stimulus-outcome learning to some degree, facilitating the compensation via regions such as OFC. The OFC, and also the closely associated vmPFC receive a wide range of information highly relevant to reinforcement learning (Groman et al., 2021; Moneta et al., 2023, 2024) and might be suitable to compensate ACC function. However, we were not able to test this as no correlate of OFC/vmPFC activity was measured. It is also worth mentioning that ACC function has not been closely defined yet. Another suitable region to compensate ACC function might be dlPFC, a region which is able to modulate activity of the motor cortex and whose stimulation is able to cause shifts in reinforcement learning strategies (Morris et al., 2014; J. X. Wang et al., 2018).

While it will be helpful to investigate this more directly using a method with a higher spatial resolution, such as fMRI, within a reinforcement learning task, it might also be helpful to investigate the effect of cerebellar TMS at a more basic level. Applying cerebellar repetitive TMS (rTMS; and several control stimulations on different appointments) and measuring resting-state fMRI before and after would be insightful to understand the effects of cerebellar TMS on cerebellar connectivity with other brain areas. rTMS can be used off-line and increase or decrease excitability of the subjacent area depending on stimulation frequency (Klomjai et al., 2015). This approach could shed light on several speculative interpretations for the studies presented here. While it would be interesting to see to which degree connectivity to areas involved in reinforcement learning changes, the direction of the effect (increased or decreased

activation/connectivity) would help interpreting whether cerebellar over- or underactivation is causal for the differences found in FRN and ERN.

Cerebellar computation in reinforcement learning

A recent study investigated feedback processing in the FRN in patients with ACC lesions (Oerlemans et al., 2024), i.e., the main generator of the FRN. This appears highly relevant in relation to the results of Manuscript 1. If the results were similar to the findings in Manuscript 1, this would speak for a driving role of the cerebellum in generating the FRN. However, Oerlemans et al. (2024) found a blunted valence effect in FRN for patients with lesions to the (right dorsal) ACC while we found intact valence coding in patients with cerebellar damage. On the other hand, we found deficits in RPE coding which is something that was not tested in the study by Oerlemans et al. (2024). This points towards a complementary role of the cerebellum. Instead of a loss of valence coding as with ACC lesions, cerebellar lesions did not result in deficits in valence coding and instead selectively seemed to affect RPE. This is in conformity with the general assumption that the cerebellar influence on the cerebrum is modulatory and does not drive processes directly (Kawato et al., 2021).

A crucial point of interest concerns whether cerebellar RPE processing is related to signed or unsigned RPE. The reflection of RPEs in FRN was decreased only for negative valence. For positive valence, we could not find RPE coding for either patients/cerebellar TMS or controls/vertex TMS. This makes an interpretation as to whether the cerebellum is required for signed or unsigned RPEs more complex. Notably, valence coding in FRN was unaffected in a control analysis, indicating that cerebellar damage/disruption affected valence to a smaller degree. This could indicate that the cerebellum is more associated with unsigned than signed RPE. The ACC, on the other hand was shown to display both signed and unsigned RPEs depending on the study (Amemori et al., 2015; Corlett et al., 2022; Kawai et al., 2015; Monosov, 2017).

The interpretation of our results as deficits within the processing of unsigned RPE fits well with recent findings in fMRI and rodents. A meta-analysis conducted by Corlett et al. (2022) yielded that cerebellar activations in reinforcement learning mainly relate to unsigned instead of signed RPE. Further supporting this interpretation, rodent studies found signal increases towards both positive and negative RPEs (Heffley et al., 2018; Heffley & Hull, 2019; Kostadinov et al., 2019; Vignali et al., 2024; M. J. Wagner et al., 2017). Only one study found signal decreases towards omission in punishment contexts (Ohmae & Medina, 2015). However, a study investigating the output of the cerebellum did indeed find signals consistent with a signed RPE (Washburn et al., 2024), although the signal overlapped with licking activity.

Importantly, the finding that the cerebellum contributes towards reinforcement learning does not indicate that the computation within the cerebellum itself follows principles of reinforcement learning. Reinforcement learning algorithms can have subprocesses that provide information to the higher-level reinforcement learning process but do not constitute reinforcement learning themselves (Sutton & Barto, 2018a, 2018b). They might for instance instead be supervised or unsupervised learning processes. In fact, supervised learning has been proposed as a ruling principle for cerebellar computations (Raymond & Medina, 2018), although recent accounts have also proposed reinforcement learning as an alternative principle within the cerebellum (Kuriyama et al., 2024).

Cerebellar subregions

In addition to the general findings within FRN and learning success, further investigations were made into what subregions of the cerebellum might be most relevant for RPE processing within the FRN for Experiment 1. Stroke patients present with inhomogeneity in lesion location and (usually) clearly circumscribed lesions, enabling examination of relations between degrees of deficits and lesion location. Exploiting this characteristic of the sample, a vbLSM was performed for Experiment 1 of Manuscript 1 in order to relate the decreased RPE processing in FRN to cerebellar lesion location.

Results of the vbLSM pointed to a special role of four subregions: a cluster in the transition between Crus II and lobule VIIb, one in medial Crus II, one in Crus I, and one in medial lobule VIIb/vermal lobule VIIIa. All these regions are part of the posterior cerebellum which is associated with higher cognitive functions (Stoodley et al., 2016; Tedesco et al., 2011). As functional boundaries present differently than anatomical boundaries, it can be helpful to consider where these regions lie in an atlas based on task data, such as the one by Nettekoven et al. (2024). Considering the statistically significant clusters against this atlas, several functions related to the task are apparent. The cluster in the transition between Crus II and lobule VIIb overlapped with region D2 in the Nettekoven atlas which is associated with working memory function. Working memory and reinforcement learning are closely intertwined, both in required brain areas and function (A. H. Yoo & Collins, 2022). It is thus not unexpected to find regions with such functions affected in patients with deficient RPE coding. The cluster in the medial Crus II corresponded to the region D1, which is also working memory (Nettekoven et al., 2024). The cluster in Crus I corresponded to S3, which is associated with the default mode network and theory of mind (Nettekoven et al., 2024). While it might seem surprising to find a region associated with theory of mind among the regions associated with deficient RPE processing, an interpretation concerning its function within the default mode network might be more sensible: a main purpose that has been suggested for the default mode network is reinforcement learning (Dohmatob et al., 2020). Lastly, the cluster in medial lobule VIIb/vermal

lobule VIIIa overlaps with region A1, that has been associated with spatial rotation and simulation (Nettekoven et al., 2024). While not specifically related to reinforcement learning, visual spatial skills have been related to the reading of Chinese characters which were used as visual stimuli in the task (D. Lin et al., 2016). It might thus be a second-tier function that is relevant for this task but likely not in general for reinforcement learning tasks.

Importantly, the parcellation by Nettekoven et al. (2024) did not include reinforcement learning tasks, making assumptions as to whether these regions overlap with areas relevant for reinforcement learning more difficult. However, considering that most clusters overlapped with regions with functionality closely related to or required for reinforcement learning, it seems likely that these are in fact regions that perform tasks in reinforcement learning. Future parcellations should use task batteries or data sets that also include reinforcement learning tasks to answer this question more directly.

It is further important to note that while we found these four clusters in connection to particularly reduced RPE processing in the FRN, the distribution of FRN difference amplitudes was overall shifted in patients compared to controls (see Figure 8C in Manuscript 1). It is therefore likely that several other regions besides the ones mentioned above are relevant for reinforcement learning. Lesions were predominantly in the posterior cerebellum. In the review of Berlijn et al. (2024), a wide range of regions was found to be active in reinforcement learning as revealed by studies using fMRI in healthy adults. It is possible that some of these activations are also task-specific, as it is presumably the case with the cluster in medial lobule VIIb/vermal lobule VIIIa found in Experiment 1. It would be useful to investigate a wider range of tasks in a larger patient sample; however, this would likely require a multi-site effort, as patients with strokes limited to the cerebellum are scarce and not always easy to recruit in the chronic state (as there is less necessity for visiting an inpatient clinic as compared to, e.g., patients with degenerative disease).

The stimulation site in Experiment 2 also allowed for conclusions concerning relevant brain regions: the initial reason for stimulating the left cerebellum was the finding that spatial processing is more strongly processed in the right cerebrum and left cerebellum (Corballis, 2003; Petrosini et al., 1998). Parallels were drawn to the complex stimuli presented in the task (Chinese stimuli or radicals). However, stimulating the left site is also consistent with studies showing that cerebellar activity towards fear extinction learning (a form of classical conditioning) is found within the left cerebellar hemisphere (Doubliez et al., 2023; Ernst et al., 2019; Nio et al., 2025; Yágüez et al., 2005).

Interestingly, a recent study found deficits in reversal learning when stimulating the medial cerebellum but not the right cerebellum or occipital lobe via rTMS (Kruithof et al., 2025). The reason for stimulating the medial cerebellum was based on a recent meta-analysis from the

same group that showed that reward is processed more strongly within the vermis (Kruithof et al., 2023). Deficits in reversal learning would be predicted when considering deficits in RPE coding in FRN, as behavioural flexibility is one of the few behavioural correlates for which some evidence points to the FRN (Fischer & Ullsperger, 2013; Kirschner et al., 2022; Ullsperger, 2024; but also see Chase et al., 2011). It thus seems consistent that a stimulation of the cerebellum would result in both a reduction of RPE processing as in Manuscript 1 and a reduction in reversal learning as in the study by Kruithof et al. (2025). It initially seems incongruent that deficits were found in FRN for stimulation on the left site, and in reversal learning for stimulation on the medial cerebellum. However, cerebellar TMS is not very focal. Modelling and measurements of the electrical field for cerebellar TMS indicate that especially the double-cone coil we used in Experiment 2, but also the figure-of-8 coil that Kruithof et al. used, stimulates a rather large area (Çan et al., 2018). There thus seems to be considerable overlap between the electrical fields of the two stimulation sites. The actual regions that might be essential for eliciting deficits in the two studies might thus well lie within either or between the left hemisphere and vermis. However, the study performed by Kruithof et al. seems to indicate that the right cerebellum is not required even for reversal learning. This seems at odds with the findings of Experiment 1 in Manuscript 1 where around half of the lesions were on the left and half on the right side. There, the overall distribution of difference FRN was shifted in the whole patient sample compared to the control participants, and not selectively for patients with lesions to the left cerebellum. Cerebellar connectivity might be changed in the side contralateral to the stroke in terms of network-level changes; however, this alone is not sufficient to clearly explain the inconsistencies in findings. It thus still stands to question whether only the left hemisphere or vermis is required. It might be helpful to make use of newer brain stimulation techniques, such as transcranial ultrasound stimulation (TUS). TUS has been explored more recently as an alternative to more established NIBS methods. It offers the advantage of a much higher spatial resolution and is easily combinable with EEG and fMRI (Darmani et al., 2022). A more focal stimulation could offer a clearer picture on the cerebellar regions involved in reinforcement learning.

TMS timing

For Experiment 2 in Manuscript 1, the interaction between feedback valence, unsigned RPE, and stimulation site did not involve TMS timing. While non-significant effects are always difficult to interpret, this finding might indicate that 1) stimulation at both time points affected the same process, 2) stimulation at the different time points affected different subprocesses which were, however, both required for RPE coding, 3) a more general rTMS-like effect emerged via the prolonged single-pulse stimulation. For 1), outcome anticipation might be a fitting candidate. Outcome anticipation builds slowly starting from the response execution towards the outcome delivery (M. J. Wagner et al., 2017). While the time window in which the disruptive effect of the

TMS is effective is unknown, it might be that both stimulation time points disrupted this process. For 2), post-stimulus TMS might have disrupted error processing and pre-feedback TMS might have disrupted feedback processing. There is evidence that both of these processes are affected by cerebellar damage (Peterburs et al., 2012, 2015; Rustemeier et al., 2016). Error processing was also indeed affected in the data used for Experiment 2, as shown in Manuscript 2. The disruption of error processing might have indirectly disrupted RPE processing, while the disruption of feedback processing might have had a direct influence. Lastly, for 3), disruption might have been induced via unintended low-frequency rTMS, with effects potentially developing across the course of the task (which was, however, not investigated). While low-frequency rTMS is usually applied at 1 Hz (Klomjai et al., 2015), a few studies have also found decreased motor excitability and long-term depression for TMS at even lower frequencies such as 0.5 or 0.25 Hz (Gorsler et al., 2003; Zhuo et al., 1994). In Experiment 2, stimulation took place once per trial with a duration of ca. 4 seconds per trial, thus approximating 0.25 Hz in stimulation frequency. However, a study performed by Muller et al. (2014) was able to show that – at least for the motor domain – effects are strongest for stimulation at 1 Hz. Additionally, stimulation was varied between post-stimulus and pre-feedback TMS, and consequently no consistent rhythm was applied. It thus seems unlikely that an unintentional rTMS was responsible for the absent effects of stimulation timing on RPE coding in FRN.

The cerebellum in error detection

Result pattern in ERN

While Manuscript 1 focussed on the role of the cerebellum in feedback processing, Manuscript 2 and 3 focussed on error processing. Interestingly, even though Manuscript 2 investigated error processing within a reinforcement learning paradigm and Manuscript 3 investigated error processing within a response conflict paradigm, the influence of cerebellar TMS on error processing in the ERN presented similarly: in both studies, the discrimination of errors and correct responses in the ERN was diminished when stimulating the cerebellum. These findings are further consistent with previous studies by Peterburs et al. (2012, 2015). In these studies, participants performed antisaccade tasks, another type of response conflict task. Participants needed to perform a saccade in the opposite direction of a peripheral stimulus. Both patients with chronic cerebellar stroke and patients with a degenerative cerebellar disease showed diminished discrimination between errors and correct responses in ERN. One other study performed by Tunc et al. (2019) in patients with cerebellar degeneration could not show this effect. In this study, a Flanker task was performed. Notably, the group difference in the difference ERN (errors – correct responses) showed a trend-level effect, indicating descriptively that the difference ERN was smaller in patients than in controls. Although the authors interpreted this effect strictly as non-significant, it would fit the general pattern of

studies presented above. The smaller effect in the study by Tunc et al. does not seem explainable purely by sample size (23 patients, 29 healthy controls) or time pressure (450 ms response time window vs. 350/400 ms in Manuscript 3). While they did use wider inclusion criteria, also including cerebellar disease with extracerebellar involvement, such as SCA 1, one would expect more severe rather than smaller deficits, as a wider range of brain areas is affected. In addition, there were some differences in preprocessing and the quantification of the ERN, although it is not apparent whether these are the reason for the differences in effect sizes. Nevertheless, the overall pattern with decreased discrimination between errors and correct responses in ERN in cerebellar disease or disruption is consistent across studies.

Result pattern in Pe

However, the result pattern for the Pe in Manuscript 2 presented much differently than for the ERN, with an *increased* error-correct differentiation. Differences in both neural generators and function have been proposed for the Pe. While it is suspected that the ACC contributes to generating the Pe, additional generators have been proposed, such as the parietal cortex (Hester et al., 2005). It is possible that these generators were not or differently affected by the cerebellar TMS. The function of the Pe is not as clear as for the ERN (van Veen & Carter, 2006). A differentiation into an early and a late Pe has been proposed, with different functionality: while the early Pe should show a signal similar to and highly correlated with the ERN that is generated potentially by the same source (i.e., ACC), differences in functionality from ERN have been proposed for the late Pe (Wessel, 2012). For the late Pe and later ERP signal in general, error awareness has been suggested as a potential underlying process (Del Cul et al., 2007). While early and late Pe were not separately assessed and, instead, only the peak Pe was detected, the major differences between result patterns in ERN and Pe indicate that we might have captured a different process in Pe than in ERN.

The complementary effects in ERN and Pe in Manuscript 2 with no deficits in behaviour appeared to be highly similar to the findings reported by Peterburs et al. (2012) in a response conflict task in patients with chronic cerebellar stroke. Peterburs et al. quoted long-term compensatory mechanisms as a potential reason for this result pattern in chronic cerebellar stroke, with an increased error-correct differentiation in Pe compensating for the decreased error-correct differentiation in the earlier-peaking ERN, resulting in an intact performance. However, as TMS in Manuscript 2 was applied instantaneous, a long-term compensation does not seem fitting to explain the result pattern. Two other options stand to reason: first, the increased error-correct differentiation might yet constitute compensation, however, in a short-term manner. In favour of this argument would be the indeed intact learning performance. Error processing might thus have been taken over by the Pe instead of ERN. This interpretation calls into question whether the findings shown by Peterburs et al. truly reflected long-term

compensation, or whether these also showed a short-term compensation available instantaneously. Notably, the compensation in the two studies might differ, as 1) compensation available in reinforcement learning and response inhibition might differ, and 2), the manipulation applied via cerebellar spTMS might differ greatly from the effects of cerebellar degeneration and stroke. It thus cannot be excluded that Peterburs et al. observed long-term compensation and Manuscript 2 showed short-term compensation. It is important to note that late error processing (in Pe) might not result in intact performance in all contexts: it might prove more problematic in contexts that require a fast-paced line of action, such as in sports or the play of instruments. However, intact performance does not evidence that increased error-correct differentiation in the Pe constitute compensation. Compensation could also have taken place at other stages of the task, such as feedback anticipation or processing, or even in the inter-trial-interval, and the changes to Pe might have a different underlying cause than compensation. For example, the increased error-correct differentiation in Pe might constitute a hypermetria, i.e., a maladjusted, overly high signal. A potential variable in which hypermetria might have occurred could be salience which is associated with Pe (Overbeek et al., 2005). This interpretation would be consistent with the dysmetria of thought hypothesis (Schmahmann, 1998), i.e., that dysmetria concurrent with cerebellar dysfunction occurs not only in the motor but also in the cognitive domain. This interpretation could be testable in settings with a wider range of error saliences.

Another important point of consideration is that results between Manuscript 2 and 3 were not consistent for the Pe: while for Manuscript 2, an increased error-correct differentiation in Pe was found for cerebellar TMS, no significant effects were observed in Pe in Manuscript 2. First, differences in sample or other external parameters do not offer an explanation for these differences, as samples were almost the same and data were acquired within the same session (first, the pre-test for Manuscript 3, followed by the probabilistic feedback learning study for Manuscript 2, then the Go/Nogo Flanker task for Manuscript 3). The only notable difference concerning the sample appears to be the smaller final sample size for Manuscript 3, as more subjects needed to be excluded. Besides sample size, reasons might lie within differences in the tasks: Manuscript 3 used a fast-paced response conflict task while Manuscript 2 used a slow-paced reinforcement learning task. Potential differences might be pace, task difficulty, or reliance on error awareness. Another reason might lie within the timing of the stimulation which took place much closer to the ERN (and also Pe) latency in Manuscript 3 compared to Manuscript 2. The stimulation in Manuscript 3 might have consequently been more effective than in Manuscript 2. Importantly, the absence of effects within Pe in Manuscript 3, with simultaneously no deficits within behavioural performance, prompts the question whether the interpretation of the increased error-correct differentiation in Pe in Manuscript 2 can truly be compensation. However, differences in reliance on processes reflected in Pe between

response conflict and reinforcement learning are also an important point of consideration. The Pe presented with a less pronounced peak in the grand average in Manuscript 2, consistent with studies that examined Pe in reinforcement learning paradigms (Unger et al., 2012; Zhuang et al., 2021). The Pe might present different in reinforcement learning task, potentially due to errors being more ambiguous than in response conflict tasks. This is also a question of basic research into the background of the Pe, which has been less extensively investigated than ERN.

Association of error and feedback processing

Manuscript 2 investigated the influence of cerebellar TMS onto error processing in a reinforcement learning task – importantly, in this data, the RPE coding in the FRN was blunted when receiving cerebellar TMS. This is an important consideration for the effects in the ERN, as deficits might thus also be caused by deficient feedback processing. Stimulation was applied at two time points (but only once per stimulus/trial): either at 100 ms after stimulus presentation (thus before the response) or 100 ms before the feedback presentation. Considering the processing deficits in ERN with cerebellar TMS, two potential explanations arise: 1) The deficit in ERN might have been caused by the blunted RPE coding in FRN. This would indicate that RPE coding and consequentially the updating of action values is essential for error detection in reinforcement learning. 2) The effect stems from the post-stimulus stimulation directly affecting error processing. While this interpretation indicates that the deficit in FRN did not affect ERN, the causality might be inverted: for example, a disruption of action value representation could affect both error detection and RPE processing, as action value representation is required for both. A trend-level interaction in ERN indicated a stronger blunting of the response type effect in ERN under post-stimulus cerebellar TMS. This finding supports a more direct effect of TMS on ERN, and not indirectly via blunted RPE coding during the feedback stage. Nevertheless, this alone does not allow for the conclusion that the deficit in ERN is causal for the deficit in FRN. It might yet be that both deficits are completely separate from each other. The finding in the FRN presented in Manuscript 1 did not show any interaction indicating that any of the stimulation time points resulted in stronger blunting of RPE coding in FRN. It might thus well be that the ERN is affected by only post-stimulus TMS while the FRN is affected by both post-stimulus and pre-feedback TMS.

The finding that both error coding in ERN and RPE coding in FRN is blunted while error coding in Pe and RPE coding in P300 is not, proves interesting in relation to the networks and functionality involved. The ACC, the likely neural generator of the ERN and FRN, has been implicated within both the salience and executive network (Carter et al., 1999; Ham et al., 2013). While the Pe has been less well researched, the P300 has been implicated in the executive network and several sensory networks (Guerrero et al., 2022; Li et al., 2018). The

findings in Manuscript 1 and 2 taken together might thus indicate differences in functional significance of connectivity between the cerebellum and these networks in reinforcement learning or different capabilities of these networks to compensate cerebellar deficits.

TMS timing

While TMS timing in Manuscript 2 was rigidly set to 100 ms post-stimulus, the timing was more varied and individually adjusted in Manuscript 3. This followed the question of whether a clear time window could be established for an effect of cerebellar TMS towards a disruption of ERN. For the motor domain, this has been established more clearly in terms of cerebellar brain inhibition (Ugawa et al., 1991). Here, one coil is placed on the cerebellum and one over the contralateral motor cortex. It could be shown that cerebellar TMS around 5 ms before TMS over M1 results in decreased motor output (Fernandez et al., 2018). Considering the effects found in Manuscript 2, this time window needs to be larger for the cognitive domain, as the distance between stimulation and response/ERN latency varied depending on response time, and stimulation seemed to still be effective. In Manuscript 3, TMS timing was applied at four different stimulation time points: either 100 or 50 ms before, at the calculated ERN latency, or 50 ms afterwards. However, to increase the number of trials per condition, stimulation timings were pooled for analysis: the stimulation at 100 or 50 ms before the ERN latency were pooled together as *early* stimulation and the stimulation at ERN latency or 50 ms afterwards were pooled together as *late* stimulation. The blunting of error-correct discrimination in ERN was, however, only found for the late stimulation. This appears to be inconsistent with the findings of Manuscript 2 which showed a blunting of the error-correct discrimination in ERN with a rather large temporal distance between stimulation and response/ERN (stimulation 100 ms post-stimulus, median response time at 453.5 ms post-stimulus with an average individual standard deviation of 98.8 ms). A potential reason for this might be different requirements of the task. Reinforcement learning tasks rely strongly on the representation and updating of action values. However, there might be a difference in reliance on action values for response conflicts. It was previously shown that the ERN (but not the Pe) requires knowledge of which action is correct, i.e., the action value (Di Gregorio et al., 2018); however, it is conceivable that there is no necessity for an updating of these values. As detailed in the introduction, behaviour is not only regulated by action values but may also be directed by policy. There is a difference in brain regions associated with value- and policy-based functions, with VTA, ventral striatum, OFC, and vmPFC being more associated with value-based function and SNc, dorsal striatum, and dlPFC being more associated with policy-based functions (Araújo et al., 2024; Balleine et al., 2007; Fraser et al., 2023; Groman et al., 2021; Lerner et al., 2021; Moneta et al., 2023, 2024; Morris et al., 2014; O'Doherty et al., 2004; Ott et al., 2011; Overman et al., 2023). It might be the case that response conflicts require a higher degree of policy updating and a lower degree of action value representation. As policy functions are more closely connected with motor

functions, processing might be faster, making cerebellar TMS only effective in this close range around the ERN latency while a wider time window works for more cognitive tasks.

In addition, the relation between response times and ERN latency in the pre-task (that was used to calculate the individual ERN latency for stimulation) and response times and ERN latency in the experimental task needs to be considered. With the median response time in the pre-task at around 250 ms and the mean ERN latency at around 50 ms, the average ERN latency should roughly be at 300 ms. The stimulation at 50 ms after this calculated time would thus happen after the ERN, and close to the end of the response time window (at 350 ms). An influence on the ERN via this stimulation time point is thus only conceivable if reaction times or ERN latency in the experimental task were higher – otherwise it would still occur after the ERN. While reaction times in the experimental task seemed to have been slightly lower than 250 ms, the ERN latency appears to be higher in the experimental task compared to the pre-task. The late stimulation time points thus seemed to occur closely before or at ERN latency in the experimental task.

More research is necessary concerning the temporal relation between cerebellar and cerebral error processing in the cognitive domain. Future studies might want to stimulate at a wider range of timings, but it would also be interesting to see whether error processing is deficient in response conflict tasks with cerebellar rTMS. Such a study would make an important contribution as to determine whether cerebellar TMS does not affect behavioural performance in general in response conflict tasks or whether cerebellar spTMS does not have a strong enough effect to see behavioural deficits.

Limitations

Vertex as a control condition

In all three manuscripts, vertex was used as a control site. Vertex is a commonly used control site for cerebellar stimulation (Gatti et al., 2023). A sham stimulation does not suffice as a control site, as the cerebellar stimulation is quite distracting. This does not only make differences between the stimulation site quite noticeable to participants but also creates problems when comparing performance parameters between stimulation sites, as the distraction might be causal for differences. In our study, vertex seemed to offer a good match in several parameters of side effects, such as inattentiveness, headaches, and discomfort (see Figure 5 in Manuscript 1).

However, in Study 2 of Manuscript 1, it is apparent that vertex TMS induced changes to the RPE effect within the FRN. Instead of finding enhanced FRN amplitudes for higher compared to lower RPEs as one would expect from previous studies (Burnside et al., 2019; Chase et al., 2011; Fischer & Ullsperger, 2013; Frömer et al., 2021; Hoy et al., 2021; Humann et al., 2020;

Kirschner et al., 2022; Rawls & Lamm, 2021; Weber & Bellebaum, 2024), the pattern was reversed, with a decreased FRN amplitude for higher compared to lower RPEs. A likely reason seems to be a direct stimulation of the ACC. A study performed by Jung et al. (2016) could show a deactivation of the ACC concurrent with a series of 12 short 1 Hz TMS pulses. Vertex stimulation thus cannot serve as a true control stimulation, leaving Experiment 2 of Manuscript 1 without a control condition. This makes comparisons in learning performance impossible. No learning differences between cerebellar and vertex TMS were found. However, it is not clear whether this is due to no influence of cerebellar TMS on learning, or due to a similar influence of vertex and cerebellar TMS on learning. Nevertheless, it is still meaningful to regard the cerebellar TMS in Experiment 2 as a comparison to the cerebellar patients in Experiment 1. Both showed the same pattern of a blunted RPE coding in the FRN.

Interestingly, no influence of vertex TMS was apparent for the ERN, for which the ACC also serves as the likely generator (Herrmann et al., 2004; Hochman et al., 2009; Ladouceur et al., 2006; Roger et al., 2010). As detailed in both Manuscript 2 and 3, the expected error-correct differentiation was found.

Nevertheless, the present results speak against using vertex TMS as the sole control site, at least in reinforcement learning paradigms, but, if possible, also in other paradigms, as the ACC is involved a wide range of processes in the emotional, motor, and cognitive domain (Devinsky et al., 1995). Unfortunately, no alternative active control sites have been tested robustly. Kruithof et al. (2025) used the occipital cortex as a control site, which can, however, lead to problems in visual perception (Kammer, 1998). They used the right cerebellum as an additional stimulation site, which was useful in showing differences in effects within the same region (cerebellum). From the current status of the literature, it might be sensible to use several control sites, both to compare effects across control sites within studies and to potentially find a valid control site in the long term. For learning paradigms, this makes within-subject designs, such as the one in Experiment 2, difficult if not impossible, as repetition effects will increase with increasing repetition of the same paradigm. Instead, for healthy participants, between-subject paradigms should be considered.

Lack of learning success

Even though pilots were conducted in elderly participants to assess whether task difficulty was appropriate, many participants in Experiment 1 of Manuscript 1 did not learn the stimulus contingency and did not increase their performance significantly above chance level. This made comparisons between pre- and post-learning, as originally pre-registered, impossible. Instead, an alternative approach using RPE modelling was applied. Of note, the learning success was not substantially lower than in the study of Rustemeier et al. (2016; ca. 75 % vs. ca. 70 % in the last block).

A similar issue arose for Experiment 2, which was likely due to the distracting effect of the TMS. This was reported in spontaneous self-reports at the end of the sessions and was also apparent from the side effects questionnaire.

Alternatively, adaptive tasks might help ensure that most participants learn. This is particularly important when considering adding a reversal learning phase, where contingencies are reversed. For reversal to have a meaningful effect, participants need to understand how to correctly perform the task. Otherwise, the reversal might just further confuse participants and lead to decreased engagement with the task.

Conclusions

In summary, the presented studies showed that cerebellar function is required for cerebral processing in reinforcement learning as measured in the ERN and FRN. Both the processing of RPEs at the feedback stage and the processing of response errors at the response stage were affected under cerebellar dysfunction. Cerebellar disruption also affected response error processing in a response conflict task, substantiating the importance of cerebellar function in performance monitoring in its entirety. Behavioural deficits were absent or minor. The presented findings converge with previous initial studies in humans and a growing body of studies showing signals consistent with reinforcement learning in the rodent cerebellum. Future research should focus on determining behavioural deficits concurrent with cerebellar dysfunction and further comprehending the role of the cerebellum in disorders with abnormal reinforcement learning, such as addiction, anxiety disorders, and psychosis. Understanding the mechanisms in which the cerebellum is involved in the emergence of these diseases might prove particularly helpful in light of recent research into the cerebellum as a target for brain stimulation (Basavaraju et al., 2024).

References

Abele, M., Minnerop, M., Urbach, H., Specht, K., & Klockgether, T. (2007). Sporadic adult onset ataxia of unknown etiology. *Journal of Neurology*, *254*(10), 1384–1389. https://doi.org/10.1007/s00415-007-0556-1

Adamaszek, M., D'Agata, F., Ferrucci, R., Habas, C., Keulen, S., Kirkby, K. C., Leggio, M., Mariën, P., Molinari, M., Moulton, E., Orsi, L., Van Overwalle, F., Papadelis, C., Priori, A., Sacchetti, B., Schutter, D. J., Styliadis, C., & Verhoeven, J. (2017). Consensus paper: Cerebellum and emotion. *The Cerebellum*, *16*(2), 552–576. https://doi.org/10.1007/s12311-016-0815-8

Afzal, S., Recio, M., & Shamim, S. (2015). Paraneoplastic cerebellar ataxia and the paraneoplastic syndromes. *Baylor University Medical Center Proceedings*, *28*(2), 217–220. https://doi.org/10.1080/08998280.2015.11929234

Ahmadian, N., van Baarsen, K., van Zandvoort, M., & Robe, P. A. (2019). The Cerebellar Cognitive Affective Syndrome—A meta-analysis. *The Cerebellum*, *18*(5), 941–950. https://doi.org/10.1007/s12311-019-01060-2

Akam, T., Rodrigues-Vaz, I., Marcelo, I., Zhang, X., Pereira, M., Oliveira, R. F., Dayan, P., & Costa, R. M. (2021). The anterior cingulate cortex predicts future states to mediate model-based action selection. *Neuron*, *109*(1), 149-163.e7. https://doi.org/10.1016/j.neuron.2020.10.013

Albrecht, C., & Bellebaum, C. (2023). Slip or fallacy? Effects of error severity on own and observed pitch error processing in pianists. *Cognitive, Affective, & Behavioral Neuroscience*, *23*(4), 1076–1094. https://doi.org/10.3758/s13415-023-01097-1

Albus, J. S. (1971). A theory of cerebellar function. *Mathematical Biosciences*, *10*(1–2), 25–61. https://doi.org/10.1016/0025-5564(71)90051-4

Alexander, W. H., & Brown, J. W. (2011). Medial prefrontal cortex as an action-outcome predictor. *Nature Neuroscience*, *14*(10), 1338–1344. https://doi.org/10.1038/nn.2921

Alexander, W. H., & Brown, J. W. (2019). The role of the anterior cingulate cortex in prediction error and signaling surprise. *Topics in Cognitive Science*, *11*(1), 119–135. https://doi.org/10.1111/tops.12307

Amemori, K., Amemori, S., & Graybiel, A. M. (2015). Motivation and affective judgments differentially recruit neurons in the primate dorsolateral prefrontal and anterior cingulate cortex. *The Journal of Neuroscience*, *35*(5), 1939–1953. https://doi.org/10.1523/JNEUROSCI.1731-14.2015

Amiez, C., Sallet, J., Procyk, E., & Petrides, M. (2012). Modulation of feedback related activity in the rostral anterior cingulate cortex during trial and error exploration. *NeuroImage*, *63*(3), 1078–1090. https://doi.org/10.1016/j.neuroimage.2012.06.023

Andreasen, N. C., & Pierson, R. (2008). The role of the cerebellum in schizophrenia. *Biological Psychiatry*, *64*(2), 81–88. https://doi.org/10.1016/j.biopsych.2008.01.003

Araújo, A., Duarte, I. C., Sousa, T., Oliveira, J., Pereira, A. T., Macedo, A., & Castelo-Branco, M. (2024). Neural inhibition as implemented by an actor-critic model involves the human dorsal striatum and ventral tegmental area. *Scientific Reports*, *14*(1), 6363. https://doi.org/10.1038/s41598-024-56161-8

Arbel, Y., Hong, L., Baker, T. E., & Holroyd, C. B. (2017). It's all about timing: An electrophysiological examination of feedback-based learning with immediate and delayed feedback. *Neuropsychologia*, *99*, 179–186. https://doi.org/10.1016/j.neuropsychologia.2017.03.003

Ashida, R., Cerminara, N. L., Brooks, J., & Apps, R. (2018). Principles of organization of the human cerebellum: Macro- and microanatomy. In M.-U. Manto & T. A. G. M. Huisman (Eds.), *Handbook of Clinical Neurology* (Vol. 154, pp. 45–58). Elsevier. https://doi.org/10.1016/B978-0-444-63956-1.00003-5

Aupperle, R. L., & Paulus, M. (2010). Neural systems underlying approach and avoidance in anxiety disorders. *Dialogues in Clinical Neuroscience*, *12*(4), 517–531. https://doi.org/10.31887/DCNS.2010.12.4/raupperle

Averbeck, B. B., & Costa, V. D. (2017). Motivational neural circuits underlying reinforcement learning. *Nature Neuroscience*, *20*(4), 505–512. https://doi.org/10.1038/nn.4506

Averbeck, B. B., & O'Doherty, J. P. (2022). Reinforcement-learning in fronto-striatal circuits. *Neuropsychopharmacology*, *47*(1), 147–162. https://doi.org/10.1038/s41386-021-01108-0

Azevedo, F. A. C., Carvalho, L. R. B., Grinberg, L. T., Farfel, J. M., Ferretti, R. E. L., Leite, R. E. P., Filho, W. J., Lent, R., & Herculano-Houzel, S. (2009). Equal numbers of neuronal and nonneuronal cells make the human brain an isometrically scaled-up primate brain. *Journal of Comparative Neurology*, *513*(5), 532–541. https://doi.org/10.1002/cne.21974

Bagnall, M. W., Zingg, B., Sakatos, A., Moghadam, S. H., Zeilhofer, H. U., & Lac, S. du. (2009). Glycinergic projection neurons of the cerebellum. *The Journal of Neuroscience*, *29*(32), 10104–10110. https://doi.org/10.1523/JNEUROSCI.2087-09.2009

Balconi, M., & Scioli, S. (2012). Error monitoring functions in response to an external feedback when an explicit judgement is required: ERP modulation and cortical source localisation. *International Journal of Psychophysiology*, *83*(3), 295–301. https://doi.org/10.1016/j.ijpsycho.2011.11.005

Balleine, B. W., Delgado, M. R., & Hikosaka, O. (2007). The role of the dorsal striatum in reward and decision-making. *The Journal of Neuroscience*, *27*(31), 8161–8165. https://doi.org/10.1523/JNEUROSCI.1554-07.2007

Balsters, J. H., Cussans, E., Diedrichsen, J., Phillips, K. A., Preuss, T. M., Rilling, J. K., & Ramnani, N. (2010). Evolution of the cerebellar cortex: The selective expansion of prefrontal-projecting cerebellar lobules. *NeuroImage*, *49*(3), 2045–2052. https://doi.org/10.1016/j.neuroimage.2009.10.045

Balsters, J. H., & Ramnani, N. (2011). Cerebellar plasticity and the automation of first-order rules. *The Journal of Neuroscience*, *31*(6), 2305–2312. https://doi.org/10.1523/JNEUROSCI.4358-10.2011

Balsters, J. H., Whelan, C. D., Robertson, I. H., & Ramnani, N. (2013). Cerebellum and cognition: Evidence for the encoding of higher order rules. *Cerebral Cortex*, *23*(6), 1433–1443. https://doi.org/10.1093/cercor/bhs127

Bandura, A. (2008). Observational learning. In W. Donsbach (Ed.), *The International Encyclopedia of Communication* (1st ed.). John Wiley & Sons, Ltd. https://doi.org/10.1002/9781405186407.wbieco004

Bandura, A., Jeffery, R., & Bachicha, D. L. (1974). Analysis of memory codes and cumulative rehearsal in observational learning. *Journal of Research in Personality*, *7*(4), 295–305. https://doi.org/10.1016/0092-6566(74)90051-8

Barash, S., Melikyan, A., Sivakov, A., Zhang, M., Glickstein, M., & Thier, P. (1999). Saccadic dysmetria and adaptation after lesions of the cerebellar cortex. *The Journal of Neuroscience*, *19*(24), 10931–10939. https://doi.org/10.1523/JNEUROSCI.19-24-10931.1999

Bariselli, S., Fobbs, W. C., Creed, M. C., & Kravitz, A. V. (2019). A competitive model for striatal action selection. *Brain Research*, *1713*, 70–79. https://doi.org/10.1016/j.brainres.2018.10.009

Barto, A. G., Sutton, R. S., & Anderson, C. W. (1983). Neuronlike adaptive elements that can solve difficult learning control problems. *IEEE Transactions on Systems, Man, and Cybernetics*, *SMC-13*(5), 834–846. https://doi.org/10.1109/TSMC.1983.6313077

Basavaraju, R., Kaur, S., & Mehta, U. M. (2024). Cerebellar transcranial magnetic stimulation in psychiatric disorders: A systematic review. *Current Behavioral Neuroscience Reports*, *11*(1), 23–32. https://doi.org/10.1007/s40473-024-00270-1

Basile, G. A., Bertino, S., Bramanti, A., Ciurleo, R., Anastasi, G. P., Milardi, D., & Cacciola, A. (2021). Striatal topographical organization: Bridging the gap between molecules, connectivity and behavior. *European Journal of Histochemistry*, *65*(s1), 3284. https://doi.org/10.4081/ejh.2021.3284

Bates, D., Mächler, M., Bolker, B., & Walker, S. (2015). Fitting linear mixed-effects models using lme4. *Journal of Statistical Software*, *67*(1), 1–48. https://doi.org/10.18637/jss.v067.i01

Bauswein, E., Kolb, F. P., Leimbeck, B., & Rubia, F. J. (1983). Simple and complex spike activity of cerebellar Purkinje cells during active and passive movements in the awake monkey. *The Journal of Physiology*, *339*(1), 379–394. https://doi.org/10.1113/jphysiol.1983.sp014722

Bayer, H. M., & Glimcher, P. W. (2005). Midbrain dopamine neurons encode a quantitative reward prediction error signal. *Neuron*, *47*(1), 129–141. https://doi.org/10.1016/j.neuron.2005.05.020

Becker, M. P. I., Nitsch, A. M., Miltner, W. H. R., & Straube, T. (2014). A single-trial estimation of the feedback-related negativity and its relation to BOLD responses in a time-estimation task. *The Journal of Neuroscience*, *34*(8), 3005–3012. https://doi.org/10.1523/JNEUROSCI.3684-13.2014

Beier, K. T., Steinberg, E. E., DeLoach, K. E., Xie, S., Miyamichi, K., Schwarz, L., Gao, X. J., Kremer, E. J., Malenka, R. C., & Luo, L. (2015). Circuit architecture of VTA dopamine neurons revealed by systematic input-output mapping. *Cell*, *162*(3), 622–634. https://doi.org/10.1016/j.cell.2015.07.015

Bellebaum, C., & Colosio, M. (2014). From feedback- to response-based performance monitoring in active and observational learning. *Journal of Cognitive Neuroscience*, *26*(9), 2111–2127. https://doi.org/10.1162/jocn_a_00612

Bellebaum, C., & Daum, I. (2008). Learning-related changes in reward expectancy are reflected in the feedback-related negativity. *European Journal of Neuroscience*, *27*(7), 1823–1835. https://doi.org/10.1111/j.1460-9568.2008.06138.x

Bengtsson, F., & Hesslow, G. (2006). Cerebellar control of the inferior olive. *The Cerebellum*, *5*(1), 7–14. https://doi.org/10.1080/14734220500462757

Berciano, J. (2001). Multiple system atrophy and idiopathic late-onset cerebellar ataxia. In M.-U. Manto & M. Pandolfo (Eds.), *The Cerebellum and its Disorders* (pp. 178–197). Cambridge University Press; Cambridge Core. https://doi.org/10.1017/CBO9780511666469.013

Berlijn, A. M., Huvermann, D. M., Bechler, E., Thieme, A., Schnitzler, A., Bellebaum, C., Timmann, D., Minnerop, M., & Peterburs, J. (in press). Impaired reinforcement learning and coding of prediction errors in patients with cerebellar degeneration—A study with EEG and voxel-based morphometry. *Cognitive, Affective, & Behavioral Neuroscience*.

Berlijn, A. M., Huvermann, D. M., Schneider, S., Bellebaum, C., Timmann, D., Minnerop, M., & Peterburs, J. (2024). The role of the human cerebellum for learning from and processing of external feedback in non-motor learning: A systematic review. *The Cerebellum*, *23*, 1532–1551. https://doi.org/10.1007/s12311-024-01669-y

Bernstein, P. S., Scheffers, M. K., & Coles, M. G. H. (1995). “Where did I go wrong?” A psychophysiological analysis of error detection. *Journal of Experimental Psychology: Human Perception and Performance*, *21*(6), 1312–1322. https://doi.org/10.1037/0096-1523.21.6.1312

Bhatia, K. P., Bain, P., Bajaj, N., Elble, R. J., Hallett, M., Louis, E. D., Raethjen, J., Stamelou, M., Testa, C. M., Deuschl, G., & the Tremor Task Force of the International Parkinson and Movement Disorder Society. (2018). Consensus statement on the classification of tremors. From the task force on tremor of the International Parkinson and Movement Disorder Society. *Movement Disorders*, *33*(1), 75–87. https://doi.org/10.1002/mds.27121

Biswas, M. S., Roy, S. K., Hasan, R., & PK, M. M. U. (2024). The crucial role of the cerebellum in autism spectrum disorder: Neuroimaging, neurobiological, and anatomical insights. *Health Science Reports*, *7*(7), e2233. https://doi.org/10.1002/hsr2.2233

Błaszczyk, M., Ochwat, K., Necka, S., Kwiecińska, M., Ostrowski, P., Bonczar, M., Żytkowski, A., Walocha, J., Mituś, J., & Koziej, M. (2024). The arterial anatomy of the cerebellum—A comprehensive review. *Brain Sciences*, *14*(8), 763. https://doi.org/10.3390/brainsci14080763

Blithikioti, C., Nuño, L., Guell, X., Pascual-Diaz, S., Gual, A., Balcells-Olivero, M., & Miquel, L. (2022). The cerebellum and psychological trauma: A systematic review of neuroimaging studies. *Neurobiology of Stress*, *17*, 100429. https://doi.org/10.1016/j.ynstr.2022.100429

Bodranghien, F., Bastian, A., Casali, C., Hallett, M., Louis, E. D., Manto, M., Mariën, P., Nowak, D. A., Schmahmann, J. D., Serrao, M., Steiner, K. M., Strupp, M., Tilikete, C., Timmann, D., & van

Dun, K. (2016). Consensus paper: Revisiting the symptoms and signs of cerebellar syndrome. *The Cerebellum*, *15*(3), 369–391. https://doi.org/10.1007/s12311-015-0687-3

Boltzmann, L. (1868). Studien über das Gleichgewicht der lebenden Kraft. *Wissenschaftliche Abhandlungen*, *1*, 49–96.

Bostan, A. C., & Strick, P. L. (2018). The basal ganglia and the cerebellum: Nodes in an integrated network. *Nature Reviews Neuroscience*, *19*(6), 338–350. https://doi.org/10.1038/s41583-018-0002-7

Bostan, A. C., & Strick, P. L. (2022). Cerebellar outputs in non-human primates: An anatomical perspective using transsynaptic tracers. In M.-U. Manto, D. L. Gruol, J. D. Schmahmann, N. Koibuchi, & R. V. Sillitoe (Eds.), *Handbook of the Cerebellum and Cerebellar Disorders* (2nd ed., pp. 681–702). Springer Nature.

Botvinick, M., Nystrom, L. E., Fissell, K., Carter, C. S., & Cohen, J. D. (1999). Conflict monitoring versus selection-for-action in anterior cingulate cortex. *Nature*, *402*(6758), 179–181. https://doi.org/10.1038/46035

Bötzel, K., Rottach, K., & Büttner, U. (1993). Normal and pathological saccadic dysmetria. *Brain*, *116*(2), 337–353. https://doi.org/10.1093/brain/116.2.337

Brockett, A. T., Tennyson, S. S., deBettencourt, C. A., Gaye, F., & Roesch, M. R. (2020). Anterior cingulate cortex is necessary for adaptation of action plans. *Proceedings of the National Academy of Sciences*, *117*(11), 6196–6204. https://doi.org/10.1073/pnas.1919303117

Brunamonti, E., Chiricozzi, F. R., Clausi, S., Olivito, G., Giusti, M. A., Molinari, M., Ferraina, S., & Leggio, M. (2014). Cerebellar damage impairs executive control and monitoring of movement generation. *PLOS ONE*, *9*(1), e85997. https://doi.org/10.1371/journal.pone.0085997

Buckner, R. L., Krienen, F. M., Castellanos, A., Diaz, J. C., & Yeo, B. T. T. (2011). The organization of the human cerebellum estimated by intrinsic functional connectivity. *Journal of Neurophysiology*, *106*(5), 2322–2345. https://doi.org/10.1152/jn.00339.2011

Burnside, R., Fischer, A. G., & Ullsperger, M. (2019). The feedback-related negativity indexes prediction error in active but not observational learning. *Psychophysiology*, *56*(9), e13389. https://doi.org/10.1111/psyp.13389

Busch, S. E., & Hansel, C. (2023). Climbing fiber multi-innervation of mouse Purkinje dendrites with arborization common to human. *Science*, *381*(6656), 420–427. https://doi.org/10.1126/science.adi1024

Busch, S. E., & Hansel, C. (2024). Non-allometric expansion and enhanced compartmentalization of Purkinje cell dendrites in the human cerebellum. *bioRxiv*, 2024.09.09.612113. https://doi.org/10.1101/2024.09.09.612113

Camille, N., Tsuchida, A., & Fellows, L. K. (2011). Double dissociation of stimulus-value and action-value learning in humans with orbitofrontal or anterior cingulate cortex damage. *The Journal of Neuroscience*, *31*(42), 15048–15052. https://doi.org/10.1523/JNEUROSCI.3164-11.2011

Çan, M. K., Laakso, I., Nieminen, J. O., Murakami, T., & Ugawa, Y. (2018). Coil model comparison for cerebellar transcranial magnetic stimulation. *Biomedical Physics & Engineering Express*, *5*(1), 015020. https://doi.org/10.1088/2057-1976/aaee5b

Caplan, L. (2022). Vascular supply and territories of the cerebellum. In M.-U. Manto, D. L. Gruol, J. D. Schmahmann, N. Koibuchi, & R. V. Sillitoe (Eds.), *Handbook of the Cerebellum and Cerebellar Disorders* (2nd ed., pp. 451–466). Springer Nature.

Carta, I., Chen, C. H., Schott, A. L., Dorizan, S., & Khodakhah, K. (2019). Cerebellar modulation of the reward circuitry and social behavior. *Science*, *363*(6424), eaav0581. https://doi.org/10.1126/science.aav0581

Carter, Cameron S., Botvinick, Matthew M., & Cohen, Jonathan D. (1999). The contribution of the anterior cingulate cortex to executive processes in cognition. *Reviews in the Neurosciences*, *10*(1), 49–58. https://doi.org/10.1515/REVNEURO.1999.10.1.49

Castejon, O. J., & Sims, P. (2000). Three-dimensional morphology of cerebellar climbing fibers. A study by means of confocal laser scanning microscopy and scanning electron microscopy. *Scanning*, *22*(3), 211–217. https://doi.org/10.1002/sca.4950220309

Cauda, F., Cavanna, A. E., D'agata, F., Sacco, K., Duca, S., & Geminiani, G. C. (2011). Functional connectivity and coactivation of the nucleus accumbens: A combined functional connectivity and structure-based meta-analysis. *Journal of Cognitive Neuroscience*, *23*(10), 2864–2877. https://doi.org/10.1162/jocn.2011.21624

Cavanagh, J. F. (2015). Cortical delta activity reflects reward prediction error and related behavioral adjustments, but at different times. *NeuroImage*, *110*, 205–216. https://doi.org/10.1016/j.neuroimage.2015.02.007

Cavanagh, J. F., Bismark, A. W., Frank, M. J., & Allen, J. J. B. (2019). Multiple dissociations between comorbid depression and anxiety on reward and punishment processing: Evidence from computationally informed EEG. *Computational Psychiatry*, 1–17. https://doi.org/10.1162/CPSY_a_00024

Chase, H. W., Swainson, R., Durham, L., Benham, L., & Cools, R. (2011). Feedback-related negativity codes prediction error but not behavioral adjustment during probabilistic reversal learning. *Journal of Cognitive Neuroscience*, *23*(4), 936–946. https://doi.org/10.1162/jocn.2010.21456

Chatrian, G. E., Lettich, E., & Nelson, P. L. (1985). Ten percent electrode system for topographic studies of spontaneous and evoked EEG activities. *American Journal of EEG Technology*, *25*(2), 83–92. https://doi.org/10.1080/00029238.1985.11080163

Chaves, C. J., Caplan, L. R., Chung, C.-S., Tapia, J., Amarenco, P., Teal, P., Wityk, R., Estol, C., Tettenborn, B., Rosengart, A., Vemmos, K., DeWitt, L. D., & Pessin, M. S. (1994). Cerebellar infarcts in the New England Medical Center Posterior Circulation Stroke Registry. *Neurology*, *44*(8), 1385–1385. https://doi.org/10.1212/WNL.44.8.1385

Chen, Z., Zhang, R., Huo, H., Liu, P., Zhang, C., & Feng, T. (2022). Functional connectome of human cerebellum. *NeuroImage*, *251*, 119015. https://doi.org/10.1016/j.neuroimage.2022.119015

Chirino-Pérez, A., Marrufo-Meléndez, O. R., Muñoz-López, J. I., Hernandez-Castillo, C. R., Ramirez-Garcia, G., Díaz, R., Nuñez-Orozco, L., & Fernandez-Ruiz, J. (2022). Mapping the Cerebellar Cognitive Affective Syndrome in patients with chronic cerebellar strokes. *The Cerebellum*, *21*(2), 208–218. https://doi.org/10.1007/s12311-021-01290-3

Chowdhury, R., Lambert, C., Dolan, R. J., & Düzel, E. (2013). Parcellation of the human substantia nigra based on anatomical connectivity to the striatum. *NeuroImage*, *81*, 191–198. https://doi.org/10.1016/j.neuroimage.2013.05.043

Clairis, N., & Lopez-Persem, A. (2023). Debates on the dorsomedial prefrontal/dorsal anterior cingulate cortex: Insights for future research. *Brain*, *146*(12), 4826–4844. https://doi.org/10.1093/brain/awad263

Clarac, F., Massion, J., & Smith, A. M. (2009). Duchenne, Charcot and Babinski, three neurologists of La Salpetrière Hospital, and their contribution to concepts of the central organization of motor synergy. *Journal of Physiology-Paris*, *103*(6), 361–376. https://doi.org/10.1016/j.jphysparis.2009.09.001

Clark, R. E., & Squire, L. R. (1998). Classical conditioning and brain systems: The role of awareness. *Science*, *280*(5360), 77–81. https://doi.org/10.1126/science.280.5360.77

Clower, D. M., West, R. A., Lynch, J. C., & Strick, P. L. (2001). The inferior parietal lobule is the target of output from the superior colliculus, hippocampus, and cerebellum. *The Journal of Neuroscience*, *21*(16), 6283–6291. https://doi.org/10.1523/JNEUROSCI.21-16-06283.2001

Coenen, V. A., Schumacher, L. V., Kaller, C., Schlaepfer, T. E., Reinacher, P. C., Egger, K., Urbach, H., & Reisert, M. (2018). The anatomy of the human medial forebrain bundle: Ventral tegmental area connections to reward-associated subcortical and frontal lobe regions. *NeuroImage: Clinical*, *18*, 770–783. https://doi.org/10.1016/j.nicl.2018.03.019

Cohen, J. Y., Haesler, S., Vong, L., Lowell, B. B., & Uchida, N. (2012). Neuron-type-specific signals for reward and punishment in the ventral tegmental area. *Nature*, *482*(7383), 85–88. https://doi.org/10.1038/nature10754

Cohen, M. X., Elger, C. E., & Ranganath, C. (2007). Reward expectation modulates feedback-related negativity and EEG spectra. *NeuroImage*, *35*(2), 968–978. https://doi.org/10.1016/j.neuroimage.2006.11.056

Cohen, M. X., & Ranganath, C. (2007). Reinforcement learning signals predict future decisions. *The Journal of Neuroscience*, *27*(2), 371. https://doi.org/10.1523/JNEUROSCI.4421-06.2007

Coles, M. G. H., Scheffers, M. K., & Holroyd, C. B. (2001). Why is there an ERN/Ne on correct trials? Response representations, stimulus-related components, and the theory of error-processing. *Biological Psychology*, *56*(3), 173–189. https://doi.org/10.1016/S0301-0511(01)00076-X

Colin, F., Ris, L., & Godaux, E. (2001). Neuroanatomy of the cerebellum. In M.-U. Manto & M. Pandolfo (Eds.), *The Cerebellum and its Disorders* (pp. 6–29). Cambridge University Press; Cambridge Core. https://doi.org/10.1017/CBO9780511666469.013

Cook, R. D. (1977). Detection of influential observation in linear regression. *Technometrics*, *19*(1), 15–18. https://doi.org/10.1080/00401706.1977.10489493

Corballis, P. M. (2003). Visuospatial processing and the right-hemisphere interpreter. *Brain and Cognition*, *53*(2), 171–176. https://doi.org/10.1016/S0278-2626(03)00103-9

Corlett, P. R., Mollick, J. A., & Kober, H. (2022). Meta-analysis of human prediction error for incentives, perception, cognition, and action. *Neuropsychopharmacology*, *47*(7), 1339–1349. https://doi.org/10.1038/s41386-021-01264-3

Costa, V. D., Dal Monte, O., Lucas, D. R., Murray, E. A., & Averbeck, B. B. (2016). Amygdala and ventral striatum make distinct contributions to reinforcement learning. *Neuron*, *92*(2), 505–517. https://doi.org/10.1016/j.neuron.2016.09.025

Craig, B. T., Morrill, A., Anderson, B., Danckert, J., & Striemer, C. L. (2021). Cerebellar lesions disrupt spatial and temporal visual attention. *Cortex*, *139*, 27–42. https://doi.org/10.1016/j.cortex.2021.02.019

D'Angelo, E. (2016). Granule cells and parallel fibers. In D. L. Gruol, N. Koibuchi, M.-U. Manto, M. Molinari, J. D. Schmahmann, & Y. Shen (Eds.), *Essentials of Cerebellum and Cerebellar Disorders* (1st ed., pp. 177–182). Springer Nature.

Daniel, H., & Crepel, F. (2022). Purkinje neurons: Synaptic plasticity. In M.-U. Manto, D. L. Gruol, J. D. Schmahmann, N. Koibuchi, & R. V. Sillitoe (Eds.), *Handbook of the Cerebellum and Cerebellar Disorders* (2nd ed., pp. 863–880). Springer Nature.

D'Ardenne, K., McClure, S. M., Nystrom, L. E., & Cohen, J. D. (2008). BOLD responses reflecting dopaminergic signals in the human ventral tegmental area. *Science*, *319*(5867), 1264–1267. https://doi.org/10.1126/science.1150605

Darley, F. L., Aronson, A. E., & Brown, J. R. (1969a). Clusters of deviant speech dimensions in the dysarthrias. *Journal of Speech and Hearing Research*, *12*(3), 462–496. https://doi.org/10.1044/jshr.1203.462

Darley, F. L., Aronson, A. E., & Brown, J. R. (1969b). Differential diagnostic patterns of dysarthria. *Journal of Speech and Hearing Research*, *12*(2), 246–269. https://doi.org/10.1044/jshr.1202.246

Darmani, G., Bergmann, T. O., Butts Pauly, K., Caskey, C. F., de Lecea, L., Fomenko, A., Fouragnan, E., Legon, W., Murphy, K. R., Nandi, T., Phipps, M. A., Pinton, G., Ramezanpour, H., Sallet, J., Yaakub, S. N., Yoo, S. S., & Chen, R. (2022). Non-invasive transcranial ultrasound stimulation for neuromodulation. *Clinical Neurophysiology*, *135*, 51–73. https://doi.org/10.1016/j.clinph.2021.12.010

Davie, J. T., Clark, B. A., & Häusser, M. (2008). The origin of the complex spike in cerebellar Purkinje cells. *The Journal of Neuroscience*, *28*(30), 7599–7609. https://doi.org/10.1523/JNEUROSCI.0559-08.2008

Davies, P. L., Segalowitz, S. J., Dywan, J., & Pailing, P. E. (2001). Error-negativity and positivity as they relate to other ERP indices of attentional control and stimulus processing. *Biological Psychology*, *56*(3), 191–206. https://doi.org/10.1016/S0301-0511(01)00080-1

Dayan, P. (2004). Reinforcement learning. In H. Pashler & R. Gallistel (Eds.), *Steven's Handbook of Experimental Psychology* (3rd ed., Vol. 3, pp. 103–130). John Wiley & Sons.

Dayan, P., & Balleine, B. W. (2002). Reward, motivation, and reinforcement learning. *Neuron*, *36*(2), 285–298. https://doi.org/10.1016/S0896-6273(02)00963-7

De Smet, H. J., Baillieux, H., Wackenier, P., De Praeter, M., Engelborghs, S., Paquier, P. F., De Deyn, P. P., & Mariën, P. (2009). Long-term cognitive deficits following posterior fossa tumor resection: A neuropsychological and functional neuroimaging follow-up study. *Neuropsychology*, *23*(6), 694–704. https://doi.org/10.1037/a0016106

De Zeeuw, C. I., Hoogenraad, C. C., Koekkoek, S. K. E., Ruigrok, T. J. H., Galjart, N., & Simpson, J. I. (1998). Microcircuitry and function of the inferior olive. *Trends in Neurosciences*, *21*(9), 391–400. https://doi.org/10.1016/S0166-2236(98)01310-1

Del Cul, A., Baillet, S., & Dehaene, S. (2007). Brain dynamics underlying the nonlinear threshold for access to consciousness. *PLOS Biology*, *5*(10), e260. https://doi.org/10.1371/journal.pbio.0050260

Delion, M., Dinomais, M., & Mercier, P. (2017). Arteries and veins of the cerebellum. *The Cerebellum*, *16*(5), 880–912. https://doi.org/10.1007/s12311-016-0828-3

Derdeyn, P., Hui, M., Macchia, D., & Beier, K. T. (2022). Uncovering the connectivity logic of the ventral tegmental area. *Frontiers in Neural Circuits*, *15*, 799688. https://doi.org/10.3389/fncir.2021.799688

Desmond, J. E., Chen, S. H. A., & Shieh, P. B. (2005). Cerebellar transcranial magnetic stimulation impairs verbal working memory. *Annals of Neurology*, *58*(4), 553–560. https://doi.org/10.1002/ana.20604

Devinsky, O., Morrell, M. J., & Vogt, B. A. (1995). Contributions of anterior cingulate cortex to behaviour. *Brain*, *118*(1), 279–306. https://doi.org/10.1093/brain/118.1.279

Di Gregorio, F., Maier, M. E., & Steinhauser, M. (2018). Errors can elicit an error positivity in the absence of an error negativity: Evidence for independent systems of human error monitoring. *NeuroImage*, *172*, 427–436. https://doi.org/10.1016/j.neuroimage.2018.01.081

di Pellegrino, G., Ciaramelli, E., & Làdavas, E. (2007). The regulation of cognitive control following rostral anterior cingulate cortex lesion in humans. *Journal of Cognitive Neuroscience*, *19*(2), 275–286. https://doi.org/10.1162/jocn.2007.19.2.275

Dickson, P. E., Cairns, J., Goldowitz, D., & Mittleman, G. (2017). Cerebellar contribution to higher and lower order rule learning and cognitive flexibility in mice. *Neuroscience*, *345*, 99–109. https://doi.org/10.1016/j.neuroscience.2016.03.040

Diedrichsen, J. (2006). A spatially unbiased atlas template of the human cerebellum. *NeuroImage*, *33*(1), 127–138. https://doi.org/10.1016/j.neuroimage.2006.05.056

Diedrichsen, J., Balsters, J. H., Flavell, J., Cussans, E., & Ramnani, N. (2009). A probabilistic MR atlas of the human cerebellum. *NeuroImage*, *46*(1), 39–46. https://doi.org/10.1016/j.neuroimage.2009.01.045

Diedrichsen, J., King, M., Hernandez-Castillo, C., Sereno, M., & Ivry, R. B. (2019). Universal transform or multiple functionality? Understanding the contribution of the human cerebellum across task domains. *Neuron*, *102*(5), 918–928. https://doi.org/10.1016/j.neuron.2019.04.021

Diedrichsen, J., Maderwald, S., Küper, M., Thürling, M., Rabe, K., Gizewski, E. R., Ladd, M. E., & Timmann, D. (2011). Imaging the deep cerebellar nuclei: A probabilistic atlas and normalization procedure. *NeuroImage*, *54*(3), 1786–1794. https://doi.org/10.1016/j.neuroimage.2010.10.035

Dieudonné, S. (2016). Golgi neurons. In D. L. Gruol, N. Koibuchi, M.-U. Manto, M. Molinari, J. D. Schmahmann, & Y. Shen (Eds.), *Essentials of Cerebellum and Cerebellar Disorders* (1st ed., pp. 201–206). Springer Nature.

Dirnberger, G., Novak, J., Nasel, C., & Zehnter, M. (2010). Separating coordinative and executive dysfunction in cerebellar patients during motor skill acquisition. *Neuropsychologia*, *48*(5), 1200–1208. https://doi.org/10.1016/j.neuropsychologia.2009.12.016

D'Mello, A. M., & Stoodley, C. J. (2015). Cerebro-cerebellar circuits in autism spectrum disorder. *Frontiers in Neuroscience*, *9*, 408. https://doi.org/10.3389/fnins.2015.00408

Dohmatob, E., Dumas, G., & Bzdok, D. (2020). Dark control: The default mode network as a reinforcement learning agent. *Human Brain Mapping*, *41*(12), 3318–3341. https://doi.org/10.1002/hbm.25019

Domenech, P., & Koechlin, E. (2015). Executive control and decision-making in the prefrontal cortex. *Current Opinion in Behavioral Sciences*, *1*, 101–106. https://doi.org/10.1016/j.cobeha.2014.10.007

Doubliez, A., Nio, E., Senovilla-Sanz, F., Spatharioti, V., Apps, R., Timmann, D., & Lawrenson, C. L. (2023). The cerebellum and fear extinction: Evidence from rodent and human studies. *Frontiers in Systems Neuroscience*, *17*, 1166166. https://doi.org/10.3389/fnsys.2023.1166166

Duquette, P. (2001). Immune diseases. In M.-U. Manto & M. Pandolfo (Eds.), *The Cerebellum and its Disorders* (pp. 228–236). Cambridge University Press; Cambridge Core. https://doi.org/10.1017/CBO9780511666469.016

Edlow, J. A., Newman-Toker, D. E., & Savitz, S. I. (2008). Diagnosis and initial management of cerebellar infarction. *The Lancet Neurology*, *7*(10), 951–964. https://doi.org/10.1016/S1474-4422(08)70216-3

Elston, T. W., Croy, E., & Bilkey, D. K. (2019). Communication between the anterior cingulate cortex and ventral tegmental area during a cost-benefit reversal task. *Cell Reports*, *26*(9), 2353-2361.e3. https://doi.org/10.1016/j.celrep.2019.01.113

Elston, T. W., Kalhan, S., & Bilkey, D. K. (2018). Conflict and adaptation signals in the anterior cingulate cortex and ventral tegmental area. *Scientific Reports*, *8*(1), 11732. https://doi.org/10.1038/s41598-018-30203-4

Emeric, E. E., Brown, J. W., Leslie, M., Pouget, P., Stuphorn, V., & Schall, J. D. (2008). Performance monitoring local field potentials in the medial frontal cortex of primates: Anterior cingulate cortex. *Journal of Neurophysiology*, *99*(2), 759–772. https://doi.org/10.1152/jn.00896.2006

Eppinger, B., Kray, J., Mock, B., & Mecklinger, A. (2008). Better or worse than expected? Aging, learning, and the ERN. *Neuropsychologia*, *46*(2), 521–539. https://doi.org/10.1016/j.neuropsychologia.2007.09.001

Erdlenbruch, F., Timmann, D., & Thieme, A. (2024). Clinical cerebellar neuroscience: Ataxias—Cognitive and affective symptoms in focal cerebellar lesions. *Current Opinion in Behavioral Sciences*, *55*, 101331. https://doi.org/10.1016/j.cobeha.2023.101331

Ernst, T. M., Brol, A. E., Gratz, M., Ritter, C., Bingel, U., Schlamann, M., Maderwald, S., Quick, H. H., Merz, C. J., & Timmann, D. (2019). The cerebellum is involved in processing of predictions and prediction errors in a fear conditioning paradigm. *eLife*, *8*, e46831. https://doi.org/10.7554/eLife.46831

Etkin, A., Prater, K. E., Schatzberg, A. F., Menon, V., & Greicius, M. D. (2009). Disrupted amygdalar subregion functional connectivity and evidence of a compensatory network in generalized anxiety disorder. *Archives of General Psychiatry*, *66*(12), 1361–1372. https://doi.org/10.1001/archgenpsychiatry.2009.104

Falkenstein, M., Hohnsbein, J., Hoormann, J., & Blanke, L. (1991). Effects of crossmodal divided attention on late ERP components. II. Error processing in choice reaction tasks. *Electroencephalography and Clinical Neurophysiology*, *78*(6), 447–455. https://doi.org/10.1016/0013-4694(91)90062-9

Fan, L., Hu, J., Ma, W., Wang, D., Yao, Q., & Shi, J. (2019). Altered baseline activity and connectivity associated with cognitive impairment following acute cerebellar infarction: A resting-state fMRI study. *Neuroscience Letters*, *692*, 199–203. https://doi.org/10.1016/j.neulet.2018.11.007

Faßbender, L., Krause, D., & Weigelt, M. (2023). Feedback processing in cognitive and motor tasks: A meta-analysis on the feedback-related negativity. *Psychophysiology*, *60*(12), e14439. https://doi.org/10.1111/psyp.14439

Faull, R. L. M., & Carman, J. B. (1968). Ascending projections of the substantia nigra in the rat. *Journal of Comparative Neurology*, *132*(1), 73–91. https://doi.org/10.1002/cne.901320104

Fellows, L. K., & Farah, M. J. (2007). The role of ventromedial prefrontal cortex in decision making: Judgment under uncertainty or judgment per se? *Cerebral Cortex*, *17*(11), 2669–2674. https://doi.org/10.1093/cercor/bhl176

Fernandez, L., Major, B. P., Teo, W.-P., Byrne, L. K., & Enticott, P. G. (2018). Assessing cerebellar brain inhibition (CBI) via transcranial magnetic stimulation (TMS): A systematic review. *Neuroscience & Biobehavioral Reviews*, *86*, 176–206. https://doi.org/10.1016/j.neubiorev.2017.11.018

Fernandez, L., Rogasch, N. C., Do, M., Clark, G., Major, B. P., Teo, W.-P., Byrne, L. K., & Enticott, P. G. (2020). Cerebral cortical activity following non-invasive cerebellar stimulation—A systematic review of combined TMS and EEG studies. *The Cerebellum*, *19*(2), 309–335. https://doi.org/10.1007/s12311-019-01093-7

Fiorillo, C. D. (2013). Two dimensions of value: Dopamine neurons represent reward but not aversiveness. *Science*, *341*(6145), 546–549. https://doi.org/10.1126/science.1238699

Fischer, A. G., & Ullsperger, M. (2013). Real and fictive outcomes are processed differently but converge on a common adaptive mechanism. *Neuron*, *79*(6), 1243–1255.

Foerde, K., & Shohamy, D. (2011). Feedback timing modulates brain systems for learning in humans. *The Journal of Neuroscience*, *31*(37), 13157–13167. https://doi.org/10.1523/JNEUROSCI.2701-11.2011

Fouragnan, E., Retzler, C., & Philiastides, M. G. (2018). Separate neural representations of prediction error valence and surprise: Evidence from an fMRI meta-analysis. *Human Brain Mapping*, *39*(7), 2887–2906. https://doi.org/10.1002/hbm.24047

Fraser, K. M., Pribut, H. J., Janak, P. H., & Keiflin, R. (2023). From prediction to action: Dissociable roles of ventral tegmental area and substantia nigra dopamine neurons in instrumental reinforcement. *The Journal of Neuroscience*, *43*(21), 3895–3908. https://doi.org/10.1523/JNEUROSCI.0028-23.2023

Frings, M., Boenisch, R., Gerwig, M., Diener, H.-C., & Timmann, D. (2004). Learning of sensory sequences in cerebellar patients. *Learning and Memory*, *11*(3), 347–355. https://doi.org/10.1101/lm.66904

Frömer, R., Nassar, M. R., Bruckner, R., Stürmer, B., Sommer, W., & Yeung, N. (2021). Response-based outcome predictions and confidence regulate feedback processing and learning. *eLife*, *10*, e62825. https://doi.org/10.7554/eLife.62825

Galliano, E., Mazzarello, P., & D'Angelo, E. (2010). Discovery and rediscoveries of Golgi cells. *The Journal of Physiology*, *588*(19), 3639–3655. https://doi.org/10.1113/jphysiol.2010.189605

Gardner, R., Coleman, L. T., Mitchell, L., Smith, L., Harvey, A. S., Scheffer, I. E., Storey, E., Nowotny, M., Sloane, R., & Lubitz, L. (2001). Near-total absence of the cerebellum. *Neuropediatrics*, *32*(2), 62–68. https://doi.org/10.1055/s-2001-13882

Gatti, D., Rinaldi, L., Vecchi, T., & Ferrari, C. (2023). Understanding cerebellar cognitive and social functions: Methodological challenges and new directions for future transcranial magnetic stimulation studies. *Current Opinion in Behavioral Sciences*, *53*, 101300. https://doi.org/10.1016/j.cobeha.2023.101300

Gehring, W. J., Goss, B., Coles, M. G. H., Meyer, D. E., & Donchin, E. (1993). A neural system for error detection and compensation. *Psychological Science*, *4*(6), 385–390. https://doi.org/10.1111/j.1467-9280.1993.tb00586.x

Gehring, W. J., Goss, B., Coles, M. G. H., Meyer, D. E., & Donchin, E. (2018). The error-related negativity. *Perspectives on Psychological Science*, *13*(2), 200–204. https://doi.org/10.1177/1745691617715310

Gershman, S. J., Norman, K. A., & Niv, Y. (2015). Discovering latent causes in reinforcement learning. *Neuroeconomics*, *5*, 43–50. https://doi.org/10.1016/j.cobeha.2015.07.007

Glickstein, M. (2022). Visual circuits from cerebral cortex to cerebellum; The link through pons. In M.-U. Manto, D. L. Gruol, J. D. Schmahmann, N. Koibuchi, & R. V. Sillitoe (Eds.), *Handbook of the Cerebellum and Cerebellar Disorders* (2nd ed., pp. 595–604). Springer Nature.

Glickstein, M., Gerrits, N., Kralj-Hans, I., Mercier, B., Stein, J., & Voogd, J. (1994). Visual pontocerebellar projections in the macaque. *Journal of Comparative Neurology*, *349*(1), 51–72. https://doi.org/10.1002/cne.903490105

Glickstein, M., May III, J. G., & Mercier, B. E. (1985). Corticopontine projection in the macaque: The distribution of labelled cortical cells after large injections of horseradish peroxidase in the pontine nuclei. *Journal of Comparative Neurology*, *235*(3), 343–359. https://doi.org/10.1002/cne.902350306

Glickstein, M., Strata, P., & Voogd, J. (2009). Cerebellum: History. *Neuroscience*, *162*(3), 549–559. https://doi.org/10.1016/j.neuroscience.2009.02.054

Gołembiowska, K., Berghauzen-Maciejewska, K., Górska, A., Kamińska, K., & Ossowska, K. (2013). A partial lesion of the substantia nigra pars compacta and retrorubral field decreases the harmaline-induced glutamate release in the rat cerebellum. *Brain Research*, *1537*, 303–311. https://doi.org/10.1016/j.brainres.2013.08.059

Gorsler, A., Bäumer, T., Weiller, C., Münchau, A., & Liepert, J. (2003). Interhemispheric effects of high and low frequency rTMS in healthy humans. *Clinical Neurophysiology*, *114*(10), 1800–1807. https://doi.org/10.1016/S1388-2457(03)00157-3

Gottwald, B., Mihajlovic, Z., Wilde, B., & Mehdorn, H. M. (2003). Does the cerebellum contribute to specific aspects of attention? *Neuropsychologia*, *41*(11), 1452–1460. https://doi.org/10.1016/S0028-3932(03)00090-3

Grangeray, A., Dorgans, K., Roux, S., & Bossu, J.-L. (2016). The Purkinje cell: As an integrative machine. In D. L. Gruol, N. Koibuchi, M.-U. Manto, M. Molinari, J. D. Schmahmann, & Y. Shen (Eds.), *Essentials of Cerebellum and Cerebellar Disorders* (1st ed., pp. 183–188). Springer Nature.

Groman, S. M., Lee, D., & Taylor, J. R. (2021). Unlocking the reinforcement-learning circuits of the orbitofrontal cortex. *Behavioral Neuroscience*, *135*(2), 120–128. https://doi.org/10.1037/bne0000414

Guell, X., Gabrieli, J. D. E., & Schmahmann, J. D. (2018). Embodied cognition and the cerebellum: Perspectives from the dysmetria of thought and the universal cerebellar transform theories. *Cortex*, *100*, 140–148. https://doi.org/10.1016/j.cortex.2017.07.005

Guerrero, L., Bouazzaoui, B., Isingrini, M., & Angel, L. (2022). Involvement of executive control in neural capacity related to working memory in aging: An ERP P300 study. *Cognitive, Affective, & Behavioral Neuroscience*, *22*(6), 1311–1333. https://doi.org/10.3758/s13415-022-01018-8

Habas, C. (2021). Functional connectivity of the cognitive cerebellum. *Frontiers in Systems Neuroscience*, *15*, 642225. https://doi.org/10.3389/fnsys.2021.642225

Habas, C., Kamdar, N., Nguyen, D., Prater, K., Beckmann, C. F., Menon, V., & Greicius, M. D. (2009). Distinct cerebellar contributions to intrinsic connectivity networks. *The Journal of Neuroscience*, *29*(26), 8586–8594. https://doi.org/10.1523/JNEUROSCI.1868-09.2009

Haber, S. N. (2011). Neuroanatomy of reward: A view from the ventral striatum. In J. A. Gottfried (Ed.), *Neurobiology of Sensation and Reward.* (pp. 235–262). CRC Press/Taylor & Francis.

Haines, D. E. (2016). Pivotal insights: The contributions of Gordon Holmes (1876–1965) and Olof Larsell (1886–1964) to our understanding of cerebellar function and structure. In D. L. Gruol, N.

Koibuchi, M.-U. Manto, M. Molinari, J. D. Schmahmann, & Y. Shen (Eds.), *Essentials of Cerebellum and Cerebellar Disorders* (1st ed., pp. 21–32). Springer Nature.

Hajcak, G., & Foti, D. (2008). Errors are aversive: Defensive motivation and the error-related negativity. *Psychological Science*, *19*(2), 103–108. https://doi.org/10.1111/j.1467-9280.2008.02053.x

Hajcak, G., Holroyd, C. B., Moser, J. S., & Simons, R. F. (2005). Brain potentials associated with expected and unexpected good and bad outcomes. *Psychophysiology*, *42*(2), 161–170. https://doi.org/10.1111/j.1469-8986.2005.00278.x

Hajcak, G., Moser, J. S., Holroyd, C. B., & Simons, R. F. (2007). It's worse than you thought: The feedback negativity and violations of reward prediction in gambling tasks. *Psychophysiology*, *44*(6), 905–912. https://doi.org/10.1111/j.1469-8986.2007.00567.x

Ham, T., Leff, A., de Boissezon, X., Joffe, A., & Sharp, D. J. (2013). Cognitive control and the salience network: An investigation of error processing and effective connectivity. *The Journal of Neuroscience*, *33*(16), 7091–7098. https://doi.org/10.1523/JNEUROSCI.4692-12.2013

Hannah, R., Rocchi, L., Tremblay, S., Wilson, E., & Rothwell, J. C. (2020). Pulse width biases the balance of excitation and inhibition recruited by transcranial magnetic stimulation. *Brain Stimulation: Basic, Translational, and Clinical Research in Neuromodulation*, *13*(3), 536–538. https://doi.org/10.1016/j.brs.2020.01.011

Harris, J. A., Clifford, C. W. G., & Miniussi, C. (2008). The functional effect of transcranial magnetic stimulation: Signal suppression or neural noise generation? *Journal of Cognitive Neuroscience*, *20*(4), 734–740. https://doi.org/10.1162/jocn.2008.20048

Haruno, M., & Kawato, M. (2006). Heterarchical reinforcement-learning model for integration of multiple cortico-striatal loops: fMRI examination in stimulus-action-reward association learning. *Neural Networks*, *19*(8), 1242–1254. https://doi.org/10.1016/j.neunet.2006.06.007

Hattori, R., Hedrick, N. G., Jain, A., Chen, S., You, H., Hattori, M., Choi, J.-H., Lim, B. K., Yasuda, R., & Komiyama, T. (2023). Meta-reinforcement learning via orbitofrontal cortex. *Nature Neuroscience*, *26*(12), 2182–2191. https://doi.org/10.1038/s41593-023-01485-3

Hauser, T. U., Iannaccone, R., Stämpfli, P., Drechsler, R., Brandeis, D., Walitza, S., & Brem, S. (2014). The feedback-related negativity (FRN) revisited: New insights into the localization, meaning and network organization. *NeuroImage*, *84*, 159–168. https://doi.org/10.1016/j.neuroimage.2013.08.028

Hawkins, R. D., & Byrne, J. H. (2015). Associative learning in invertebrates. *Cold Spring Harbor Perspectives in Biology*, *7*(5), a021709. https://doi.org/10.1101/cshperspect.a021709

Heffley, W., & Hull, C. (2019). Classical conditioning drives learned reward prediction signals in climbing fibers across the lateral cerebellum. *eLife*, *8*, e46764. https://doi.org/10.7554/eLife.46764

Heffley, W., Song, E. Y., Xu, Z., Taylor, B. N., Hughes, M. A., McKinney, A., Joshua, M., & Hull, C. (2018). Coordinated cerebellar climbing fiber activity signals learned sensorimotor predictions. *Nature Neuroscience*, *21*(10), 1431–1441. https://doi.org/10.1038/s41593-018-0228-8

Herbert, M., Eppinger, B., & Kray, J. (2011). Younger but not older adults benefit from salient feedback during learning. *Frontiers in Psychology*, *2*. https://doi.org/10.3389/fpsyg.2011.00171

Herculano-Houzel, S. (2010). Coordinated scaling of cortical and cerebellar numbers of neurons. *Frontiers in Neuroanatomy*, *4*, 12. https://doi.org/10.3389/fnana.2010.00012

Herrmann, M. J., Römmler, J., Ehlis, A.-C., Heidrich, A., & Fallgatter, A. J. (2004). Source localization (LORETA) of the error-related-negativity (ERN/Ne) and positivity (Pe). *Cognitive Brain Research*, *20*(2), 294–299. https://doi.org/10.1016/j.cogbrainres.2004.02.013

Hester, R., Foxe, J. J., Molholm, S., Shpaner, M., & Garavan, H. (2005). Neural mechanisms involved in error processing: A comparison of errors made with and without awareness. *NeuroImage*, *27*(3), 602–608. https://doi.org/10.1016/j.neuroimage.2005.04.035

Hinneberg, B. M., & Hegele, M. (2022). Acting in temporal contexts: On the behavioral and neurophysiological consequences of feedback delays. *Neuroscience*, *486*, 91–102. https://doi.org/10.1016/j.neuroscience.2021.06.028

Hirono, M. (2016). Lugaro cells. In D. L. Gruol, N. Koibuchi, M.-U. Manto, M. Molinari, J. D. Schmahmann, & Y. Shen (Eds.), *Essentials of Cerebellum and Cerebellar Disorders* (1st ed., pp. 207–212). Springer Nature.

Hiser, J., & Koenigs, M. (2018). The multifaceted role of the ventromedial prefrontal cortex in emotion, decision making, social cognition, and psychopathology. *Biological Psychiatry*, *83*(8), 638–647. https://doi.org/10.1016/j.biopsych.2017.10.030

Hoche, F., Guell, X., Vangel, M. G., Sherman, J. C., & Schmahmann, J. D. (2018). The Cerebellar Cognitive Affective/Schmahmann Syndrome Scale. *Brain*, *141*(1), 248–270. https://doi.org/10.1093/brain/awx317

Hochman, E. Y., Eviatar, Z., Breznitz, Z., Nevat, M., & Shaul, S. (2009). Source localization of error negativity: Additional source for corrected errors. *NeuroReport*, *20*(13), 1144–1148. https://doi.org/10.1097/WNR.0b013e32832f84ed

Holmes, G. (1917). The symptoms of acute cerebellar injuries due to gunshot injuries. *Brain*, *40*(4), 461–535.

Holroyd, C. B., & Coles, M. G. H. (2002). The neural basis of human error processing: Reinforcement learning, dopamine, and the error-related negativity. *Psychological Review*, *109*(4), 679–709. https://doi.org/10.1037/0033-295X.109.4.679

Holroyd, C. B., Nieuwenhuis, S., Mars, R. B., & Coles, M. G. (2004). Anterior cingulate cortex, selection for action, and error processing. *Cognitive Neuroscience of Attention*, 219–231.

Holroyd, C. B., Pakzad-Vaezi, K. L., & Krigolson, O. E. (2008). The feedback correct-related positivity: Sensitivity of the event-related brain potential to unexpected positive feedback. *Psychophysiology*, *45*(5), 688–697. https://doi.org/10.1111/j.1469-8986.2008.00668.x

Holroyd, C. B., & Verguts, T. (2021). The best laid plans: Computational principles of anterior cingulate cortex. *Trends in Cognitive Sciences*, *25*(4), 316–329. https://doi.org/10.1016/j.tics.2021.01.008

Höltje, G., & Mecklinger, A. (2020). Feedback timing modulates interactions between feedback processing and memory encoding: Evidence from event-related potentials. *Cognitive, Affective, & Behavioral Neuroscience*, *20*(2), 250–264. https://doi.org/10.3758/s13415-019-00765-5

Hore, J., Wild, B., & Diener, H. C. (1991). Cerebellar dysmetria at the elbow, wrist, and fingers. *Journal of Neurophysiology*, *65*(3), 563–571. https://doi.org/10.1152/jn.1991.65.3.563

Hoshi, E., Tremblay, L., Féger, J., Carras, P. L., & Strick, P. L. (2005). The cerebellum communicates with the basal ganglia. *Nature Neuroscience*, *8*(11), 1491–1493. https://doi.org/10.1038/nn1544

Hoshino, M., Miyashita, S., Seto, Y., & Yamada, M. (2022). Specification of cerebellar and precerebellar neurons. In M.-U. Manto, D. L. Gruol, J. D. Schmahmann, N. Koibuchi, & R. V. Sillitoe (Eds.), *Handbook of the Cerebellum and Cerebellar Disorders* (2nd ed., pp. 83–98). Springer Nature.

Hosp, J. A., Coenen, V. A., Rijntjes, M., Egger, K., Urbach, H., Weiller, C., & Reisert, M. (2019). Ventral tegmental area connections to motor and sensory cortical fields in humans. *Brain Structure and Function*, *224*(8), 2839–2855. https://doi.org/10.1007/s00429-019-01939-0

Hoy, C. W., Steiner, S. C., & Knight, R. T. (2021). Single-trial modeling separates multiple overlapping prediction errors during reward processing in human EEG. *Communications Biology*, *4*(1), 910. https://doi.org/10.1038/s42003-021-02426-1

Hudson, D. B., Valcana, T., Bean, G., & Timiras, P. S. (1976). Glutamic acid: A strong candidate as the neurotransmitter of the cerebellar granule cell. *Neurochemical Research*, *1*(1), 73–81. https://doi.org/10.1007/BF00965633

Hüfner, K., Stephan, T., Kalla, R., Deutschländer, A., Wagner, J., Holtmannspötter, M., Schulte-Altedorneburg, G., Strupp, M., Brandt, T., & Glasauer, S. (2007). Structural and functional MRIs

disclose cerebellar pathologies in idiopathic downbeat nystagmus. *Neurology*, *69*(11), 1128–1135. https://doi.org/10.1212/01.wnl.0000276953.00969.48

Hull, C. (2020). Prediction signals in the cerebellum: Beyond supervised motor learning. *Elife*, *9*, e54073. https://doi.org/10.7554/eLife.54073

Humann, J., Fischer, A. G., & Ullsperger, M. (2020). The dynamics of feedback-based learning is modulated by working memory capacity. *Psyarxiv*. https://doi.org/10.31234/osf.io/8qzu2

Ichikawa, N., Siegle, G. J., Dombrovski, A., & Ohira, H. (2010). Subjective and model-estimated reward prediction: Association with the feedback-related negativity (FRN) and reward prediction error in a reinforcement learning task. *International Journal of Psychophysiology*, *78*(3), 273–283. https://doi.org/10.1016/j.ijpsycho.2010.09.001

Ichinohe, N., Mori, F., & Shoumura, K. (2000). A di-synaptic projection from the lateral cerebellar nucleus to the laterodorsal part of the striatum via the central lateral nucleus of the thalamus in the rat. *Brain Research*, *880*(1), 191–197. https://doi.org/10.1016/S0006-8993(00)02744-X

Ilango, A., Kesner, A. J., Keller, K. L., Stuber, G. D., Bonci, A., & Ikemoto, S. (2014). Similar roles of substantia nigra and ventral tegmental dopamine neurons in reward and aversion. *The Journal of Neuroscience*, *34*(3), 817–822. https://doi.org/10.1523/JNEUROSCI.1703-13.2014

Ilg, W., Christensen, A., Mueller, O. M., Goericke, S. L., Giese, M. A., & Timmann, D. (2013). Effects of cerebellar lesions on working memory interacting with motor tasks of different complexities. *Journal of Neurophysiology*, *110*(10), 2337–2349. https://doi.org/10.1152/jn.00062.2013

Ishikawa, T., Tomatsu, S., Izawa, J., & Kakei, S. (2016). The cerebro-cerebellum: Could it be loci of forward models? *Neuroscience Research*, *104*, 72–79. https://doi.org/10.1016/j.neures.2015.12.003

Ito, M. (1998). Cerebellar learning in the vestibulo–ocular reflex. *Trends in Cognitive Sciences*, *2*(9), 313–321. https://doi.org/10.1016/S1364-6613(98)01222-4

Ito, M. (2009). Cerebellar microcircuitry. In L. R. Squire (Ed.), *Encyclopedia of Neuroscience* (pp. 723–728). Academic Press. https://doi.org/10.1016/B978-008045046-9.01306-1

Ito, M., Yoshida, M., Obata, K., Kawai, N., & Udo, M. (1970). Inhibitory control of intracerebellar nuclei by the Purkinje cell axons. *Experimental Brain Research*, *10*(1), 64–80. https://doi.org/10.1007/BF00340519

Jocham, G., Klein, T. A., & Ullsperger, M. (2011). Dopamine-mediated reinforcement learning signals in the striatum and ventromedial prefrontal cortex underlie value-based choices. *The Journal of Neuroscience*, *31*(5), 1606–1613. https://doi.org/10.1523/JNEUROSCI.3904-10.2011

Johnson, J. F., Belyk, M., Schwartze, M., Pinheiro, A. P., & Kotz, S. A. (2019). The role of the cerebellum in adaptation: ALE meta-analyses on sensory feedback error. *Human Brain Mapping*, *40*(13), 3966–3981. https://doi.org/10.1002/hbm.24681

Jung, J., Bungert, A., Bowtell, R., & Jackson, S. R. (2016). Vertex stimulation as a control site for transcranial magnetic stimulation: A concurrent TMS/fMRI study. *Brain Stimulation*, *9*(1), 58–64. https://doi.org/10.1016/j.brs.2015.09.008

Kammer, T. (1998). Phosphenes and transient scotomas induced by magnetic stimulation of the occipital lobe: Their topographic relationship. *Neuropsychologia*, *37*(2), 191–198. https://doi.org/10.1016/S0028-3932(98)00093-1

Kaplan, A., Mizrahi-Kliger, A. D., Israel, Z., Adler, A., & Bergman, H. (2020). Dissociable roles of ventral pallidum neurons in the basal ganglia reinforcement learning network. *Nature Neuroscience*, *23*(4), 556–564. https://doi.org/10.1038/s41593-020-0605-y

Kawai, T., Yamada, H., Sato, N., Takada, M., & Matsumoto, M. (2015). Roles of the lateral habenula and anterior cingulate cortex in negative outcome monitoring and behavioral adjustment in nonhuman primates. *Neuron*, *88*(4), 792–804. https://doi.org/10.1016/j.neuron.2015.09.030

Kawato, M., Ohmae, S., Hoang, H., & Sanger, T. (2021). 50 years since the Marr, Ito, and Albus models of the cerebellum. *Neuroscience*, *462*, 151–174. https://doi.org/10.1016/j.neuroscience.2020.06.019

Kebschull, J. M., Casoni, F., Consalez, G. G., Goldowitz, D., Hawkes, R., Ruigrok, T. J. H., Schilling, K., Wingate, R., Wu, J., Yeung, J., & Uusisaari, M. Y. (2024). Cerebellum lecture: The cerebellar nuclei—Core of the cerebellum. *The Cerebellum*, *23*(2), 620–677. https://doi.org/10.1007/s12311-022-01506-0

Kelly, P. J., Stein, J., Shafqat, S., Eskey, C., Doherty, D., Chang, Y., Kurina, A., & Furie, K. L. (2001). Functional recovery after rehabilitation for cerebellar stroke. *Stroke*, *32*(2), 530–534. https://doi.org/10.1161/01.STR.32.2.530

Kelly, R. M., & Strick, P. L. (2003). Cerebellar loops with motor cortex and prefrontal cortex of a nonhuman primate. *The Journal of Neuroscience*, *23*(23), 8432–8444. https://doi.org/10.1523/JNEUROSCI.23-23-08432.2003

Kennerley, S. W., Walton, M. E., Behrens, T. E. J., Buckley, M. J., & Rushworth, M. F. S. (2006). Optimal decision making and the anterior cingulate cortex. *Nature Neuroscience*, *9*(7), 940–947. https://doi.org/10.1038/nn1724

Kent, R. D., Kent, J. F., Duffy, J. R., Thomas, J. E., Weismer, G., & Stuntebeck, S. (2000). Ataxic dysarthria. *Journal of Speech, Language, and Hearing Research*, *43*(5), 1275–1289. https://doi.org/10.1044/jslhr.4305.1275

Kiehl, K. A., Liddle, P. F., & Hopfinger, J. B. (2000). Error processing and the rostral anterior cingulate: An event-related fMRI study. *Psychophysiology*, *37*(2), 216–223. Cambridge Core. https://doi.org/10.1111/1469-8986.3720216

King, M., Hernandez-Castillo, C. R., Poldrack, R. A., Ivry, R. B., & Diedrichsen, J. (2019). Functional boundaries in the human cerebellum revealed by a multi-domain task battery. *Nature Neuroscience*, *22*(8), 1371–1378. https://doi.org/10.1038/s41593-019-0436-x

Kirchkamp, O., Nagel, R. C., Sarin, R., Montuori, A., Rowe, J., Mott, B., Lester, J., Armstrong, J. S., Spector, M. J., & Burns, G. W. (2012). Nonassociative learning. In N. M. Seel (Ed.), *Encyclopedia of the Sciences of Learning* (pp. 2475–2477). Springer US.

Kirschner, H., Fischer, A. G., & Ullsperger, M. (2022). Feedback-related EEG dynamics separately reflect decision parameters, biases, and future choices. *NeuroImage*, *259*, 119437. https://doi.org/10.1016/j.neuroimage.2022.119437

Klockgether, T., Synofzik, M., Alhusaini, S., Anheim, M., Antonijevic, I., Ashizawa, T., Bataller, L., Berard, M., Bertini, E., Boesch, S., Braga-Neto, P., Cassou, E., Chan, E., Chuang, R., Collins, A., Damásio, J., Donis, K., Duquette, A., Durães, J., … AGI working group on COAs and Registries. (2024). Consensus recommendations for clinical outcome assessments and registry development in ataxias: Ataxia Global Initiative (AGI) working group expert guidance. *The Cerebellum*, *23*(3), 924–930. https://doi.org/10.1007/s12311-023-01547-z

Klomjai, W., Katz, R., & Lackmy-Vallée, A. (2015). Basic principles of transcranial magnetic stimulation (TMS) and repetitive TMS (rTMS). *Annals of Physical and Rehabilitation Medicine*, *58*(4), 208–213. https://doi.org/10.1016/j.rehab.2015.05.005

Koeppen, A. H. (2001). Neuropathology of the inherited ataxias. In M.-U. Manto & M. Pandolfo (Eds.), *The Cerebellum and its Disorders* (pp. 387–406). Cambridge University Press; Cambridge Core. https://doi.org/10.1017/CBO9780511666469.027

Köhler, W. (1921). *Intelligenzprüfungen an Menschenaffen* (2nd ed.). Springer.

Koibuchi, N. (2001). Thyroid hormone and cerebellar development. In M.-U. Manto & M. Pandolfo (Eds.), *The Cerebellum and its Disorders* (pp. 305–315). Cambridge University Press; Cambridge Core. https://doi.org/10.1017/CBO9780511666469.021

Konczak, J., Schoch, B., Dimitrova, A., Gizewski, E., & Timmann, D. (2005). Functional recovery of children and adolescents after cerebellar tumour resection. *Brain*, *128*(6), 1428–1441. https://doi.org/10.1093/brain/awh385

Kostadinov, D., Beau, M., Blanco-Pozo, M., & Häusser, M. (2019). Predictive and reactive reward signals conveyed by climbing fiber inputs to cerebellar Purkinje cells. *Nature Neuroscience*, *22*(6), 950–962. https://doi.org/10.1038/s41593-019-0381-8

Kostadinov, D., & Häusser, M. (2022). Reward signals in the cerebellum: Origins, targets, and functional implications. *Neuron*, *110*(8), 1290–1303. https://doi.org/10.1016/j.neuron.2022.02.015

Kriete, A. L., & Hollis, K. L. (2022). Learning in insects: Perspectives and possibilities. In M. A. Krause, K. L. Hollis, & M. R. Papini (Eds.), *Evolution of Learning and Memory Mechanisms* (pp. 52–70). Cambridge University Press; Cambridge Core. https://doi.org/10.1017/9781108768450.006

Krigolson, O. E. (2018). Event-related brain potentials and the study of reward processing: Methodological considerations. *International Journal of Psychophysiology*, *132*, 175–183. https://doi.org/10.1016/j.ijpsycho.2017.11.007

Kruithof, E. S., Drop, E. M., Gerits, D., Klaus, J., & Schutter, D. J. L. G. (2025). Continuous theta burst stimulation to the medial posterior cerebellum impairs reversal learning in healthy volunteers. *Cognitive, Affective, & Behavioral Neuroscience*. https://doi.org/10.3758/s13415-025-01273-5

Kruithof, E. S., Klaus, J., & Schutter, D. J. L. G. (2023). The human cerebellum in reward anticipation and outcome processing: An activation likelihood estimation meta-analysis. *Neuroscience & Biobehavioral Reviews*, *149*, 105171. https://doi.org/10.1016/j.neubiorev.2023.105171

Kuriyama, R., Yoshimura, H., & Yamazaki, T. (2024). A theory of cerebellar learning as a spike-based reinforcement learning in continuous time and space. *bioRxiv*, 2024.06.23.600300. https://doi.org/10.1101/2024.06.23.600300

Kuypers, H., & Ugolini, G. (1990). Viruses as transneuronal tracers. *Trends in Neurosciences*, *13*(2), 71–75. https://doi.org/10.1016/0166-2236(90)90071-H

Kuznetsova, A., Brockhoff, P., & Christensen, R. (2017). lmerTest package: Tests in linear mixed effects models. *Journal of Statistical Software*, *82*(13), 1–26.

Kwon, H. G., & Jang, S. H. (2014). Differences in neural connectivity between the substantia nigra and ventral tegmental area in the human brain. *Frontiers in Human Neuroscience*, *8*, 41. https://doi.org/10.3389/fnhum.2014.00041

Kyan, M., Muneesawang, P., Jarrah, K., & Guan, L. (2014). Introduction. In *Unsupervised Learning* (pp. 1–8). https://doi.org/10.1002/9781118875568.ch1

Ladouceur, C. D., Dahl, R. E., Birmaher, B., Axelson, D. A., & Ryan, N. D. (2006). Increased error-related negativity (ERN) in childhood anxiety disorders: ERP and source localization. *Journal of Child Psychology and Psychiatry*, *47*(10), 1073–1082. https://doi.org/10.1111/j.1469-7610.2006.01654.x

Lainé, J., & Axelrad, H. (1994). The candelabrum cell: A new interneuron in the cerebellar cortex. *Journal of Comparative Neurology*, *339*(2), 159–173. https://doi.org/10.1002/cne.903390202

Lainé, J., & Axelrad, H. (1998). Lugaro cells target basket and stellate cells in the cerebellar cortex. *NeuroReport*, *9*(10), 2399–2403.

Larson, M. J., Baldwin, S. A., Good, D. A., & Fair, J. E. (2010). Brief reports: Temporal stability of the error-related negativity (ERN) and post-error positivity (Pe): The role of number of trials. *Psychophysiology*, *47*(6), 1167–1171. https://doi.org/10.1111/j.1469-8986.2010.01022.x

LeDoux, J. (2007). The amygdala. *Current Biology*, *17*(20), R868–R874. https://doi.org/10.1016/j.cub.2007.08.005

Lee, D., & Seo, H. (2007). Mechanisms of reinforcement learning and decision making in the primate dorsolateral prefrontal cortex. *Annals of the New York Academy of Sciences*, *1104*(1), 108–122. https://doi.org/10.1196/annals.1390.007

Lee, D., Seo, H., & Jung, M. W. (2012). Neural basis of reinforcement learning and decision making. *Annual Review of Neuroscience*, *35*, 287–308. https://doi.org/10.1146/annurev-neuro-062111-150512

Leggio, M. (2016). Clinical functional topography in cognition. In D. L. Gruol, N. Koibuchi, M.-U. Manto, M. Molinari, J. D. Schmahmann, & Y. Shen (Eds.), *Essentials of Cerebellum and Cerebellar Disorders* (1st ed., pp. 391–396). Springer Nature.

Lenka, A., & Louis, E. D. (2019). Revisiting the clinical phenomenology of “cerebellar tremor”: Beyond the intention tremor. *The Cerebellum*, *18*(3), 565–574. https://doi.org/10.1007/s12311-018-0994-6

Lerner, T. N., Holloway, A. L., & Seiler, J. L. (2021). Dopamine, updated: Reward prediction error and beyond. *Current Opinion in Neurobiology*, *67*, 123–130. https://doi.org/10.1016/j.conb.2020.10.012

Li, F., Yi, C., Jiang, Y., Liao, Y., Si, Y., Yao, D., Zhang, Y., & Xu, P. (2018). The construction of large-scale cortical networks for P300 from scalp EEG. *IEEE Access*, *6*, 68498–68506. https://doi.org/10.1109/ACCESS.2018.2879487

Lin, D., Sun, H., & Zhang, X. (2016). Bidirectional relationship between visual spatial skill and Chinese character reading in chinese kindergartners: A cross-lagged analysis. *Contemporary Educational Psychology*, *46*, 94–100. https://doi.org/10.1016/j.cedpsych.2016.04.008

Lin, Y.-C., Hsu, C.-C. H., Wang, P.-N., Lin, C.-P., & Chang, L.-H. (2020). The relationship between zebrin expression and cerebellar functions: Insights from neuroimaging studies. *Frontiers in Neurology*, *11*, 315. https://doi.org/10.3389/fneur.2020.00315

Liu, Q., Rubarth, K., Faber, J., Sulzer, P., Dogan, I., Barkhoff, M., Minnerop, M., Berlijn, A. M., Elben, S., Jacobi, H., Aktories, J.-E., Huvermann, D. M., Erdlenbruch, F., Van der Veen, R., Müller, J., Nio, E., Frank, B., Köhrmann, M., Wondzinski, E., … Thieme, A. (2024). Subtypes of cognitive impairment in cerebellar disease identified by cross-diagnostic cluster-analysis: Results from a German multicenter study. *Journal of Neurology*, *272*(1), 83. https://doi.org/10.1007/s00415-024-12831-1

Liu, S. J., & Dubois, C. J. (2016). Stellate cells. In D. L. Gruol, N. Koibuchi, M.-U. Manto, M. Molinari, J. D. Schmahmann, & Y. Shen (Eds.), *Essentials of Cerebellum and Cerebellar Disorders* (1st ed., pp. 189–194). Springer Nature.

Lopiano, L., de’sperati, C., & Montarolo, P. G. (1990). Long-term habituation of the acoustic startle response: Role of the cerebellar vermis. *Neuroscience*, *35*(1), 79–84. https://doi.org/10.1016/0306-4522(90)90122-K

Loyola, S., Bosman, L. W. J., De Gruijl, J. R., De Jeu, M. T. G., Negrello, M., Hoogland, T. M., & De Zeeuw, C. I. (2022). Inferior olive: All ins and outs. In M.-U. Manto, D. L. Gruol, J. D. Schmahmann, N. Koibuchi, & R. V. Sillitoe (Eds.), *Handbook of the Cerebellum and Cerebellar Disorders* (2nd ed., pp. 1137–1192). Springer Nature.

Luciani, L. (1891). *Il cervelletto: Nuovi studi di fisiologia normale e patologica* (Vol. 20). Le Monnier.

Lupo, M., Troisi, E., Chiricozzi, F. R., Clausi, S., Molinari, M., & Leggio, M. (2015). Inability to process negative emotions in cerebellar damage: A functional transcranial doppler sonographic study. *The Cerebellum*, *14*(6), 663–669. https://doi.org/10.1007/s12311-015-0662-z

Lütcke, H., & Frahm, J. (2008). Lateralized anterior cingulate function during error processing and conflict monitoring as revealed by high-resolution fMRI. *Cerebral Cortex*, *18*(3), 508–515. https://doi.org/10.1093/cercor/bhm090

Maas, R. P. P. W. M., Killaars, S., van de Warrenburg, B. P. C., & Schutter, D. J. L. G. (2021). The Cerebellar Cognitive Affective Syndrome scale reveals early neuropsychological deficits in SCA3 patients. *Journal of Neurology*, *268*(9), 3456–3466. https://doi.org/10.1007/s00415-021-10516-7

Madden, M. B., Stewart, B. W., White, M. G., Krimmel, S. R., Qadir, H., Barrett, F. S., Seminowicz, D. A., & Mathur, B. N. (2022). A role for the claustrum in cognitive control. *Trends in Cognitive Sciences*, *26*(12), 1133–1152. https://doi.org/10.1016/j.tics.2022.09.006

Maier, M. E., Di Gregorio, F., Muricchio, T., & Di Pellegrino, G. (2015). Impaired rapid error monitoring but intact error signaling following rostral anterior cingulate cortex lesions in humans. *Frontiers in Human Neuroscience*, *9*, 339. https://doi.org/10.3389/fnhum.2015.00339

Mak, M., Tyburski, E., Madany, Ł., Sokołowski, A., & Samochowiec, A. (2016). Executive function deficits in patients after cerebellar neurosurgery. *Journal of the International Neuropsychological Society*, *22*(1), 47–57. Cambridge Core. https://doi.org/10.1017/S1355617715001174

Malicki, M., Szmyd, B. M., Bobeff, E. J., Karuga, F. F., Piotrowski, M. M., Kościołek, D., Wanibuchi, S., Radek, M., & Jaskólski, D. J. (2023). The superior cerebellar artery: Variability and clinical significance. *Biomedicines*, *11*(7). https://doi.org/10.3390/biomedicines11072009

Manto, M.-U. (2001a). Clinical signs of cerebellar disorders. In M.-U. Manto & M. Pandolfo (Eds.), *The Cerebellum and its Disorders* (pp. 97–120). Cambridge University Press; Cambridge Core. https://doi.org/10.1017/CBO9780511666469.009

Manto, M.-U. (2001b). Other infectious diseases. In M.-U. Manto & M. Pandolfo (Eds.), *The Cerebellum and its Disorders* (pp. 248–264). Cambridge University Press; Cambridge Core. https://doi.org/10.1017/CBO9780511666469.018

Manto, M.-U. (2009). Mechanisms of human cerebellar dysmetria: Experimental evidence and current conceptual bases. *Journal of NeuroEngineering and Rehabilitation*, *6*(1), 10. https://doi.org/10.1186/1743-0003-6-10

Manto, M.-U., Adamaszek, M., Apps, R., Carlson, E., Guarque-Chabrera, J., Heleven, E., Kakei, S., Khodakhah, K., Kuo, S.-H., Lin, C.-Y. R., Joshua, M., Miquel, M., Mitoma, H., Larry, N., Péron, J. A., Pickford, J., Schutter, D. J. L. G., Singh, M. K., Tan, T., … Yamashiro, K. (2024). Consensus paper: Cerebellum and reward. *The Cerebellum*, *23*(5), 2169–2192. https://doi.org/10.1007/s12311-024-01702-0

Manto, M.-U., & Jacquy, J. (2001a). Corticobasal degeneration. In M.-U. Manto & M. Pandolfo (Eds.), *The Cerebellum and its Disorders* (pp. 198–201). Cambridge University Press; Cambridge Core. https://doi.org/10.1017/CBO9780511666469.014

Manto, M.-U., & Jacquy, J. (2001b). Other cerebellotoxic agents. In M.-U. Manto & M. Pandolfo (Eds.), *The Cerebellum and its Disorders* (pp. 342–366). Cambridge University Press; Cambridge Core. https://doi.org/10.1017/CBO9780511666469.025

Manto, M.-U., & Zulewski, H. (2001). Endocrine disorders: Clinical aspects. In M.-U. Manto & M. Pandolfo (Eds.), *The Cerebellum and its Disorders* (pp. 316–324). Cambridge University Press; Cambridge Core. https://doi.org/10.1017/CBO9780511666469.022

Marblestone, A. H., Wayne, G., & Kording, K. P. (2016). Toward an integration of deep learning and neuroscience. *Frontiers in Computational Neuroscience*, *10*, 94. https://doi.org/10.3389/fncom.2016.00094

Margulies, D. S., Kelly, A. M. C., Uddin, L. Q., Biswal, B. B., Castellanos, F. X., & Milham, M. P. (2007). Mapping the functional connectivity of anterior cingulate cortex. *NeuroImage*, *37*(2), 579–588. https://doi.org/10.1016/j.neuroimage.2007.05.019

Marr, D. (1969). A theory of cerebellar cortex. *Journal of Physiology*, *202*, 437–470.

Martina, M. (2016). Unipolar brush cells. In D. L. Gruol, N. Koibuchi, M.-U. Manto, M. Molinari, J. D. Schmahmann, & Y. Shen (Eds.), *Essentials of Cerebellum and Cerebellar Disorders* (1st ed., pp. 213–218). Springer Nature.

Maschke, M., Drepper, J., Kindsvater, K., Kolb, F. P., Diener, H.-C., & Timmann, D. (2000). Fear conditioned potentiation of the acoustic blink reflex in patients with cerebellar lesions. *Journal of Neurology, Neurosurgery & Psychiatry*, *68*(3), 358–364. https://doi.org/10.1136/jnnp.68.3.358

McDannald, M. A., Lucantonio, F., Burke, K. A., Niv, Y., & Schoenbaum, G. (2011). Ventral striatum and orbitofrontal cortex are both required for model-based, but not model-free, reinforcement learning. *The Journal of Neuroscience*, *31*(7), 2700–2705. https://doi.org/10.1523/JNEUROSCI.5499-10.2011

McDougle, S. D., Butcher, P. A., Parvin, D. E., Mushtaq, F., Niv, Y., Ivry, R. B., & Taylor, J. A. (2019). Neural signatures of prediction errors in a decision-making task are modulated by action execution failures. *Current Biology*, *29*(10), 1606-1613.e5. https://doi.org/10.1016/j.cub.2019.04.011

Meadows, C. C., Gable, P. A., Lohse, K. R., & Miller, M. W. (2016). The effects of reward magnitude on reward processing: An averaged and single trial event-related potential study. *Biological Psychology*, *118*, 154–160. https://doi.org/10.1016/j.biopsycho.2016.06.002

Meder, D., Madsen, K. H., Hulme, O., & Siebner, H. R. (2016). Chasing probabilities—Signaling negative and positive prediction errors across domains. *NeuroImage*, *134*, 180–191. https://doi.org/10.1016/j.neuroimage.2016.04.019

Merz, J., Lehrl, S., Galster, V., & Erzigkeit, H. (1975). MWT-B—Ein Intelligenzkurztest. *Psychiatrie, Neurologie Und Medizinische Psychologie*, *27*(7), 423–428.

Miall, R. C., & Wolpert, D. M. (1996). Forward models for physiological motor control. *Neural Networks*, *9*(8), 1265–1279. https://doi.org/10.1016/S0893-6080(96)00035-4

Middleton, F. A., & Strick, P. L. (2001). Cerebellar projections to the prefrontal cortex of the primate. *The Journal of Neuroscience*, *21*(2), 700–712. https://doi.org/10.1523/JNEUROSCI.21-02-00700.2001

Mies, G. W., van der Molen, M. W., Smits, M., Hengeveld, M. W., & van der Veen, F. M. (2011). The anterior cingulate cortex responds differently to the validity and valence of feedback in a time-estimation task. *NeuroImage*, *56*(4), 2321–2328. https://doi.org/10.1016/j.neuroimage.2011.04.015

Miltner, W. H. R., Braun, C. H., & Coles, M. G. H. (1997). Event-related brain potentials following incorrect feedback in a time-estimation task: Evidence for a “generic” neural system for error detection. *Journal of Cognitive Neuroscience*, *9*(6), 788–798. https://doi.org/10.1162/jocn.1997.9.6.788

Miquel, M., Vazquez-Sanroman, D., Carbo-Gas, M., Gil-Miravet, I., Sanchis-Segura, C., Carulli, D., Manzo, J., & Coria-Avila, G. A. (2016). Have we been ignoring the elephant in the room? Seven arguments for considering the cerebellum as part of addiction circuitry. *Neuroscience & Biobehavioral Reviews*, *60*, 1–11. https://doi.org/10.1016/j.neubiorev.2015.11.005

Mirenowicz, J., & Schultz, W. (1996). Preferential activation of midbrain dopamine neurons by appetitive rather than aversive stimuli. *Nature*, *379*(6564), 449–451. https://doi.org/10.1038/379449a0

Miyazaki, T., Yamasaki, M., Tanaka, K. F., & Watanabe, M. (2021). Compartmentalized input–output organization of Lugaro cells in the cerebellar cortex. *Neuroscience*, *462*, 89–105. https://doi.org/10.1016/j.neuroscience.2020.05.026

Moneta, N., Garvert, M. M., Heekeren, H. R., & Schuck, N. W. (2023). Task state representations in vmPFC mediate relevant and irrelevant value signals and their behavioral influence. *Nature Communications*, *14*(1), 3156. https://doi.org/10.1038/s41467-023-38709-w

Moneta, N., Grossman, S., & Schuck, N. W. (2024). Representational spaces in orbitofrontal and ventromedial prefrontal cortex: Task states, values, and beyond. *Trends in Neurosciences*, *47*(12), 1055–1069. https://doi.org/10.1016/j.tins.2024.10.005

Monosov, I. E. (2017). Anterior cingulate is a source of valence-specific information about value and uncertainty. *Nature Communications*, *8*(1), 134. https://doi.org/10.1038/s41467-017-00072-y

Morales, M., & Margolis, E. B. (2017). Ventral tegmental area: Cellular heterogeneity, connectivity and behaviour. *Nature Reviews Neuroscience*, *18*(2), 73–85. https://doi.org/10.1038/nrn.2016.165

Moreno-Rius, J. (2018). The cerebellum in fear and anxiety-related disorders. *Progress in Neuro-Psychopharmacology and Biological Psychiatry*, *85*, 23–32. https://doi.org/10.1016/j.pnpbp.2018.04.002

Morris, R. W., Dezfouli, A., Griffiths, K. R., & Balleine, B. W. (2014). Action-value comparisons in the dorsolateral prefrontal cortex control choice between goal-directed actions. *Nature Communications*, *5*(1), 4390. https://doi.org/10.1038/ncomms5390

Moulton, E. A., Elman, I., Becerra, L. R., Goldstein, R. Z., & Borsook, D. (2014). The cerebellum and addiction: Insights gained from neuroimaging research. *Addiction Biology*, *19*(3), 317–331. https://doi.org/10.1111/adb.12101

Mugnaini, E., Sekerková, G., & Martina, M. (2011). The unipolar brush cell: A remarkable neuron finally receiving deserved attention. *Brain Research Reviews*, *66*(1), 220–245. https://doi.org/10.1016/j.brainresrev.2010.10.001

Mukhopadhyay, P., Dutt, A., Kumar Das, S., Basu, A., Hazra, A., Dhibar, T., & Roy, T. (2007). Identification of neuroanatomical substrates of set-shifting ability: Evidence from patients with focal brain lesions. In R. Banerjee & B. K. Chakrabarti (Eds.), *Progress in Brain Research* (Vol. 168, pp. 95–104). Elsevier. https://doi.org/10.1016/S0079-6123(07)68008-X

Muller, P. A., Dhamne, S. C., Vahabzadeh-Hagh, A. M., Pascual-Leone, A., Jensen, F. E., & Rotenberg, A. (2014). Suppression of motor cortical excitability in anesthetized rats by low frequency repetitive transcranial magnetic stimulation. *PLOS ONE*, *9*(3), e91065. https://doi.org/10.1371/journal.pone.0091065

Myers, J. L. (1958). Secondary reinforcement: A review of recent experimentation. *Psychological Bulletin*, *55*(5), 284–301. https://doi.org/10.1037/h0046125

Naeije, G., Rai, M., Allaerts, N., Sjogard, M., De Tiège, X., & Pandolfo, M. (2020). Cerebellar cognitive disorder parallels cerebellar motor symptoms in Friedreich ataxia. *Annals of Clinical and Translational Neurology*, *7*(6), 1050–1054. https://doi.org/10.1002/acn3.51079

Nakano, K., Kayahara, T., Tsutsumi, T., & Ushiro, H. (2000). Neural circuits and functional organization of the striatum. *Journal of Neurology*, *247*(5), V1–V15. https://doi.org/10.1007/PL00007778

Neau, J.-Ph., Anllo, E. A., Bonnaud, V., Ingrand, P., & Gil, R. (2000). Neuropsychological disturbances in cerebellar infarcts. *Acta Neurologica Scandinavica*, *102*(6), 363–370. https://doi.org/10.1034/j.1600-0404.2000.102006363.x

Nettekoven, C., Zhi, D., Shahshahani, L., Pinho, A. L., Saadon-Grosman, N., Buckner, R. L., & Diedrichsen, J. (2024). A hierarchical atlas of the human cerebellum for functional precision mapping. *Nature Communications*, *15*(1), 8376. https://doi.org/10.1038/s41467-024-52371-w

Nicholas, J., Amlang, C., Lin, C.-Y. R., Montaser-Kouhsari, L., Desai, N., Pan, M.-K., Kuo, S.-H., & Shohamy, D. (2024). The role of the cerebellum in learning to predict reward: Evidence from cerebellar ataxia. *The Cerebellum*, *23*(4), 1355–1368. https://doi.org/10.1007/s12311-023-01633-2

Nieoullon, A., Cheramy, A., & Glowinski, J. (1978). Release of dopamine in both caudate nuclei and both substantia nigrae in response to unilateral stimulation of cerebellar nuclei in the cat. *Brain Research*, *148*(1), 143–152. https://doi.org/10.1016/0006-8993(78)90384-0

Nieuwenhuis, S., Ridderinkhof, K. R., Blom, J., Band, G. P. H., & Kok, A. (2001). Error-related brain potentials are differentially related to awareness of response errors: Evidence from an antisaccade task. *Psychophysiology*, *38*(5), 752–760. https://doi.org/10.1111/1469-8986.3850752

Nio, E., Pereira, P. P., Diekmann, N., Petrenko, M., Doubliez, A., Ernst, T. M., Batsikadze, G., Maderwald, S., Deuschl, C., Üngör, M., Cheng, S., Merz, C. J., Quick, H. H., & Timmann, D. (2025). Human cerebellum and ventral tegmental area interact during extinction of learned fear. *eLife*. https://doi.org/10.7554/elife.105399.1

Niv, Y. (2009). Reinforcement learning in the brain. *Journal of Mathematical Psychology*, *53*(3), 139–154. https://doi.org/10.1016/j.jmp.2008.12.005

Niv, Y., & Schoenbaum, G. (2008). Dialogues on prediction errors. *Trends in Cognitive Sciences*, *12*(7), 265–272. https://doi.org/10.1016/j.tics.2008.03.006

Nomoto, K., Schultz, W., Watanabe, T., & Sakagami, M. (2010). Temporally extended dopamine responses to perceptually demanding reward-predictive stimuli. *The Journal of Neuroscience*, *30*(32), 10692–10702. https://doi.org/10.1523/JNEUROSCI.4828-09.2010

O'Doherty, J., Dayan, P., Schultz, J., Deichmann, R., Friston, K., & Dolan, R. J. (2004). Dissociable roles of ventral and dorsal striatum in instrumental conditioning. *Science*, *304*(5669), 452–454. https://doi.org/10.1126/science.1094285

O'Doherty, J. P. (2011). Contributions of the ventromedial prefrontal cortex to goal-directed action selection. *Annals of the New York Academy of Sciences*, *1239*(1), 118–129. https://doi.org/10.1111/j.1749-6632.2011.06290.x

Oerlemans, J., Alejandro, R. J., Hemelsoet, D., Genbrugge, E., Bouche, K., Defreyne, L., De Herdt, V., & Holroyd, C. B. (2024). Lesions of anterior cingulate cortex disrupt an electrophysiological signature of reward processing in humans. *bioRxiv*, 2024.12.04.626789. https://doi.org/10.1101/2024.12.04.626789

Oerlemans, J., Alejandro, R. J., Van Roost, D., Boon, P., De Herdt, V., Meurs, A., & Holroyd, C. B. (2025). Unravelling the origin of reward positivity: A human intracranial event-related brain potential study. *Brain*, *148*(1), 199–211. https://doi.org/10.1093/brain/awae259

Ohmae, S., & Medina, J. F. (2015). Climbing fibers encode a temporal-difference prediction error during cerebellar learning in mice. *Nature Neuroscience*, *18*(12), 1798–1803. https://doi.org/10.1038/nn.4167

Olmedo-Saura, G., Pérez-Pérez, J., Xuclà-Ferrarons, T., Collet, R., Martínez-Viguera, A., & Kulisevsky, J. (2023). Cerebellar syndrome induced by hypomagnesemia: A treatable cause of ataxia not to be missed. Report of three cases and a review of the literature. *Movement Disorders Clinical Practice*, *10*(6), 1004–1012. https://doi.org/10.1002/mdc3.13739

Olson, I. R., Hoffman, L. J., Jobson, K. R., Popal, H. S., & Wang, Y. (2023). Little brain, little minds: The big role of the cerebellum in social development. *Developmental Cognitive Neuroscience*, *60*, 101238. https://doi.org/10.1016/j.dcn.2023.101238

Orban de Xivry, J.-J., & Diedrichsen, J. (2024). Diversity of the nature of input and output signals in the cerebellum suggests a diversity of function. *Current Opinion in Behavioral Sciences*, *57*, 101386. https://doi.org/10.1016/j.cobeha.2024.101386

Orozco, E. A., Jiménez, R. B., Alvarez-Tostado, J. L., Vogt, W., & Silva, G. R. (2010). The specific origin of the simple and complex spikes in Purkinje neurons. *The Journal of Physiology*, *588*(20), 3853. https://doi.org/10.1113/jphysiol.2010.198325

Osorno, T., Rudolph, S., Nguyen, T., Kozareva, V., Nadaf, N. M., Norton, A., Macosko, E. Z., Lee, W.-C. A., & Regehr, W. G. (2022). Candelabrum cells are ubiquitous cerebellar cortex interneurons with specialized circuit properties. *Nature Neuroscience*, *25*(6), 702–713. https://doi.org/10.1038/s41593-022-01057-x

Ott, D. V. M., Ullsperger, M., Jocham, G., Neumann, J., & Klein, T. A. (2011). Continuous theta-burst stimulation (cTBS) over the lateral prefrontal cortex alters reinforcement learning bias. *NeuroImage*, *57*(2), 617–623. https://doi.org/10.1016/j.neuroimage.2011.04.038

Overbeek, T. J. M., Nieuwenhuis, S., & Ridderinkhof, K. R. (2005). Dissociable components of error processing. *Journal of Psychophysiology*, *19*(4), 319–329. https://doi.org/10.1027/0269-8803.19.4.319

Overman, M. J., Sarrazin, V., Browning, M., & O'Shea, J. (2023). Stimulating human prefrontal cortex increases reward learning. *NeuroImage*, *271*, 120029. https://doi.org/10.1016/j.neuroimage.2023.120029

Palau, F., & Arpa, J. (2016). Differential diagnosis of cerebellar ataxias on the basis of the age at onset. In D. L. Gruol, N. Koibuchi, M.-U. Manto, M. Molinari, J. D. Schmahmann, & Y. Shen (Eds.), *Essentials of Cerebellum and Cerebellar Disorders* (1st ed., pp. 523–529). Springer Nature.

Palesi, F., De Rinaldis, A., Castellazzi, G., Calamante, F., Muhlert, N., Chard, D., Tournier, J. D., Magenes, G., D'Angelo, E., & Gandini Wheeler-Kingshott, C. A. M. (2017). Contralateral cortico-ponto-cerebellar pathways reconstruction in humans in vivo: Implications for reciprocal cerebro-cerebellar structural connectivity in motor and non-motor areas. *Scientific Reports*, *7*(1), 12841. https://doi.org/10.1038/s41598-017-13079-8

Papageorgi, I. (2021). Positive and negative reinforcement and punishment. In T. K. Shackelford & V. A. Weekes-Shackelford (Eds.), *Encyclopedia of Evolutionary Psychological Science* (1st ed., pp. 6079–6081). Springer Nature Switzerland AG. https://doi.org/10.1007/978-3-319-19650-3

Park, C., Chang, W. H., Ohn, S. H., Kim, S. T., Bang, O. Y., Pascual-Leone, A., & Kim, Y.-H. (2011). Longitudinal changes of resting-state functional connectivity during motor recovery after stroke. *Stroke*, *42*(5), 1357–1362. https://doi.org/10.1161/STROKEAHA.110.596155

Parsons, L. M., Petacchi, A., Schmahmann, J. D., & Bower, J. M. (2009). Pitch discrimination in cerebellar patients: Evidence for a sensory deficit. *Brain Research*, *1303*, 84–96. https://doi.org/10.1016/j.brainres.2009.09.052

Patel, S. H., & Azzam, P. N. (2005). Characterization of N200 and P300: Selected studies of the event-related potential. *International Journal of Medical Sciences*, *2*(4), 147–154. https://doi.org/10.7150/ijms.2.147

Paul, K., Angus, D. J., Bublatzky, F., Wüllhorst, R., Endrass, T., Greenwood, L.-M., Hajcak, G., Jack, B. N., Korinth, S. P., Kroczek, L. O. H., Lucero, B., Mundorf, A., Nolden, S., Peterburs, J., Pfabigan, D. M., Schettino, A., Severo, M. C., Lee Shing, Y., Turan, G., … Pourtois, G. (2025). Revisiting the electrophysiological correlates of valence and expectancy in reward processing – A multi-lab replication. *Cortex*, *184*, 150–171. https://doi.org/10.1016/j.cortex.2024.12.017

Pearson, J. M., Heilbronner, S. R., Barack, D. L., Hayden, B. Y., & Platt, M. L. (2011). Posterior cingulate cortex: Adapting behavior to a changing world. *Trends in Cognitive Sciences*, *15*(4), 143–151. https://doi.org/10.1016/j.tics.2011.02.002

Pentney, R. (2001). Alcohol toxicity in the cerebellum: Fundamental aspects. In M.-U. Manto & M. Pandolfo (Eds.), *The Cerebellum and its Disorders* (pp. 327–335). Cambridge University Press; Cambridge Core. https://doi.org/10.1017/CBO9780511666469.023

Pereira, S., & van der Kooy, D. (2013). Entwined engrams. *Worm*, *2*(2), e22725. https://doi.org/10.4161/worm.22725

Peterburs, J., & Desmond, J. E. (2016). The role of the human cerebellum in performance monitoring. *Current Opinion in Neurobiology*, *40*, 38–44. https://doi.org/10.1016/j.conb.2016.06.011

Peterburs, J., Gajda, K., Koch, B., Schwarz, M., Hoffmann, K.-P., Daum, I., & Bellebaum, C. (2012). Cerebellar lesions alter performance monitoring on the antisaccade task—An event-related potentials study. *Neuropsychologia*, *50*(3), 379–389. https://doi.org/10.1016/j.neuropsychologia.2011.12.009

Peterburs, J., Hofmann, D., Becker, M. P. I., Nitsch, A. M., Miltner, W. H. R., & Straube, T. (2018). The role of the cerebellum for feedback processing and behavioral switching in a reversal-learning task. *Brain and Cognition*, *125*, 142–148. https://doi.org/10.1016/j.bandc.2018.07.001

Peterburs, J., Kobza, S., & Bellebaum, C. (2016). Feedback delay gradually affects amplitude and valence specificity of the feedback-related negativity (FRN). *Psychophysiology*, *53*(2), 209–215. https://doi.org/10.1111/psyp.12560

Peterburs, J., Thürling, M., Rustemeier, M., Göricke, S., Suchan, B., Timmann, D., & Bellebaum, C. (2015). A cerebellar role in performance monitoring–Evidence from EEG and voxel-based morphometry in patients with cerebellar degenerative disease. *Neuropsychologia*, *68*, 139–147. https://doi.org/10.1016/j.neuropsychologia.2015.01.017

Peters, A., Helming, H., Bruchmann, M., Wiegandt, A., Straube, T., & Schindler, S. (2024). How and when social evaluative feedback is processed in the brain: A systematic review on ERP studies. *Cortex*, *173*, 187–207. https://doi.org/10.1016/j.cortex.2024.02.003

Petrosini, L., Leggio, M. G., & Molinari, M. (1998). The cerebellum in the spatial problem solving: A co-star or a guest star? *Progress in Neurobiology*, *56*(2), 191–210. https://doi.org/10.1016/S0301-0082(98)00036-7

Pfabigan, D. M., Alexopoulos, J., Bauer, H., & Sailer, U. (2011). Manipulation of feedback expectancy and valence induces negative and positive reward prediction error signals manifest in event-related brain potentials. *Psychophysiology*, *48*(5), 656–664. https://doi.org/10.1111/j.1469-8986.2010.01136.x

Picton, T. W. (1992). The P300 wave of the human event-related potential. *Journal of Clinical Neurophysiology*, *9*, 456–456.

Pietschmann, M., Simon, K., Endrass, T., & Kathmann, N. (2008). Changes of performance monitoring with learning in older and younger adults. *Psychophysiology*, *45*(4), 559–568. https://doi.org/10.1111/j.1469-8986.2008.00651.x

Pinheiro, A. P., Johnson, J. F., Amorim, M., Roberto, M., Schwartze, M., Kotz, S. A., & Shenton, M. E. (2021). The cerebellum links to positive symptoms of psychosis: A systematic review and meta-analysis. *Schizophrenia Bulletin Open*, *2*(1), sgab039. https://doi.org/10.1093/schizbullopen/sgab039

Popa, L. S., & Ebner, T. J. (2022). Cerebellum and internal models. In M.-U. Manto, D. L. Gruol, J. D. Schmahmann, N. Koibuchi, & R. V. Sillitoe (Eds.), *Handbook of the Cerebellum and Cerebellar Disorders* (2nd ed., pp. 1461–1486). Springer Nature.

Postuma, R. B., & Dagher, A. (2006). Basal ganglia functional connectivity based on a meta-analysis of 126 positron emission tomography and functional magnetic resonance imaging publications. *Cerebral Cortex*, *16*(10), 1508–1521. https://doi.org/10.1093/cercor/bhj088

Potts, G. F., Martin, L. E., Kamp, S.-M., & Donchin, E. (2011). Neural response to action and reward prediction errors: Comparing the error-related negativity to behavioral errors and the feedback-related negativity to reward prediction violations. *Psychophysiology*, *48*(2), 218–228. https://doi.org/10.1111/j.1469-8986.2010.01049.x

Prekop, H.-T., & Wingate, R. J. T. (2016). Cerebellar nucleus development. In D. L. Gruol, N. Koibuchi, M.-U. Manto, M. Molinari, J. D. Schmahmann, & Y. Shen (Eds.), *Essentials of Cerebellum and Cerebellar Disorders* (1st ed., pp. 149–154). Springer Nature.

Prevosto, V., Graf, W., & Ugolini, G. (2010). Cerebellar inputs to intraparietal cortex areas LIP and MIP: Functional frameworks for adaptive control of eye movements, reaching, and arm/eye/head movement coordination. *Cerebral Cortex*, *20*(1), 214–228. https://doi.org/10.1093/cercor/bhp091

Priddy, K., & Keller, P. (2005). Supervised training methods. In *Artificial Neural Networks: An Introduction* (pp. 35–48). SPIE Press.

Proudfit, G. H. (2015). The reward positivity: From basic research on reward to a biomarker for depression. *Psychophysiology*, *52*(4), 449–459. https://doi.org/10.1111/psyp.12370

Ramayya, A. G., Misra, A., Baltuch, G. H., & Kahana, M. J. (2014). Microstimulation of the human substantia nigra alters reinforcement learning. *The Journal of Neuroscience*, *34*(20), 6887–6895. https://doi.org/10.1523/JNEUROSCI.5445-13.2014

Ramnani, N. (2012). Frontal lobe and posterior parietal contributions to the cortico-cerebellar system. *The Cerebellum*, *11*(2), 366–383. https://doi.org/10.1007/s12311-011-0272-3

Ravizza, S. M., McCormick, C. A., Schlerf, J. E., Justus, T., Ivry, R. B., & Fiez, J. A. (2006). Cerebellar damage produces selective deficits in verbal working memory. *Brain*, *129*(2), 306–320. https://doi.org/10.1093/brain/awh685

Rawls, E., & Lamm, C. (2021). The aversion positivity: Mediofrontal cortical potentials reflect parametric aversive prediction errors and drive behavioral modification following negative reinforcement. *Cortex*, *140*, 26–39. https://doi.org/10.1016/j.cortex.2021.03.012

Raymond, J. L., & Medina, J. F. (2018). Computational principles of supervised learning in the cerebellum. *Annual Review of Neuroscience*, *41*, 233–253. https://doi.org/10.1146/annurev-neuro-080317-061948

Rentiya, Z., Hutnik, R., Mekkam, Y. Q., & Bae, J. (2020). The pathophysiology and clinical manifestations of spinocerebellar ataxia type 6. *The Cerebellum*, *19*(3), 459–464. https://doi.org/10.1007/s12311-020-01120-y

Rescorla, R. A., & Wagner, A. R. (1972). A theory of Pavlovian conditioning: Variations in the effectiveness of reinforcement and nonreinforcement. In A. H. Black & W. F. Prokasy (Eds.), *Classical conditioning II: Current research and theory* (pp. 64–99). Appleton-Century-Crofts.

Ridderinkhof, K. R., Ramautar, J. R., & Wijnen, J. G. (2009). To PE or not to PE: A P3-like ERP component reflecting the processing of response errors. *Psychophysiology*, *46*(3), 531–538. https://doi.org/10.1111/j.1469-8986.2009.00790.x

Rodríguez-Labrada, R., Batista-Izquierdo, A., González-Melix, Z., Reynado-Cejas, L., Vázquez-Mojena, Y., Sanz, Y. A., Canales-Ochoa, N., González-Zaldívar, Y., Dogan, I., Reetz, K., & Velázquez-Pérez, L. (2022). Cognitive decline is closely associated with ataxia severity in spinocerebellar ataxia type 2: A validation study of the Schmahmann Syndrome Scale. *The Cerebellum*, *21*(3), 391–403. https://doi.org/10.1007/s12311-021-01305-z

Roger, C., Bénar, C. G., Vidal, F., Hasbroucq, T., & Burle, B. (2010). Rostral cingulate zone and correct response monitoring: ICA and source localization evidences for the unicity of correct- and error-negativities. *NeuroImage*, *51*(1), 391–403. https://doi.org/10.1016/j.neuroimage.2010.02.005

Rolls, E. T. (2023). Emotion, motivation, decision-making, the orbitofrontal cortex, anterior cingulate cortex, and the amygdala. *Brain Structure and Function*, *228*(5), 1201–1257. https://doi.org/10.1007/s00429-023-02644-9

Romaniello, R., & Borgatti, R. (2022). Cerebellar agenesis. In M.-U. Manto, D. L. Gruol, J. D. Schmahmann, N. Koibuchi, & R. V. Sillitoe (Eds.), *Handbook of the Cerebellum and Cerebellar Disorders* (2nd ed., pp. 2113–2134). Springer Nature.

Romero, M. C., Davare, M., Armendariz, M., & Janssen, P. (2019). Neural effects of transcranial magnetic stimulation at the single-cell level. *Nature Communications*, *10*(1), 2642. https://doi.org/10.1038/s41467-019-10638-7

Roy, A. K., Fudge, J. L., Kelly, C., Perry, J. S. A., Daniele, T., Carlisi, C., Benson, B., Xavier Castellanos, F., Milham, M. P., Pine, D. S., & Ernst, M. (2013). Intrinsic functional connectivity of amygdala-based networks in adolescent generalized anxiety disorder. *Journal of the American Academy of Child & Adolescent Psychiatry*, *52*(3), 290-299.e2. https://doi.org/10.1016/j.jaac.2012.12.010

Rudebeck, P. H., Behrens, T. E., Kennerley, S. W., Baxter, M. G., Buckley, M. J., Walton, M. E., & Rushworth, M. F. S. (2008). Frontal cortex subregions play distinct roles in choices between actions and stimuli. *The Journal of Neuroscience*, *28*(51), 13775–13785. https://doi.org/10.1523/JNEUROSCI.3541-08.2008

Ruigrok, T. J. H., Sillitoe, R. V., & Voogd, J. (2015). Cerebellum and cerebellar connections. In G. Paxinos (Ed.), *The Rat Nervous System* (4th ed., pp. 133–205). Academic Press. https://doi.org/10.1016/B978-0-12-374245-2.00009-7

Rushworth, M. F. S., Hadland, K. A., Gaffan, D., & Passingham, R. E. (2003). The effect of cingulate cortex lesions on task switching and working memory. *Journal of Cognitive Neuroscience*, *15*(3), 338–353. https://doi.org/10.1162/089892903321593072

Rustemeier, M., Koch, B., Schwarz, M., & Bellebaum, C. (2016). Processing of positive and negative feedback in patients with cerebellar lesions. *The Cerebellum*, *15*, 425–438. https://doi.org/10.1007/s12311-015-0702-8

Salari, M., Etemadifar, M., Rashedi, R., & Mardani, S. (2024). A review of ocular movement abnormalities in hereditary cerebellar ataxias. *The Cerebellum*, *23*(2), 702–721. https://doi.org/10.1007/s12311-023-01554-0

Sambrook, T. D., & Goslin, J. (2015). A neural reward prediction error revealed by a meta-analysis of ERPs using great grand averages. *Psychological Bulletin*, *141*(1), 213–235. https://doi.org/10.1037/bul0000006

San Martín, R. (2012). Event-related potential studies of outcome processing and feedback-guided learning. *Frontiers in Human Neuroscience*, *6*, 304. https://doi.org/10.3389/fnhum.2012.00304

Sanger, T. D., Yamashita, O., & Kawato, M. (2020). Expansion coding and computation in the cerebellum: 50 years after the Marr–Albus codon theory. *The Journal of Physiology*, *598*(5), 913–928. https://doi.org/10.1113/JP278745

Sarikaya, H., & Steinlin, M. (2018). Cerebellar stroke in adults and children. In M.-U. Manto & T. A. G. M. Huisman (Eds.), *Handbook of Clinical Neurology* (Vol. 155, pp. 301–312). Elsevier. https://doi.org/10.1016/B978-0-444-64189-2.00020-2

Satolli, S., Rossi, S., Vegezzi, E., Pellerin, D., Manca, M. L., Barghigiani, M., Battisti, C., Bilancieri, G., Bruno, G., Capacci, E., Casali, C., Ceravolo, R., Cocozza, S., Cotti Piccinelli, S., Criscuolo, C., Danzi, M. C., De Micco, R., De Michele, G., Dicaire, M.-J., … Santorelli, F. M. (2024). Spinocerebellar ataxia 27B: A frequent and slowly progressive autosomal-dominant cerebellar ataxia—Experience from an Italian cohort. *Journal of Neurology*, *271*(8), 5478–5488. https://doi.org/10.1007/s00415-024-12506-x

Schmahmann, J. D. (1998). Dysmetria of thought: Clinical consequences of cerebellar dysfunction on cognition and affect. *Trends in Cognitive Sciences*, *2*(9), 362–371. https://doi.org/10.1016/S1364-6613(98)01218-2

Schmahmann, J. D. (2000). The role of the cerebellum in affect and psychosis. *Journal of Neurolinguistics*, *13*(2), 189–214. https://doi.org/10.1016/S0911-6044(00)00011-7

Schmahmann, J. D. (2016). A brief history of the cerebellum. In D. L. Gruol, N. Koibuchi, M.-U. Manto, M. Molinari, J. D. Schmahmann, & Y. Shen (Eds.), *Essentials of Cerebellum and Cerebellar Disorders* (1st ed., pp. 5–20). Springer Nature.

Schmahmann, J. D., MacMore, J., & Vangel, M. (2009). Cerebellar stroke without motor deficit: Clinical evidence for motor and non-motor domains within the human cerebellum. *Neuroscience*, *162*(3), 852–861. https://doi.org/10.1016/j.neuroscience.2009.06.023

Schmahmann, J. D., & Pandya, D. N. (1991). Projections to the basis pontis from the superior temporal sulcus and superior temporal region in the Rhesus monkey. *Journal of Comparative Neurology*, *308*(2), 224–248. https://doi.org/10.1002/cne.903080209

Schmahmann, J. D., & Pandya, D. N. (1992). Course of the fiber pathways to pons from parasensory association areas in the Rhesus monkey. *Journal of Comparative Neurology*, *326*(2), 159–179. https://doi.org/10.1002/cne.903260202

Schmahmann, J. D., & Pandya, D. N. (1993). Prelunate, occipitotemporal, and parahippocampal projections to the basis pontis in Rhesus monkey. *Journal of Comparative Neurology*, *337*(1), 94–112. https://doi.org/10.1002/cne.903370107

Schmahmann, J. D., & Pandya, D. N. (1997). Anatomic organization of the basilar pontine projections from prefrontal cortices in Rhesus monkey. *The Journal of Neuroscience*, *17*(1), 438. https://doi.org/10.1523/JNEUROSCI.17-01-00438.1997

Schmahmann, J. D., & Sherman, J. C. (1997). Cerebellar Cognitive Affective Syndrome. In J. D. Schmahmann (Ed.), *International Review of Neurobiology* (Vol. 41, pp. 433–440). Academic Press. https://doi.org/10.1016/S0074-7742(08)60363-3

Schmahmann, J. D., & Sherman, J. C. (1998). The Cerebellar Cognitive Affective Syndrome. *Brain*, *121*(4), 561–579. https://doi.org/10.1093/brain/121.4.561

Schneider, B., & Koenigs, M. (2017). Human lesion studies of ventromedial prefrontal cortex. *Neuropsychologia*, *107*, 84–93. https://doi.org/10.1016/j.neuropsychologia.2017.09.035

Schuck, N. W., Wilson, R., & Niv, Y. (2018). A state representation for reinforcement learning and decision-making in the orbitofrontal cortex. In R. Morris, A. Bornstein, & A. Shenhav (Eds.), *Goal-Directed Decision Making* (pp. 259–278). Academic Press. https://doi.org/10.1016/B978-0-12-812098-9.00012-7

Schuelke, M. (2005). Ataxia with vitamin E deficiency. In M. P. Adam, J. Feldman, G. M. Mirzaa, R. A. Pagon, S. E. Wallace, & A. Amemiya (Eds.), *GeneReviews*. University of Washington.

Schulreich, S., Pfabigan, D. M., Derntl, B., & Sailer, U. (2013). Fearless dominance and reduced feedback-related negativity amplitudes in a time-estimation task – Further neuroscientific evidence for dual-process models of psychopathy. *Biological Psychology*, *93*(3), 352–363. https://doi.org/10.1016/j.biopsycho.2013.04.004

Schultz, W. (2016). Dopamine reward prediction error coding. *Dialogues in Clinical Neuroscience*, *18*(1), 23–32. https://doi.org/10.31887/DCNS.2016.18.1/wschultz

Schultz, W., Apicella, P., & Ljungberg, T. (1993). Responses of monkey dopamine neurons to reward and conditioned stimuli during successive steps of learning a delayed response task. *The*

Journal of Neuroscience, *13*(3), 900–913. https://doi.org/10.1523/JNEUROSCI.13-03-00900.1993

Schultz, W., Dayan, P., & Montague, P. R. (1997). A neural substrate of prediction and reward. *Science*, *275*(5306), 1593–1599. https://doi.org/10.1126/science.275.5306.1593

Schutter, D. J. L. G. (2021a). Disorders of fear and anxiety. In *The Cerebellum in Emotions and Psychopathology* (1st ed., pp. 38–63). Routledge.

Schutter, D. J. L. G. (2021b). Evolution and basic anatomy of the cerebellum. In *The Cerebellum in Emotions and Psychopathology* (pp. 1–19). Routledge.

Schutter, D. J. L. G., & van Honk, J. (2006). An electrophysiological link between the cerebellum, cognition and emotion: Frontal theta EEG activity to single-pulse cerebellar TMS. *NeuroImage*, *33*(4), 1227–1231. https://doi.org/10.1016/j.neuroimage.2006.06.055

Schweighofer, N., Arbib, M. A., & Kawato, M. (1998). Role of the cerebellum in reaching movements in humans. I. Distributed inverse dynamics control. *European Journal of Neuroscience*, *10*(1), 86–94. https://doi.org/10.1046/j.1460-9568.1998.00006.x

Sen, P. C., Hajra, M., & Ghosh, M. (2020). Supervised classification algorithms in machine learning: A survey and review. In J. K. Mandal & D. Bhattacharya (Eds.), *Emerging Technology in Modelling and Graphics* (pp. 99–111). Springer Singapore.

Sendhilnathan, N., Ipata, A., & Goldberg, M. E. (2021). Mid-lateral cerebellar complex spikes encode multiple independent reward-related signals during reinforcement learning. *Nature Communications*, *12*(1), 6475. https://doi.org/10.1038/s41467-021-26338-0

Sendhilnathan, N., Semework, M., Goldberg, M. E., & Ipata, A. E. (2020). Neural correlates of reinforcement learning in mid-lateral cerebellum. *Neuron*, *106*(1), 188-198.e5. https://doi.org/10.1016/j.neuron.2019.12.032

Sereno, M. I., Diedrichsen, J., Tachrount, M., Testa-Silva, G., d'Arceuil, H., & De Zeeuw, C. (2020). The human cerebellum has almost 80% of the surface area of the neocortex. *Proceedings of the National Academy of Sciences*, *117*(32), 19538–19543. https://doi.org/10.1073/pnas.2002896117

Sharpe, J. A. (2008). Neurophysiology and neuroanatomy of smooth pursuit: Lesion studies. *Brain and Cognition*, *68*(3), 241–254. https://doi.org/10.1016/j.bandc.2008.08.015

Shenkin, H. A., & Zavala, M. (1982). Cerebellar strokes: Mortality, surgical indications, and results of ventricular drainage. *The Lancet*, *320*(8295), 429–432. https://doi.org/10.1016/S0140-6736(82)90453-6

Shidara, M., Kawano, K., Gomi, H., & Kawato, M. (1993). Inverse-dynamics model eye movement control by Purkinje cells in the cerebellum. *Nature*, *365*(6441), 50–52. https://doi.org/10.1038/365050a0

Shiner, T., Seymour, B., Wunderlich, K., Hill, C., Bhatia, K. P., Dayan, P., & Dolan, R. J. (2012). Dopamine and performance in a reinforcement learning task: Evidence from Parkinson's disease. *Brain*, *135*(6), 1871–1883. https://doi.org/10.1093/brain/aws083

Shinoda, Y., & Sugihara. (2022). Axonal trajectories of single climbing and mossy fiber neurons in the cerebellar cortex and nucleus. In M.-U. Manto, D. L. Gruol, J. D. Schmahmann, N. Koibuchi, & R. V. Sillitoe (Eds.), *Handbook of the Cerebellum and Cerebellar Disorders* (2nd ed., pp. 559–594). Springer Nature.

Shobeiri, P., Hosseini Shabanan, S., Haghshomar, M., Khanmohammadi, S., Fazeli, S., Sotoudeh, H., & Kamali, A. (2024). Cerebellar microstructural abnormalities in obsessive–compulsive disorder (OCD): A systematic review of diffusion tensor imaging studies. *The Cerebellum*, *23*(2), 778–801. https://doi.org/10.1007/s12311-023-01573-x

Silberberg, G., & Bolam, J. P. (2015). Local and afferent synaptic pathways in the striatal microcircuitry. *Current Opinion in Neurobiology*, *33*, 182–187. https://doi.org/10.1016/j.conb.2015.05.002

Silvetti, M., & Verguts, T. (2012). Reinforcement learning, high-level cognition, and the human brain. In P. Bright (Ed.), *Neuroimaging–Cognitive and Clinical Neuroscience* (pp. 283–296). InTech.

Siman-Tov, T., Granot, R. Y., Shany, O., Singer, N., Hendler, T., & Gordon, C. R. (2019). Is there a prediction network? Meta-analytic evidence for a cortical-subcortical network likely subserving prediction. *Neuroscience & Biobehavioral Reviews*, *105*, 262–275. https://doi.org/10.1016/j.neubiorev.2019.08.012

Skinner, B. F. (1963). Operant behavior. *American Psychologist*, *18*(8), 503–515. https://doi.org/10.1037/h0045185

Smith, D. M., & Torregrossa, M. M. (2024). The ventral tegmental area dopamine to basolateral amygdala projection supports acquisition of cocaine self-administration. *Neuropharmacology*, *261*, 110160. https://doi.org/10.1016/j.neuropharm.2024.110160

Smith, J. B., Lee, A. K., & Jackson, J. (2020). The claustrum. *Current Biology*, *30*(23), R1401–R1406. https://doi.org/10.1016/j.cub.2020.09.069

Spencer, K. A., & Slocomb, D. L. (2007). The neural basis of ataxic dysarthria. *The Cerebellum*, *6*(1), 58–65. https://doi.org/10.1080/14734220601145459

Stemmer, B., Segalowitz, S. J., Witzke, W., & Schönle, P. W. (2004). Error detection in patients with lesions to the medial prefrontal cortex: An ERP study. *Neuropsychologia*, *42*(1), 118–130. https://doi.org/10.1016/S0028-3932(03)00121-0

Stevens, F. L., Hurley, R. A., Taber, K. H., Hurley, R. A., Hayman, L. A., & Taber, K. H. (2011). Anterior cingulate cortex: Unique role in cognition and emotion. *The Journal of Neuropsychiatry and Clinical Neurosciences*, *23*(2), 121–125. https://doi.org/10.1176/jnp.23.2.jnp121

Stewardson, H. J., & Sambrook, T. D. (2020). Evidence for parietal reward prediction errors using great grand average meta-analysis. *International Journal of Psychophysiology*, *152*, 81–86. https://doi.org/10.1016/j.ijpsycho.2020.03.002

Stockert, A., Schwartze, M., Poeppel, D., Anwander, A., & Kotz, S. A. (2021). Temporo-cerebellar connectivity underlies timing constraints in audition. *eLife*, *10*, e67303. https://doi.org/10.7554/eLife.67303

Stoodley, C. J., MacMore, J. P., Makris, N., Sherman, J. C., & Schmahmann, J. D. (2016). Location of lesion determines motor vs. Cognitive consequences in patients with cerebellar stroke. *NeuroImage: Clinical*, *12*, 765–775. https://doi.org/10.1016/j.nicl.2016.10.013

Strick, P. L., Dum, R. P., & Fiez, J. A. (2009). Cerebellum and nonmotor function. *Annual Review of Neuroscience*, *32*, 413–434. https://doi.org/10.1146/annurev.neuro.31.060407.125606

Su, T.-Z., Campbell, G. W., & Oxender, D. L. (1997). Glutamine transport in cerebellar granule cells in culture. *Brain Research*, *757*(1), 69–78. https://doi.org/10.1016/S0006-8993(97)00139-X

Sutton, R. S., & Barto, A. G. (2018a). Introduction. In *Reinforcement Learning: An introduction* (2nd ed., pp. 1–22). The MIT press.

Sutton, R. S., & Barto, A. G. (2018b). On-policy prediction with approximation. In *Reinforcement Learning: An introduction* (2nd ed., pp. 197–242). The MIT press.

Sutton, R. S., & Barto, A. G. (2018c). *Reinforcement learning: An introduction*. MIT press.

Svaldi, C., Paquier, P., Keulen, S., van Elp, H., Catsman-Berrevoets, C., Kingma, A., Jonkers, R., Kohnen, S., & de Aguiar, V. (2024). Characterising the long-term language impairments of children following cerebellar tumour surgery by extracting psycholinguistic properties from spontaneous language. *The Cerebellum*, *23*(2), 523–544. https://doi.org/10.1007/s12311-023-01563-z

Swain, R. A., Kerr, A. L., & Thompson, R. F. (2011). The cerebellum: A neural system for the study of reinforcement learning. *Frontiers in Behavioral Neuroscience*, *5*, 8. https://doi.org/10.3389/fnbeh.2011.00008

Szmulewicz, D. J., Waterston, J. A., MacDougall, H. G., Mossman, S., Chancellor, A. M., McLean, C. A., Merchant, S., Patrikios, P., Halmagyi, G. M., & Storey, E. (2011). Cerebellar Ataxia, Neuropathy,

Vestibular Areflexia Syndrome (CANVAS): A review of the clinical features and video-oculographic diagnosis. *Annals of the New York Academy of Sciences*, *1233*(1), 139–147. https://doi.org/10.1111/j.1749-6632.2011.06158.x

Takahashi, Y. K., Stalnaker, T. A., Mueller, L. E., Harootonian, S. K., Langdon, A. J., & Schoenbaum, G. (2023). Dopaminergic prediction errors in the ventral tegmental area reflect a multithreaded predictive model. *Nature Neuroscience*, *26*(5), 830–839. https://doi.org/10.1038/s41593-023-01310-x

Talmi, D., Atkinson, R., & El-Deredy, W. (2013). The feedback-related negativity signals salience prediction errors, not reward prediction errors. *The Journal of Neuroscience*, *33*(19), 8264–8269. https://doi.org/10.1523/JNEUROSCI.5695-12.2013

Tanaka, H., Ishikawa, T., & Kakei, S. (2021). Neural predictive computation in the cerebellum. In H. Mizusawa & S. Kakei (Eds.), *Cerebellum as a CNS Hub* (pp. 371–390). Springer International Publishing.

Tang, W., Kochubey, O., Kintscher, M., & Schneggenburger, R. (2020). A VTA to basal amygdala dopamine projection contributes to signal salient somatosensory events during fear learning. *The Journal of Neuroscience*, *40*(20), 3969–3980. https://doi.org/10.1523/JNEUROSCI.1796-19.2020

Taron, F., Chiapparini, L., & Mariotti, C. (2022). Autosomal dominant spinocerebellar ataxias and episodic ataxias. In M.-U. Manto, D. L. Gruol, J. D. Schmahmann, N. Koibuchi, & R. V. Sillitoe (Eds.), *Handbook of the Cerebellum and Cerebellar Disorders* (2nd ed., pp. 2483–2560). Springer Nature.

Tedesco, A. M., Chiricozzi, F. R., Clausi, S., Lupo, M., Molinari, M., & Leggio, M. G. (2011). The cerebellar cognitive profile. *Brain*, *134*(12), 3672–3686. https://doi.org/10.1093/brain/awr266

Teive, H. A. G., Munhoz, R. P., Arruda, W. O., Raskin, S., Werneck, L. C., & Ashizawa, T. (2011). Spinocerebellar ataxia type 10 – A review. *Parkinsonism & Related Disorders*, *17*(9), 655–661. https://doi.org/10.1016/j.parkreldis.2011.04.001

Thieme, A., Faber, J., Sulzer, P., Reetz, K., Dogan, I., Barkhoff, M., Krahe, J., Jacobi, H., Aktories, J.-E., Minnerop, M., Elben, S., van der Veen, R., Müller, J., Batsikadze, G., Konczak, J., Synofzik, M., Roeske, S., & Timmann, D. (2022). The CCAS-scale in hereditary ataxias: Helpful on the group level, particularly in SCA3, but limited in individual patients. *Journal of Neurology*, *269*(8), 4363–4374. https://doi.org/10.1007/s00415-022-11071-5

Thieme, A., Roeske, S., Faber, J., Sulzer, P., Minnerop, M., Elben, S., Jacobi, H., Reetz, K., Dogan, I., Barkhoff, M., Konczak, J., Wondzinski, E., Siebler, M., Mueller, O., Sure, U., Schmahmann, J. D., Klockgether, T., Synofzik, M., & Timmann, D. (2020). Validation of a German version of the Cerebellar Cognitive Affective/ Schmahmann Syndrome Scale: Preliminary version and study protocol. *Neurological Research and Practice*, *2*(1), 39. https://doi.org/10.1186/s42466-020-00071-3

Thieme, A., Röske, S., Faber, J., Sulzer, P., Minnerop, M., Elben, S., Reetz, K., Dogan, I., Barkhoff, M., Konczak, J., Wondzinski, E., Siebler, M., Hetze, S., Müller, O., Sure, U., Klockgether, T., Synofzik, M., & Timmann, D. (2021). Reference values for the Cerebellar Cognitive Affective Syndrome Scale: Age and education matter. *Brain*, *144*(2), e20–e20. https://doi.org/10.1093/brain/awaa417

Thieme, A., & Timmann, D. (2022). Ataxien – Eine aktuelle Übersicht über die weiter wachsende Anzahl möglicher Diagnosen. *Psychiatrie*, *90*(5), 233–251. https://doi.org/10.1055/a-1772-8897

Thoma, P., Bellebaum, C., Koch, B., Schwarz, M., & Daum, I. (2008). The cerebellum is involved in reward-based reversal learning. *The Cerebellum*, *7*, 433–443. https://doi.org/10.1007/s12311-008-0046-8

Thorndike, E. L. (1911). *Animal intelligence; Experimental studies*. Macmillan.

Thorndike, E. L. (1933). A proof of the law of effect. *Science*, *77*(1989), 173–175. https://doi.org/10.1126/science.77.1989.173.b

Thorwart, A., & Livesey, E. J. (2016). Three ways that non-associative knowledge may affect associative learning processes. *Frontiers in Psychology*, *7*, 2024. https://doi.org/10.3389/fpsyg.2016.02024

Timmann, D., Küper, M., Gizewski, E. R., Schoch, B., & Donchin, O. (2022). Lesion-symptom mapping of the human cerebellum. In M.-U. Manto, D. L. Gruol, J. D. Schmahmann, N. Koibuchi, & R. V. Sillitoe (Eds.), *Handbook of the Cerebellum and Cerebellar Disorders* (2nd ed., pp. 1857–1890). Springer Cham.

Tinazzi, M., Morgante, F., Peretti, A., Mariotti, C., Panzeri, M., Fiorio, M., & Fasano, A. (2013). Impaired temporal processing of tactile and proprioceptive stimuli in cerebellar degeneration. *PLOS ONE*, *8*(11), e78628. https://doi.org/10.1371/journal.pone.0078628

Todd, N. P. M., Govender, S., & Colebatch, J. G. (2018). The human electrocerebellogram (EcEG) recorded non-invasively using scalp electrodes. *Neuroscience Letters*, *682*, 124–131. https://doi.org/10.1016/j.neulet.2018.06.012

Tohgi, H., Takahashi, S., Chiba, K., & Hirata, Y. (1993). Cerebellar infarction. Clinical and neuroimaging analysis in 293 patients. The Tohoku Cerebellar Infarction Study Group. *Stroke*, *24*(11), 1697–1701. https://doi.org/10.1161/01.STR.24.11.1697

Topka, H., & Massaquoi, S. G. (2001). Pathophysiology of clinical cerebellar signs. In M.-U. Manto & M. Pandolfo (Eds.), *The Cerebellum and its Disorders* (pp. 121–135). Cambridge University Press; Cambridge Core. https://doi.org/10.1017/CBO9780511666469.010

Tricomi, E., & Fiez, J. A. (2008). Feedback signals in the caudate reflect goal achievement on a declarative memory task. *NeuroImage*, *41*(3), 1154–1167. https://doi.org/10.1016/j.neuroimage.2008.02.066

Trouillas, P., Takayanagi, T., Hallett, M., Currier, R. D., Subramony, S. H., Wessel, K., Bryer, A., Diener, H. C., Massaquoi, S., Gomez, C. M., Coutinho, P., Hamida, M. B., Campanella, G., Filla, A., Schut, L., Timann, D., Honnorat, J., Nighoghossian, N., & Manyam, B. (1997). International cooperative ataxia rating scale for pharmacological assessment of the cerebellar syndrome. *Journal of the Neurological Sciences*, *145*(2), 205–211. https://doi.org/10.1016/S0022-510X(96)00231-6

Trutti, A. C., Mulder, M. J., Hommel, B., & Forstmann, B. U. (2019). Functional neuroanatomical review of the ventral tegmental area. *NeuroImage*, *191*, 258–268. https://doi.org/10.1016/j.neuroimage.2019.01.062

Tsutsui, K.-I., Grabenhorst, F., Kobayashi, S., & Schultz, W. (2016). A dynamic code for economic object valuation in prefrontal cortex neurons. *Nature Communications*, *7*(1), 12554. https://doi.org/10.1038/ncomms12554

Tunc, S., Baginski, N., Lubs, J., Bally, J. F., Weissbach, A., Baaske, M. K., Tadic, V., Brüggemann, N., Bäumer, T., Beste, C., & Münchau, A. (2019). Predictive coding and adaptive behavior in patients with genetically determined cerebellar ataxia—A neurophysiology study. *NeuroImage: Clinical*, *24*, 102043. https://doi.org/10.1016/j.nicl.2019.102043

Turing, A. M. (1969). Intelligent machinery. In B. Meltzer & D. Michie (Eds.), *Machine Intelligence* (Vol. 5). Edinburgh University Press.

Turner, B. M., Paradiso, S., Marvel, C. L., Pierson, R., Boles Ponto, L. L., Hichwa, R. D., & Robinson, R. G. (2007). The cerebellum and emotional experience. *Neuropsychologia*, *45*(6), 1331–1341. https://doi.org/10.1016/j.neuropsychologia.2006.09.023

Ugawa, Y., Day, B. L., Rothwell, J. C., Thompson, P. D., Merton, P. A., & Marsden, C. D. (1991). Modulation of motor cortical excitability by electrical stimulation over the cerebellum in man. *The Journal of Physiology*, *441*(1), 57–72. https://doi.org/10.1113/jphysiol.1991.sp018738

Ullsperger, M. (2024). Beyond peaks and troughs: Multiplexed performance monitoring signals in the EEG. *Psychophysiology*, *61*(7), e14553. https://doi.org/10.1111/psyp.14553

Unger, K., Heintz, S., & Kray, J. (2012). Punishment sensitivity modulates the processing of negative feedback but not error-induced learning. *Frontiers in Human Neuroscience*, *6*. https://doi.org/10.3389/fnhum.2012.00186

Uusisaari, M., & De Schutter, E. (2011). The mysterious microcircuitry of the cerebellar nuclei. *The Journal of Physiology*, *589*(14), 3441–3457. https://doi.org/10.1113/jphysiol.2010.201582

Uusisaari, M., & Knöpfel, T. (2010). GlyT2+ neurons in the lateral cerebellar nucleus. *The Cerebellum*, *9*(1), 42–55. https://doi.org/10.1007/s12311-009-0137-1

Uusisaari, M., Obata, K., & Knöpfel, T. (2007). Morphological and electrophysiological properties of GABAergic and non-GABAergic cells in the deep cerebellar nuclei. *Journal of Neurophysiology*, *97*(1), 901–911. https://doi.org/10.1152/jn.00974.2006

Vaghi, M. M., Vértes, P. E., Kitzbichler, M. G., Apergis-Schoute, A. M., van der Flier, F. E., Fineberg, N. A., Sule, A., Zaman, R., Voon, V., Kundu, P., Bullmore, E. T., & Robbins, T. W. (2017). Specific frontostriatal circuits for impaired cognitive flexibility and goal-directed planning in obsessive-compulsive disorder: Evidence from resting-state functional connectivity. *Biological Psychiatry*, *81*(8), 708–717. https://doi.org/10.1016/j.biopsych.2016.08.009

van der Meer, M. A., & Redish, A. D. (2011). Ventral striatum: A critical look at models of learning and evaluation. *Current Opinion in Neurobiology*, *21*(3), 387–392. https://doi.org/10.1016/j.conb.2011.02.011

van Es, D. M., van der Zwaag, W., & Knapen, T. (2019). Topographic maps of visual space in the human cerebellum. *Current Biology*, *29*(10), 1689-1694.e3. https://doi.org/10.1016/j.cub.2019.04.012

van Gaalen, J., Kerstens, F. G., Maas, R. P. P. W. M., Härmark, L., & van de Warrenburg, B. P. C. (2014). Drug-induced cerebellar ataxia: A systematic review. *CNS Drugs*, *28*(12), 1139–1153. https://doi.org/10.1007/s40263-014-0200-4

van Kemenade, B. M., Arikan, B. E., Podranski, K., Steinsträter, O., Kircher, T., & Straube, B. (2019). Distinct roles for the cerebellum, angular gyrus, and middle temporal gyrus in action-feedback monitoring. *Cerebral Cortex*, *29*(4), 1520–1531. https://doi.org/10.1093/cercor/bhy048

van Veen, V., & Carter, C. S. (2002). The anterior cingulate as a conflict monitor: fMRI and ERP studies. *Physiology & Behavior*, *77*(4), 477–482. https://doi.org/10.1016/S0031-9384(02)00930-7

van Veen, V., & Carter, C. S. (2006). Error detection, correction, and prevention in the brain: A brief review of data and theories. *Clinical EEG and Neuroscience*, *37*(4), 330–335. https://doi.org/10.1177/155005940603700411

van Essen, D. C., Donahue, C. J., & Glasser, M. F. (2018). Development and evolution of cerebral and cerebellar cortex. *Brain Behavior and Evolution*, *91*(3), 158–169. https://doi.org/10.1159/000489943

Verleger, R., Kuniecki, M., Möller, F., Fritzmannova, M., & Siebner, H. R. (2009). On how the motor cortices resolve an inter-hemispheric response conflict: An event-related EEG potential-guided TMS study of the Flankers task. *European Journal of Neuroscience*, *30*(2), 318–326. https://doi.org/10.1111/j.1460-9568.2009.06817.x

Vignali, C., Mutersbaugh, M., & Hull, C. (2024). Cerebellar climbing fibers signal flexible, rapidly adapting reward predictions. *bioRxiv*, 2024.10.09.617467. https://doi.org/10.1101/2024.10.09.617467

Viñas-Guasch, N., Ng, T. H. B., Heng, J. G., Chan, Y. C., Chew, E., Desmond, J. E., & Chen, S. H. A. (2023). Cerebellar transcranial magnetic stimulation (TMS) impairs visual working memory. *The Cerebellum*, *22*(3), 332–347. https://doi.org/10.1007/s12311-022-01396-2

Volz, K. G., Schubotz, R. I., & von Cramon, D. Y. (2005). Frontomedian activation depends on both feedback validity and valence: fMRI evidence for contextual feedback evaluation. *NeuroImage*, *27*(3), 564–571. https://doi.org/10.1016/j.neuroimage.2005.04.026

Voogd, J., & Glickstein, M. (1998). The anatomy of the cerebellum. *Trends in Cognitive Sciences*, *2*(9), 307–313. https://doi.org/10.1016/S1364-6613(98)01210-8

Voogd, J., & Marani, E. (2016). Gross anatomy of the cerebellum. In D. L. Gruol, N. Koibuchi, M.-U. Manto, M. Molinari, J. D. Schmahmann, & Y. Shen (Eds.), *Essentials of Cerebellum and Cerebellar Disorders* (1st ed., pp. 33–36). Springer Nature.

Wagner, A. R., & Rescorla, R. A. (1972). Inhibition in Pavlovian conditioning: Application of a theory. In R. A. Boakes & M. S. Halliday (Eds.), *Inhibition and Learning* (pp. 301–336). Academic Press.

Wagner, M. J., Kim, T. H., Savall, J., Schnitzer, M. J., & Luo, L. (2017). Cerebellar granule cells encode the expectation of reward. *Nature*, *544*(7648), 96–100. https://doi.org/10.1038/nature21726

Walsh, J. J., & Han, M. H. (2014). The heterogeneity of ventral tegmental area neurons: Projection functions in a mood-related context. *Neuroscience*, *282*, 101–108. https://doi.org/10.1016/j.neuroscience.2014.06.006

Wang, J. X., Kurth-Nelson, Z., Kumaran, D., Tirumala, D., Soyer, H., Leibo, J. Z., Hassabis, D., & Botvinick, M. (2018). Prefrontal cortex as a meta-reinforcement learning system. *Nature Neuroscience*, *21*(6), 860–868. https://doi.org/10.1038/s41593-018-0147-8

Wang, Y., & Lan, Y. (2023). The role of the cerebellum in drug reward: A review. *JIN*, *22*(6), 147. https://doi.org/10.31083/j.jin2206147

Warren, C. M., Hyman, J. M., Seamans, J. K., & Holroyd, C. B. (2015). Feedback-related negativity observed in rodent anterior cingulate cortex. *Journal of Physiology-Paris*, *109*(1–3), 87–94. https://doi.org/10.1016/j.jphysparis.2014.08.008

Washburn, S., Oñate, M., Yoshida, J., Vera, J., Bhuvanasundaram, R., Khatami, L., Nadim, F., & Khodakhah, K. (2024). The cerebellum directly modulates the substantia nigra dopaminergic activity. *Nature Neuroscience*, *27*(3), 497–513. https://doi.org/10.1038/s41593-023-01560-9

Watabe-Uchida, M., Zhu, L., Ogawa, S. K., Vamanrao, A., & Uchida, N. (2012). Whole-brain mapping of direct inputs to midbrain dopamine neurons. *Neuron*, *74*(5), 858–873. https://doi.org/10.1016/j.neuron.2012.03.017

Watanabe, M. (2016). Basket cells. In D. L. Gruol, N. Koibuchi, M.-U. Manto, M. Molinari, J. D. Schmahmann, & Y. Shen (Eds.), *Essentials of Cerebellum and Cerebellar Disorders* (1st ed., pp. 195–200). Springer Nature.

Weber, C., & Bellebaum, C. (2024). Prediction-error-dependent processing of immediate and delayed positive feedback. *Scientific Reports*, *14*(1), 9674. https://doi.org/10.1038/s41598-024-60328-8

Weeks, H. M., Therrien, A. S., & Bastian, A. J. (2017). Proprioceptive localization deficits in people with cerebellar damage. *The Cerebellum*, *16*(2), 427–437. https://doi.org/10.1007/s12311-016-0819-4

Weinberg, A., Luhmann, C. C., Bress, J. N., & Hajcak, G. (2012). Better late than never? The effect of feedback delay on ERP indices of reward processing. *Cognitive, Affective, & Behavioral Neuroscience*, *12*(4), 671–677. https://doi.org/10.3758/s13415-012-0104-z

Weismüller, B., & Bellebaum, C. (2016). Expectancy affects the feedback-related negativity (FRN) for delayed feedback in probabilistic learning. *Psychophysiology*, *53*(11), 1739–1750. https://doi.org/10.1111/psyp.12738

Wessel, J. R. (2012). Error awareness and the error-related negativity: Evaluating the first decade of evidence. *Frontiers in Human Neuroscience*, *6*, 8. https://doi.org/10.3389/fnhum.2012.00088

Windholz, G. (1997). Ivan P. Pavlov: An overview of his life and psychological work. *American Psychologist*, *52*(9), 941–946. https://doi.org/10.1037/0003-066X.52.9.941

Wolpert, D. M., & Kawato, M. (1998). Multiple paired forward and inverse models for motor control. *Neural Networks*, *11*(7), 1317–1329. https://doi.org/10.1016/S0893-6080(98)00066-5

Wolpert, D. M., Miall, R. C., & Kawato, M. (1998). Internal models in the cerebellum. *Trends in Cognitive Sciences*, *2*(9), 338–347. https://doi.org/10.1016/S1364-6613(98)01221-2

Wong, A. H. K., Wirth, F. M., & Pittig, A. (2022). Avoidance of learnt fear: Models, potential mechanisms, and future directions. *Behaviour Research and Therapy*, *151*, 104056. https://doi.org/10.1016/j.brat.2022.104056

Wu, W., Keller, C. J., Rogasch, N. C., Longwell, P., Shpigel, E., Rolle, C. E., & Etkin, A. (2018). ARTIST: A fully automated artifact rejection algorithm for single-pulse TMS-EEG data. *Human Brain Mapping*, *39*(4), 1607–1625. https://doi.org/10.1002/hbm.23938

Xue, A., Kong, R., Yang, Q., Eldaief, M. C., Angeli, P. A., DiNicola, L. M., Braga, R. M., Buckner, R. L., & Yeo, B. T. T. (2021). The detailed organization of the human cerebellum estimated by intrinsic functional connectivity within the individual. *Journal of Neurophysiology*, *125*(2), 358–384. https://doi.org/10.1152/jn.00561.2020

Yágüez, L., Coen, S., Gregory, L. J., Amaro, E., Altman, C., Brammer, M. J., Bullmore, E. T., Williams, S. C. R., & Aziz, Q. (2005). Brain response to visceral aversive conditioning: A functional magnetic resonance imaging study. *Gastroenterology*, *128*(7), 1819–1829. https://doi.org/10.1053/j.gastro.2005.02.068

Yamada, M., & Hoshino, M. (2016). Precerebellar nuclei. In D. L. Gruol, N. Koibuchi, M. Manto, M. Molinari, J. D. Schmahmann, & Y. Shen (Eds.), *Essentials of Cerebellum and Cerebellar Disorders: A Primer For Graduate Students* (pp. 63–67). Springer International Publishing. https://doi.org/10.1007/978-3-319-24551-5_7

Yates, J. R. (2023). Neuroanatomical and neurochemical substrates of addiction. In J. R. Yates (Ed.), *Determinants of Addiction* (pp. 91–132). Academic Press. https://doi.org/10.1016/B978-0-323-90578-7.00001-3

Yee, R. D. (1989). Downbeat nystagmus: Characteristics and localization of lesions. *Transactions of the American Ophthalmological Society*, *87*, 984–1032.

Yin, H., Wang, Y., Zhang, X., & Li, P. (2018). Feedback delay impaired reinforcement learning: Principal components analysis of reward positivity. *Neuroscience Letters*, *685*, 179–184. https://doi.org/10.1016/j.neulet.2018.08.039

Yoo, A. H., & Collins, A. G. E. (2022). How working memory and reinforcement learning are intertwined: A cognitive, neural, and computational perspective. *Journal of Cognitive Neuroscience*, *34*(4), 551–568. https://doi.org/10.1162/jocn_a_01808

Yoo, J. H., Zell, V., Gutierrez-Reed, N., Wu, J., Ressler, R., Shenasa, M. A., Johnson, A. B., Fife, K. H., Faget, L., & Hnasko, T. S. (2016). Ventral tegmental area glutamate neurons co-release GABA and promote positive reinforcement. *Nature Communications*, *7*(1), 13697. https://doi.org/10.1038/ncomms13697

Yoshida, J., Oñate, M., Khatami, L., Vera, J., Nadim, F., & Khodakhah, K. (2022). Cerebellar contributions to the basal ganglia influence motor coordination, reward processing, and movement vigor. *The Journal of Neuroscience*, *42*(45), 8406–8415. https://doi.org/10.1523/JNEUROSCI.1535-22.2022

Yoshida, T., Sugino, H., Yamamoto, H., Tanno, S., Tamura, M., Igarashi, J., Isomura, Y., & Hira, R. (2024). Synergistic reinforcement learning by cooperation of the cerebellum and basal ganglia. *bioRxiv*, 2024.07.12.603330. https://doi.org/10.1101/2024.07.12.603330

Yu, A. J., & Rankin, C. H. (2022). Learning and memory in the nematode Caenorhabditis elegans. In M. A. Krause, K. L. Hollis, & M. R. Papini (Eds.), *Evolution of Learning and Memory Mechanisms* (pp. 15–32). Cambridge University Press; Cambridge Core. https://doi.org/10.1017/9781108768450.004

Yu, R., Zhou, W., & Zhou, X. (2011). Rapid processing of both reward probability and reward uncertainty in the human anterior cingulate cortex. *PLOS ONE*, *6*(12), e29633. https://doi.org/10.1371/journal.pone.0029633

Zaghloul, K. A., Blanco, J. A., Weidemann, C. T., McGill, K., Jaggi, J. L., Baltuch, G. H., & Kahana, M. J. (2009). Human substantia nigra neurons encode unexpected financial rewards. *Science*, *323*(5920), 1496–1499. https://doi.org/10.1126/science.1167342

Zhang, H., Wang, B., Li, K., Wang, X., Li, X., Zhu, J., Zhao, Q., Yang, Y., Lv, L., Zhang, M., & Zhang, H. (2019). Altered functional connectivity between the cerebellum and the cortico-striato-thalamo-cortical circuit in obsessive-compulsive disorder. *Frontiers in Psychiatry*, *10*, 522. https://doi.org/10.3389/fpsyt.2019.00522

Zhang, L., Lengersdorff, L., Mikus, N., Gläscher, J., & Lamm, C. (2020). Using reinforcement learning models in social neuroscience: Frameworks, pitfalls and suggestions of best practices. *Social Cognitive and Affective Neuroscience*, *15*(6), 695–707. https://doi.org/10.1093/scan/nsaa089

Zhang, S., Hu, S., Chao, H. H., & Li, C.-S. R. (2016). Resting-state functional connectivity of the locus coeruleus in humans: In comparison with the ventral tegmental area/substantia nigra pars compacta and the effects of age. *Cerebral Cortex*, *26*(8), 3413–3427. https://doi.org/10.1093/cercor/bhv172

Zhang, X., Suo, X., Yang, X., Lai, H., Pan, N., He, M., Li, Q., Kuang, W., Wang, S., & Gong, Q. (2022). Structural and functional deficits and couplings in the cortico-striato-thalamo-cerebellar circuitry in social anxiety disorder. *Translational Psychiatry*, *12*(1), 26. https://doi.org/10.1038/s41398-022-01791-7

Zhang, Y., Larcher, K. M.-H., Misic, B., & Dagher, A. (2017). Anatomical and functional organization of the human substantia nigra and its connections. *eLife*, *6*, e26653. https://doi.org/10.7554/eLife.26653

Zhang, Z., Cheng, Z., Lin, Z., Nie, C., & Yang, T. (2018). A neural network model for the orbitofrontal cortex and task space acquisition during reinforcement learning. *PLOS Computational Biology*, *14*(1), e1005925. https://doi.org/10.1371/journal.pcbi.1005925

Zheng, N., & Raman, I. M. (2010). Synaptic inhibition, excitation, and plasticity in neurons of the cerebellar nuclei. *The Cerebellum*, *9*(1), 56–66. https://doi.org/10.1007/s12311-009-0140-6

Zhuang, Q., Zhu, S., Yang, X., Zhou, X., Xu, X., Chen, Z., Lan, C., Zhao, W., Becker, B., Yao, S., & Kendrick, K. M. (2021). Oxytocin-induced facilitation of learning in a probabilistic task is associated with reduced feedback- and error-related negativity potentials. *Journal of Psychopharmacology*, *35*(1), 40–49. https://doi.org/10.1177/0269881120972347

Zhuo, M., Kandel, E. R., & Hawkins, R. D. (1994). Nitric oxide and cGMP can produce either synaptic depression or potentiation depending on the frequency of presynaptic stimulation in the hippocampus. *NeuroReport*, *5*(9), 1033–1036.

Affidavit

Eidesstattliche Erklärung gemäß § 5 der Promotionsordnung vom 15.06.2018 der Mathematisch-Naturwissenschaftlichen Fakultät der Heinrich-Heine-Universität Düsseldorf:

Ich versichere an Eides Statt, dass die Dissertation von mir selbständig und ohne unzulässige fremde Hilfe unter Beachtung der „Grundsätze zur Sicherung guter wissenschaftlicher Praxis an der Heinrich-Heine-Universität Düsseldorf“ erstellt worden ist. Die Dissertation wurde in der vorliegenden oder ähnlichen Form noch bei keiner anderen Institution eingereicht. Ich habe bisher keine erfolglosen Promotionsversuche unternommen.

Düsseldorf, den _____ _____

Datum Dana Maria Huvermann

Acknowledgements

The work presented here would not have been possible without the help, support, and love of many people.

I could not have been luckier with my team of supervisors, Prof. Jutta Peterburs, Prof. Dagmar Timmann, Prof. Christian Bellebaum, and PD Dr. Martina Minnerop. I am extremely thankful to have had your guidance, especially considering the turbulent times of Covid and post-Covid in which all the experiments were conducted.

All of the experiments conducted were an effort beyond myself and would have not been possible without my project twin, Adam Berlijn, who worked side by side with me, and who endured many precarious days in the TMS lab with me. On a similar note, I would like to thank Andreas Thieme, Friedrich Erdlenbruch and Simone Lobrecht, who spent many weekends and evenings helping me collect data.

The emotional and physical labour of one Marc André Kellert shall not be forgotten. Without you, this doctoral thesis would not have been finished.

Besonders dankbar bin ich auch meiner Familie, die immer an mich geglaubt hat, sich mit mir gefreut hat, und sich mit mir geärgert hat. Papa und Mama, nur durch euer Beispiel und eure Unterstützung konnte ich zu der Person werden, die ich heute bin. Mama, du tanzt gerade sicherlich irgendwo ganz doll vor Freude. Meinen Geschwistern, Maya, Lynn und Luis danke ich für Ihren unerschütterlichen Glauben an mich. Luis, auch wenn du diesen Moment nicht mehr miterleben darfst, so bist du doch in jedem Schritt dieses Weges bei mir gewesen. Dein Einfluss reicht weit über diesen Moment hinaus, und ich trage ihn immer in mir. Oma und Opa, auch euch danke ich für eure Unterstützung. Eure Liebe, Geduld und Vertrauen in mich haben mir immer Halt gegeben – sei es in Momenten des Zweifels oder wenn es einfach nur gut tat, bei euch zu sein.

Special thanks also goes to Dr. Laura Bartylla, who introduced me to the world of science and has always listened and supported me throughout these years.

I would also like to thank my fellow lab members, in particular Alice Doubliez, Enzo Nio, and Julian Vahedi, with whom I have shared many years of companionship. Thank you, guys, for this exciting time we spent together!

Last, I would like to thank all the lovely participants who took part in the studies leading up to this dissertation.

Appendix

Original article of Manuscript 1

Huvermann, D. M., Berlijn, A. M., Thieme, A., Erdlenbruch, F., Groiss, S. J., Deistung, A., … & Peterburs, J. (2025). The cerebellum contributes to prediction error coding in reinforcement learning in humans. *Journal of Neuroscience*, e1972242025.

I was the corresponding and first author of this article. My co-authors and I conceptualised the study and created the experimental setup. I acquired the behavioural and EEG data for Study 1 on my own, while MRI data for Study 1 was acquired with the support of several co-authors. For Study 2, data acquisition was conducted by Adam Berlijn and me. I wrote all code for data preprocessing and behavioural/prediction error modelling. I performed the statistical analysis and wrote the first draft of the manuscript. All authors contributed to results interpretation, discussion, revision, and read and approved the final version of the manuscript.

Original article of Manuscript 2

Huvermann, D. M.*, Berlijn, A. M.*, Groiss, S. J., Mittelstaedt, M., Schnitzler, A., Bellebaum, C., … & Peterburs, J. (2025). Cerebellar single-pulse TMS differentially affects early and late error processing in reinforcement learning. *Manuscript submitted for publication*.

I was the corresponding and shared first author of this article. My co-authors and I conceptualised the study and created the experimental setup. Adam Berlijn and I conducted the data acquisition. I performed the preprocessing and statistical analysis and wrote the first draft of the manuscript. All authors contributed to results interpretation, discussion, revision, and read and approved the final version of the manuscript.

Original article of Manuscript 3

Berlijn, A. M.*, Huvermann, D. M.*, Groiss, S. J., Schnitzler, A., Mittelstaedt, M., Bellebaum, C., ... & Peterburs, J. (2024). The effect of cerebellar TMS on error processing: A combined single-pulse TMS and ERP study. *Imaging Neuroscience*, *2*, 1-19.

I was the shared first author of this manuscript. My co-authors and I conceptualised the study and created the experimental setup. Adam Berlijn and I conducted the data acquisition, statistical analysis, and wrote the first draft of the manuscript. All authors contributed to results interpretation, discussion, revision, and read and approved the final version of the manuscript.

Systems/Circuits

The Cerebellum Contributes to Prediction Error Coding in Reinforcement Learning in Humans

Dana M. Huvermann,[1,2] Adam M. Berlijn,[2,3] Andreas Thieme,[1] Friedrich Erdlenbruch,[1] Stefan J. Groiss,[4,5] Andreas Deistung,[6] Manfred Mittelstaedt,[2] Elke Wondzinski,[7] Heike Sievers,[7] Benedikt Frank,[1] Sophia L. Göricke,[1] Michael Gliem,[8] Martin Köhrmann,[1] Mario Siebler,[7,8] Alfons Schnitzler,[4,5] Christian Bellebaum,[2] Martina Minnerop,[3,4,5] Dagmar Timmann,[1]* and Jutta Peterburs[2,9]*

[1]Department of Neurology and Center for Translational and Behavioral Neurosciences (C-TNBS), Essen University Hospital, University of Duisburg-Essen, Essen 45147, Germany, [2]Faculty of Mathematics and Natural Sciences, Heinrich Heine University Düsseldorf, Düsseldorf 40225, Germany, [3]Institute of Neuroscience and Medicine (INM-1), Research Centre Jülich, Jülich 52428, Germany, [4]Institute of Clinical Neuroscience and Medical Psychology, Medical Faculty & University Hospital Düsseldorf, Heinrich Heine University Düsseldorf, Düsseldorf 40225, Germany, [5]Department of Neurology, Center for Movement Disorders and Neuromodulation, Medical Faculty & University Hospital Düsseldorf, Heinrich-Heine University Düsseldorf, Düsseldorf 40225, Germany, [6]University Clinic and Outpatient Clinic for Radiology, Department for Radiation Medicine, University Hospital Halle (Saale), University Medicine Halle, Halle (Saale) 06120, Germany, [7]Department of Neurology and Neurorehabilitation, MediClin Fachklinik Rhein/Ruhr, Essen 45219, Germany, [8]Department of Neurology, Medical Faculty & University Hospital Düsseldorf, Heinrich Heine University Düsseldorf, Düsseldorf 40225, Germany, and [9]Institute for Systems Medicine & Department of Human Medicine, MSH Medical School Hamburg, Hamburg 20457, Germany

Recent rodent data suggest that the cerebellum—a region typically associated with processing sensory prediction errors (PEs)—also processes PEs in reinforcement learning (RL-PEs; i.e., learning from action outcomes). We tested whether cerebellar output is necessary for RL-PE processing in regions more traditionally associated with action-outcome processing, such as the striatum and anterior cingulate cortex. The feedback-related negativity (FRN) was measured as a proxy of cerebral RL-PE processing in a probabilistic feedback learning task using electroencephalography. Two complementary experiments were performed in humans. First, patients with chronic cerebellar stroke (20 male, 6 female) and matched healthy controls (19 male, 7 female) were tested. Second, single-pulse cerebellar transcranial magnetic stimulation (TMS) was applied in healthy participants (7 male, 17 female), thus implementing a virtual lesion approach. Consistent with previous studies, learning of action-outcome associations was intact with only minor changes in behavioral flexibility. Importantly, no significant RL-PE processing was observed in the FRN in patients with cerebellar stroke and in participants receiving cerebellar TMS. Findings in both experiments show that RL-PE processing in the forebrain depends on cerebellar output in humans, complementing and extending previous findings in rodents.

Key words: **cerebellum; event-related potentials (ERPs); executive functions; lesion; noninvasive brain stimulation; performance monitoring**

Significance Statement

While processing of prediction errors in reinforcement learning (RL-PEs) is usually attributed to midbrain and forebrain, recent rodent studies have recorded RL-PE signals in the cerebellum. It is not yet clear whether these cerebellar RL-PE signals contribute to RL-PE processing in the forebrain/midbrain. In the current study, we could show that forebrain RL-PE coding is blunted when the cerebellum is affected across two complementary lesion models (patients with cerebellar stroke, cerebellar TMS). Our results support direct involvement of the cerebellum in RL-PE processing. We can further show that the cerebellum is necessary for RL-PE coding in the forebrain.

Received Oct. 17, 2024; revised March 12, 2025; accepted March 14, 2025.

Author contributions: D.M.H., A.M.B., S.J.G., C.B., Martina Minnerop, D.T., and J.P. designed research; D.M.H., A.M.B., A.T., F.E., and S.J.G. performed research; Manfred Mittelstaedt, E.W., H.S., B.F., M.G., M.K., M.S., and A.S. contributed unpublished reagents/analytic tools; D.M.H., A.D., and S.L.G. analyzed data; D.M.H., C.B., Martina Minnerop, D.T., and J.P. wrote the paper.

We thank the German Research Foundation (Deutsche Forschungsgemeinschaft, DFG; project number: 437661157 awarded to J.P., D.T., and Martina Minnerop) for supporting this research. D.M.H. was partially supported by the Bernd Fink Foundation. We thank Greta Wippich for drawing the Experimental Procedure in Figures 2*A* and 4*A*; Simone Lohbeck, Michael Klein, and Naomi Johanna Müller for their help with data acquisition; Thomas Ernst for his help with setting up the MRI protocol and conversion of MR data into BIDS format; and Beate Brol for her help with lesion symptom mapping.

*D.T. and J.P. contributed equally to this work.

The authors declare no competing financial interests.

Correspondence should be addressed to Dana Huvermann at dana.huvermann@hhu.de.

https://doi.org/10.1523/JNEUROSCI.1972-24.2025

Introduction

In our fast-paced world, we need to constantly monitor our environment and our actions and choose according to the anticipated consequences of our actions. In such reinforcement learning contexts, we rely on external feedback (e.g., reward/success, punishment/failure) to acquire action-outcome associations and thereby improve our behavior. Thus, we need to learn to predict action outcomes, for which we rely heavily on processing prediction errors, i.e., the difference between predicted and actual outcomes.

Prediction errors in reinforcement learning contexts (RL-PEs) have mainly been linked to basal ganglia, midbrain, and prefrontal areas (Fouragnan et al., 2018). Predictive functions beyond the motor domain have also been proposed for the cerebellum (Ramnani, 2006; Sokolov et al., 2017). More recent studies have shown cerebellar activation patterns consistent with RL-PEs in both humans and rodents (Kostadinov and Häusser, 2022; Manto et al., 2024; Berlijn et al., 2024b). Moreover, psychiatric disorders with cerebellar involvement, such as schizophrenia, autism spectrum disorder, and major depression (Phillips et al., 2015), have been reliably associated with altered and/or impaired reinforcement learning (Balsters et al., 2017; Halahakoon et al., 2020; Katthagen et al., 2020). However, deficits cannot clearly be attributed to cerebellar dysfunction, as multiple brain areas are typically affected in these disorders. Causal evidence for cerebellar involvement in reinforcement learning in humans is scarce. Patients with cerebellar damage showed deficits in reversal, but not acquisition learning within reinforcement learning (Thoma et al., 2008; Nicholas et al., 2024). An initial study using electroencephalography (EEG) showed altered outcome/feedback processing in patients with cerebellar stroke without impaired acquisition learning (Rustemeier et al., 2016).

In humans, RL-PE processing is typically studied using feedback learning tasks. Here, participants have to learn through trial and error that, for example, one of several response options leads to a higher probability of monetary reward over punishment (Eppinger et al., 2008). EEG can be used to measure an approximation of activity in one of the main drivers of RL-PE processing, the anterior cingulate cortex (ACC; Fouragnan et al., 2018): the feedback-related negativity (FRN) is a frontocentral negative deflection in the event-related potential (ERP) that emerges ~250 ms after feedback onset (e.g., presentation of a reward or punishment; Miltner et al., 1997; San Martín, 2012). Reflecting the activity of dopaminergic target regions, such as the ACC and striatum (Holroyd and Coles, 2002; Hauser et al., 2014; Foti et al., 2015), FRN amplitudes covary with the estimated RL-PE at the single-trial level (Fischer and Ullsperger, 2013; Hoy et al., 2021; Rawls and Lamm, 2021).

Despite findings of RL-PE-like signals in the cerebellum in rodents and initial accounts of altered reinforcement learning in humans with cerebellar damage, acquisition learning seems to be largely unaffected in cerebellar lesion patients (Thoma et al., 2008; Rustemeier et al., 2016). In the present study, we therefore studied the interplay between the cerebellum and cerebral cortex with respect to RL-PE processing more directly by investigating the impact of cerebellar damage/disruption on cortical RL-PE coding in the FRN and learning success. This approach extends previous observations of RL-PE signals in the cerebellum toward the question whether these are necessary for intact cerebral RL-PE processing. In two experiments, we studied patients with chronic cerebellar stroke and used single-pulse transcranial magnetic stimulation (TMS) in healthy adults to create a "virtual lesion." Single-pulse TMS offers the advantage of examining effects of deficits with a high temporal precision. Reinforcement learning success was assessed using a probabilistic feedback learning task. RL-PE processing was assessed using the FRN on a trial-by-trial basis. If the cerebellum contributes to reinforcement learning, RL-PE processing as reflected in the FRN should be reduced in cerebellar stroke patients compared with healthy controls (Experiment 1) and for cerebellar single-pulse TMS (Experiment 2). Indeed, no significant RL-PE processing as indexed by the FRN was found in cerebellar stroke patients and for cerebellar TMS. Concerning behavior, only minor abnormalities in behavioral flexibility were observed, with reinforcement learning success generally preserved.

Materials and Methods

Experiment 1

Participants

Thirty-one adults with a chronic stroke restricted to the cerebellum were recruited from the university hospitals Essen and Düsseldorf as well as the Rhein-Ruhr Clinic in Essen-Kettwig, Germany. Only patients with a postacute stroke, i.e., at least 6 months after the stroke event (with one exception who was only 42 d poststroke), were included. Lesions had to be confined to the cerebellum. Thirty-three adults without stroke were recruited as controls. Inclusion criteria were no current psychiatric and no current or past neurological disease, no use of medications affecting the central nervous system, and no alcohol or illicit drug abuse. Five patients and four controls were excluded because they did not meet these inclusion criteria. In total, data from 26 patients (20 men and 6 women) and the 26 controls (19 men and 7 women) who provided the best match regarding demographic parameters entered the analyses. Three controls were excluded during matching to ensure that nontask-related parameters (Table 1) did not result in group differences in task-related variables. Means and standard deviations on the main demographic variables are listed in Table 1 (for details, see Table 2 for patients and Table 3 for controls). Of note, three patients with depression and antidepressant medication and three matched controls (who also had a clinical diagnosis of depression and antidepressant medication, roughly matched on BDI score) were included in the analyses, as we could not exclude this to be part of a cerebellar cognitive affective symptom (CCAS; Schmahmann and Sherman, 1998), and to ensure that target sample size was met.

Handedness was assessed with the Edinburgh Handedness Inventory (EHI; Table 1; Oldfield, 1971). According to LQ_{EHI}, 19 patients and 21 controls were right-handed, 3 patients and 1 control were left-handed, and 4 patients and 4 controls were ambidextrous. IQ estimates were obtained using the Mehrfachwahl-Wortschatz-Test-B score (MWT-B; multiple choice vocabulary test; Table 1; Merz et al., 1975). As depression might affect feedback processing (Keren et al., 2018) and has a higher incidence poststroke (Robinson and Jorge, 2016), we assessed depression using the Beck Depression Inventory II (BDI; Beck et al., 1996).

Figure 1 shows the overlaid lesion regions for all 26 patients. Overall, 21 patients had a stroke in the posterior inferior cerebellar artery (PICA) territory (9 left, 9 right, 3 bilateral), 3 patients had a stroke in the superior

Table 1. Demographic data for patients and controls as well as group comparisons

Variable	$M_{controls}$ (SD)	$M_{patients}$ (SD)	t	df	p
Age	56.4 (12.7)	56.2 (12.1)	0.04	49.86	0.964
Education (years)	13.5 (2.3)	14.1 (2.9)	0.90	47.44	0.371
LQ_{EHI}	70.9 (47.2)	56.6 (54.0)	1.01	49.11	0.316
MWT-B (IQ)	118.8 (16.1)	113.4 (13.9)	1.28	48.91	0.205
WML rating	0.31 (0.47)	0.69 (0.79)	2.14	40.81	0.039
BDI-II	5.3 (7.5)	6.3 (9.1)	0.42	48.17	0.679

$n_{controls} = 26$, $n_{patients} = 26$. *M*, mean; SD, standard deviation. Age and education are given in years. LQ, laterality quotient; EHI, Edinburgh Handedness Inventory; MWT-B, Mehrfachwahl-Wortschatz-test B (a vocabulary-based German intelligence test); WML, white matter lesion; BDI-II, Beck depression inventory II.

Table 2. Patients' and lesion characteristics

ID	Age	Sex	Edu.	Hnd.	Vascular territory	Time since stroke (years)	Affected cerebellar regions	Additional information
005	55–59	m	16–20	r	PICA-L (lacunar)	0–5	Left Crus II, left Crus I, left VIIIa	
011	45–49	m	16–20	r	PICA-R	0–5	Right Crus II, right VIIIa, right VIIb, right VIIIb, right IX, right Crus I	External MRI
012	30–34	m	16–20	r	PICA-R	0–5	Right VIIIa, right VIIb, right VIIIb, right IX, right Crus II	
014	65–69	m	11–15	a	PICA-R	21–25	Right VIIb, right Crus II, right VIIIa, right VIIIb, right IX, vermal VIIIa, vermal VIIIb	
018	55–59	m	11–15	a	PICA-L	11–15	Left Crus I, left Crus II, left VIIIa, left VIIb, left VIIIb, left VI	
020	70–74	m	11–15	r	SCA-R	11–15	Right I-IV, right V, right Dentate	
023	55–59	f	11–15	l	PICA-R	16–20	Right Crus I, right VIIIb, right IX, right Crus II, right VIIb, right VIIIa	
024	60–64	m	11–15	r	PICA-L+R (lacunar)	6–10	Right VIIb, left VIIb	
026	65–69	f	6–10	r	PICA-R, PICA-L (lacunar)	6–10	Right VIIIa, right VIIb, right IX, right Crus II, right VIIIb, left VIIIa, left IX, left VIIIb	Migraine
029	50–54	m	16–20	a	SCA-R	11–15	Right VI, right V, right Dentate, right Crus I	Recent history of AD, negative BAI
031	45–49	m	11–15	r	PICA-R (lacunar)	0–5	right Crus I, right Crus II, right VIIIa	
033	50–54	f	11–15	r	PICA-L, SCA-R (lacunar)	6–10	Left Crus I, left Crus II, left VIIb, right Crus I, left VIIIa, vermal Crus II	MDD, intake of antidepressants
035	60–64	m	16–20	a	PICA-L	16–20	Left VIIIa, left VIIb, left VIIIb, left Crus II, left IX, left Crus I	MDD, antidepressants
037	55–59	f	16–20	r	PICA-L	0–5	Left IX, left VIIIb, left VIIb, left VIIIa, left Crus II, left Dentate	External MRI
038	55–59	f	11–15	r	PICA-L, PICA-R (lacunar)	6–10	Left Crus II, left VIIb, left VIIIa, left IX, left Crus I, left VIIIb	
039	60–64	m	16–20	l	PICA-R (lacunar)	n/a[a]	Right Crus I	External MRI
040	60–64	m	16–20	r	PICA-L	0–5	Left Crus II, left VIIb, left VIIIa, left VIIIb, left Crus I, left IX	Not a native German speaker
042	50–54	m	11–15	r	PICA-R	6–10	Right Crus II, right VIIb, right Crus I, right VIIIa	
046	18–24	m	11–15	r	PICA-R	0–5	Right VIIb, right VIIIa, right VIIIb	External MRI
047	65–69	m	16–20	r	PICA-R	0–5	Right Crus II, right Crus I, right VIIb, right VIIIa, right VIIIb, right IX	
048	65–69	m	16–20	l	PICA-L	6–10	Left Crus II, left VIIb, left VIIIa, left VIIIb, left Crus I, left IX, left dentate	
055	70–74	m	6–10	r	PICA-L	6–10	Left Crus II, left Crus I	
056	65–69	m	11–15	r	SCA-L	6–10	Left V, left VI, left I-IV, left dentate	
058	45–49	f	11–15	r	PICA-L (lacunar)	0–5	Left VIIIb, left IX	MDD, childhood diagnosis of ADD, antidepressants
060	50–54	m	11–15	r	SCA-L, PICA-R	16–20	Left V, left VI, right Crus II, left I-IV, right VIIb, left Dentate	
061	55–59	m	16–20	r	PICA-L	0–5	Left Crus II, left Crus I, left VIIb, left VIIIa, left VIIIb, left IX	

Age is given in years. m, male; f, female; edu., years of education; hnd., handedness according to Edinburgh Handedness Inventory; l, left; r, right; a, ambidextrous; PICA, posterior inferior cerebellar artery; SCA, superior inferior artery; SARA, scale for the assessment and rating of ataxia (maximum score = 40); MDD, major depressive disorder; AD, anxiety disorder; ADD, attention deficit disorder; BAI, Beck anxiety inventory (Beck et al., 1988). For affected regions, only those that made out >1% of total lesion volume were included. Regions are sorted according to percentage of total lesion volume. Age, education, and time since stroke are given in ranges to comply with data protection requirements.
[a]Time since stroke was unknown in this case, as the lacunar stroke was an incidental finding.

cerebellar artery (SCA) territory (1 left, 2 right), and 2 patients had a stroke in both the PICA and SCA territory (1 in the left PICA and right SCA territory, 1 in the right PICA and left SCA territory). Lesions were thus unilateral in all but five patients (Table 2). Images of individual lesions are provided in Extended Data Figure 1-1. Mean time between cerebellar infarct and participation in the experiment was 8.4 years (SD = 6.0 years, range from 1.5 months to 22 years; unknown in one case).

Both patients and controls were assessed for clinical neurological symptoms. While patients showed overall higher scores on the scale for the assessment and rating of ataxia (SARA; Schmitz-Hübsch et al., 2006) than controls ($t_{(47.01)} = 2.74$, $p = 0.009$), no participants showed deficits in oculomotor function in the neurological examination (which might have affected task performance).

All participants gave written informed consent prior to participation. They received monetary compensation for participation and were reimbursed for travel costs. The experiment was preregistered on the Open Science Framework (OSF; https://osf.io/rd3xb), conducted in accordance with the ethical principles for medical research involving human subjects outlined in the Declaration of Helsinki, and approved by the Ethics Committees at the Faculty of Medicine of Heinrich-Heine-University Düsseldorf and at the University Hospital Essen.

Procedure

The experiment usually took place on 2 consecutive days. The temporal gap between sessions was longer for three patients (56, 29, and 43 d) and two controls (9 and 2 d) due to participants' time constraints or scheduling issues. The experimental task with EEG was conducted on both days with different versions (short and long feedback delay version, respectively; see below for details). On the first day, we initially obtained informed consent and participants filled in a demographic questionnaire, the EHI, the BDI-II, and the MWT-B. Following EEG preparations, participants were informed about EEG artifacts and how to avoid them.

Subsequently, participants completed one of two feedback delay versions of a probabilistic feedback learning task as described by Eppinger et al. (2008; see Fig. 2*A* for the experimental procedure), which was conducted using Presentation software (version 20.0, Neurobehavioral Systems). Order of the versions was counterbalanced among participants. Figure 2*B* illustrates the sequence and time course of stimulus presentation in one trial. The task consisted of 8 blocks of 40 trials, thus 320 trials in total. Five practice trials with different stimuli were provided. Each trial began with a fixation cross presented for 500–1,500 ms. Next, one of four abstract stimuli (Chinese characters and radicals) was presented for 1,500 ms. Participants had to respond by pressing the left or right button on a response box (Cedrus RB-740, Cedrus Corporation) within a response time window of 3,000 ms. Choices were highlighted on the screen for 200 ms, followed by a black screen for 500 ms in the short delay condition and 6,500 ms in the long delay condition. Different delay durations were used as previous studies had shown differential involvement of cerebral brain areas depending on feedback delay (Foerde and Shohamy, 2011). While immediate delay

Table 3. Characteristics of controls for Experiment 1 (patient study)

ID	Age	Sex	Handedness (EHI)	Years of education	Additional information
001	55–59	f	Right	11–15	
002	75–79	m	Right	16–20	Excluded (matching)
004	60–64	m	Right	11–15	Excluded (developmental venous anomaly)
006	70–74	m	Right	11–15	
007	55–59	f	Right	11–15	
008	55–59	m	Right	6–10	MD, intake of antidepressants
009	70–74	m	Right	11–15	
010	50–54	f	Right	11–15	
013	55–59	m	Right	16–20	
017	70–74	f	Right	11–15	
019	60–64	m	Right	11–15	
021	50–54	m	Right	16–20	
022	55–59	f	Right	16–20	MD, intake of antidepressants
025	55–59	m	Right	11–15	Excluded (moderate brain volume loss)
027	70–74	m	Right	16–20	
028	45–49	f	Right	11–15	MD, intake of antidepressants
030	45–49	m	Right	11–15	
032	55–59	m	Right	16–20	Excluded (matching)
034	55–59	m	Right	11–15	
036	25–29	m	Right	6–10	Excluded (intake of antidepressants)
043	18–24	m	Right	11–15	
044	55–59	m	Left	11–15	
045	65–69	m	Ambidextrous	11–15	
049	70–74	m	Right	11–15	Not a native German speaker
050	50–54	f	Right	6–10	
051	50–54	m	Right	11–15	MD, intake of antidepressants, excluded (matching)
052	18–24	m	Ambidextrous	6–10	
054	55–59	m	Ambidextrous	11–15	
057	70–74	m	Right	11–15	Excluded (extensive white matter lesions)
059	55–59	m	Ambidextrous	16–20	
062	50–54	m	Right	11–15	
063	55–59	m	Right	11–15	
064	65–69	m	Right	11–15	

Age is given in years. m, male; f, female; EHI, Edinburgh Handedness Inventory; SARA, Scale for the Assessment and Rating of Ataxia; MD, major depression. Age and education are given in ranges to comply with data protection requirements.

activated areas typically associated with reward processing, such as the striatum, activations for delayed feedback shifted toward the hippocampus (Foerde and Shohamy, 2011). This shift was also apparent in FRN, with a decreased FRN amplitude with longer feedback delays (Peterburs et al., 2016). This shift in activation could affect potential deficits in cerebellar patients due to differences in connectivity of these brain regions with the cerebellum. Finally, feedback was displayed for 1,000 ms. Feedback consisted of either the display of "+20 ct" in green font as positive feedback or "−10 ct" in red font as negative feedback.

Two of the four stimuli were linked to random feedback (50% positive and 50% negative regardless of response), while the other two were linked to contingent feedback. Here, correct responses were followed by positive feedback 90% of the time and by negative feedback 10% of the time (and vice versa for incorrect responses). Correctness was balanced for the two response buttons, so that for one of these stimuli, the chance of positive feedback was higher for the left button, while for the other stimulus, the chance of positive feedback was higher for the right button. In case a participant exceeded the learning criterion of 65% correct answers by the second of eight blocks, a new stimulus set was provided to increase the number of prelearning trials. This was the case for eight patients and eight controls in one feedback delay condition/session (of which 1 and 5, respectively, were second sessions) and for six patients and eight controls in both conditions. In case a participant did not exceed the learning criterion until the eighth and last block, a ninth block was added to increase the number of postlearning trials. This was the case for three patients and two controls in one of the two conditions.

Following this task on Day 1, participants underwent cranial MRI and a clinical neurological examination.

On the second day, following EEG preparations, the remaining other version (short or long feedback delay version) of the probabilistic feedback task was completed. Versions were counterbalanced between sessions. Two different stimulus sets were used per session, and order was counterbalanced. Responses (choice, choice accuracy) and response times were recorded during the experiment.

EEG recording and preprocessing

EEG was recorded from 28 active Ag/AgCl electrodes (F7, F3, Fz, F4, F8, FC5, FC1, FC2, FC6, T7, C3, Cz, C4, T8, CP5, CP1, CP2, CP6, P7, P3, Pz, P4, P8, PO9, O1, Oz, O2, PO10) positioned on a BrainCap (Brain Products) according to the 10–20 system. FCz was used as an on-line reference, and AFz was used as ground electrode. Fp1 was used as vertical electrooculogram (vEOG) and an electrode was placed next to the outer canthus of the left eye as horizontal electrooculogram (hEOG). Impedances were kept below 25 kΩ. Data were amplified with a BrainAmp DC amplifier and recorded at 1,000 Hz using BrainVision Recorder 1.21 (Brain Products). Data preprocessing was performed using BrainVision Analyzer 2 software (version 2.2, Brain Products) and MATLAB (MathWorks).

First, data were rereferenced to the mastoid electrodes and FCz was reestablished. Next, a DC detrend was applied and data were filtered using zero phase shift Butterworth filters with a low cutoff of 1 Hz and high cutoff of 30 Hz, as well as a notch filter at 50 Hz to remove powerline artifacts. Subsequently, we removed vertical and horizontal eye movement artifacts using a semiautomatic Ocular Correction ICA as implemented in BrainVision Analyzer 2. vEOG was used for blinks and vertical activity, and hEOG for horizontal activity. The first 177.2 s were used for ICA. We then segmented data from the start marker of the experiment to end of experiment, and segmented them around the feedback markers, starting 200 ms before and ending 600 ms after each marker. Only feedback markers for learnable stimuli were segmented. Baseline correction was performed based on the 200 ms preceding feedback onset, followed by automated artifact rejection. Segments with a voltage step exceeding 50 μV/ms, an amplitude above 100 μV or below −100 μV, or activity not exceeding 0.1 μV were excluded. Single-trial data were then exported via generic data export. On average, 1.1% of segments (SD = 2.5%) were rejected. Additionally, data for learnable stimuli were averaged and exported according to feedback valence (positive, negative) and feedback delay (short, long).

The EEG system had to be switched from an actiCAP system to a newer actiCAP snap system after the first 27 participants due to a defect in impedance measurement.

In MATLAB, peak detection was performed on the averaged data separately for each condition [feedback valence (positive, negative) × feedback delay (short, long)]. The FRN was defined as the local maximal negative peak within the time window between 200 and 350 ms at electrode site FCz (Sambrook and Goslin, 2015). If no local maximum/minimum could be detected, the corresponding single-trial segments were excluded. For the single-trial data, the mean amplitude in a time window of 40 ms around the respective FRN latency determined by the peak detection on the averaged data was extracted (Meadows et al., 2016).

Prediction error estimation

Prediction errors on each trial were estimated based on choices participants made and feedback they received using a reinforcement learning model (Sutton and Barto, 2018) consistent with previous studies (Ichikawa et al., 2010; Fischer and Ullsperger, 2013; McDougle et al., 2019) which has been shown to be highly correlated with the gold standard (i.e., subjective ratings; Ichikawa et al., 2010). We modeled action values Q and PEs δ based on the actually received feedback R and

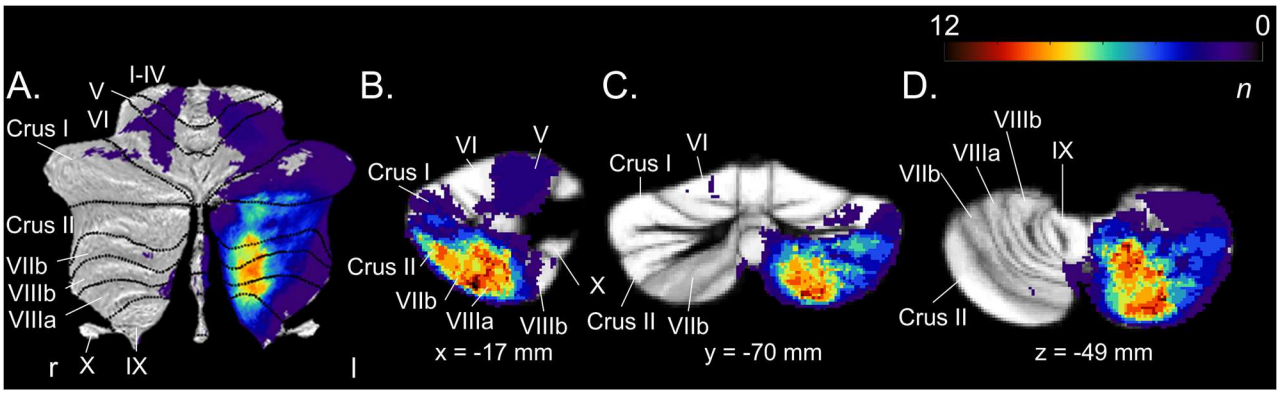

Figure 1. Overlap plot of all lesions in the patient group ($n = 26$) superimposed on (***A***) a cerebellar flatmap (Diedrichsen and Zotow, 2015) and in 2D (***B***) sagittal, (***C***) coronal, and (***D***) axial views. Lesions on the right side were mirrored to the left side. Color code shown on the top right denotes total lesion overlap (from purple = 0 to red = 12). Individual lesions are depicted in Extended Data Figure 1-1.

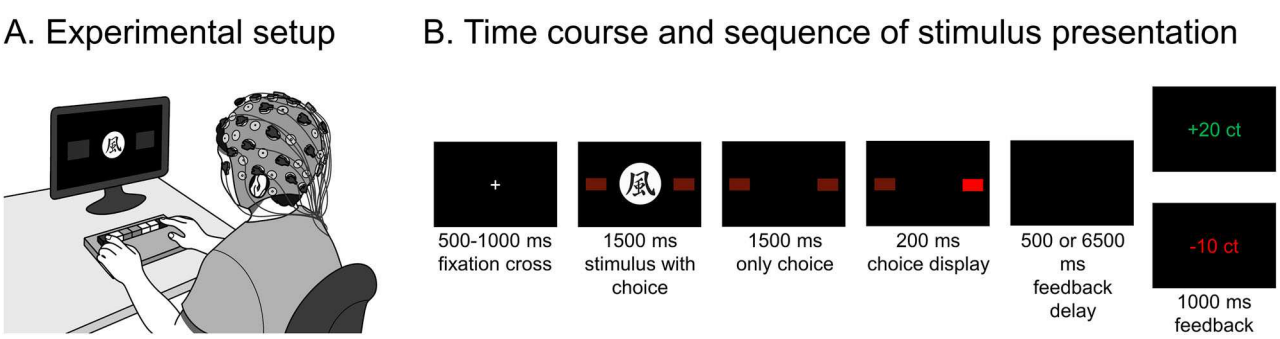

Figure 2. Experimental procedure of Experiment 1 (patient study). ***A***, Experimental setup. EEG was recorded while participants performed the probabilistic feedback task. ***B***, Time course and sequence of stimulus presentation in one trial of the feedback learning task. After a fixation cross was presented for 500–1,000 ms, one of four stimuli was presented, toward which participants were required to respond by pressing the left or right button on a response pad within 3,000 ms. The stimulus was only shown for the first 1,500 ms. After the response, the respective choice was highlighted on screen for 200 ms, followed by either 500 or 6,500 ms of blank screen (depending on feedback delay version). Positive ("+20 ct") or negative feedback ("−10 ct") was then presented on screen for 1,000 ms. Participants needed to learn by trial and error whether one of the choices was related to higher chance of positive/negative feedback depending on stimulus. Feedback for two of the stimuli had a 90% contingency, while for the other two it had a 50% (random) contingency. A total of 320 trials were used in the task.

participants' chosen response a, using a Rescorla–Wagner model (Rescorla and Wagner, 1972; Wagner and Rescorla, 1972):

$$Q_{a,t+1} = Q_{a,t} + \alpha * \delta_t,$$

$$\delta_t = R_{a,t} - Q_{a,t}.$$

To model response probabilities, we used a softmax function (Sutton and Barto, 2018), which estimates the probability p of the chosen action with the estimated action values Q per action a and time point t (in this case, the trial):

$$p_{a_1,t} = \frac{e^{\beta * Q_{a_1,t}}}{e^{\beta * Q_{a_1,t}} + e^{\beta * Q_{a_2,t}}}.$$

The function *fmincon* provided by MATLAB was used to fit this model to the data via minimizing the negative sum of log-likelihoods minus a gamma distribution of β with a shape parameter of 2 and scale parameter of 3 (as to penalize high β; McDougle et al., 2019). We estimated a learning rate α as well as an inverse temperature β for exploration behavior, separately for each stimulus and reward and punishment. We allowed α to assume any value between 0 and 1 and β to assume any value between 0 and 50.

Experimental design and statistical analysis

This study was preregistered to OSF (https://osf.io/rd3xb). Necessary sample size was determined via power analysis to be $N = 48$, i.e., 24 per group, as detailed in the preregistration. Required sample size was thus matched ($n = 26$ per group). Raw data and code used for preprocessing and analysis are available from https://osf.io/cqf97.

Analysis focused on differences in the FRN between controls and patients (on group level), especially in relation to coding of RL-PEs. As the signed RL-PE overlaps with feedback valence, we split the signed RL-PE into the unsigned RL-PE (on a scale from 0/low to 1/high) and feedback valence (positive, negative), which were used as separate predictors in the analysis. We further examined learning success as reflected in choice accuracy and choice switching as an index of behavioral flexibility. The analysis was restricted to stimuli with a 90% contingency, as participants were not able to learn in the 50% contingency condition.

Data were analyzed in R (version 4.2.3; R Core Team, 2023) using RStudio (version 2023.3.0.386, Posit Team, 2023). Concerning choice accuracy, the preregistered ANOVA was performed. For the FRN, since only 14 patients and 12 controls exceeded the learning criterion of >65% correct responses within at least one block of the task in either version, the preregistered ANOVA analysis with learning phase (pre-/postlearning) as a factor was not feasible. With the factor learning phase, we had aimed to investigate to what extent feedback processing changed over the course of the task as participants learned which responses resulted in a higher chance of reward/punishment. Instead, we decided to pursue a single-trial–based analysis approach using LME models including the trial-by-trial unsigned RL-PE. Analyses based on single trials have increasingly been used in recent studies as they offer the possibility to use variables that vary from trial to trial as factors in the statistical analysis (Volpert-Esmond et al., 2021). LME analyses based on single-trial data have also been shown to deliver less biased results compared

with ANOVAs based on averaged data (Heise et al., 2022). The lme4 library (version 1.1-32; Bates et al., 2015) was used for LME modeling, and the lmertest library (version 3.1-3; Kuznetsova et al., 2017) was used to evaluate statistical significance. Significance was evaluated using restricted maximum likelihood with p values computed using Satterthwaite approximation, following the findings by Luke (Luke, 2017). While we initially tested a maximal fit for random effects, in case of singular fit, we reduced the originally maximal random effects structure up to the random intercept and highest-order interaction as random slope per participant (Brauer and Curtin, 2018). For all LME analyses, outliers were identified via Cook's distance (Cook, 1977) using the influence.ME package (version 0.9-9; Nieuwenhuis et al., 2012) and an outlier criterion of $4/(n\text{-}p\text{-}1)$, where n is the number of subjects and p is the number of fixed effects. Significant interactions were followed up using simple slope analyses via the interactions library (version 1.1.5; Long, 2019). p values were Bonferroni-corrected according to the number of simple slopes in the respective analysis.

Choice accuracy. We conducted a mixed ANOVA with the factors group (patients, controls), feedback delay (short, long), and block (1–8). Significant effects were followed up with Bonferroni-corrected t tests using the *emmeans_test* function (Lenth, 2025). No participant exceeded the outlier criterion of $M \pm 2.5$ SD per feedback delay/study session.

Choice switching. As an additional behavioral measure, we analyzed whether choice switching following feedback was influenced by the categorical fixed effects feedback valence (−0.5: negative, 0.5: positive), response type (−0.5: false, 0.5: correct), group (−0.5: control, 0.5: patient), feedback delay (−0.5: short, 0.5: long), and the continuous effect block which was scaled via the built-in *scale* function. Choice switching for a given trial was defined as whether the choice for the current stimulus was switched (choice switching = 1) or sustained (choice switching = 0) in the next trial that the same stimulus was presented in. The variable was scaled via the built-in *scale* function. We also included all interactions of these factors as fixed effects. No participants exceeded our Cook's distance criterion. The model equation was as follows:

$$\begin{aligned}\text{choice switching} \sim\ & 1 + \text{feedback valence} * \text{response type} * \text{group} \\ & * \text{feedback delay} * \text{block} + (1 + \text{feedback valence:} \\ & \text{response type:feedback delay:block}|\text{subject})\end{aligned}$$

FRN. For FRN amplitudes, we again employed an LME model with the fixed effects feedback valence (negative: −0.5, positive: 0.5), group (−0.5: control, 0.5: patient), feedback delay (−0.5: short, 0.5: long), and the continuous fixed effect unsigned RL-PE which was the absolute of the signed RL-PE minus 0.5 (thus with minimal values of −0.5 and maximal values of 0.5). We also included all interactions of these factors as fixed effects. Here, we deviated from the preregistration (which only included the signed RL-PE), because analyzing the signed RL-PE in an LME model is confounded by valence effects and disregards possible U-shaped relations which are identifiable by separating feedback valence and unsigned RL-PE (i.e., RL-PE magnitude). Initial convergence issues were solved via changing the optimizer to *bobyqa*. Four controls were excluded due to exceeding the Cook's distance criterion. The model equation was as follows:

$$\begin{aligned}\text{FRN} \sim\ & 1 + \text{unsigned PE} * \text{feedback valence} * \text{group} * \text{feedback delay} \\ & + (1 + \text{unsigned PE:feedback valence:feedback delay} + \\ & \text{unsigned PE:feedback valence} + \text{unsigned PE:feedback delay} \\ & + \text{feedback valence:feedback delay}|\text{subject})\end{aligned}$$

Structural MRI and lesion symptom mapping

For 21 patients and all controls, a 3D T1-weighted magnetization-prepared rapid acquisition gradient-echo (MPRAGE) sequence was acquired [176 slices, repetition time (TR), 2,530 ms; echo time (TE), 2.27 ms; inversion time (TI), 1,100 ms; flip angle (FA), 7°; voxel size, 1 × 1 × 1 mm; acceleration factor, 2 (GRAPPA); field of view, 256 × 256 mm; acquisition time (TA), 6:03 min:s]. A MAGNETOM Vida 3T system (Siemens Healthcare) with a 64-channel coil was used. For the remaining five patients, an MR scan was not possible due to implants ($n = 4$) or claustrophobia ($n = 1$), and instead, existing diagnostic structural MR images were used.

We first confirmed that lesions were isolated to the cerebellum, which was also reconfirmed by an experienced neuroradiologist (SGö). T2-weighted images were also assessed for white matter lesions (see below).

Non-normalized 3D T1 images were first manually aligned to the AC-PC line. Cerebellar, postischemic lesions were then manually traced and saved as regions of interest using MRIcron (https://www.nitrc.org/projects/mricron). Next, the cerebellum was isolated, and datasets were segmented using the *suit_isolate_seg* function provided by SUIT toolbox (https://www.diedrichsenlab.org/imaging/suit.htm). Isolation masks were manually corrected. Datasets were then normalized with the function *suit_isolate_mask*, using the lesion mask as optional input, thus ignoring the respective area(s). Finally, lesion ROIs were transformed via *suit_reslice* into the spatially unbiased atlas template of the cerebellum (SUIT; Diedrichsen, 2006).

For statistical analysis of whether deficits corresponded to specific lesion locations, voxel-based lesion symptom mapping (vbLSM) was conducted using NPM as implemented with MRIcron (Stoodley et al., 2016; Timmann et al., 2022). For this purpose, all lesion ROIs on the right side were mirrored to the left side (in the five patients with bilateral lesions, the side with the larger lesion was considered). For one subject (sub-060) with bilateral lesions, the lesion of higher interest for our cognitive task in posterolateral regions (Crus II, lobule VIIb) was mirrored to the left side instead of the larger lesion in anterior cerebellar motor regions. vbLSM compares for each voxel, whether patients with this voxel affected differ from patients with this voxel unaffected within a variable of interest. A Brunner–Munzel test was employed (Brunner and Munzel, 2000) with a statistical threshold of $p < 0.05$. Only variables with statistical differences between patients and controls were considered, which in our case was the interaction effect between RL-PE, feedback valence, and group onto FRN amplitude. We collapsed this effect into one variable per participant by taking the difference between the mean FRN amplitude for high RL-PE (≥−0.5) and low RL-PE (<0.5) for negative feedback (because FRN amplitudes differed between high and low RL-PE only for negative feedback valence in controls). Signs were reversed for the analysis, as lower values are related to more dysfunction in vbLSM (while in our case positive values were associated with more dysfunction). Clusters of voxels with significant effects were extracted using MRIcroGL (Brett et al., 2001), considering clusters larger than 32 mm^3. Affected lobules and nuclei were defined based on the probabilistic atlases of the human cerebellum by Diedrichsen et al. (2009, 2011).

White matter lesion assessment

3D dark fluid T2-weighted spin-echo sequences [SPACE; 160 slices; TR, 7,000 ms; TE, 428 ms; TI, 2,050 ms; voxel size, 1 × 1 × 1 mm; acceleration factor, 2 (GRAPPA), field of view, 256 × 256 mm; TA, 5:24 min:s] were acquired and examined for white matter lesions. They were rated following Wahlund et al. (2001; Table 1). Even though we excluded patients with particularly pronounced and widespread white matter lesions, we still found higher white matter lesion ratings for cerebellar stroke patients than controls. White matter lesions have previously been shown to contribute to deficits in cognition (Filley and Fields, 2016), although findings specifically concerning reinforcement learning appear as yet lacking. To exclude effects of WMLs in our data, we checked our cognitive scores (CCAS) and did not find any general cognitive deficits in patients compared with controls ($t_{(40.89)} = 1.03$, $p = 0.310$). Our finding concerning RL-PE processing in stroke patients additionally coincides with our findings for cerebellar TMS in Experiment 2, where cerebellar and control stimulation was applied within-subject, excluding between-subject factors like white matter lesions as a cause. It thus seems likely that the deficits in RL-PE processing in our patients are caused by the cerebellar stroke itself.

Quantitative susceptibility mapping

In an additional analysis, we examined whether lesions within the dentate nucleus had a special impact on RL-PE processing, as the dentate

nucleus constitutes the main output of the cerebellum, with more than half of its projection relating to non-motor functions (Palesi et al., 2021). To identify the dentate nucleus based on its high iron levels (Deistung et al., 2016), quantitative susceptibility mapping (QSM) was conducted based on data collected using a multi-echo gradient-echo scan [176 axial slices; TR, 27 ms; $TE_{1–4}$, 3.66 ms/9.74 ms/15.83 ms/21.91 ms; FA, 15°; voxel size, 0.9 × 0.9 × 0.9 mm; acceleration factor, 2 (GRAPPA); field of view, 230 mm × 230 mm; TA, 8:15 min:s] as described in Deistung et al. (2022). Outlines of the dentate nucleus as well as dentate nucleus lesion (if present) were manually drawn in ITK-SNAP (Yushkevich et al., 2006). We identified six patients who had a lesion in the dentate nucleus, with two of those previously classified as impaired concerning the differentiation between negative low and high RL-PE in FRN. We coregistered both dentate nucleus regions of interest and lesions to the T1 images and then normalized and resliced them into SUIT space. Functions included within the SUIT toolbox were used, i.e., *suit_normalize_dentate* for normalization and *suit_reslice_dartel* for reslicing. However, as overlaps between lesions were too few and did not allow meaningful statistical analysis, we abstained from an additional analysis and instead provide images of the individual dentate lesions in Figure 3.

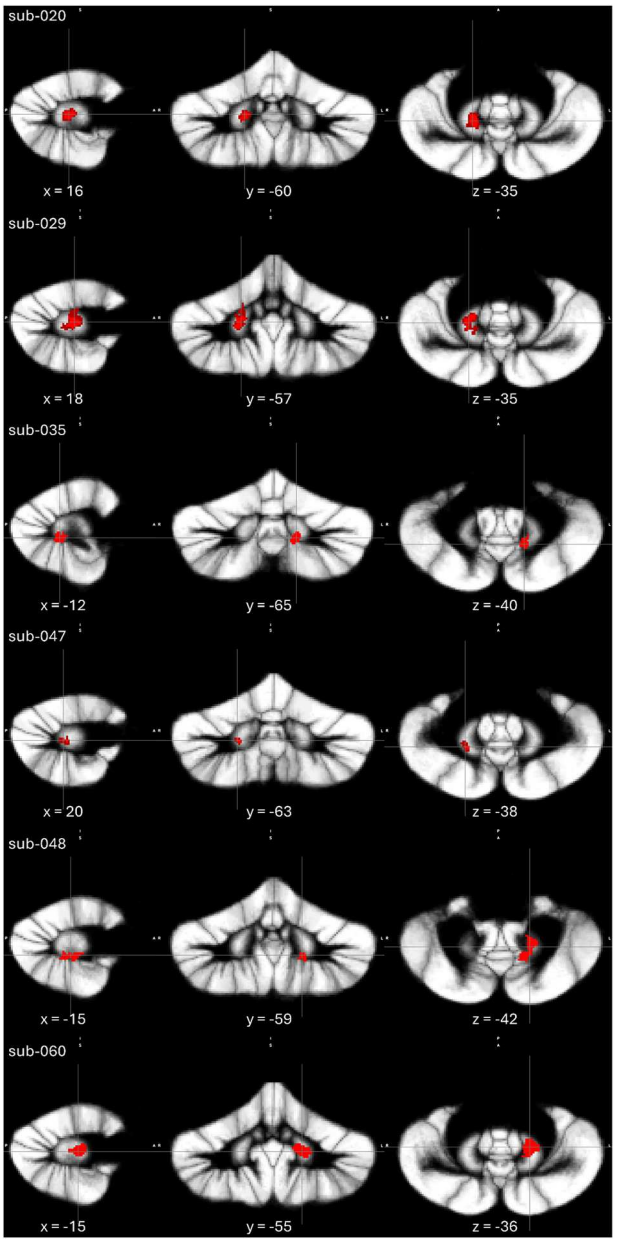

Figure 3. Individual, unmirrored dentate nucleus lesions for Experiment 1 (patient study), normalized to SUIT space, are presented in sagittal (left column), coronal (middle column), and axial view (right column) for patients with dentate lesions (sub-004, sub-005, sub-019, sub-022, sub-026, and sub-036). Lesion are marked in red.

Experiment 2

Participants

Twenty-nine healthy adults were recruited for participation. Four participants completed only one of two sessions and were thus excluded; one participant was excluded due to stimulation at a false output strength in one of the sessions. Thus, data from 24 participants (7 men, 17 women) with a mean age of 23.3 years (SD = 2.9 years, range from 19 to 30 years) were analyzed. Handedness was assessed with the EHI (Oldfield, 1971), with a mean LQ score of 62.3 (SD = 53.3, range from −85.7 to 100.0). According to LQ_{EHI}, 20 participants were right-handed, 2 left-handed, and 2 ambidextrous. All participants reported no neurological or psychiatric diseases and no metal implants in or near their head. Further exclusion criteria were pregnancy, alcohol or illicit substance abuse, and intake of psychotropic medication. IQ estimates were obtained using the MWT-B (Merz et al., 1975), yielding a mean IQ of 103.5 (SD = 15.4). Participants received monetary compensation for participation in two sessions.

All participants gave written informed consent prior to participation. The experiment was conducted in accordance with the ethical principles for medical research involving human subjects outlined in the Declaration of Helsinki and approved by the Ethics Committee at the Faculty of Medicine of Heinrich-Heine-University Düsseldorf.

Procedure

The experiment took place on 2 separate days with at least 48 h in between to decrease repetition effects (M = 101.6 d, SD = 152.1 d, range from 2 to 448 d). Note that due to a technical defect of the TMS system and a consequent pause of experiments, the time between sessions was exceptionally long for five individuals included in the analysis (362–448 d). Without these participants, the average time between sessions was 26.6 d (SD = 28.0 d, range from 2 to 98 d).

While one session of Experiment 2 comprised the experimental task with vertex (control) stimulation, the other session comprised the cerebellar stimulation. Order for stimulation site was counterbalanced.

After participants arrived in the lab, informed consent was obtained and they filled in a demographic questionnaire, the EHI, and the MWT-B. Following EEG and EMG preparations and the subsequent motor threshold estimation, we placed the double cone TMS coil on their head with a custom mounting and further secured it with an elastic band (see below for a detailed description; Fig. 4*A*). Before and after the experimental task, an additional Flanker task was performed for which results are reported elsewhere (Berlijn et al., 2024a).

Participants completed a probabilistic feedback learning task that closely followed procedures as described for Experiment 1. Figure 4*B* illustrates the sequence and time course of stimulus presentation in each trial. The task consisted of six blocks of 56 trials, thus 336 trials in total. Again, five practice trials with different stimuli were provided. Due to the younger sample, stimulus presentation was reduced to 500 ms and the response time window was shortened to 1,000 ms. Only short feedback delays (i.e., 500 ms) were used. Two stimuli were again linked to random feedback while the other two stimuli were linked to contingent feedback. For the contingent stimuli, correct responses were followed by positive feedback in 80% of the cases and by negative feedback in 20% of the cases (vice versa for incorrect responses). In both contingency conditions, TMS was delivered 100 ms poststimulus for one stimulus and 100 ms prefeedback for the other. In case a participant had learnt so fast that they exceeded the learning criterion of 75% correct answers by the second of six blocks, a new stimulus set was provided to increase the number of prelearning trials. This was the case for seven participants in one condition (of which four were second sessions) and for one participant in both conditions. In case a participant did not exceed the learning criterion until the sixth and last block, a seventh

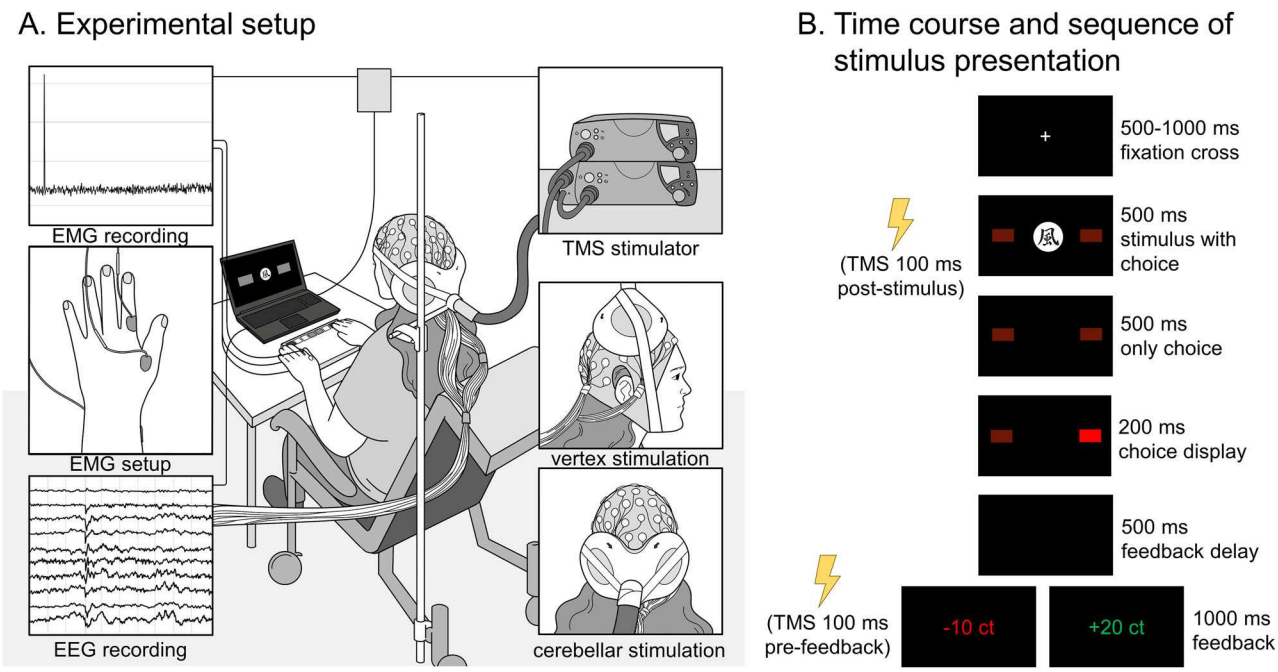

Figure 4. Experimental procedure of Experiment 2 (TMS study). ***A***, Experimental setup. A double cone coil was placed on either the left cerebellum (1 cm down and 3 cm to the left of the inion) or vertex depending on session. Simultaneously, EEG and EMG were recorded. ***B***, Time course and sequence of stimulus presentation and timing of TMS pulses in one trial in the experimental task. After a fixation cross was presented for 500–1,000 ms, one of four stimuli was presented, toward which participants could respond by pressing the left or right button on a response pad within 1,000 ms. The stimulus was only shown for the first 500 ms. After response, the respective choice was highlighted on screen for 200 ms, followed by 500 ms of blank screen. Positive ("+20 ct") or negative feedback ("−10 ct") was then presented on screen for 1,000 ms. Participants needed to learn by trial and error whether one of the choices was related to a higher chance of positive/negative feedback depending on stimulus. Feedback for two of the stimuli had an 80% contingency, while for the other two, it had a 50% contingency. TMS stimulation was applied either 100 ms poststimulus presentation or 100 ms prefeedback stimulation. A total of 336 trials were used in the task.

block was added to increase the number of postlearning trials. This was the case for three participants in one condition and for one participant in both conditions.

TMS application and EMG recording

The complete experimental setup is depicted in Figure 4*A*. Stimulation was applied at 120% of motor threshold (MT) as measured in the first session. MT was measured again on the second session. While there was a trend for a lower motor threshold on the second ($M = 36.8\%$, $SD = 7.4\%$) compared with the first session ($M = 37.8\%$, $SD = 7.4\%$; $t_{(22)} = 1.72$, $p = 0.100$), there was no significant difference in MT between cerebellar and vertex stimulation session ($t_{(22)} = 0.44$, $p = 0.663$).

MT was determined as the lowest intensity that still triggered a motor-evoked potential in at least 5 of 10 stimulations. MEPs were recorded by AgCl surface electrodes (Ambu) from the left M. abductor pollicis brevis in resting condition. The signal was amplified with a Digitimer D360 (Digitimer). The frequency band of the filter was set to 100–5,000 Hz and digitized at a sampling rate of 5 kHz (Signal version 6.02, Cambridge Electronic Design). We monitored for MEPs during the experimental task as to avoid stimulating too close to the brainstem.

TMS was applied via a Magstim Double Cone Coil using a Magstim BiStim^2 unit (Magstim). To enable a fast-paced task flow, we alternated stimulation between two Bistim units. Stimulation was applied either to the left lateral cerebellum (1 cm below and 3 cm to the left of the inion; confer Hardwick et al., 2014) or vertex (at electrode position Cz, Jung et al., 2016), both with inferior voltage flow. The coil was wrapped in plastic wrap to reduce electrode motion artifacts caused by direct contact between TMS and EEG. Participants were given earplugs to reduce auditory artifacts. After the coil was positioned, we fixed it with a custom stand and to the participant's forehead (cerebellar TMS) or chin (vertex TMS). Coil position was constantly monitored and adjusted during the breaks if necessary.

Vertex was chosen as a control site, as it is common choice of control site (Gatti et al., 2023). We did not use sham cerebellar TMS as it provides participants with a very different experience in terms of vibrations, coil clicks, and magnetic field build-up (Duecker and Sack, 2015).

Single-pulse TMS was chosen over rTMS due to its advantage of examining effects of deficits with a high temporal resolution. Instead of examining processing and task performance with a relatively steady deficit across all processing stages, like with rTMS, single-pulse TMS can be applied at different time points within the trial. This offers the advantage of differentiating effects stemming from deficits at different processing stages.

Side effects questionnaire

As participants spontaneously reported side effects after the experiment, we introduced a postexperimental side effect questionnaire halfway through the study in which participants were asked to rate symptoms (headaches, neck pain, toothaches, inattentiveness, discomfort, phosphenes, others) associated with TMS on a scale from 1 to 5 (see Fig. 5 for a plot of the side effect ratings). Ten participants completed this questionnaire in both of their sessions and five participants completed it in one session. There were no significant differences between vertex and cerebellar TMS (all $p \geq 0.343$) in terms of reported side effects.

EEG recording and preprocessing

All EEG equipment used was explicitly suitable for concurrent TMS. EEG was recorded from 30 passive Ag/AgCl Multitrode electrodes (Fp1, Fp2, F7, F3, Fz, F4, F8, FC5, FC1, FC2, FC6, T7, C3, Cz, C4, T8, CP5, CP1, CPz, CP2, CP6, P7, P3, Pz, P4, P8, O1, Oz, O2, Iz) positioned on a BrainCap (Brain Products) according to the 10–20 system. FCz was used as an on-line reference, and AFz was used as ground electrode. Impedances were kept below 5 kΩ. Data were amplified with a BrainAmp MR amplifier and recorded at 1,000 Hz using BrainVision Recorder 1.21 (Brain Products).

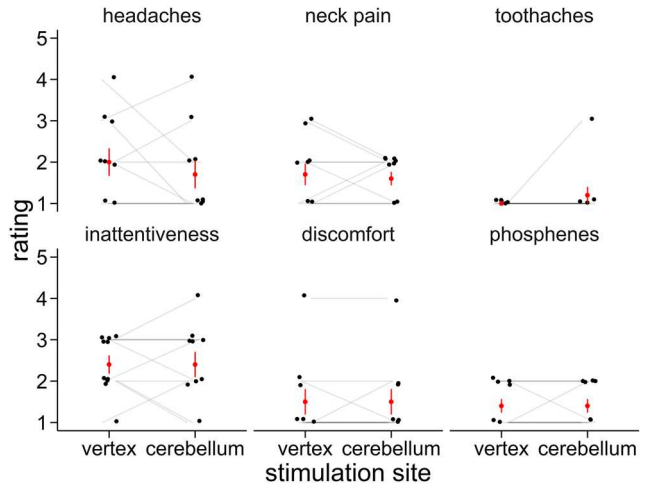

Figure 5. Side effects reported in the postexperimental questionnaire in Experiment 2 (TMS study). Means and standard errors are shown in red, individual ratings are shown in black.

Preprocessing was conducted using the ARTIST algorithm by Wu et al. (2018; see Bertazzoli et al., 2021 for a comparison of TMS-EEG preprocessing methods) and Brain Vision Analyzer. Nevertheless, a remainder of the TMS pulse artifact was still seen in the ERP.

Data were initially checked for missing TMS pulses (TMS marker was sent but pulse was not) both by visual inspection and via an explorative artifact detection: first, trials were segmented around the TMS marker (starting 100 ms before and ending 100 ms after it). Since TMS pulses cause large spikes in the raw data, an automatic artifact detection was employed on the ERP data to identify whether a pulse was sent. Segments with an amplitude >400 or less than −400 μV at electrode Fz were considered to contain a TMS artifact. For all except one participant, all segments contained this artifact, meaning that for each TMS marker in the ERP, a TMS pulse was triggered. Segments in which the above criterion was not met were visually confirmed to contain no TMS pulse artifact and were subsequently excluded from analysis. Marker timings for delayed markers (due to port conflicts) were adjusted in the marker files. This was the case for one marker in 10 participants and two markers in one participant. In two participants, one of these markers indicated a TMS pulse, thus also indicating delay of the corresponding TMS trigger. We excluded the corresponding segments as the TMS pulse had thus not been sent at the correct time.

For preprocessing, we used the ARTIST algorithm by Wu et al. (2018), which is based on EEGLAB (v2022.1; Delorme and Makeig, 2004). This algorithm is designed to decrease artifacts in the EEG signal caused by TMS pulses. In a first step, the ARTIST algorithm corrected for direct current drift, removed the TMS pulse artifact by interpolating the EEG signal around the TMS marker (here: 15 ms prior to until 5 ms after the TMS marker), and removed the decay artifact via ICA. Data were then notch-filtered (50 Hz) and bandpass filtered (high-pass filter: 1 Hz; low-pass filter: 30 Hz). Next, data were segmented into epochs beginning 1,500 ms before and ending 2,200 ms after the TMS markers. Following this, segments containing movement artifacts were rejected ($M = 2.8\%$ of segments, SD = 2.6%) and bad channels were interpolated ($M = 0.96$ channels, SD = 1.15 channels). In a final step, bad independent components were removed via a second ICA, after which the signal was rereferenced to an average reference. Deviating from the ARTIST algorithm, we restored electrode FCz after this, because FCz was essential for our data analysis. For baseline correction, the time window between 300 and 100 ms preceding the TMS pulse was used to avoid confounding the baseline correction with the TMS pulse deflection. We always excluded electrode Iz before any preprocessing because it was particularly noisy in pilot testing. Data were then saved in the BrainVision exchange format.

The segment size needed to be rather large, because initial segments were created around the TMS pulse, while in a later step the ERPs needed to be time locked to feedback onset. Therefore, some markers existed in more than one segment (when they were overlapping). To correct this, marker files were edited with a custom MATLAB script, deleting all excess markers. In this step, segments with more than one response were also excluded.

Data were then further preprocessed in BrainVision Analyzer 2.2. Due to only 10 participants exceeding the learning criterion of 75% correct responses in both conditions, the planned data analysis using ANOVA was not feasible. As a result, we pursued a single-trial analysis approach in parallel to data analysis for Experiment 1 and thus deviated from the preregistered procedures. We segmented data around feedback onset, starting 200 ms before and ending 500 ms after feedback markers. Next, we performed an additional baseline correction using the time window from 200 to 0 ms before feedback onset (thus including parts of the remaining pulse artifact for those pulses that were applied 100 ms before the feedback). We then exported single-trial ERPs with a generic data export, on average resulting in 329.3 segments (SD = 18.8 segments) per participant. Data were then exported via a generic data export for further processing in MATLAB. We additionally averaged data according to conditions (stimulation site, TMS timing, feedback valence) to extract FRN peak latencies. Only trials with contingent feedback were included. Peak detection was performed in parallel to Experiment 1.

Prediction error estimation

Prediction errors were again modeled as described in Experiment 1. Before merging the behavioral, RL-PE, and EEG data, we excluded all trials in the behavioral and RL-PE data that were not included in the preprocessed EEG data. These were either trials that did not enter the segmentation in ARTIST because the TMS marker/trigger had not been sent (e.g., when participants did not respond in time and thus no feedback-locked TMS trigger was sent) or trials/segments that ARTIST excluded during artifact rejection. Behavioral, RL-PE, and EEG data were then merged.

Experimental design and statistical analysis

The study was preregistered to OSF (https://osf.io/a24rg). We had aimed for a sample size of 20–25 participants (see preregistration for more details). The targeted sample size was thus matched ($n = 24$). Raw data and code used for preprocessing and analysis are available from https://osf.io/9n7yp.

Data were again analyzed in R (version 4.2.3; R Core Team, 2023) using RStudio (version 2023.3.0.386; Posit Team, 2023). Concerning choice accuracy, the preregistered ANOVA analysis as well as an additional linear mixed effects (LME) analysis were performed (see below). Since only 10 participants exceeded the learning criterion of >75% correct responses in at least one block for both stimulation sites, the preregistered ANOVA with learning (pre-/postlearning) as a factor was not possible for the FRN analysis. We again decided to pursue a single-trial–based analysis approach using LME models including the unsigned RL-PE instead.

Analyses were conducted to match procedures in Experiment 1, only deviating within the Cook's distance criterion for the choice switching LME analysis where the original criterion was not applicable, so that we instead used the criterion of $4/n$ (Nieuwenhuis et al., 2012).

Choice accuracy. We conducted a repeated-measures ANOVA with the within-subjects factors stimulation site (cerebellum, vertex), TMS timing (poststimulus, prefeedback), and block (1–6), as preregistered. Significant effects were followed up with Bonferroni-corrected t tests using the function *emmeans_test*. No participant exceeded the outlier criterion of $M \pm 2.5$ SD per stimulation site/study session.

Choice switching. We analyzed whether choice switching was influenced by the categorical fixed effects feedback valence (−0.5: negative, 0.5: positive), response type (−0.5: false, 0.5: correct), stimulation site (−0.5: vertex, 0.5: cerebellum), TMS timing (−0.5: poststimulus, 0.5: prefeedback), and the continuous effect block which was scaled via the built-in *scale* function. We also included all interactions of these factors as fixed effects. Three participants had to be excluded

because they exceeded the Cook's distance criterion. The model equation was as follows:

$$\text{choice switching} \sim 1 + \text{feedback valence} * \text{response type} * \text{stimulation site} * \text{TMS timing} * \text{block} + (1 + \text{feedback valence: response type:stimulation site:TMS timing:block}|\text{subject}).$$

FRN. For FRN amplitudes, we again employed LME models with the fixed effects feedback valence (negative: −0.5, positive: 0.5), stimulation site (−0.5: vertex, 0.5: cerebellum), TMS timing (−0.5: poststimulus, 0.5: prefeedback), and the continuous fixed effect unsigned RL-PE which was the absolute of the signed RL-PE minus 0.5 (thus with minimal values of −0.5 and maximal values of 0.5). We also included all interactions of these factors as fixed effects. While we were initially also able to keep random slopes up to third-level interactions, solving convergence issues via changing the optimizer to *bobyqa*, due to singular fit after the subsequent exclusion of one Cook's distance outlier, we had to revert to a random effects structure with only the fourth-level interactions and random intercept. Two outliers identified by Cook's distance were excluded. The model equation was as follows:

$$\text{FRN} \sim 1 + \text{unsigned PE} * \text{feedback valence} * \text{TMS condition} * \text{TMS timing} * \text{learnability} + (1 + \text{unsigned PE:feedback valence:TMS condition: TMS timing:learnability}|\text{subject}).$$

Results

Experiment 1: RL-PE processing in cerebellar stroke patients

In Experiment 1, we studied patients with chronic cerebellar stroke ($n = 26$) and a matched healthy control group ($n = 26$) to investigate reinforcement learning success and RL-PE processing, quantified by ACC-driven FRN amplitude. Participants performed a probabilistic feedback learning task (Fig. 2*A*,*B*) in which they had to optimize their behavior via trial and error to obtain a monetary reward ("+20 ct" per trial) and avoid a monetary punishment ("−10 ct"). Responses were made by pressing one of two buttons on a response pad. Two out of four stimuli were associated with a 90% reward contingency (i.e., pressing the "correct" button resulted in a reward in 90% of the time and a punishment 10% of the time; vice versa for the "incorrect" button), while the other two stimuli were associated with random feedback. As learning was only possible for the 90% contingency stimuli, the analysis was restricted to these (see Materials and Methods for a more detailed description of the task). Two different feedback delays were used (short, 500 ms; long, 6,500 ms), as previous work has shown differences in FRN depending on feedback timing (Peterburs et al., 2016).

During task performance, EEG was recorded to analyze the FRN (Fig. 2*A*). To see whether potential deficits were associated with specific lesion locations, lesion symptom mapping was conducted based on T1-weighted MR images in patients.

Choice accuracy

Mean choice accuracy by group (patients, controls), feedback delay (short delay, long delay), and block (1–8) is shown in Figure 6*A*. The effect of these factors on choice accuracy was analyzed within an ANOVA. We expected no differences in accuracy between groups and only a general learning effect. This expectation was based on a previous study which did not find deficient learning

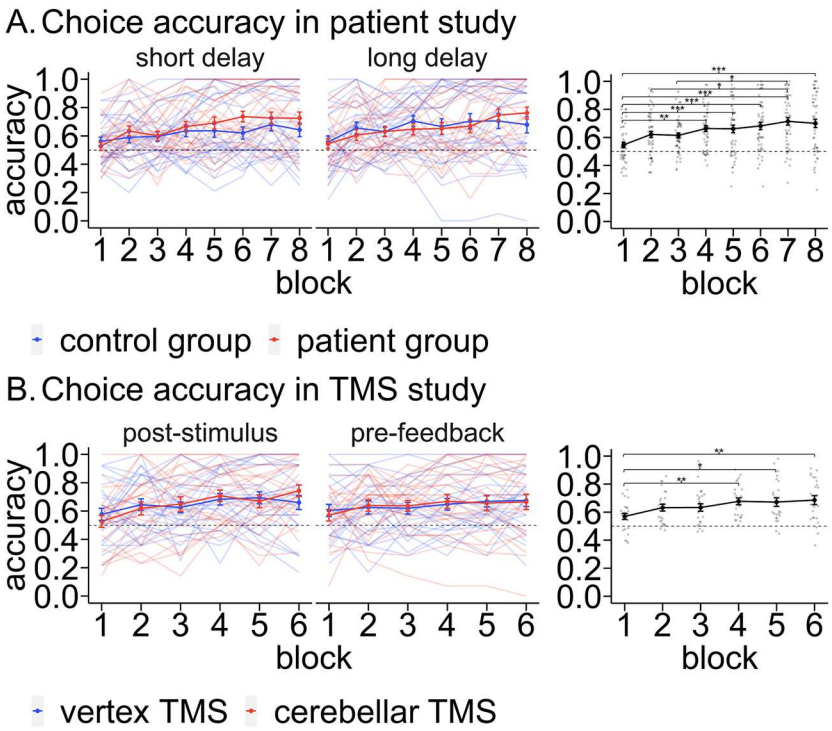

Figure 6. Accuracy for Experiments 1 (patient study) and 2 (TMS study). ***A***, Left, Choice accuracy in the probabilistic feedback task in Experiment 1 (patient study) according to group (patients, controls), feedback delay (short delay, long delay), and block (1–8). Red lines denote patients and blue lines controls. Opaque lines denote group means. Error bars indicate standard errors. Translucent lines denote individual mean accuracy. Right, Choice accuracy according to block. Opaque lines denote means across groups and feedback delays. Error bars indicate standard errors. Translucent dots denote individual mean accuracy. ***B***, Left, Choice accuracy in the probabilistic feedback task in Experiment 2 (TMS study) according to stimulation site (cerebellum, vertex), TMS timing (poststimulus, prefeedback), and block (1–6). Red lines denote vertex TMS and blue lines cerebellar TMS. Opaque lines denote means per stimulation site. Error bars indicate standard errors. Translucent lines denote individual mean accuracy per stimulation site. Right, Choice accuracy according to block. Opaque lines denote means across TMS timings and stimulations sites. Error bars indicate standard errors. Translucent dots denote individual mean accuracy. $*p < 0.05$. $**p < 0.01$. $***p < 0.001$.

in patients with cerebellar stroke (Rustemeier et al., 2016), which is likely due to compensatory mechanisms in this patient group (Peterburs et al., 2012). Overall, we found a significant main effect of block, i.e., a learning effect, but none of the effects involving the factor group (patients vs controls) reached significance.

Statistical analysis showed a main effect of block ($F_{(3.15,154.26)} = 15.65$, $p < 0.001$), indicating that subjects had learned to optimize their behavior over the course of the task. Post hoc t tests revealed that choice accuracy was significantly higher in block 4 ($t_{(823)} = 3.97$, $p = 0.002$), block 5 ($t_{(823)} = 3.91$, $p < 0.001$), block 6 ($t_{(823)} = 4.61$, $p < 0.001$), block 7 ($t_{(823)} = 5.72$, $p < 0.001$), and block 8 ($t_{(823)} = 5.26$, $p < 0.001$) compared with that in block 1. Additionally, choice accuracy was higher in block 7 compared with that in block 2 ($t_{(823)} = 3.18$, $p = 0.042$) and block 3 ($t_{(823)} = 3.42$, $p = 0.018$). All other pairwise comparisons were nonsignificant (all $p \geq 0.087$). No other effects reached significance (all $p \geq 0.179$; see Table 4 for the complete inferential statistics).

Choice switching

The effects of response type, feedback valence, block, group, and feedback delay on choice switching were analyzed using LME analysis. We found the expected effects of increased choice switching after negative feedback, false responses, short feedback delays, as well as early in the experiment. Importantly, while in controls, choice switching was increased for negative compared with positive feedback for both short and long feedback delays, in patients, this effect was present only for short but not for long feedback delay (Fig. 7*A*).

Statistical analysis showed that choice switching was increased after incorrect compared with correct responses ($\beta = -0.23$, SE = 0.03, $t_{(15,948.01)} = 8.65$, $p < 0.001$). The effect of response type was further modulated by block ($\beta = -0.10$, SE = 0.03, $t_{(15,919.59)} = 3.78$, $p < 0.001$), such that the differentiation between correct and false responses was stronger late in the task ($\beta = -0.33$, SE = 0.04, $t = 7.79$, $p < 0.001$) but already present early in the task ($\beta = -0.14$, SE = 0.04, $t = 3.77$, $p < 0.001$).

Choice switching was also increased after negative compared with positive feedback ($\beta = -0.20$, SE = 0.03, $t_{(15,920.60)} = 7.60$, $p < 0.001$). This effect was further modulated by feedback delay and group ($\beta = 0.32$, SE = 0.10, $t_{(15,826.98)} = 3.10$, $p = 0.002$; Fig. 7*A*). For controls, negative compared with positive feedback resulted in increased choice switching for both short ($\beta = -0.16$, SE = 0.05, $t = 3.27$, $p = 0.004$) and long feedback delay ($\beta = -0.23$, SE = 0.05, $t = 4.58$, $p < 0.001$). For patients, negative compared with positive feedback resulted in increased choice switching for short ($\beta = -0.34$, SE = 0.05, $t = 6.97$, $p < 0.001$) but not for long feedback delay ($\beta = -0.11$, SE = 0.05, $t = 2.13$, $p = 0.134$).

Choice switching was also reduced for the long compared with the short feedback delay ($\beta = -0.08$, SE = 0.03, $t_{(15,880.70)} = 3.21$, $p = 0.001$) and across blocks ($\beta = -0.08$, SE = 0.01, $t_{(15,896.82)} = 5.82$, $p < 0.001$). Complete inferential statistics can be found in Table 5.

Table 4. Inferential statistics for the ANOVA investigating the influence of group, feedback delay, and block on accuracy in Experiment 1 (patient study)

Effect	df_n	df_d	F	p
Group	1.00	49.00	0.28	0.600
Feedback delay	1.00	49.00	0.50	0.484
Block	3.15	154.26	15.65	<0.001
Group × feedback delay	1.00	49.00	0.96	0.331
Group × block	3.15	154.26	1.64	0.179
Feedback delay × block	4.18	204.87	0.24	0.923
Group × feedback delay × block	4.18	204.87	1.24	0.295

$n = 52$.

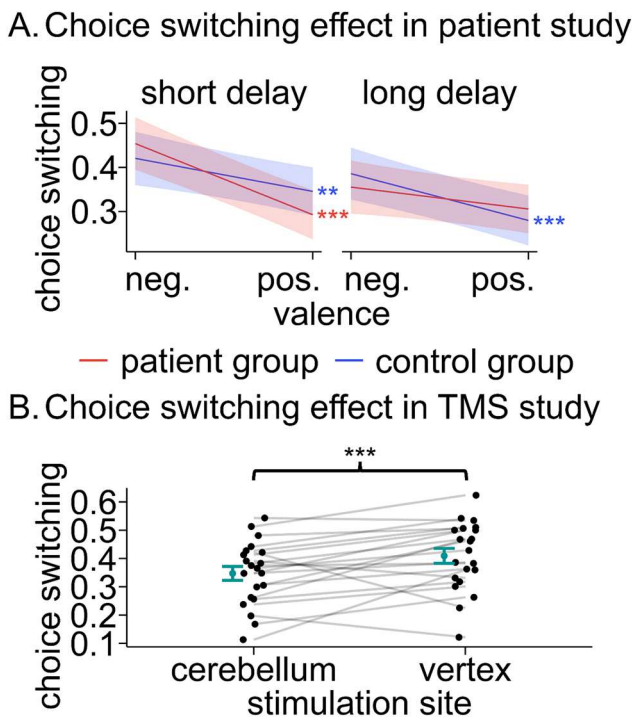

Figure 7. Choice switching results for Experiments 1 (patient study) and 2 (TMS study). ***A***, Slope estimates for choice switching predicted by feedback valence and modulated by feedback delay and group in Experiment 1 (patient study). pos., positive feedback valence; neg., negative feedback valence. Red lines denote patients and blue lines controls. Colored bands indicate 95% confidence intervals. *$p < 0.05$. **$p < 0.01$. ***$p < 0.001$. ***B***, Mean choice switching according to stimulation site in Experiment 2 (TMS study). Means per stimulation site are displayed in cyan while individual means per stimulation site are displayed in black. Error bars indicate standard errors.

FRN

The effects of (signed) RL-PE (reflected by the factors unsigned RL-PE and feedback valence), group, and feedback delay on FRN amplitude were analyzed using LME analysis. We expected the FRN to be increased for high compared with low unsigned RL-PEs for negative feedback and decreased for high compared with low unsigned RL-PEs for positive feedback and expected this effect to be reduced in the patient group. Grand averages of the feedback-locked ERP at FCz show that the FRN amplitude was increased (i.e., more negative) for high compared with low RL-PEs for negative feedback for controls but not for patients (Fig. 8*A*). This effect could also be confirmed in statistical analysis. For grand average feedback-locked ERPs for all conditions, see Figure 9*A*.

Statistical analysis showed that the FRN was enhanced for negative compared with positive feedback ($\beta = 0.48$, SE = 0.11, $t_{(1,535.59)} = 4.15$, $p < 0.001$) and for high compared with low RL-PEs ($\beta = -0.39$, SE = 0.18, $t_{(769.27)} = 2.16$, $p = 0.031$). Importantly, within an interaction between RL-PE, feedback valence, and group ($\beta = 3.28$, SE = 1.34, $t_{(37.08)} = 2.44$, $p = 0.020$), the FRN reflected the RL-PE for controls only in negative ($\beta = -2.10$, SE = 0.44, $t = 4.78$, $p < 0.001$), but not positive feedback contexts ($\beta = 0.73$, SE = 0.39, $t = 1.88$, $p = 0.242$; see Fig. 8*B* for simple slope plots). For patients, the RL-PE was not reflected for either feedback valence, both $p > 0.999$.

Table 5. Inferential statistics for the LME analysis examining the effect of feedback valence, response type, feedback delay, group, and block onto choice switching in Experiment 1 (patient study)

Fixed effects					
	Est/β	SE	df	t	p
(Intercept)	0.08	0.04	58.56	1.96	0.055
Feedback valence	−0.20	0.03	15,920.60	−7.60	<0.001
Response type	−0.23	0.03	15,948.01	−8.65	<0.001
Feedback delay	−0.08	0.03	15,880.70	−3.21	0.001
Group	0.00	0.08	58.56	−0.02	0.988
Block	−0.08	0.01	15,896.82	−5.82	<0.001
Feedback valence × response type	−0.07	0.05	15,895.70	−1.26	0.208
Feedback valence × feedback delay	0.09	0.05	15,826.98	1.77	0.076
Response type × feedback delay	−0.10	0.05	15,926.76	−1.92	0.054
Feedback valence × group	−0.05	0.05	15,920.60	−0.87	0.387
Response type × group	−0.08	0.05	15,948.01	−1.45	0.148
Feedback delay × group	0.03	0.05	15,880.70	0.61	0.544
Feedback valence × block	0.02	0.03	15,528.96	0.61	0.542
Response type × block	−0.10	0.03	15,919.59	−3.78	<0.001
Feedback delay × block	0.05	0.03	15,885.45	1.90	0.057
Group × block	0.04	0.03	15,896.82	1.67	0.095
Feedback valence × response type × feedback delay	−0.05	0.10	15,910.73	−0.46	0.648
Feedback valence × response type × group	0.09	0.10	15,895.70	0.85	0.396
Feedback valence × feedback delay × group	0.32	0.10	15,826.98	3.10	0.002
Response type × feedback delay × group	−0.11	0.10	15,926.76	−1.01	0.312
Feedback valence × response type × block	0.05	0.05	15,914.81	1.03	0.305
Feedback valence × feedback delay × block	−0.03	0.05	12,591.80	−0.62	0.535
Response type × feedback delay × block	−0.02	0.05	15,922.19	−0.43	0.670
Feedback valence × group × block	−0.03	0.05	15,528.96	−0.61	0.540
Response type × group × block	−0.06	0.05	15,919.59	−1.12	0.262
Feedback delay × group × block	0.05	0.05	15,885.45	1.02	0.309
Feedback valence × response type × feedback delay × group	−0.13	0.21	15,910.73	−0.64	0.522
Feedback valence × response type × feedback delay × block	−0.12	0.11	322.87	−1.09	0.276
Feedback valence × response type × group × block	−0.15	0.10	15,914.81	−1.44	0.149
Feedback valence × feedback delay × group × block	−0.16	0.10	12,591.80	−1.49	0.136
Response type × feedback delay × group × block	0.14	0.10	15,922.19	1.31	0.190
Feedback valence × response type × feedback delay × group × block	−0.12	0.22	322.87	−0.54	0.587
Random effects					
	Variance	SD	Corr		
Subject (intercept)	0.07	0.26			
Subject (feedback valence × response type × feedback delay × block)	0.05	0.23	−0.62		
Residual	0.86	0.93			
Model fit					
	Marginal		Conditional		
R^2	0.05		0.12		

Key: p values for fixed effects calculated using Satterthwaite's approximations. Model equation: choice switch ~ 1 + feedback valence * response type * feedback delay * group * block + (1 + feedback valence:response type:feedback delay:block | subject). $n_{subjects} = 52$, $n_{observations} = 16{,}001$.

Within an interaction between feedback valence and feedback delay ($\beta = -1.09$, SE = 0.27, $t_{(73.82)} = 4.04$, $p < 0.001$), the FRN was enhanced for negative compared with positive feedback only for short ($\beta = 0.89$, SE = 0.16, $t = 5.66$, $p < 0.001$) but not long feedback delay ($\beta = -0.06$, SE = 0.16, $t = 0.37$, $p > 0.999$).

It was also increased within a feedback delay main effect for long over short feedback delay ($\beta = -0.94$, SE = 0.13, $t_{(2,765.36)} = 7.24$, $p < 0.001$). This effect was further modulated by group within an interaction ($\beta = 0.59$, SE = 0.26, $t_{(2,765.36)} = 2.27$, $p = 0.024$). The FRN amplitude was more strongly increased for long feedback delays for controls ($\beta = -1.51$, SE = 0.19, $t = 7.93$, $p < 0.001$) than patients ($\beta = -0.68$, SE = 0.16, $t = 4.15$, $p < 0.001$).

Complete inferential statistics can be found in Table 6.

Lesion symptom mapping

Lesions were mainly located in posterolateral regions, with highest overlap in lobules Crus II, l, VIIb, VIIIa, and VIIIb (Fig. 1). Six patients had a lesion extending into the dentate nucleus. Images of individual lesions are displayed in Extended Data Figure 1-1. For analysis, all lesions were mirrored to the left side (in case of bilateral lesions, the side with the larger lesion was mirrored to the left side if necessary).

To investigate whether the FRN changes were linked to specific cerebellar lesion locations, voxel-based lesion symptom mapping (vbLSM) was performed. While controls mostly showed the expected coding of RL-PEs in the FRN in the anticipated direction (i.e., increased/more negative FRN amplitude for high over low RL-PEs), only few patients showed this pattern, and some patients even showed the opposite (i.e., decreased/more positive FRN for high over low RL-PE; Fig. 8*C*). We used the difference FRN for negative feedback as a parameter for the vbLSM (FRN for high RL-PEs [≥0.5] – FRN for low RL-PEs [<0.5]). We expected aberrant processing to be associated with damage to posterolateral regions, especially Crus I and II. Indeed, a more aberrant difference FRN was associated with more four posterior lesion clusters: in Crus II extending toward lobule VIIb (peak $z = 3.0$, peak coordinates: $x = -26$ mm, $y = -78$ mm, $z = -51$ mm, 535 mm^3), medial Crus II (peak $z = 2.6$, peak coordinates: $x = -5$ mm, $y = -79$ mm, $z = -35$ mm, 37 mm^3), Crus I (peak $z = 2.5$, peak coordinates: $x = -27$ mm, $y = -86$ mm, $z = -34$ mm, 149 mm^3), and medial lobule VIIb/vermal VIIIa (peak $z = 2.3$, peak coordinates: $x = -6$ mm, $y = -68$ mm, $z = -45$ mm, 550 mm^3; Fig. 10).

In an additional step, we examined lesions in the dentate nucleus (see Materials and Methods). There were only six patients with lesions in the dentate nucleus (of which two had been classified as impaired) with only minimal overlap. Meaningful analyses could thus not be performed. Plots of individual dentate nucleus lesions are shown in Figure 3.

Experiment 2: RL-PE processing in healthy young adults receiving cerebellar TMS

In Experiment 2, we investigated reinforcement learning and RL-PE processing in young healthy adults ($n = 24$) for cerebellar and control (vertex) single-pulse TMS using the same probabilistic feedback learning task as in Experiment 1 (Fig. 4*A*). Pulses were applied once per trial and either at the response stage (100 ms poststimulus onset) or at the feedback stage (100 ms prefeedback; Fig. 4*B*). Single-pulse TMS has the advantage of transient effects on behavior and neural processing (Gatti et al.,

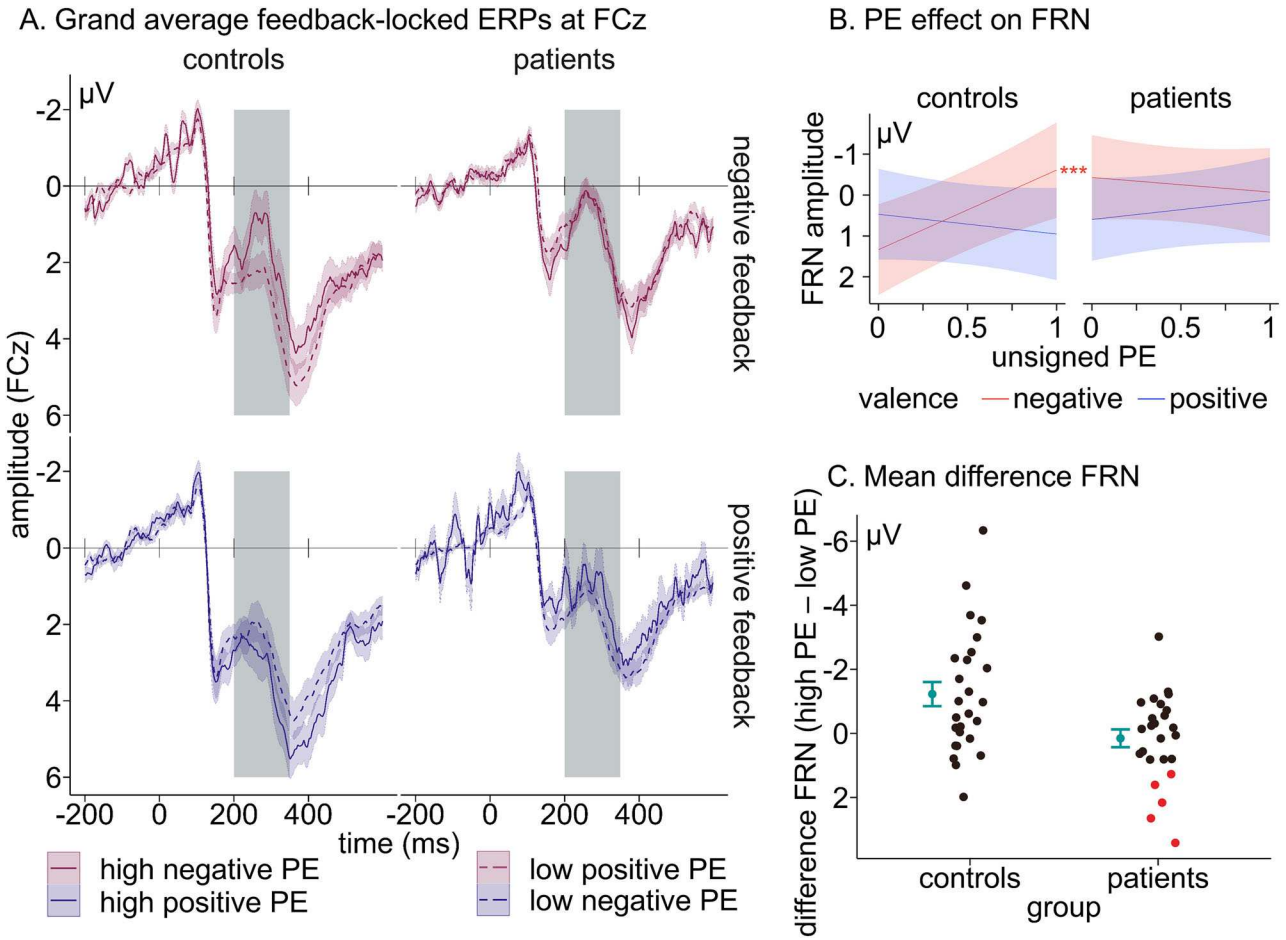

Figure 8. ERP results for Experiment 1 (patient study). ***A***, Grand average feedback-locked ERPs at FCz according to unsigned RL-PE (low, high), feedback valence (positive, negative), and group (patients, controls). Red lines denote high unsigned RL-PE (>0.5) and blue lines low unsigned RL-PE (≤0.5). Colored bands indicate standard errors. ***B***, Slope estimates for FRN amplitude predicted by unsigned RL-PE and modulated by feedback valence and group. Red lines denote positive feedback valence and blue lines negative feedback valence. Colored bands indicate 95% confidence intervals. *$p < 0.05$. **$p < 0.01$. ***$p < 0.001$. ***C***, Mean difference FRN (mean negative high RL-PE − mean negative low RL-PE) separately for groups (controls, patients). Group means are displayed in cyan while individual means are displayed in black. Error bars indicate standard errors. Patients with a difference FRN above 1 μV (i.e., decreased/more positive difference FRN) are marked in red who are used as impaired group in lesion symptom mapping.

2023) within-subject, excluding the possibility of long-term compensation that may be present in chronic stroke patients (Peterburs et al., 2012).

Choice accuracy

Mean choice accuracy as a function of stimulation site (cerebellum, vertex), TMS timing (poststimulus, prefeedback), and block (1–8) is shown in Figure 6*B*. The effects of these factors on choice accuracy were analyzed using an ANOVA. We expected a main effect of block, and participants to perform worse when receiving cerebellar compared with vertex TMS, as no long-term compensatory mechanisms should be available due to the instantaneous effect of the TMS. Overall, we found a main effect of block, i.e., a learning effect, while no effects involving the stimulation site factor (cerebellum/vertex) reached significance.

Statistical analysis showed a significant main effect of block ($F_{(3.18,73.05)} = 6.21$, $p < 0.001$) with higher choice accuracy in block 4 ($t_{(570)} = 3.49$, $p = 0.008$), block 5 ($t_{(570)} = 3.33$, $p = 0.014$), and block 6 ($t_{(570)} = 3.77$, $p = 0.003$) compared with block 1. All other effects were nonsignificant (all $p \geq 0.461$; see Table 7 for complete inferential statistics).

Choice switching

The effects of response type, feedback valence, block, stimulation site, and TMS timing on choice switching were analyzed using LME analysis. We found the expected effects of increased choice switching after negative feedback and false responses. Importantly, choice switching was generally reduced for cerebellar compared with vertex stimulation (Fig. 7*B*).

The main effect of stimulation site reached significance ($\beta = -0.11$, SE = 0.03, $t_{(6,475.16)} = 3.67$, $p < 0.001$), with decreased choice switching for cerebellar compared with vertex TMS (Fig. 7*B*).

Further, the main effect of response type was significant ($\beta = -0.39$, SE = 0.03, $t_{(6,502.49)} = 12.64$, $p < 0.001$), with more choice switching after incorrect compared with correct choices. This effect was further modulated by block ($\beta = -0.15$, SE = 0.03, $t_{(6,499.06)} = 5.02$, $p < 0.001$). Follow-up simple slope analyses showed that while choice switching was significantly increased both early ($\beta = -0.22$, SE = 0.04, $t = 5.22$, $p < 0.001$) and late in the task ($\beta = -0.54$, SE = 0.05, $t = 11.44$, $p < 0.001$), the effect was stronger late in the task.

Statistical analysis also showed a main effect of feedback valence ($\beta = -0.23$, SE = 0.03, $t_{(6,489.74)} = 7.74$, $p < 0.001$), with more choice switching after negative compared with positive feedback.

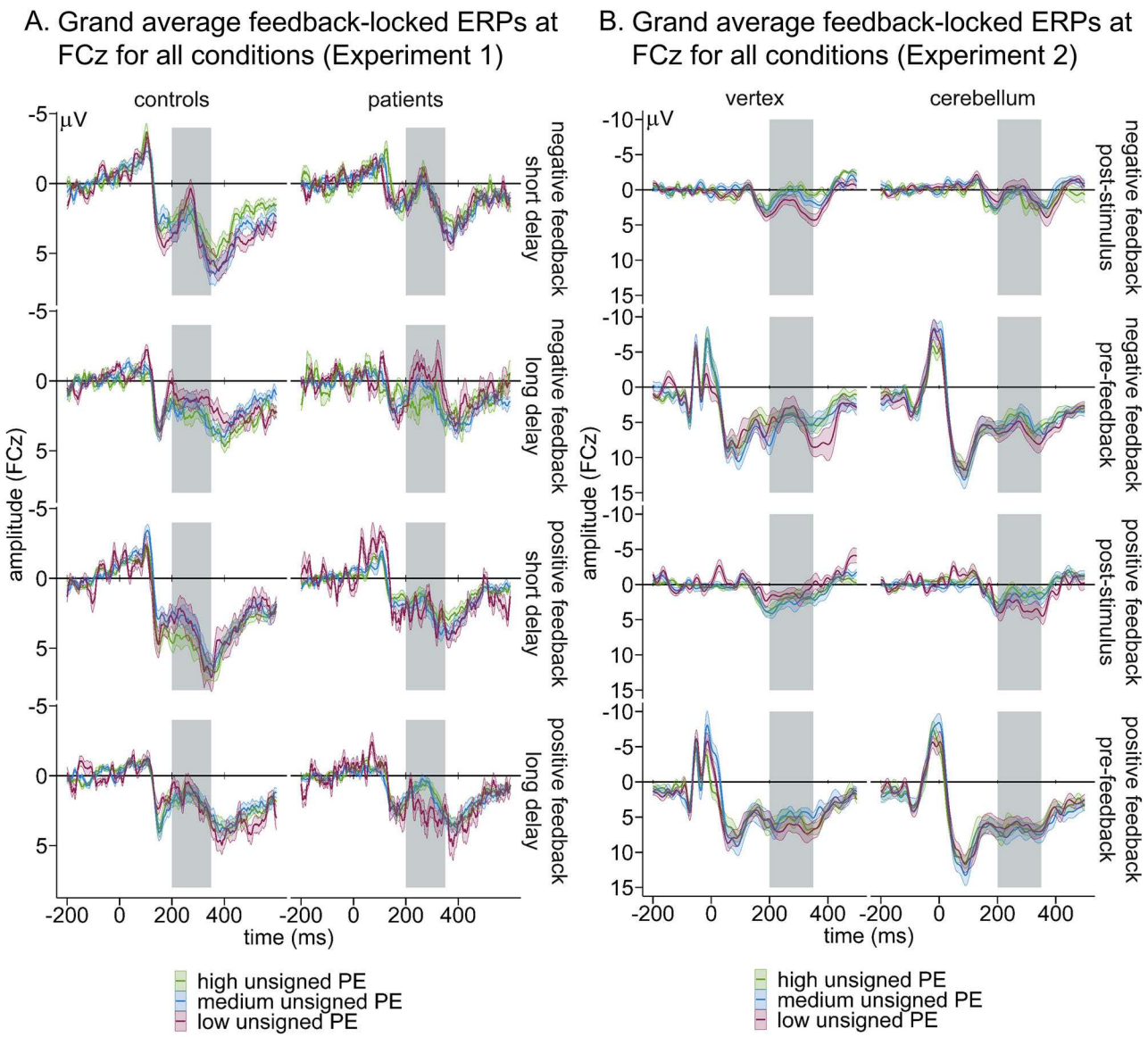

Figure 9. Grand average feedback-locked ERPs for all conditions and three RL-PE levels. ***A***, Grand average feedback-locked ERPs for Experiment 1 (patient study) at FCz according to unsigned RL-PE (low, medium, high), feedback valence (positive, negative), feedback delay (short delay, long delay), and group (patients, controls). Red lines denote low, blue lines denote medium, and green lines denote high unsigned RL-PE. Colored bands indicate standard errors. ***B***, Grand average feedback-locked ERPs for Experiment 2 (TMS study) at FCz according to unsigned RL-PE (low, medium, high), feedback valence (positive, negative), TMS timing (poststimulus, prefeedback), and stimulation site (vertex, cerebellum). Red lines denote low, blue lines denote medium, and green lines denote high unsigned RL-PE. Colored bands indicate standard errors.

No other effects involving response type or feedback valence with stimulation site or each other emerged (all $p \geq 0.246$). Complete inferential statistics can be found in Table 8.

FRN

The effects of (signed) RL-PE (reflected in unsigned RL-PE and feedback valence), stimulation site, and TMS timing on FRN amplitude were analyzed using LME analysis. We expected the FRN to be increased for higher unsigned RL-PEs for negative feedback and decreased for higher unsigned RL-PEs for positive feedback, and we expected this effect to be reduced when stimulating the cerebellum compared with the vertex. Grand averages for the feedback-locked ERP at FCz are shown in Figure 11*A*. For grand average feedback-locked ERPs for all conditions, see Figure 9*B*. FRN amplitudes were reduced for high compared with low RL-PEs for negative feedback only for control stimulation but not for cerebellar stimulation.

Statistical analysis showed that FRN was enhanced for negative compared with positive feedback ($\beta = 1.08$, SE = 0.14, $t_{(7,116.94)} = 7.90$, $p < 0.001$). Feedback valence further interacted significantly with the unsigned RL-PE, ($\beta = -1.11$, SE = 0.49, $t_{(6,506.98)} = 2.28$, $p = 0.023$). Follow-up simple slope analyses revealed that while the unsigned RL-PE modulated the FRN for negative feedback, with a reduced FRN with increasing RL-PE at trend level ($\beta = 0.70$, SE = 0.32, $t = 2.18$, $p = 0.058$), this was not the case for positive feedback ($\beta = -0.12$, SE = 0.29, $t = 0.42$, $p > 0.999$). This interaction was further modulated by stimulation site ($\beta = 2.82$, SE = 0.93, $t_{(5,523.19)} = 3.05$, $p = 0.002$; Fig. 11*B*). For vertex TMS, FRN was reduced with increasing unsigned RL-PE for negative feedback ($\beta = 1.57$, SE = 0.43, $t = 3.69$, $p < 0.001$) but not positive feedback ($\beta = -0.56$,

Table 6. Inferential statistics for the LME analysis examining the effect of unsigned RL-PE, feedback valence, feedback delay, and group onto FRN amplitude in Experiment 1 (patient study)

Fixed effects					
	Est/β	SE	df	t	p
(Intercept)	0.29	0.34	46.00	0.87	0.389
Unsigned PE	−0.39	0.18	769.27	−2.16	0.031
Feedback valence	0.48	0.11	1,535.59	4.15	<0.001
Feedback delay	−0.94	0.13	2,765.36	−7.24	<0.001
Group	−0.48	0.67	46.00	−0.72	0.477
Unsigned PE × feedback valence	0.79	0.67	37.08	1.18	0.246
Unsigned PE × feedback delay	0.56	0.47	41.99	1.19	0.239
Feedback valence × feedback delay	−1.09	0.27	73.82	−4.04	<0.001
Unsigned PE × group	0.67	0.37	769.27	1.83	0.068
Feedback valence × group	0.26	0.23	1,535.59	1.13	0.258
Feedback delay × group	0.59	0.26	2,765.36	2.27	0.024
Unsigned PE × feedback valence × feedback delay	−2.02	1.73	36.29	−1.17	0.250
Unsigned PE × feedback valence × group	−3.28	1.34	37.08	−2.44	0.020
Unsigned PE × feedback delay × group	−0.99	0.94	41.99	−1.06	0.295
Feedback valence × feedback delay × group	0.09	0.54	73.82	0.16	0.872
Unsigned PE × feedback valence × feedback delay × group	−4.03	3.45	36.29	−1.17	0.251

Random effects						
	Variance	SD	Corr			
Subject (intercept)	5.20	2.28				
Subject (unsigned PE × feedback valence)	11.10	3.33	−0.07			
Subject (unsigned PE × feedback delay)	4.16	2.04	0.42	0.65		
Subject (feedback valence × feedback delay)	0.96	0.98	−0.07	−0.96	−0.70	
Subject (unsigned PE × feedback valence × feedback delay)	104.57	10.23	−0.08	−0.52	−0.16	0.70
Residual	37.25	6.10				

Model fit		
	Marginal	Conditional
R^2	0.01	0.16

Key: p values for fixed effects calculated using Satterthwaite's approximations. Model equation: FRN ~ 1 + unsigned PE * feedback valence * feedback delay * group + (1 + unsigned PE:feedback valence:feedback delay + unsigned PE:feedback valence + unsigned PE:feedback delay + feedback valence:feedback delay| subject). $n_{subjects} = 48$, $n_{observations} = 15{,}034$.

SE = 0.39, $t = 1.45$, $p = 0.594$). When stimulating the cerebellum, the FRN was not significantly modulated by the unsigned RL-PE (both $p \geq 0.999$).

No other effects involving feedback valence or the unsigned RL-PE with stimulation site or each other emerged (all $p \geq 0.207$). Complete inferential statistics can be found in Table 9.

Control analysis

To explore whether feedback processing was generally disrupted or whether this was more specific to the processing of RL-PEs, we performed a control analysis investigating whether patients with cerebellar stroke (Experiment 1) and healthy controls receiving cerebellar TMS (Experiment 2) showed preserved valence coding in the FRN, as valence effects for short feedback delays are a well-reported finding (Sambrook and Goslin, 2015; Hinneberg and Hegele, 2022). This was investigated within the same LME model reported above, resolving the (nonsignificant) interactions between outcome valence, feedback delay, and group for Experiment 1 and outcome valence, TMS timing, and stimulation site for Experiment 2.

Indeed, result patterns were consistent with intact valence coding in FRN under short feedback delays for patients with cerebellar stroke and healthy participants receiving cerebellar TMS. In Experiment 1, the FRN was indeed more negative for negative relative to positive feedback in both controls ($\beta = 0.81$, SE = 0.23, $t = 3.54$, $p = 0.002$) and patients ($\beta = 1.01$, SE = 0.21, $t = 4.79$, $p < 0.001$) in the short delay condition but not in the long delay condition (both $p \geq 0.103$; Fig. 12*A*). In Experiment 2, where only short delays were used, the FRN was consistently more negative for negative over positive valence for both stimulation sites and TMS timings (poststimulus vertex: $\beta = 1.12$, SE = 0.27, $t = 4.13$, $p < 0.001$; poststimulus cerebellum: $\beta = 0.79$, SE = 0.27, $t = 2.96$, $p = 0.012$; prefeedback vertex: $\beta = 1.47$, SE = 0.27, $t = 5.54$, $p < 0.001$; prefeedback cerebellum: $\beta = 1.09$, SE = 0.27, $t = 4.07$, $p < 0.001$; Fig. 12*B*).

To further examine whether we could find evidence against an effect of these interactions, model comparisons were performed to extract an estimation of the Bayes factor. The full LME models were compared against a model without the interaction between outcome valence, feedback delay, and group for Experiment 1 and outcome valence, TMS timing, and stimulation site for Experiment 2. The Bayes factor was then estimated based on the difference Bayesian Information Criterion, following Shen and González (2021). In line with the control analyses, the

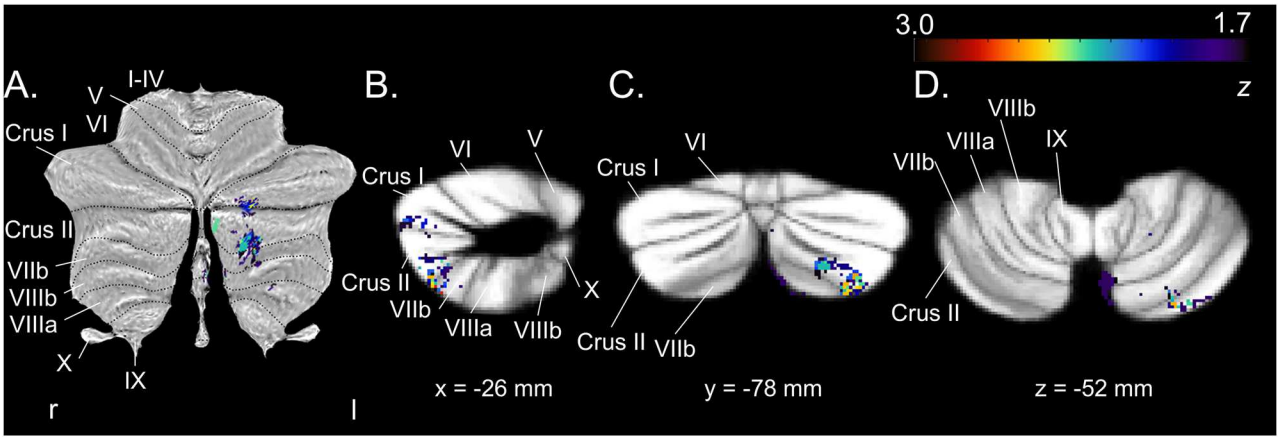

Figure 10. Lesion symptom mapping in Experiment 1 (patient study). Voxel-based lesion symptom mapping of lesion location comparing groups on (***A***) a cerebellar flatmap (Diedrichsen and Zotow, 2015) and in 2D (***B***) sagittal, (***C***) coronal, and (***D***) axial views. Color code shown on the top right denotes *z*-scores (from purple = 1.7 to red = 3.0). r, right; l, left.

Table 7. Inferential statistics for the ANOVA investigating the influence of stimulation site, TMS timing and block on accuracy in Experiment 2 (TMS study)

Effect	df_n	df_d	F	p
Stimulation site	1	23	0.01	0.938
TMS timing	1	23	0.13	0.717
Block	3.18	73.05	6.21	<0.001
Stimulation site × TMS timing	1	23	0.01	0.929
Stimulation site × block	3.12	71.87	0.88	0.461
TMS timing × block	3.33	76.65	0.62	0.619
Stimulation site × TMS timing × block	5	115	0.65	0.660

$n = 24$.

estimated Bayes Factor indicated very strong evidence for an absence of the triple interactions (BF = 90.02 for both experiments/comparisons).

Exploratory analysis of predictability of choice switching by ERP components

While differences in accuracy or choice switching between groups (Experiment 1) and stimulation sites (Experiment 2) were either not significant or not as severe, differences in RL-PE processing in the FRN were substantial. While the FRN does not seem to have a strong behavioral correlate (Ullsperger, 2024), there is some evidence linking it to behavioral flexibility (Cohen and Ranganath, 2007; Fischer and Ullsperger, 2013; Kirschner et al., 2022; but also see Chase et al., 2011). In an exploratory analysis, we added the FRN amplitude as an additional factor to the LME models with choice switching as the dependent variable. However, the respective LME models did not offer a better fit to the data than the original models (Experiment 1: $\chi^2_{(32)} = 36.01$, $p = 0.286$; Experiment 2: $\chi^2_{(32)} = 24.82$, $p = 0.813$) and neither did any effects including the FRN amplitude and the group factor reach significance within these models (all $p \geq 0.079$). In an additional analysis for Experiment 1, we tried to relate the difference FRN as presented in Figure 8*C* to choice switching using group-specific correlations. However, this correlation did not reach significance for controls ($t_{(24)} = 0.29$, $p = 0.773$) or patients ($t_{(23)} = 0.28$, $p = 0.784$).

For completeness, we also added the P3a and P3b separately to the choice switching model to see whether these would improve model fit. P3a and P3b in the feedback-related ERP peak at ∼300–500 ms postfeedback frontocentrally and parietally, respectively (Hruby and Marsalek, 2003; Polich, 2007), and have been more clearly associated with behavioral flexibility (Ullsperger, 2024). Indeed, including P3a/b in the model significantly improved model fit for both P3a ($\chi^2_{(32)} = 58.19$, $p = 0.003$) and P3b ($\chi^2_{(32)} = 54.72$, $p = 0.007$) in Experiment 1. Full statistics for the model comparisons can be found in Table 10. Several effects including both P3a and group reached significance and one effect including both P3b and group reached significance. The general effect patterns seem to indicate that the P3a is generally predictive of choice switching for healthy controls, but only under specific circumstances for patients.

For the P3a LME model in Experiment 1, the interaction between P3a and group reached significance ($\beta = 0.01$, SE = 0.00, $t_{(15,752.83)} = 2.04$, $p = 0.042$). P3a was predictive of choice switching for controls ($\beta = -0.01$, SE = 0.00, $t = -2.45$, $p = 0.028$), such that an increased P3a corresponded to decreased choice switching. This effect did not reach significance in patients ($\beta = 0.00$, SE = 0.00, $t = 0.90$, $p = 0.734$). This interaction was further modulated by block ($\beta = 0.01$, SE = 0.00, $t_{(15,710.76)} = 2.05$,

Table 8. Inferential statistics for the LME analysis examining the effect of feedback valence, response type, stimulation site, TMS timing, and block onto choice switching in Experiment 2 (TMS study)

Fixed effects

	Est/β	SE	df	t	p
(Intercept)	0.07	0.04	22.60	1.91	0.069
Feedback valence	−0.23	0.03	6,489.74	−7.74	<0.001
Response type	−0.39	0.03	6,502.49	−12.64	<0.001
Stimulation site	−0.11	0.03	6,475.16	−3.67	<0.001
TMS timing	0.00	0.03	6,477.69	0.06	0.954
Block	0.00	0.02	6,481.40	0.21	0.831
Feedback valence × response type	0.07	0.06	6,479.45	1.15	0.252
Feedback valence × stimulation site	−0.01	0.06	6,487.20	−0.19	0.852
Response type × stimulation site	−0.06	0.06	6,488.89	−1.07	0.286
Feedback valence × TMS timing	0.01	0.06	6,461.84	0.14	0.889
Response type × TMS timing	0.04	0.06	6,502.24	0.64	0.524
Stimulation site × TMS timing	−0.03	0.06	6,479.64	−0.56	0.577
Feedback valence × block	0.01	0.03	6,327.19	0.36	0.720
Response type × block	−0.15	0.03	6,499.06	−5.02	<0.001
Stimulation site × block	−0.03	0.03	6,482.72	−0.87	0.387
TMS timing × block	0.01	0.03	6,483.30	0.31	0.758
Feedback valence × response type × stimulation site	0.13	0.12	6,481.54	1.04	0.298
Feedback valence × response type × TMS timing	0.04	0.12	6,489.48	0.35	0.727
Feedback valence × stimulation site × TMS timing	−0.12	0.12	6,436.24	−0.99	0.325
Response type × stimulation site × TMS timing	0.02	0.12	6,502.30	0.19	0.848
Feedback valence × response type × block	−0.07	0.06	6,484.86	−1.11	0.268
Feedback valence × stimulation site × block	0.00	0.06	6,107.47	−0.04	0.968
Response type × stimulation site × block	−0.02	0.06	6,490.12	−0.36	0.721
Feedback valence × TMS timing × block	0.13	0.06	6,384.46	2.08	0.037
Response type × TMS timing × block	−0.03	0.06	6,485.44	−0.48	0.629
Stimulation site × TMS timing × block	−0.07	0.06	6,479.98	−1.16	0.246
Feedback valence × response type × stimulation site × TMS timing	−0.03	0.24	6,489.04	−0.12	0.906
Feedback valence × response type × stimulation site × block	−0.04	0.12	6,485.43	−0.37	0.709
Feedback valence × response type × TMS timing × block	−0.27	0.12	6,489.30	−2.22	0.027
Feedback valence × stimulation site × TMS timing × block	0.03	0.12	4,922.33	0.21	0.833
Response type × stimulation site × TMS timing × block	0.13	0.12	6,489.78	1.10	0.271
Feedback valence × response type × stimulation site × TMS timing × block	0.01	0.25	48.64	0.04	0.971

Random effects

	Variance	SD	Corr
Subject (intercept)	0.03	0.16	
Subject (feedback valence × response type × stimulation site × TMS timing × block)	0.10	0.32	0.53
Residual	0.88	0.94	

Model fit

	Marginal	Conditional
R^2	0.08	0.11

Key: p values for fixed effects calculated using Satterthwaite's approximations. Model equation: choice switching ∼ 1 + feedback valence * response type * stimulation site * TMS timing * block + (1 + feedback valence: response type:stimulation site:TMS timing:block | subject). $n_{subjects} = 21$, $n_{observations} = 6{,}541$.

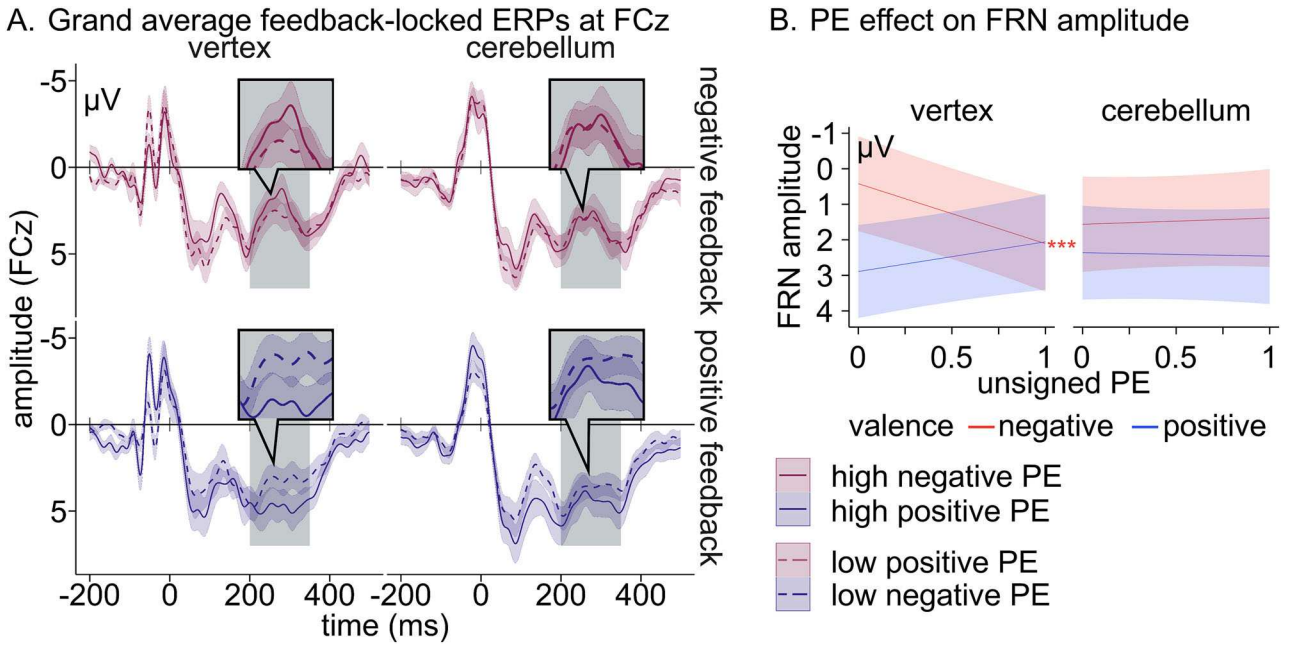

Figure 11. ERP results for Experiment 2 (TMS study). ***A***, Grand average feedback-locked ERPs at FCz according to unsigned RL-PE (low, high), feedback valence (positive, negative), and stimulation site (vertex, cerebellum). Red lines denote high unsigned RL-PE (>0.5) and blue lines low unsigned RL-PE (≤0.5). Colored bands indicate standard errors. ***B***, Slope estimates for FRN amplitude predicted by unsigned RL-PE and modulated by feedback valence and stimulation site. Red lines denote positive feedback valence and blue lines negative feedback valence. Colored bands indicate 95% confidence intervals. $*p < 0.05$. $**p < 0.01$. $***p < 0.001$.

$p = 0.041$). Choice switching was increased with increasing P3a for patients late in the task on trend level ($\beta = 0.01$, SE = 0.00, $t = 2.38$, $p = 0.068$), but not early in the task, and not at all for healthy controls (all $p \geq 0.191$). The interaction was further modulated by outcome valence in a four-way interaction ($\beta = 0.02$, SE = 0.01, $t_{(15,706.65)} = 2.31$, $p = 0.021$). Choice switching was increased on trend level with increasing P3a for patients late in the task only for positive feedback ($\beta = 0.01$, SE = 0.01, $t = 2.55$, $p = 0.087$). No other simple slopes reached significance when resolving the interaction (all $p \geq 0.168$).

A three-way interaction including P3a, group, and feedback delay ($\beta = -0.02$, SE = 0.01, $t_{(15,729.44)} = 2.23$, $p = 0.026$) showed that P3a was predictive of choice switching only for controls in the short feedback delay condition, however, only at trend level ($\beta = -0.01$, SE = 0.00, $t = 2.39$, $p = 0.067$). Larger P3a amplitudes led to reduced choice switching. The effect did not reach significance for controls in the long feedback delay condition or for patients at all (all $p \geq 0.125$). However, two higher-level interactions indicated that a P3a-choice switching relation did exist for patients under specific circumstances: The interaction between P3a, group, and feedback delay was further modulated by response type in a four-way interaction ($\beta = -0.04$, SE = 0.02, $t_{(15,712.02)} = 2.37$, $p = 0.018$). This four-way interaction revealed that P3a was significantly predictive of choice switching only for patients for short feedback delay when the choice was correct ($\beta = 0.02$, SE = 0.00, $t = 3.48$, $p = 0.004$). In no other condition did the effect reach significance (all $p \geq 0.301$). Finally, the four-way interaction was further modulated by outcome valence in a five-way interaction ($\beta = 0.08$, SE = 0.04, $t_{(15,705.28)} = 2.16$, $p = 0.031$). In this five-way interaction, P3a was predictive of choice switching on trend level only for patients for the short delay condition, when feedback was positive and the reaction was correct, with larger P3a amplitudes predicting more choice switching ($\beta = 0.01$, SE = 0.00, $t = 2.77$, $p = 0.090$). No other slope reached significance (all $p \geq 0.254$). These effect patterns might be due to a smaller, more general effect of P3a on choice switching in healthy controls, while for patients, the direction of the effect was more dependent on the experimental condition. The full statistical pattern is displayed in Table 11.

For P3b, a four-way interaction between P3b, outcome valence, group, and block emerged ($\beta = 0.02$, SE = 0.01, $t_{(14,135.18)} = 1.97$, $p = 0.049$). P3b amplitude was predictive of choice switching only for patients when receiving positive feedback and only late in the task ($\beta = 0.02$, SE = 0.01, $t = 3.97$, $p < 0.001$; all other $p \geq 0.894$).

Notably, we could not replicate these findings for Experiment 2. The stroke patient sample might have been more suitable to explore such deficits, as the single-pulse TMS we used in Experiment 2 creates a virtual lesion merely via inducing noise. A brain–behavior connection might be clearer when using rTMS protocols. Including the P3a/b in the model did not result in significant improvements in model fit (P3a: $\chi^2_{(32)} = 44.42$, $p = 0.071$; P3b: $\chi^2_{(32)} = 45.47$, $p = 0.058$).

Discussion

The current study aimed to investigate whether cerebellar output is required for reinforcement learning-prediction error (RL-PE) coding in the ACC-generated FRN. We studied this in two cerebellar lesion models (cerebellar stroke patients and single-pulse cerebellar TMS) during a probabilistic feedback learning task. While we found RL-PE coding in the FRN for healthy controls and for control stimulation (vertex) in negative outcome/feedback contexts, it was largely absent for cerebellar stroke patients and for cerebellar TMS. The results provide evidence that RL-PE computation is dependent on cerebellar output. Behavioral deficits, however, were subtle. While overall learning success was unaffected by cerebellar lesions or cerebellar TMS, behavioral flexibility, as indexed by choice switching, was reduced. Subtle deficits may be due to compensation by other brain areas within the reinforcement learning network.

Table 9. Inferential statistics for the LME analysis examining the effect of unsigned RL-PE, feedback valence, stimulation site, and TMS timing onto FRN amplitude in Experiment 2 (TMS study)

Fixed effects					
	Est/β	SE	df	t	p
(Intercept)	1.92	0.64	21.08	3.02	0.007
Unsigned PE	0.20	0.20	7,125.07	1.00	0.320
Feedback valence	1.08	0.14	7,116.94	7.90	<0.001
Stimulation site	0.08	0.14	5,953.65	0.56	0.577
TMS timing	3.38	0.15	5,521.83	22.99	<0.001
Unsigned PE × feedback valence	−1.11	0.49	6,506.98	−2.28	0.023
Unsigned PE × stimulation site	−0.46	0.40	7,120.14	−1.17	0.244
Feedback valence × stimulation site	−0.27	0.27	7,123.63	−1.00	0.317
Unsigned PE × TMS timing	0.89	0.40	7,121.23	2.24	0.025
Feedback valence × TMS timing	0.49	0.27	7,122.51	1.80	0.071
Stimulation site × TMS timing	1.28	0.31	3,279.84	4.14	<0.001
Unsigned PE × feedback valence × stimulation site	2.82	0.93	5,523.19	3.05	0.002
Unsigned PE × feedback valence × TMS timing	2.45	0.89	6,049.33	2.75	0.006
Unsigned PE × stimulation site × TMS timing	0.38	0.80	7,124.94	0.48	0.632
Feedback valence × stimulation site × TMS timing	0.21	0.54	7,124.02	0.39	0.696
Unsigned PE × feedback valence × stimulation site × TMS timing	5.31	4.07	19.75	1.30	0.207
Random effects					
	Variance	SD	Corr		
Subject (intercept)	8.82	2.97			
Subject (unsigned PE × feedback valence × stimulation site × TMS timing)	287.19	16.95	0.03		
Residual	29.10	5.39			
Model fit					
	Marginal		Conditional		
R^2	0.08		0.30		

Key: p values for fixed effects calculated using Satterthwaite's approximations. Model equation: FRN ~ 1 + unsigned PE * feedback valence * stimulation site * TMS timing + (1 + unsigned PE:feedback valence: stimulation site:TMS timing | subject). $n_{subjects} = 22$, $n_{observations} = 7{,}162$.

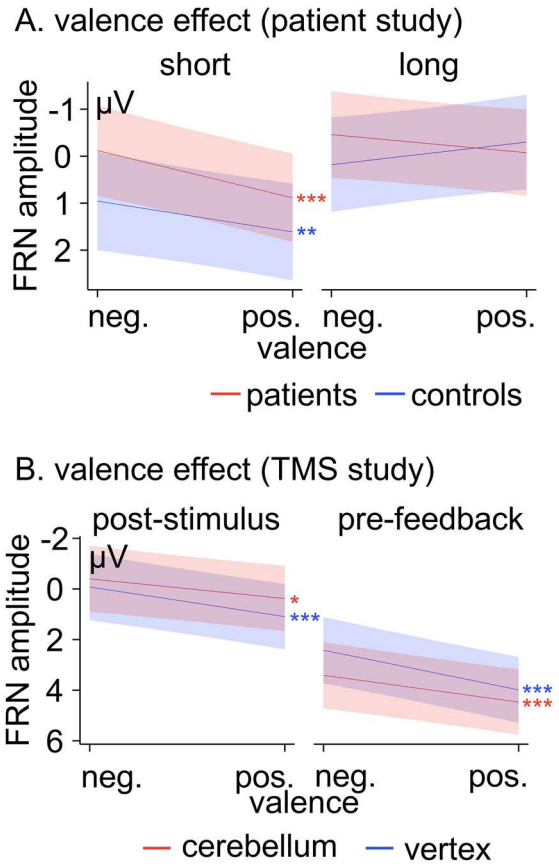

Figure 12. Slope estimates for FRN amplitude predicted by feedback valence. ***A***, Slope estimates for FRN amplitude predicted by feedback valence and modulated by feedback delay and group. Red lines denote patients and blue lines healthy controls. ***B***, Slope estimates for FRN amplitude predicted by feedback valence and modulated by TMS timing and stimulation site. Red lines denote cerebellar TMS and blue lines vertex TMS. Colored bands indicate 95% confidence intervals. *$p < 0.05$. **$p < 0.01$. ***$p < 0.001$.

For healthy controls (Experiment 1) and control stimulation (Experiment 2), RL-PE coding in the FRN was found only for negative feedback. This is consistent with previous studies in healthy participants that found the RL-PE reflected in the FRN only, or at least more strongly, for negative outcomes/feedback (Hoy et al., 2021; Rawls and Lamm, 2021). Note that the direction of the effect was unexpectedly reversed for control stimulation in Experiment 2, as discussed below. Importantly, patients with cerebellar damage and healthy participants receiving cerebellar TMS showed no significant RL-PE coding in the FRN. Activity consistent with RL-PE has previously been described in the rodent cerebellum, although mainly for reward contexts (Kostadinov and Häusser, 2022). It is thus conceivable that RL-PE processing in the cerebellum, as found in these previous studies, is necessary for further RL-PE processing in connected areas classically associated with reinforcement learning (i.e., forebrain and midbrain areas). Of note, feedback processing was not deficient in general, with an intact valence effect in the FRN under short feedback delays in cerebellar patients and in healthy participants receiving cerebellar TMS.

Closer inspection of Figure 7*A* reveals that the lack of differentiation between low and high RL-PEs in the FRN in patients was driven by an increase in FRN amplitudes for low RL-PEs rather than a decrease in FRN amplitudes for high RL-PEs. Thus, it appears that the effect is driven by over-activation toward expected outcomes rather than underactivation for unexpected outcomes, which may be indicative of exaggerated perceived salience of expected feedback.

The deficit in RL-PE coding in the FRN was most pronounced in patients with lesions at the border of Crus II and lobule VIIb and to a smaller degree in medial Crus II, Crus I, lobule VIIb, and VIIIa. Especially Crus I and II have previously been identified to be involved in decision making and executive control (Berlijn et al., 2024b) and are also connected to the reinforcement learning network (Habas, 2021). The present cluster in Crus II/lobule VIIb overlapped with regions associated with higher cognitive functions, in particular working memory (region D2 in Nettekoven et al., 2024), shown in cerebellar parcellations based on functional magnetic resonance imaging (fMRI) data. The cluster in Crus I, Crus II, and lobule VIIb/VIIIa seemed to be related to default mode network/theory of mind, working memory, and spatial rotation/simulation (regions S3, D1, and A1 in Nettekoven et al., 2024). Data on reinforcement learning tasks, however, were not included in the fMRI data on which these parcellations are based. Notably, the cluster in Crus II/lobule VIIb in the present study seems to match with a cluster found in relation to behavioral changes in a feedback learning task very similar to ours (Peterburs et al., 2018). While the abovementioned regions

Table 10. Model comparisons for the choice switching LME analysis with FRN, P3a, and P3b as additional predictors, respectively, for Experiments 1 and 2

Model	$n_{parameter}$	AIC	BIC	Log likelihood	Deviance	Model comparison χ^2	df	p
Experiment 1								
Standard model (data with valid FRN, P3a, and P3b)	36	42,815	43,091	−21,372	42,743			
Model with FRN as an additional predictor	68	42,843	43,365	−21,354	42,707	36.01	32	0.286
Model with P3a as an additional predictor	68	42,821	43,343	−21,343	42,685	58.19	32	0.003
Model with P3b as an additional predictor	68	42,825	43,346	−21,344	42,689	54.72	32	0.007
Experiment 2								
Standard model (data with valid FRN)	36	17,686	17,930	−8,807.1	17,614			
Model with FRN as an additional predictor	68	17,725	18,186	−8,794.7	17,589	24.82	32	0.813
Standard model (data with valid P3a/b)	36	17,821	18,065	−8,874.4	17,749			
Model with P3a as an additional predictor	68	17,841	18,302	−8,852.2	17,705	44.42	32	0.071
Model with P3b as an additional predictor	68	17,839	18,301	−8,851.7	17,703	45.47	32	0.058

Model comparisons based on deviance.

were associated with especially aberrant RL-PE coding, the distribution of difference FRN was overall shifted for patients compared with controls (Fig. 8*C*). Considering the overall lesion distribution in patients, it is conceivable that other posterolateral cerebellar regions also play a role in RL-PE processing.

It has to be noted that behavioral changes associated with cerebellar lesions or cerebellar TMS were quite subtle which seems unexpected given the substantial changes in the FRN. While the FRN generator, ACC, is essential for action-outcome learning (Rudebeck et al., 2008; Camille et al., 2011), the present experiments used additional visual stimuli to represent choices (i.e., button presses). It is therefore conceivable that areas involved in stimulus-outcome learning, such as the orbitofrontal cortex (OFC; Rudebeck et al., 2008; Camille et al., 2011), were able to compensate for ACC-driven deficits. Action-outcome– and stimulus-outcome–based learning might have redundancy to accommodate different environmental requirements. While both the ACC and the OFC receive a wide range of input (Heilbronner and Hayden, 2016; Groman et al., 2021), they might differ in relation to cerebellar input and dependency on predictive information processed by the cerebellum (Peterburs and Desmond, 2016). Previous studies in rodents showed that the cerebellum modulates dopaminergic activity in the substantia nigra (Washburn et al., 2024), and projections from the cerebellum to the VTA were able to modulate place preference (Carta et al., 2019). Both the substantia nigra and the VTA project toward the ACC (Zhang et al., 2017; Elston et al., 2018, 2019). The OFC, in turn, may be more independent from cerebellar processing. While there is some evidence for connections between the cerebellum and OFC (Palesi et al., 2017), we did not measure proxies of OFC activity and therefore cannot conclude whether processing in the OFC was affected. Notably, there seems to be a general pattern of reduced behavioral flexibility and intact acquisition concomitant with cerebellar damage/disruption: learning acquisition was shown to be intact in patients with cerebellar stroke (Thoma et al., 2008; Rustemeier et al., 2016; present Exp. 1) and cerebellar degeneration (A.M. Berlijn, D.M. Huvermann, E. Bechler et al., unpublished observation) as well as healthy participants receiving cerebellar single-pulse or rTMS (present Exp.2, Kruithof et al., 2025). Nicholas et al. (2024) showed deficits in behavioral flexibility in patients with cerebellar degeneration using a task with constantly changing drifting reward probabilities. In an additional exploratory analysis, we were able to link deficits not in the FRN but in later feedback processing (P3a) to deficits in choice switching, which is consistent with the current conception that the P3 has stronger behavioral correlates than the FRN (Ullsperger, 2024). There is some evidence for a relation between FRN and behavioral adjustment (Fischer and Ullsperger, 2013; Kirschner et al., 2022; but also see Chase et al., 2011), which might not have played a big enough role in the current study. FRN seems to predict choice switching in highly adaptive environments (Cohen and Ranganath, 2007). The FRN might thus be a readout of a RL-PE that depends on cerebellar output but is not strictly required for learning success in tasks which do not require a high degree of behavioral flexibility. Thoma et al. (2008) and Kruithof et al. (2025) showed that behavioral flexibility required in reversal learning is indeed impaired in cerebellar damage/disruption even in the presence of intact learning acquisition.

In Experiment 2, we varied TMS pulse timing to test whether the cerebellum is potentially involved in response and/or feedback processing selectively. The variation in pulse timing did not appear to modulate the effect of cerebellar TMS on RL-PE coding in the FRN. While this might be related to differential contributions of predictive effects (poststimulus TMS) and feedback processing (prefeedback TMS), an absence of a timing effect might also result from nonoptimal temporal placement of stimulation timings.

While in Experiment 1, the FRN reflected the RL-PE in the expected direction in control participants (i.e., more negative FRN amplitudes for higher RL-PEs), the direction was unexpectedly reversed for the control stimulation in Experiment 2. It thus seems that even though vertex is a common site for control stimulation, it did have an effect on feedback processing, challenging its use as a control condition in Experiment 2. At least one study (Jung et al., 2016) showed reduced activity in the ACC (i.e., the generator of FRN; Hauser et al., 2014) with vertex TMS, although not significantly with the inverted stimulation that we used. Nevertheless, it is still noteworthy that findings for the cerebellar TMS in Experiment 2 replicated the findings in Experiment 1 for cerebellar stroke patients. Both showed a lack of RL-PE coding in FRN. Even though the RL-PE was reflected in the FRN for vertex TMS in the opposite direction, there was a significant RL-PE coding for vertex TMS, while it could not be found for the cerebellar TMS, as well as no effect of stimulation site on learning, thus replicating the overall result pattern in Experiment 1.

In summary, feedback processing, as indexed by the FRN, was shown to be dependent on cerebellar output. While cerebellar dysfunction or damage resulted in only subtle changes in behavioral flexibility with reinforcement learning performance largely intact, processing of RL-PEs as reflected in the FRN was substantially blunted. Crucially, this pattern was consistent across two

Table 11. Inferential statistics for the LME analysis examining the effect of P3a, feedback valence, response type, feedback delay, group, and block onto choice switching in Experiment 1 (patient study)

Fixed effects					
	Est/β	SE	df	t	p
(Intercept)	0.09	0.04	64.23	2.31	0.024
P3a	0.00	0.00	15,752.83	−1.38	0.167
Feedback valence	−0.18	0.03	15,706.55	−5.87	<0.001
Response type	−0.25	0.03	15,739.13	−8.04	<0.001
Feedback delay	−0.09	0.03	15,714.33	−2.78	0.005
Group	−0.04	0.08	64.23	−0.48	0.632
Block	−0.08	0.02	15,707.24	−5.59	<0.001
P3a × feedback valence	0.00	0.00	15,709.07	−1.06	0.288
P3a × response type	0.01	0.00	15,713.92	1.80	0.072
Feedback valence × response type	−0.13	0.06	15,704.73	−2.14	0.032
P3a × feedback delay	0.00	0.00	15,729.44	−0.82	0.412
Feedback valence × feedback delay	0.12	0.06	15,707.21	1.93	0.053
Response type × feedback delay	−0.10	0.06	15,717.62	−1.61	0.108
P3a × group	0.01	0.00	15,752.83	2.04	0.042
Feedback type × group	−0.08	0.06	15,706.55	−1.34	0.180
Response type × group	−0.07	0.06	15,739.13	−1.09	0.275
Feedback delay × group	0.10	0.06	15,714.33	1.68	0.092
P3a × block	0.00	0.00	15,710.76	1.32	0.186
Feedback valence × block	0.01	0.03	15,706.32	0.33	0.738
Response type × block	−0.10	0.03	15,715.07	−3.29	0.001
Feedback delay × block	0.06	0.03	15,704.81	2.12	0.034
Group × block	0.01	0.03	15,707.24	0.39	0.700
P3a × feedback valence × response type	0.02	0.01	15,707.98	1.78	0.075
P3a × feedback valence × feedback delay	−0.01	0.01	15,708.47	−0.67	0.505
P3a × response type × feedback delay	0.00	0.01	15,712.02	−0.45	0.652
Feedback valence × response type × feedback delay	−0.07	0.12	15,704.17	−0.58	0.565
P3a × feedback valence × group	0.01	0.01	15,709.07	1.18	0.240
P3a × response type × group	0.00	0.01	15,713.92	−0.06	0.951
Feedback valence × response type × group	0.23	0.12	15,704.73	1.87	0.061
P3a × feedback delay × group	−0.02	0.01	15,729.44	−2.23	0.026
Feedback valence × feedback delay × group	0.26	0.12	15,707.21	2.14	0.033
Response type × feedback delay × group	0.03	0.12	15,717.62	0.22	0.829
P3a × feedback valence × block	0.00	0.00	15,706.65	0.33	0.740
P3a × response type × block	0.00	0.00	15,708.16	0.18	0.857
Feedback valence × response type × block	0.09	0.06	15,704.32	1.58	0.114
P3a × feedback delay × block	−0.01	0.00	15,707.03	−1.29	0.199
Feedback valence × feedback delay × block	0.01	0.06	15,705.59	0.21	0.836
Response type × feedback delay × block	−0.06	0.06	15,708.86	−0.92	0.357
P3a × group × block	0.01	0.00	15,710.76	2.05	0.041
Feedback valence × group × block	−0.10	0.06	15,706.32	−1.69	0.092
Response type × group × block	0.00	0.06	15,715.07	0.02	0.983
Feedback delay × group × block	0.06	0.06	15,704.81	1.05	0.295
P3a × feedback valence × response type × feedback delay	0.02	0.02	15,705.28	0.89	0.374
P3a × feedback valence × response type × group	−0.03	0.02	15,707.98	−1.85	0.065
P3a × feedback valence × feedback delay × group	0.02	0.02	15,708.47	1.23	0.219
P3a × response type × feedback delay × group	−0.04	0.02	15,712.02	−2.37	0.018
Feedback valence × response type × feedback delay × group	−0.43	0.25	15,704.17	−1.75	0.081
P3a × feedback valence × response type × block	−0.01	0.01	15,706.99	−1.45	0.147
P3a × feedback valence × feedback delay × block	−0.01	0.01	15,706.18	−1.11	0.268
P3a × response type × feedback delay × block	0.01	0.01	15,707.24	1.29	0.196
Feedback valence × response type × feedback delay × block	−0.14	0.12	15,704.08	−1.13	0.257
P3a × feedback valence × group × block	0.02	0.01	15,706.65	2.31	0.021
P3a × response type × group × block	−0.01	0.01	15,708.16	−1.51	0.132
Feedback valence × response type × group × block	−0.06	0.12	15,704.32	−0.47	0.638
P3a × feedback delay × group × block	−0.01	0.01	15,707.03	−1.13	0.257
Feedback valence × feedback delay × group × block	−0.14	0.12	15,705.59	−1.16	0.246
Response type × feedback delay × group × block	0.07	0.12	15,708.86	0.62	0.533
P3a × feedback valence × response type × feedback delay × group	0.08	0.04	15,705.28	2.16	0.031
P3a × feedback valence × response type × feedback delay × block	0.00	0.02	15,705.60	−0.13	0.894
P3a × feedback valence × response type × group × block	−0.03	0.02	15,706.99	−1.48	0.140
P3a × feedback valence × feedback delay × group × block	−0.01	0.02	15,706.18	−0.36	0.720
P3a × response type × feedback delay × group × block	0.02	0.02	15,707.24	0.93	0.350
Feedback valence × response type × feedback delay × group × block	−0.04	0.24	15,704.08	−0.15	0.883
P3a × feedback valence × response type × feedback delay × group × block	−0.02	0.04	15,705.60	−0.52	0.606

(*Table continues.*)

Table 11. Continued

Fixed effects					
	Est/β	SE	df	t	p
Random effects					
	Variance	SD			
Subject (intercept)	0.07	0.26			
Residual	0.86	0.93			
Model fit					
R^2	Marginal		Conditional		
	0.06		0.13		
Simple slope analyses					
P3a × group	Est/β	SE		t	p
P3a slope for controls	−0.01	0.00		2.45	0.028
P3a slope for patients	0.00	0.00		0.90	0.734
P3a × group × block	Est/β	SE		t	p
P3a slope for controls and early experiment (M − 1SD)	−0.01	0.00		1.56	0.471
P3a slope for controls and late experiment (M + 1SD)	−0.01	0.00		1.98	0.191
P3a slope for patients and early experiment (M − 1SD)	0.00	0.00		1.09	>0.999
P3a slope for patients and late experiment (M + 1SD)	0.01	0.00		2.38	0.068
P3a × group × block × feedback valence	Est/β	SE		t	p
P3a slope for controls, early experiment (M − 1SD), and negative feedback	−0.01	0.01		1.20	>0.999
P3a slope for controls, early experiment (M − 1SD), and positive feedback	0.00	0.00		1.05	>0.999
P3a slope for controls, late experiment (M + 1SD), and negative feedback	0.00	0.01		0.04	>0.999
P3a slope for controls, late experiment (M + 1SD), and positive feedback	−0.02	0.01		2.31	0.168
P3a slope for patients, early experiment (M − 1SD), and negative feedback	0.00	0.01		0.01	>0.999
P3a slope for patients, early experiment (M − 1SD), and positive feedback	−0.01	0.00		1.57	>0.999
P3a slope for patients, late experiment (M + 1SD), and negative feedback	0.01	0.01		0.76	>0.999
P3a slope for patients, late experiment (M + 1SD), and positive feedback	0.01	0.01		2.55	0.087
P3a × group × feedback delay	Est/β	SE		t	p
P3a slope for controls and short feedback delays	−0.01	0.00		2.39	0.067
P3a slope for controls and long feedback delays	0.00	0.00		1.06	>0.999
P3a slope for patients and short feedback delays	0.01	0.01		2.15	0.125
P3a slope for patients and long feedback delays	−0.01	0.00		1.44	0.600
P3a × group × feedback delay × response type	Est/β	SE		t	p
P3a slope for controls, short feedback delays, and incorrect choices	−0.01	0.01		1.49	>0.999
P3a slope for controls, short feedback delays, and correct choices	−0.01	0.00		1.96	0.403
P3a slope for controls, long feedback delays, and incorrect choices	−0.02	0.01		2.08	0.301
P3a slope for controls, long feedback delays, and correct choices	0.00	0.00		0.72	>0.999
P3a slope for patients, short feedback delays, and incorrect choices	0.00	0.01		0.03	>0.999
P3a slope for patients, short feedback delays, and correct choices	0.02	0.00		3.48	0.004
P3a slope for patients, long feedback delays, and incorrect choices	0.00	0.01		0.72	>0.999
P3a slope for patients, long feedback delays, and correct choices	−0.01	0.00		1.28	>0.999
P3a × group × feedback delay × response type × feedback valence	Est/β	SE		t	p
P3a slope for controls, short feedback delays, incorrect choices, and negative feedback	0.00	0.01		0.07	>0.999
P3a slope for controls, short feedback delays, incorrect choices, and positive feedback	−0.02	0.02		1.53	>0.999
P3a slope for controls, short feedback delays, correct choices, and negative feedback	−0.02	0.01		1.76	>0.999
P3a slope for controls, short feedback delays, correct choices, and positive feedback	0.00	0.00		0.41	>0.999
P3a slope for controls, long feedback delays, incorrect choices, and negative feedback	0.00	0.00		0.64	>0.999
P3a slope for controls, long feedback delays, incorrect choices, and positive feedback	−0.03	0.01		2.41	0.254
P3a slope for controls, long feedback delays, correct choices, and negative feedback	0.00	0.01		0.51	>0.999
P3a slope for controls, long feedback delays, correct choices, and positive feedback	0.00	0.00		0.77	>0.999
P3a slope for patients, short feedback delays, incorrect choices, and negative feedback	−0.01	0.01		1.21	>0.999
P3a slope for patients, short feedback delays, incorrect choices, and positive feedback	0.01	0.02		0.50	>0.999
P3a slope for patients, short feedback delays, correct choices, and negative feedback	0.02	0.01		2.10	>0.999
P3a slope for patients, short feedback delays, correct choices, and positive feedback	0.01	0.00		2.77	0.090
P3a slope for patients, long feedback delays, incorrect choices, and negative feedback	0.00	0.00		0.33	>0.999
P3a slope for patients, long feedback delays, incorrect choices, and positive feedback	−0.01	0.01		1.22	>0.999
P3a slope for patients, long feedback delays, correct choices, and negative feedback	−0.02	0.01		1.46	>0.999
P3a slope for patients, long feedback delays, correct choices, and positive feedback	0.00	0.00		0.03	>0.999

Key: p values for fixed effects calculated using Satterthwaite's approximations. Model equation: choice switching ~ 1 + P3a * feedback valence * response type * feedback delay * group * block + (1| subject). $n_{subjects} = 52$, $n_{observations} = 15{,}817$.

complementary lesion models (i.e., stroke patients and single-pulse TMS). Furthermore, lesion symptom mapping in patients showed that regions at the border of Crus II and Lobule VIIb, medial Crus II, and Crus I were of particular importance.

References

Balsters JH, Apps MAJ, Bolis D, Lehner R, Gallagher L, Wenderoth N (2017) Disrupted prediction errors index social deficits in autism spectrum disorder. Brain 140:235–246.

Bates D, Mächler M, Bolker B, Walker S (2015) Fitting linear mixed-effects models using lme4. J Stat Softw 67:1–48.

Beck AT, Epstein N, Brown G, Steer RA (1988) An inventory for measuring clinical anxiety: psychometric properties. J Consult Clin Psychol 56:893–897.

Beck AT, Steer RA, Brown G (1996) *Manual for the Beck depression inventory–II*. San Antonio, TX: Psychological Corporation.

Berlijn AM, Huvermann DM, Groiss SJ, Schnitzler A, Mittelstaedt M, Bellebaum C, Timmann D, Minnerop M, Peterburs J (2024a) The effect of cerebellar TMS on error processing: a combined single-pulse TMS and ERP study. Imaging Neurosci 2:1–19.

Berlijn AM, Huvermann DM, Schneider S, Bellebaum C, Timmann D, Minnerop M, Peterburs J (2024b) The role of the human cerebellum for learning from and processing of external feedback in non-motor learning: a systematic review. Cerebellum 23:1532–1551.

Bertazzoli G, Esposito R, Mutanen TP, Ferrari C, Ilmoniemi RJ, Miniussi C, Bortoletto M (2021) The impact of artifact removal approaches on TMS–EEG signal. Neuroimage 239:118272.

Brauer M, Curtin JJ (2018) Linear mixed-effects models and the analysis of nonindependent data: a unified framework to analyze categorical and continuous independent variables that vary within-subjects and/or within-items. Psychol Methods 23:389–411.

Brett M, Leff AP, Rorden C, Ashburner J (2001) Spatial normalization of brain images with focal lesions using cost function masking. Neuroimage 14:486–500.

Brunner E, Munzel U (2000) The nonparametric Behrens-Fisher problem: asymptotic theory and a small-sample approximation. Biom J 42:17–25.

Camille N, Tsuchida A, Fellows LK (2011) Double dissociation of stimulus-value and action-value learning in humans with orbitofrontal or anterior cingulate cortex damage. J Neurosci 31:15048.

Carta I, Chen CH, Schott AL, Dorizan S, Khodakhah K (2019) Cerebellar modulation of the reward circuitry and social behavior. Science 363:eaav0581.

Chase HW, Swainson R, Durham L, Benham L, Cools R (2011) Feedback-related negativity codes prediction error but not behavioral adjustment during probabilistic reversal learning. J Cogn Neurosci 23:936–946.

Cohen MX, Ranganath C (2007) Reinforcement learning signals predict future decisions. J Neurosci 27:371.

Cook RD (1977) Detection of influential observation in linear regression. Technometrics 19:15–18.

Deistung A, et al. (2022) Quantitative susceptibility mapping reveals alterations of dentate nuclei in common types of degenerative cerebellar ataxias. Brain Commun 4:fcab306.

Deistung A, Stefanescu MR, Ernst TM, Schlamann M, Ladd ME, Reichenbach JR, Timmann D (2016) Structural and functional magnetic resonance imaging of the cerebellum: considerations for assessing cerebellar ataxias. Cerebellum 15:21–25.

Delorme A, Makeig S (2004) EEGLAB: an open-source toolbox for analysis of single-trial EEG dynamics. J Neurosci Methods 134:9–21.

Diedrichsen J (2006) A spatially unbiased atlas template of the human cerebellum. Neuroimage 33:127–138.

Diedrichsen J, Balsters JH, Flavell J, Cussans E, Ramnani N (2009) A probabilistic MR atlas of the human cerebellum. Neuroimage 46:39–46.

Diedrichsen J, Maderwald S, Küper M, Thürling M, Rabe K, Gizewski ER, Ladd ME, Timmann D (2011) Imaging the deep cerebellar nuclei: a probabilistic atlas and normalization procedure. Neuroimage 54:1786–1794.

Diedrichsen J, Zotow E (2015) Surface-based display of volume-averaged cerebellar imaging data. PLoS One 10:e0133402.

Duecker F, Sack AT (2015) Rethinking the role of sham TMS. Front Psychol 6:210.

Elston TW, Croy E, Bilkey DK (2019) Communication between the anterior cingulate cortex and ventral tegmental area during a cost-benefit reversal task. Cell Rep 26:2353–2361.e3.

Elston TW, Kalhan S, Bilkey DK (2018) Conflict and adaptation signals in the anterior cingulate cortex and ventral tegmental area. Sci Rep 8:11732.

Eppinger B, Kray J, Mock B, Mecklinger A (2008) Better or worse than expected? Aging, learning, and the ERN. Neuropsychologia 46:521–539.

Filley CM, Fields RD (2016) White matter and cognition: making the connection. J Neurophysiol 116:2093–2104.

Fischer AG, Ullsperger M (2013) Real and fictive outcomes are processed differently but converge on a common adaptive mechanism. Neuron 79:1243–1255.

Foerde K, Shohamy D (2011) Feedback timing modulates brain systems for learning in humans. J Neurosci 31:13157.

Foti D, Weinberg A, Bernat EM, Proudfit GH (2015) Anterior cingulate activity to monetary loss and basal ganglia activity to monetary gain uniquely contribute to the feedback negativity. Clin Neurophysiol 126:1338–1347.

Fouragnan E, Retzler C, Philiastides MG (2018) Separate neural representations of prediction error valence and surprise: evidence from an fMRI meta-analysis. Hum Brain Mapp 39:2887–2906.

Gatti D, Rinaldi L, Vecchi T, Ferrari C (2023) Understanding cerebellar cognitive and social functions: methodological challenges and new directions for future transcranial magnetic stimulation studies. Curr Opin Behav Sci 53:101300.

Groman SM, Lee D, Taylor JR (2021) Unlocking the reinforcement-learning circuits of the orbitofrontal cortex. Behav Neurosci 135:120.

Habas C (2021) Functional connectivity of the cognitive cerebellum. Front Syst Neurosci 15:642225.

Halahakoon DC, Kieslich K, O'Driscoll C, Nair A, Lewis G, Roiser JP (2020) Reward-processing behavior in depressed participants relative to healthy volunteers: a systematic review and meta-analysis. JAMA Psychiatry 77:1286–1295.

Hardwick RM, Lesage E, Miall RC (2014) Cerebellar transcranial magnetic stimulation: the role of coil geometry and tissue depth. Brain Stimul 7:643–649.

Hauser TU, Iannaccone R, Stämpfli P, Drechsler R, Brandeis D, Walitza S, Brem S (2014) The feedback-related negativity (FRN) revisited: new insights into the localization, meaning and network organization. Neuroimage 84:159–168.

Heilbronner SR, Hayden BY (2016) Dorsal anterior cingulate cortex: a bottom-up view. Annu Rev Neurosci 39:149–170.

Heise MJ, Mon SK, Bowman LC (2022) Utility of linear mixed effects models for event-related potential research with infants and children. Dev Cogn Neurosci 54:101070.

Hinneberg BM, Hegele M (2022) Acting in temporal contexts: on the behavioral and neurophysiological consequences of feedback delays. Neuroscience 486:91–102.

Holroyd CB, Coles MGH (2002) The neural basis of human error processing: reinforcement learning, dopamine, and the error-related negativity. Psychol Rev 109:679–709.

Hoy CW, Steiner SC, Knight RT (2021) Single-trial modeling separates multiple overlapping prediction errors during reward processing in human EEG. Commun Biol 4:910.

Hruby T, Marsalek P (2003) Event-related potentials-the P3 wave. Acta Neurobiol Exp 63:55–63.

Ichikawa N, Siegle GJ, Dombrovski A, Ohira H (2010) Subjective and model-estimated reward prediction: association with the feedback-related negativity (FRN) and reward prediction error in a reinforcement learning task. Int J Psychophysiol 78:273–283.

Jung J, Bungert A, Bowtell R, Jackson SR (2016) Vertex stimulation as a control site for transcranial magnetic stimulation: a concurrent TMS/fMRI study. Brain Stimul 9:58–64.

Katthagen T, Kaminski J, Heinz A, Buchert R, Schlagenhauf F (2020) Striatal dopamine and reward prediction error signaling in unmedicated schizophrenia patients. Schizophr Bull 46:1535–1546.

Keren H, et al. (2018) Reward processing in depression: a conceptual and meta-analytic review across fMRI and EEG studies. Am J Psychiatry 175:1111–1120.

Kirschner H, Fischer AG, Ullsperger M (2022) Feedback-related EEG dynamics separately reflect decision parameters, biases, and future choices. Neuroimage 259:119437.

Kostadinov D, Häusser M (2022) Reward signals in the cerebellum: origins, targets, and functional implications. Neuron 110:1290–1303.

Kruithof ES, Drop EM, Gerits D, Klaus J, Schutter DJLG (2025) Continuous theta burst stimulation to the medial posterior cerebellum impairs reversal learning in healthy volunteers. Cogn Affect Behav Neurosci.

Kuznetsova A, Brockhoff P, Christensen R (2017) Lmertest package: tests in linear mixed effects models. J Stat Softw 82:1–26.
Lenth RV (2025) emmeans: Estimated marginal means, aka least-squares means.
Long JA (2019) interactions: comprehensive, user-friendly toolkit for probing interactions. Available at: https://cran.r-project.org/package=interactions
Luke SG (2017) Evaluating significance in linear mixed-effects models in R. Behav Res Methods 49:1494–1502.
Manto M-U, et al. (2024) Consensus paper: cerebellum and reward. Cerebellum 23:2169–2192.
McDougle SD, Butcher PA, Parvin DE, Mushtaq F, Niv Y, Ivry RB, Taylor JA (2019) Neural signatures of prediction errors in a decision-making task are modulated by action execution failures. Curr Biol 29:1606–1613.e5.
Meadows CC, Gable PA, Lohse KR, Miller MW (2016) The effects of reward magnitude on reward processing: an averaged and single trial event-related potential study. Biol Psychol 118:154–160.
Merz J, Lehrl S, Galster V, Erzigkeit H (1975) MWT-B - ein intelligenzkurztest. Psychiatr Neurol Med Psychol 27:423–428.
Miltner WHR, Braun CH, Coles MGH (1997) Event-related brain potentials following incorrect feedback in a time-estimation task: evidence for a "generic" neural system for error detection. J Cogn Neurosci 9:788–798.
Nettekoven C, Zhi D, Shahshahani L, Pinho AL, Saadon-Grosman N, Buckner RL, Diedrichsen J (2024) A hierarchical atlas of the human cerebellum for functional precision mapping. Nat Commun 15:8376.
Nicholas J, Amlang C, Lin C-YR, Montaser-Kouhsari L, Desai N, Pan M-K, Kuo S-H, Shohamy D (2024) The role of the cerebellum in learning to predict reward: evidence from cerebellar ataxia. Cerebellum 23:1355–1368.
Nieuwenhuis R, te Grotenhuis M, Pelzer B (2012) Influence.ME: tools for detecting influential data in mixed effects models. R J 4:38–47.
Oldfield RC (1971) The assessment and analysis of handedness: the Edinburgh inventory. Neuropsychologia 9:97–113.
Palesi F, De Rinaldis A, Castellazzi G, Calamante F, Muhlert N, Chard D, Tournier JD, Magenes G, D'Angelo E, Gandini Wheeler-Kingshott CAM (2017) Contralateral cortico-ponto-cerebellar pathways reconstruction in humans in vivo: implications for reciprocal cerebro-cerebellar structural connectivity in motor and non-motor areas. Sci Rep 7:12841.
Palesi F, Ferrante M, Gaviraghi M, Misiti A, Savini G, Lascialfari A, D'Angelo E, Gandini Wheeler-Kingshott CAM (2021) Motor and higher-order functions topography of the human dentate nuclei identified with tractography and clustering methods. Hum Brain Mapp 42:4348–4361.
Peterburs J, Desmond JE (2016) The role of the human cerebellum in performance monitoring. Syst Neurosci 40:38–44.
Peterburs J, Gajda K, Koch B, Schwarz M, Hoffmann K-P, Daum I, Bellebaum C (2012) Cerebellar lesions alter performance monitoring on the antisaccade task—an event-related potentials study. Neuropsychologia 50:379–389.
Peterburs J, Hofmann D, Becker MPI, Nitsch AM, Miltner WHR, Straube T (2018) The role of the cerebellum for feedback processing and behavioral switching in a reversal-learning task. Brain Cogn 125:142–148.
Peterburs J, Kobza S, Bellebaum C (2016) Feedback delay gradually affects amplitude and valence specificity of the feedback-related negativity (FRN). Psychophysiology 53:209–215.
Phillips JR, Hewedi DH, Eissa AM, Moustafa AA (2015) The cerebellum and psychiatric disorders. Front Public Health 3:66.
Polich J (2007) Updating P300: an integrative theory of P3a and P3b. Clin Neurophysiol 118:2128–2148.
R Core Team (2023) R: a language and environment for statistical computing. Available at: https://www.*R*-project.org/
Ramnani N (2006) The primate cortico-cerebellar system: anatomy and function. Nat Rev Neurosci 7:511–522.
Rawls E, Lamm C (2021) The aversion positivity: mediofrontal cortical potentials reflect parametric aversive prediction errors and drive behavioral modification following negative reinforcement. Cortex 140:26–39.
Rescorla RA, Wagner AR (1972) A theory of Pavlovian conditioning: variations in the effectiveness of reinforcement and nonreinforcement. In: *Classical conditioning II: current research and theory* (Black AH, Prokasy WF, eds), pp 64–99. New York: Appleton-Century-Crofts.
Robinson RG, Jorge RE (2016) Post-stroke depression: a review. Am J Psychiatry 173:221–231.
Posit Team (2023) RStudio: Integrated development environment for R. Available at: http://www.posit.co/
Rudebeck PH, Behrens TE, Kennerley SW, Baxter MG, Buckley MJ, Walton ME, Rushworth MFS (2008) Frontal cortex subregions play distinct roles in choices between actions and stimuli. J Neurosci 28:13775.
Rustemeier M, Koch B, Schwarz M, Bellebaum C (2016) Processing of positive and negative feedback in patients with cerebellar lesions. Cerebellum 15:425–438.
Sambrook TD, Goslin J (2015) A neural reward prediction error revealed by a meta-analysis of ERPs using great grand averages. Psychol Bull 141:213.
San Martín R (2012) Event-related potential studies of outcome processing and feedback-guided learning. Front Hum Neurosci 6:304.
Schmahmann JD, Sherman JC (1998) The cerebellar cognitive affective syndrome. Brain 121:561–579.
Schmitz-Hübsch T, et al. (2006) Scale for the assessment and rating of ataxia. Neurology 66:1717.
Shen N, González B (2021) Bayesian information criterion for linear mixed-effects models. ArXiv Prepr ArXiv210414725.
Sokolov AA, Miall RC, Ivry RB (2017) The cerebellum: adaptive prediction for movement and cognition. Trends Cogn Sci 21:313–332.
Stoodley CJ, MacMore JP, Makris N, Sherman JC, Schmahmann JD (2016) Location of lesion determines motor vs. cognitive consequences in patients with cerebellar stroke. Neuroimage Clin 12:765–775.
Sutton RS, Barto AG (2018) Temporal-difference learning. In: *Reinforcement learning: an introduction*, 2nd ed. pp 119–140. Cambridge, MA: The MIT press.
Thoma P, Bellebaum C, Koch B, Schwarz M, Daum I (2008) The cerebellum is involved in reward-based reversal learning. Cerebellum 7:433–443.
Timmann D, Küper M, Gizewski ER, Schoch B, Donchin O (2022) Lesion-symptom mapping of the human cerebellum. In: *Handbook of the cerebellum and cerebellar disorders* (Manto M-U, Gruol DL, Schmahmann JD, Koibuchi N, Sillitoe RV, eds), Ed 2, pp 1857–1890. Houston, TX: Springer Cham.
Ullsperger M (2024) Beyond peaks and troughs: multiplexed performance monitoring signals in the EEG. Psychophysiology 61:e14553.
Volpert-Esmond HI, Page-Gould E, Bartholow BD (2021) Using multilevel models for the analysis of event-related potentials. Int J Psychophysiol 162:145–156.
Wagner AR, Rescorla RA (1972) Inhibition in Pavlovian conditioning: application of a theory. In: *Inhibition and learning* (Boakes RA, Halliday MS, eds), pp 301–336. New York: Academic Press.
Wahlund LO, et al. (2001) A new rating scale for age-related white matter changes applicable to MRI and CT. Stroke 32:1318–1322.
Washburn S, Oñate M, Yoshida J, Vera J, Bhuvanasundaram R, Khatami L, Nadim F, Khodakhah K (2024) The cerebellum directly modulates the substantia nigra dopaminergic activity. Nat Neurosci 27:497–513.
Wu W, Keller CJ, Rogasch NC, Longwell P, Shpigel E, Rolle CE, Etkin A (2018) ARTIST: a fully automated artifact rejection algorithm for single-pulse TMS-EEG data. Hum Brain Mapp 39:1607–1625.
Yushkevich PA, Piven J, Hazlett HC, Smith RG, Ho S, Gee JC, Gerig G (2006) User-guided 3D active contour segmentation of anatomical structures: significantly improved efficiency and reliability. Neuroimage 31:1116–1128.
Zhang Y, Larcher KM-H, Misic B, Dagher A (2017) Anatomical and functional organization of the human substantia nigra and its connections Johansen-Berg H, ed. Elife 6:e26653.

Cerebellar single-pulse TMS differentially affects early and late error processing in reinforcement learning

Dana M. Huvermann[*,1,2,3], Adam M. Berlijn[*,1,3,5], Stefan J. Groiss[3], Manfred Mittelstaedt[1], Alfons Schnitzler[3,4], Christian Bellebaum[1], Martina Minnerop[3,4,5], Dagmar Timmann[2], Jutta Peterburs[1,6]

[1]Faculty of Mathematics and Natural Sciences, Heinrich Heine University Dusseldorf, Dusseldorf, Germany

[2]Department of Neurology and Center for Translational and Behavioral Neurosciences (C-TNBS), Essen University Hospital, University of Duisburg-Essen, Essen, Germany

[3]Institute of Clinical Neuroscience and Medical Psychology, Medical Faculty & University Hospital Düsseldorf, Heinrich-Heine University Düsseldorf, Düsseldorf, Germany

[4]Department of Neurology, Center for Movement Disorders and Neuromodulation, Medical Faculty, Heinrich-Heine University Düsseldorf, Düsseldorf, Germany

[5]Institute of Neuroscience and Medicine (INM-1), Research Centre Jülich, Jülich, Germany

[6]Institute for Systems Medicine & Department of Human Medicine, MSH Medical School Hamburg, Hamburg, Germany

Corresponding author: dana.huvermann@hhu.de, +49 211 81-12268

*Shared first authorship

Department of Experimental Psychology

Heinrich-Heine-University Düsseldorf

Universitätsstraße 1, 40225 Düsseldorf, Germany

Abstract

There is increasing evidence that the cerebellum contributes to feedback processing in reinforcement learning. As yet, it has not been investigated whether the cerebellum also contributes to error processing in reinforcement learning. Studies have shown, however, that the cerebellum is involved in the processing of response errors in non-reinforcement learning contexts, e.g., in response conflict tasks. In the present study, we aimed to extend these findings to the processing of response errors, which slowly emerges as a result of reinforcement learning. To this end, we inhibited the cerebellum via single-pulse transcranial magnetic stimulation (spTMS) and recorded cerebral electroencephalography (EEG) measures associated with error processing. If input from the cerebellum is required for error processing, error-correct differentiation should be decreased for cerebellar compared to vertex (control) stimulation. Cerebellar spTMS was applied and EEG was recorded while healthy adults performed a probabilistic feedback learning task. The error-related negativity (ERN), a component in the response-locked event-related potential (ERP), was used as a measure of error processing. It reflects a rapidly detected mismatch between representations of the actual and the desired response and is typically larger for errors than correct responses. Error-correct differentiation in the ERN was diminished for cerebellar compared to control TMS. However, increased error-correct differentiation was found in a later ERP component, the error positivity (Pe), which is more strongly associated with error awareness. Cerebellar spTMS thus impaired fast error processing reflected in the ERN and facilitated later, conscious error processing reflected in the Pe. These findings provide causal evidence of cerebellar contributions to error processing within reinforcement learning.

Impact statement

This study showed that single-pulse-TMS-induced disruption of cerebellar function alters cerebral error processing as captured in the error-related negativity (ERN). These results align with prior research on impaired error processing in patients with cerebellar damage during response inhibition tasks and extend this evidence towards reinforcement learning contexts. Our findings further add to a growing body of evidence relating the cerebellum to reinforcement learning, influencing both error and feedback processing.

Key words: cerebellum, performance monitoring, cognitive control, reinforcement learning, single-pulse transcranial magnetic stimulation, ERP, ERN

Introduction

Understanding how organisms optimise their behaviour in dynamic environments is crucial not only to improve learning processes but also to advance our understanding of disorders associated with maladaptive learning, such as addiction and depression (1,2). Reinforcement learning is a basic form of learning in which behaviour is shaped by its consequences/outcomes, i.e., rewards that reinforce and punishments that inhibit a specific behaviour (3). Initially, in an unfamiliar context, information about actions and outcomes must be gathered on a trial-and-error basis. With learning, actions are then chosen based on their predicted outcomes. Learning success thus strongly depends on the accuracy of outcome predictions. While improving these predictions, the individual gets a better understanding of which action is correct and which is false. Ultimately, the individual is able to identify an error already at the stage of action execution, rather than having to wait for external feedback/the outcome. This shift from outcome-level processing to response-level processing underlying the distinction between right and wrong responses throughout the learning process could be shown in a reinforcement learning task by recording brain activity using electroencephalography (EEG; 4,5).

Processing of both actions/responses and outcomes has been predominantly linked to structures in the fore- and midbrain (6). In EEG studies, error processing has been shown to emerge with learning/task progression when an understanding of correct and false responses has been developed (4,5,7). In later stages of a learning task, a more pronounced negative deflection in the response-locked signal is typically found for errors relative to correct responses (4,5,7), i.e., the error-related negativity (ERN; 8,9). The ERN has a frontocentral scalp distribution and typically peaks within 100 ms post-response. Its origin lies primarily in the anterior cingulate cortex (ACC, 10–12, but also

see 13) which has been associated with error processing (14). The ERN is followed by the more posterior error positivity (Pe, peaking 200-400 ms post-response, 8,15). ERN and Pe have been proposed to be functionally distinct (15), with the ERN reflecting a fast-paced mismatch between the actual and desired response (16,17), and the Pe reflecting more conscious error processing (17,18). On the other hand, feedback processing, as reflected in the feedback-related negativity (FRN), is typically found at early stages of reinforcement learning where participants strongly depend on the external feedback to perform the task accurately (4,5,7). The FRN has been described as a functional equivalent of the ERN during feedback processing, as both seem to contribute towards an adjustment of behaviour towards error correction (19). In addition, there seems to be a high overlap in topography and neural generators (19–21).

Interestingly, recent studies in rodents (22) and humans (23–25) have provided evidence for a potentially supportive role of the cerebellum in feedback processing during reinforcement learning (26). The cerebellum is best known for predictive processes in the context of motor control (27) but in the last decades increasingly also for cognitive processes (28,29). The cerebellum is thought to support both motor and cognitive function by predicting outcomes via internal forward models (27,30,31), connecting with a wide range of cerebral brain areas, including the ACC, in a closed-loop fashion (32–37). Cerebellar dysfunction might thus influence feedback processing as reflected in the FRN via maladaptive support of ACC function. Indeed, in recent studies (23,25), we found that cerebellar lesions, degeneration, and TMS disrupted feedback processing in the sense that the prediction error was not represented in the FRN.

111 These previous studies (23–25) have focussed on the role of cerebellum at the
112 outcome stage. However, prediction at the response stage (i.e., error processing), as
113 described above, is also a prominent part of reinforcement learning. Cerebellar
114 damage and disruption of cerebellar function by non-invasive brain stimulation have
115 already been associated with deficits in error processing in response conflict tasks (38–
116 41). Specifically, differentiation between errors and correct responses in the ERN was
117 consistently reduced for cerebellar dysfunction (38–40, only on trend level in 41). For
118 the Pe, findings are more heterogeneous, with most studies not finding effects of
119 cerebellar dysfunction, except for one study in cerebellar post-acute stroke which
120 showed increased error-correct differentiation that was interpreted as compensatory
121 for deficient error processing in ERN (38). Response conflict tasks, however, contain
122 no feedback and can instead be performed based on the initial instructions. For
123 example, in a flanker task, participants need to indicate the direction of a central arrow
124 in the presence of flanking arrow. Predictions thus do not evolve slowly with learning
125 as in reinforcement learning.

126 In summary, previous studies support a cerebellar role in outcome processing in
127 reinforcement learning and error processing in response conflict tasks. This is
128 consistent with the proposed role of the cerebellum in performance monitoring, i.e., in
129 functions which support adaptive behaviour, to which both reinforcement learning and
130 error processing contribute (26). Error and feedback processing are closely
131 intertwined, and it seems conceivable that in reinforcement learning tasks, disrupted
132 feedback processing (on which participants rely in particular early in the task) as
133 caused by cerebellar dysfunction leads to changes in error processing (which emerges
134 later in the task, with learning from feedback). These changes may be similar to those

found for error processing under cerebellar dysfunction in response conflict tasks (38–41).

In the current study, we aimed to examine if aberrant feedback processing in cerebellar dysfunction transfers to the response phase with learning progression in a reinforcement learning task. We disrupted cerebellar function by non-invasive brain stimulation in young adults. Single-pulse TMS (spTMS) excites the subjacent neuronal populations followed by a prolonged period of reduced activity (42), potentially leading to inhibition or facilitation depending on various factors including stimulation site and timing (43,44). For cerebellar stimulation, an inhibitory effect of spTMS on cortical function is mostly assumed (45–47, but also see 48, for a review see 49). We analysed data from a previous study by our group (23) which were collected in young, healthy adults who received cerebellar spTMS while performing a probabilistic feedback learning task with trial-by-trial feedback. Importantly, overall learning performance was not affected by the TMS, in theory enabling error processing as the task progresses and learning takes place (4,5,7). ERN and Pe were analysed as EEG indices of error processing. In accordance with previous work in response conflict tasks (38–40), we expected to see reduced or absent error-correct differentiation in the ERN for cerebellar TMS (12, but also see 28). We expected to see this effect more strongly later in the task when response-outcome contingencies have been learnt and error processing is more pronounced (4,5,7). However, we did not expect to see distinct compensatory mechanisms indexed by an increased Pe as observed in cerebellar stroke patients (38) due to the immediate effect of spTMS. Two stimulation timings were used, to differentiate direct disruption of error processing (via post-stimulus/pre-response TMS) from indirect effects of disrupted feedback processing on error processing (pre-feedback TMS) due to maladjusted predictive processes.

In line with the hypotheses, we found decreased error-correct differentiation in the ERN for cerebellar TMS. In addition, error-correct differentiation in the Pe was increased for cerebellar stimulation while behavioural performance was overall preserved.

Material and Methods

The present study was part of a larger investigation of cerebellar contributions to reinforcement learning and presents novel, follow-up analyses of data reported previously by our group (23). There, we focused on outcome/feedback processing and thus did not analyse response-locked ERPs. We performed two studies on reinforcement learning, one with cerebellar stroke patients and respective controls, the other with healthy adults using cerebellar (vs. vertex) spTMS. The present work is focused on the spTMS study, because older adults typically show only weak error-correct differentiation in the response-locked ERP in reinforcement learning (4,7,50). However, analogous analyses were also performed for data from the patient study and are provided in Supplementary Analysis S1.

Participants

Sample characteristics are detailed in Huvermann et al. (23). Data from 24 healthy participants (7 men, 17 women; mean age 23.3 years, *SD* = 2.9 years, age range 19 to 30 years) entered the analyses. According to Edinburgh Handedness Inventory (51) scores, 20 participants were right-handed, two left-handed, and two ambidextrous.

All participants gave written informed consent prior to participation. The study was conducted in accordance with the ethical principles for medical research involving human subjects outlined in the Declaration of Helsinki and approved by the Ethics Committees at the Faculty of Medicine of Heinrich-Heine-University Düsseldorf (2018-240_1) and the University Hospital Essen (18-8477-BO).

Procedure

Please see Huvermann et al. (23) for a detailed description. In brief, cerebellar and vertex TMS took place in separate sessions at least 48 hours apart to decrease

repetition effects in the task. After EEG and EMG preparations and motor threshold estimation, the double cone TMS coil was positioned and secured to the participant's head (see Figure 1). Before and after the experimental task, an additional cognitive task was performed for which results are reported in Berlijn et al. (40).

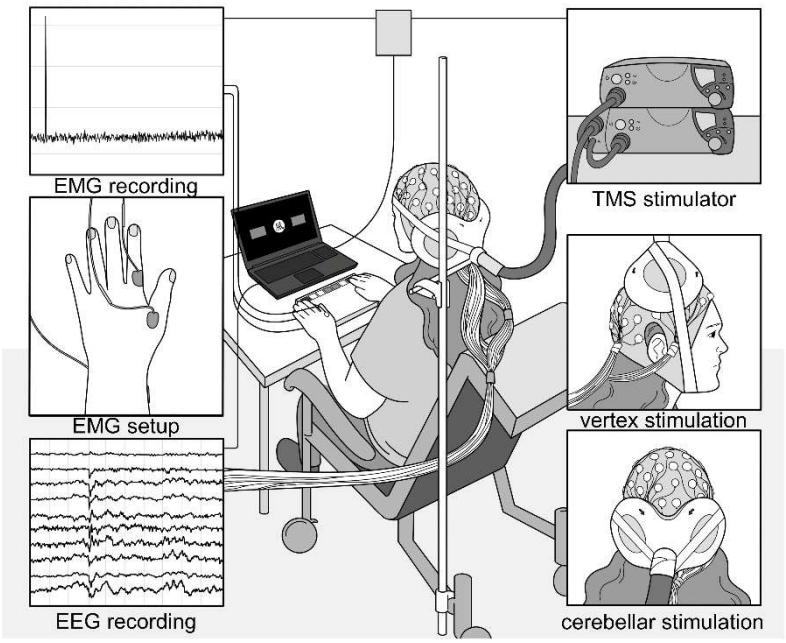

Figure 1. Experimental setup. Depending on session, TMS was applied to either the left cerebellum (1 cm down and 3 cm to the left of the inion) or vertex using a double cone coil. EEG and EMG were recorded simultaneously.

Participants completed a probabilistic feedback learning task (4,5). Figure 2 illustrates the sequence and time course of stimulus presentation in each trial. The task consisted of 6 blocks of 56 trials, thus 336 trials in total. Each trial began with a fixation cross, followed by one of four stimuli (Chinese characters). Participants responded by pressing the left or right button on a response box within a response window of 1000 ms. Choices were highlighted on the screen, followed by a black screen before feedback was displayed, with "+20ct" in green font as positive feedback or "-10ct" in red font as negative feedback. Two stimuli were linked to random feedback (50% positive and 50% negative, independent of response), while the other two stimuli were

linked to contingent feedback. Here, correct responses were followed by positive feedback in 80% of the cases and by negative feedback in 20% of the cases (vice versa for errors). Contingencies could thus be learnt. TMS was delivered 100 ms post-stimulus for one stimulus and 100 ms pre-feedback for the other.

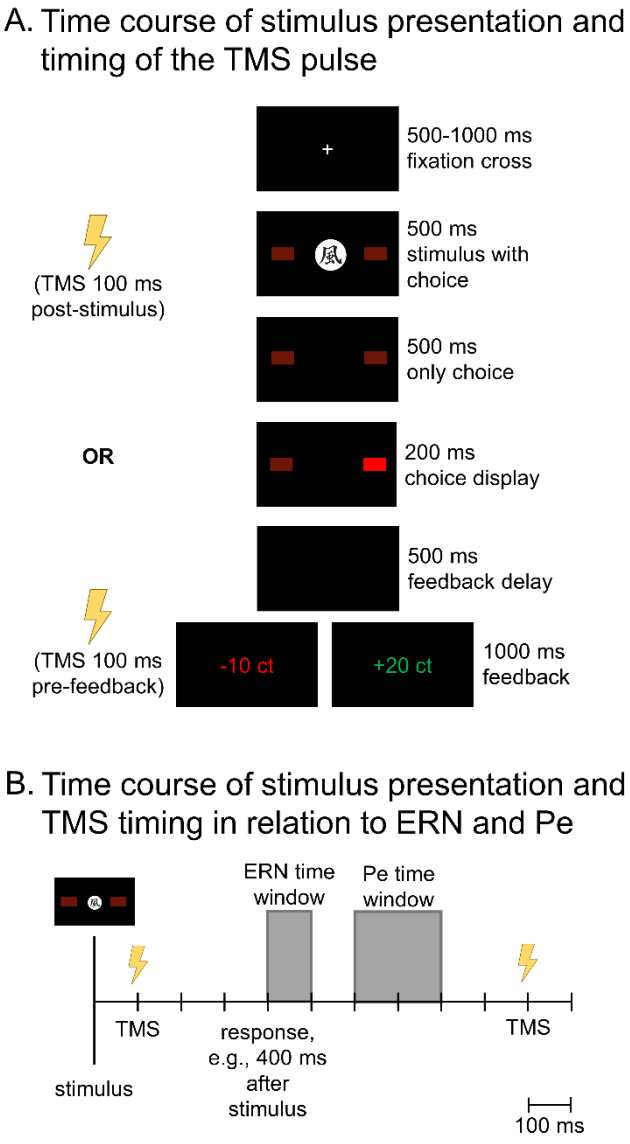

Figure 2. Time course in one trial in the experimental task. A. Time course of stimulus presentation and timing of TMS pulses in one trial in the experimental task. First, a fixation cross was presented for 500-1000 ms. Subsequently, one of four stimuli was presented for 500 ms together with flanking rectangles representing the response options. Participants responded by pressing the left or right button on a response pad up until 500 ms after the stimulus was presented. The respective rectangle was highlighted for 200 ms. After 500 ms of blank screen, positive ('+20 ct') or negative feedback ('-10 ct') was presented for 1000 ms. Participants had to learn by trial and error which of the two options was more likely to result in positive/negative feedback, separately for each of the four stimuli. Feedback for two stimuli had an 80 % contingency, and a 50 % contingency for the other two. Stimulation in a particular

trial was applied either 100 ms post-stimulus or 100 ms pre-feedback. The task consisted of 336 trials. B. Time course of stimulus presentation and timing of TMS pulse in relation to ERN and Pe time windows in one trial in the experimental task. ERN was quantified in the time window between 0 and 100 ms following response while Pe was quantified in the time window between 200 and 400 ms following response. Distance to the post-stimulus TMS pulse thus differed and depended on response time in the respective trial, while the pre-feedback TMS pulse always occurred after ERN and Pe. Note that the TMS pulse in a particular trial was given either post-stimulus or pre-feedback.

TMS was applied at 120% of motor threshold using a Magstim Double Cone Coil and a Magstim BiStim^2 unit (Magstim Co., Whitland, United Kingdom). A fast-paced task flow was enabled by alternating stimulation between two Bistim units. Stimulation was applied either to the left lateral cerebellum (1 cm below and 3 cm to the left of the inion; confer 52–54) or position vertex as a control site (at electrode position Cz, 55,56). Stimulation of the left cerebellar hemisphere is consistent with its implication in processing of visual-spatial information (57) and stronger activations of the left hemisphere in a previous fMRI study using a similar feedback learning task (58). Following spontaneous reports of side effects in the initial testing sessions, a post-experimental questionnaire was introduced in which participants were asked to rate symptoms associated with TMS (see ref. 23 for more details). No significant differences between vertex and cerebellar stimulation were observed regarding headaches, neck pain, toothaches, inattentiveness, discomfort, phosphenes ratings, or free field responses for other symptoms (all $p \geq .343$, see Figure 3).

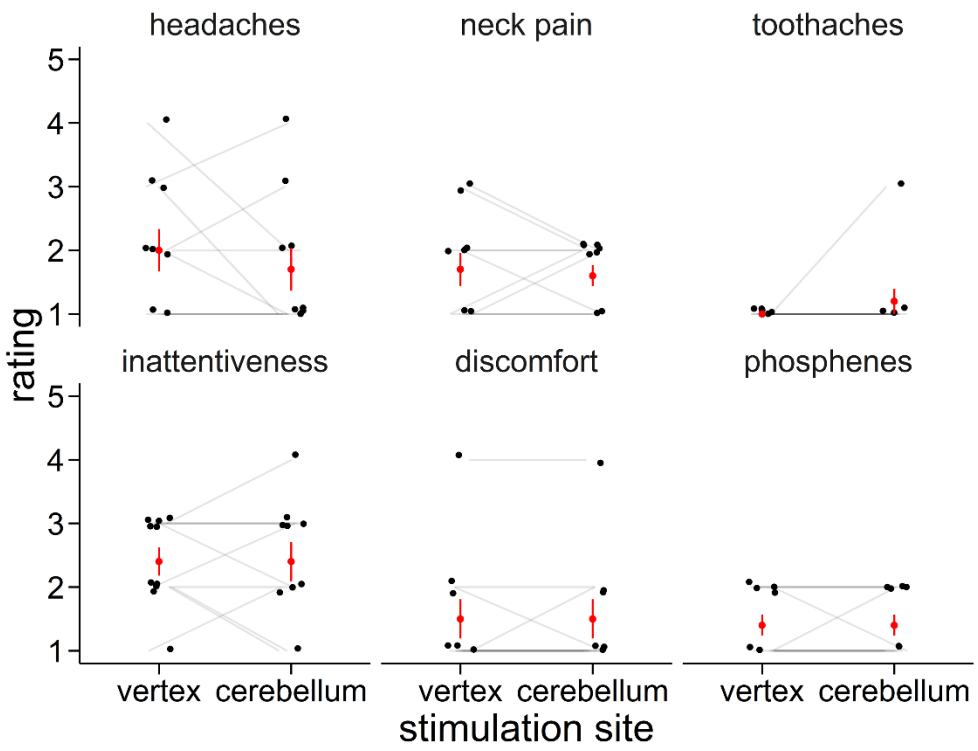

Figure 3. Ratings of side effects in the post-experimental questionnaire, as reported in Huvermann et al. (23). Means and standard errors are shown in red, individual ratings are shown in black.

EEG recording and preprocessing

Data were recorded at 1,000 Hz from 30 passive Ag/AgCl Multitrode electrodes positioned in the 10-20 system (59), using BrainAmp MR amplifier and BrainVision Recorder 1.21 (Brain Products GmbH, Gilching, Germany). Impedances were kept below 5 kΩ.

For preprocessing, the ARTIST algorithm by Wu et al. (60) based on EEGLAB (v2022.1; 61) was used. This algorithm decreases artefacts in the EEG signal caused by TMS pulses (see ref. 23 for a detailed description of preprocessing procedures).

Using Brainvision Analyzer 2 software (version 2.2, Brain Products GmbH, Gilching, Germany), data were segmented around responses, starting 200 ms before and ending 500 ms after the response. Next, a baseline correction was performed using

the time window from 200 to 100 ms before response onset. Data were then exported for further processing in MATLAB. Although data were analysed on a single-trial basis, we additionally averaged the data according to conditions (stimulation site, TMS timing, response type) to extract peak latencies of the ERP components of interest (described below). Only trials for stimuli with learnable contingencies (i.e., 80-20) were included.

Peak detection was performed on the averaged data and separately for each condition for the ERN and Pe using MATLAB. The time windows and electrode sites that had been pre-registered based on previous related studies (38–41) were used. For the ERN, peak detection was performed at FCz in the time window starting at response onset and ending 100 ms thereafter. For the Pe, we used the maximal positive peak within the time window between 200 and 400 ms at Pz. For the single-trial data, the mean amplitude in a time window around the respective latency determined by the peak detection on the averaged data for each condition was extracted (20 ms for ERN; 40 ms for Pe, 62,63).

Statistical data analysis

Data were analysed in R (version 4.2.3, 64) using RStudio (version 2023.3.0.386, 65). Analyses of accuracy and choice switching (i.e., choosing a different response than before following e.g., positive/negative feedback) are reported in Huvermann et al. (23). As data was not clearly separable into pre- and post-learning for a majority of participants, we opted for a single trial-based analysis approach using linear mixed effects (LME) models including the trial-by-trial factor trial number, thus capturing the course of error-correct differentiation across the experiment. This also overcame a common concern of unequal numbers of trials for errors and correct responses as well as (too) few error trials per condition (66–68) due to learning throughout the task. Exclusion of participants with too few error trials would systematically exclude good

learners (69) and including an equal number of trials in the analysis does not salvage the concern (70). Multilevel approaches using single-trial data, however, overcome these limitations by taking into account different numbers of data points per factor level and being relatively robust to large numbers of missing data points (69,71,72).

The packages lme4 (version 1.1-32, 73) and lmertest (version 3.1-3, 74) were used for LME modelling. We used restricted maximum likelihood with *p*-values computed using Satterthwaite approximation to evaluate significance, following Luke (75). Participants with a Cook's distance (76) above 4/(*n*-*p*-1) were identified as outliers (using the influence.ME package, version 0.9-9, 77). We strived for a maximal random effects structure but in case of singular fit gradually reduced random effects starting with main effects and then lower-grade interactions until fit was ensured. Significant interactions were followed up using simple slope analyses (interactions package, version 1.1.5, 78). *P*-values were Bonferroni-corrected according to the number of simple slopes.

LME analyses were conducted with the categorical fixed effects response type (-0.5: error, 0.5: correct), stimulation site (-0.5: vertex, 0.5: cerebellum), TMS timing (-0.5: post-stimulus, 0.5: pre-feedback), and the continuous factor trial number, which was scaled via the built-in *scale* function. We also included all interactions of these factors as fixed effects. No participants were identified as outliers based on Cook's distance. The model equation for both ERN and Pe was as follows:

$$ERN/Pe \sim 1 + response\ type * TMS\ condition * TMS\ timing * trial\ number\ +$$

$$(1 + response\ type{:}TMS\ condition{:}TMS\ timing{:}trial\ number \mid subject)$$

Note that we also performed a complementary analysis using action value modelling, as commonly conducted for analyses involving prediction error modelling in reinforcement learning contexts (see e.g., 79,80). Analyses involved a new measure,

Q_{diff}, which reflects the relative subjective action value (action value of the unchosen choice subtracted from the action value of the chosen option). It should thus offer a better measure for subjective error processing than the objective response type (see Supplementary Analysis S2 for further details), especially because, due to the probabilistic nature of our task, errors and correct responses are not as clearly defined as in response-conflict tasks. Relative action values have been shown to be more reliable than absolute action values (81), although the procedure of action value/prediction error estimation in general has been shown to be highly correlated to subjective measures (80).

Results

Accuracy

While a main effect of block, i.e., a general learning effect, was found ($F(3.18, 73.05) = 6.21$, $p < .001$), no differences between cerebellar and vertex TMS emerged, $p \geq .461$. These results indicate that error rates decreased over the course of the task and were not affected by cerebellar TMS. On average, 9.6 errors per block, stimulation site, and participant were committed ($SD = 4.4$ errors). The full results concerning accuracy are reported in Huvermann et al. (23).

ERN – effects of response type (error/correct)

Grand averages for the ERPs at FCz time-locked to individual ERN latencies for correct responses and errors (i.e., response type) according to stimulation site, TMS timing, and trial number (early, late experiment) are provided in Figure 4A.

The ERN was more negative for errors compared to correct responses ($\beta = 0.81$, $SE = 0.16$, $t(7451.23) = 4.94$, $p < .001$). This effect was further modulated by trial number ($\beta = 0.51$, $SE = 0.16$, $t(7394.78) = 3.22$, $p = .001$). While response types did not differ

in ERN amplitude early on (β = 0.29, *SE* = 0.22, *t* = 1.30, *p* = .386), errors as compared to correct responses were associated with increased negativity late in the task (β = 1.35, *SE* = 0.24, *t* = 5.75, *p* < .001).

Importantly, this interaction was further modulated by stimulation site (β = -0.80, *SE* = 0.32, *t*(7431.03) = 2.53, *p* = .012; see Figure 4B). Follow-up simple-slope analyses showed that for both cerebellar and vertex TMS, response types were not distinguished in the ERN early in the task (both *p* ≥ .453). However, late in the task, the ERN was more pronounced for errors than correct responses for vertex TMS (β = 1.94, *SE* = 0.32, *t* = 6.01, *p* < .001) but not for cerebellar TMS (β = 0.75, *SE* = 0.34, *t* = 2.22, *p* = .106).

Additionally, a trend-level interaction between response type, stimulation site, and TMS timing emerged (β = 1.22, *SE* = 0.65, *t*(7448.34) = 1.88, *p* = .060; see Supplementary Figure S1 for the slope plots). Descriptively, response types were distinguished in the ERN for vertex TMS and pre-feedback cerebellar TMS but not when stimulating the cerebellum post-stimulus.

Complete inferential statistics are provided in Supplementary Table S1. Effects that include the TMS timing factor independent of stimulation site are reported in Supplementary Analysis S3.

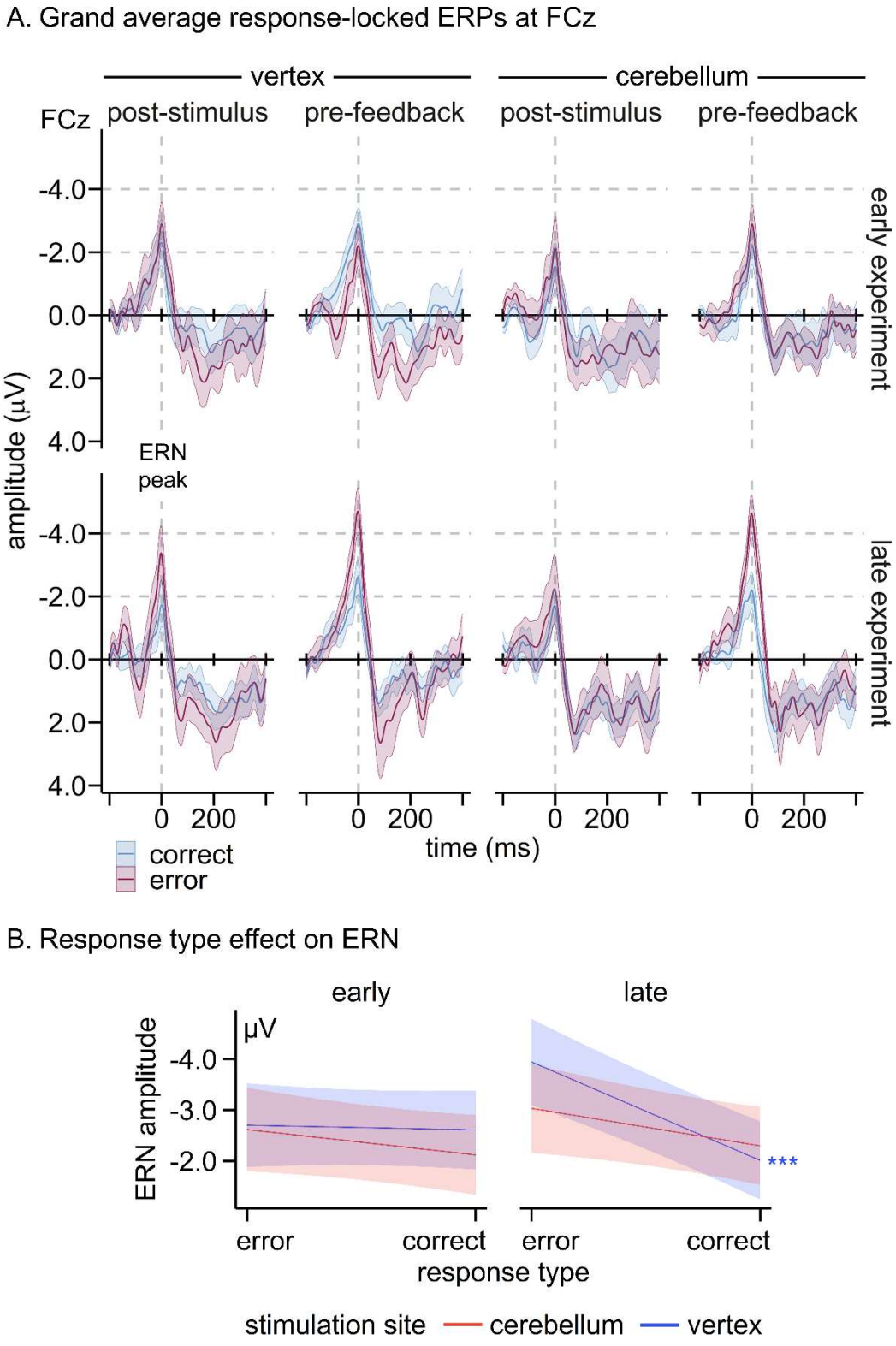

Figure 4. A) Grand-average ERPs at FCz locked to individual ERN latencies per condition (response type × stimulation site × TMS timing): early and late in the task according to response type (correct, error), stimulation site (cerebellum, vertex), and TMS timing (post-stimulus, pre-feedback). Blue lines denote correct responses, red lines errors. Coloured bands display standard errors. See Supplementary Figure S2 for a response-locked grand-average ERP. B) Slope estimates for ERN amplitude predicted by response type and modulated by stimulation site and trial number (early, late experiment). Red lines denote cerebellar stimulation and blue lines vertex stimulation. Coloured bands indicate 95 % confidence intervals. * $p < .05$. ** $p < .01$. *** $p < .001$. $n_{error} = 2702$, $n_{correct} = 4777$.

Pe – effects of response type (error/correct)

Grand averages for the response-locked ERPs at Pz for correct responses and errors (i.e., response type) according to stimulation site, TMS timing, and trial number (early, late experiment) are provided in Figure 5A.

The Pe was more pronounced for errors compared to correct responses (β = -0.99, *SE* = 0.15, $t(7848.81) = 6.68$, $p < .001$), and late compared to early in the experiment (β = 0.24, *SE* = 0.07, $t(7734.12) = 3.37$, $p = .001$).

Importantly, the effect of response type was modulated by stimulation site and TMS timing (β = 2.07, *SE* = 0.58, $t(7855.11) = 3.55$, $p < .001$; see Figure 5B). Post-hoc simple slope analyses showed that the Pe differentiated errors and correct responses for vertex TMS applied both pre-feedback (β = -0.76, *SE* = 0.29, $t = 2.63$, $p = .034$) and post-stimulus (β = -0.74, *SE* = 0.29, $t = 2.54$, $p = .044$). For cerebellar TMS, Pe amplitudes did not differ between errors and correct responses when TMS was applied pre-feedback (β = 0.20, *SE* = 0.29, $t = 0.70$, $p > .999$). However, a strong response type effect emerged for cerebellar TMS applied post-stimulus (β = -2.25, *SE* = 0.30, $t = 7.58$, $p < .001$), with more positive amplitudes for errors compared to correct responses. To check whether this response type differentiation in the Pe for post-stimulus TMS was truly stronger for cerebellar compared to vertex TMS, we checked the interaction effect (stimulation site × response type) for post-stimulus TMS trials via simple slope analysis, which proved to be significant (β = -1.51, *SE* = 0.41, $t(7835.18) = 3.64$, $p < .001$). Notably, the interaction effect did not reach significance for pre-feedback TMS trials (β = 0.55, *SE* = 0.41, $t(7838.69) = 1.34$, $p = .182$), indicating that the differences within post-stimulus TMS were more decisive for the triple interaction.

Complete inferential statistics can be found in Supplementary Table S2. Effects that include the TMS timing factor independent of stimulation site are reported in Supplementary Analysis S3.

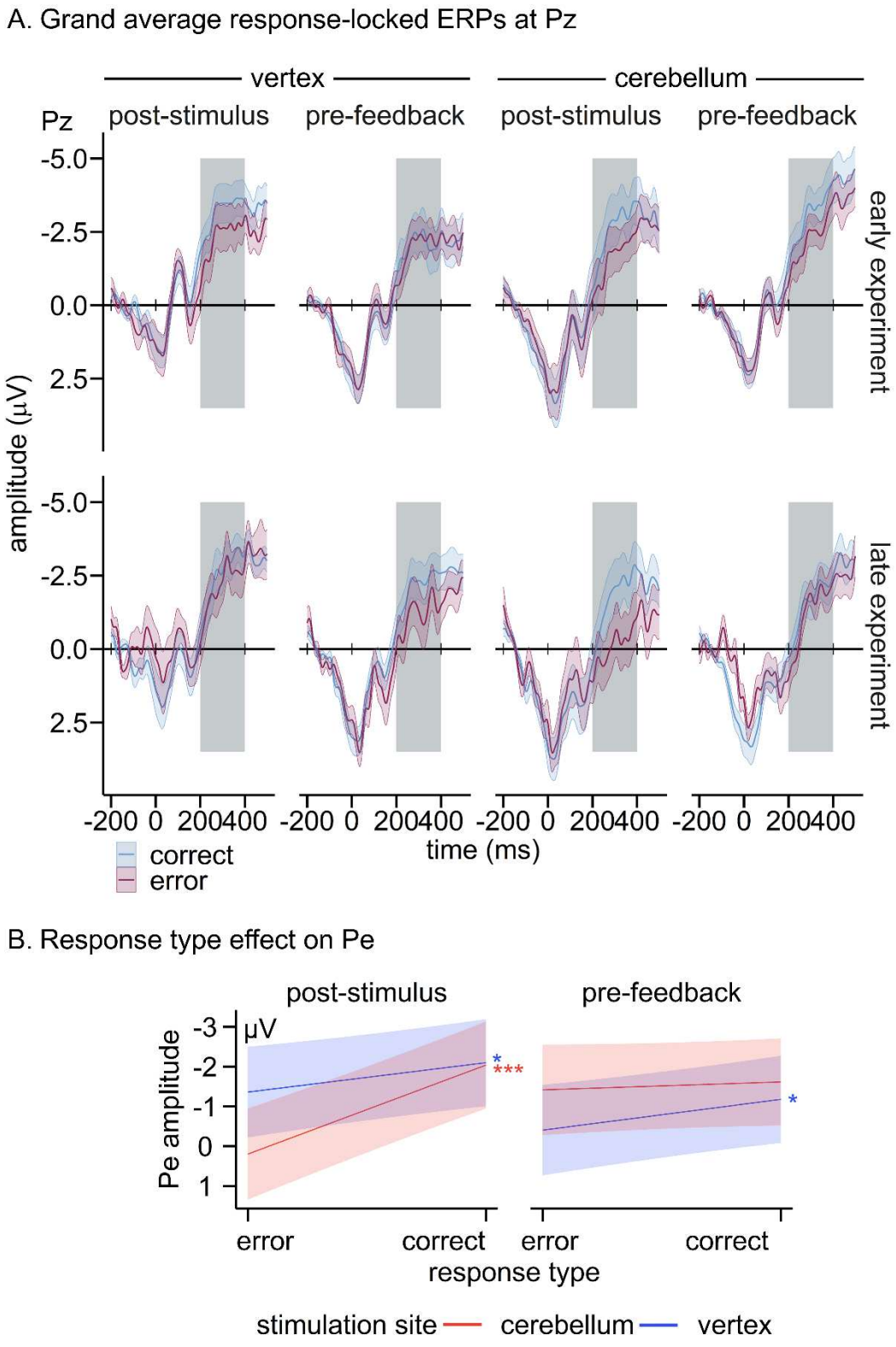

Figure 5. A) Grand-average response-locked ERPs early and late in the task at Pz according to response type (correct, error), stimulation site (cerebellum, vertex) and TMS timing (post-stimulus, pre-feedback). Blue lines denote correct responses, red lines errors. Coloured bands display standard errors. B) Slope estimates for Pe amplitude predicted by response type and modulated by stimulation site and TMS timing. Red lines denote cerebellar stimulation and blue lines vertex stimulation. Coloured bands indicate 95 % confidence intervals. * $p < .05$. ** $p < .01$. *** $p < .001$. $n_{error} = 2769$, $n_{correct} = 5122$.

Control analysis – predictability of Pe by ERN

In an additional analysis we explored whether the effects of spTMS in ERN and Pe were separate effects or whether spTMS only had an effect on ERN which in turn influenced Pe amplitude. The amplitudes of ERN and Pe correlated significantly with each other (r = -0.04, $t(7477) = 3.35$, $p < .001$), although the correlation strength was very low (82–85). To check whether the pattern in the Pe is explainable by ERN amplitudes without considering TMS effects, we fitted two additional models: one with the factors response type, trial number, and ERN amplitude (thus disregarding effects of the TMS), and one with the factors response type, trial number, stimulation site, TMS timing, and ERN (thus including both the effects of TMS and ERN). Both models included all interaction terms in the fixed effects. The model including the TMS effects provided a better fit ($X^2(16) = 116.7$, $p < .001$) and the triple interaction between response type, stimulation site, and TMS timing remained significant even when ERN was included as an additional factor ($\beta = 2.64$, $SE = 0.65$, $t(7429.14) = 4.05$, $p < .001$). To examine whether, conversely, the ERN amplitude adds information to the analysis of the Pe, we compared the original model to the model with the ERN as an additional factor. The model fit improved when adding the ERN ($X^2(16) = 72.60$, $p > .001$), indicating that the ERN amplitude does explain variance in the Pe amplitude that cannot be explained solely by the other factors. We did not perform the same analysis with ERN amplitude as dependent and Pe as independent variable as the Pe occurs after the ERN, preventing effects of the Pe onto the ERN (at least within the same trial).

While we used the objective correctness of the responses as predictor in these analyses (i.e., response type), subjective perception of which action is better/worse might have differed from this, especially considering that responses were associated

with outcomes over time in the experiment, that not all participants learnt the contingencies and that errors and correct responses were not as clearly defined as in response-conflict tasks due to the probabilistic nature of action-outcome associations. We therefore conducted an additional analysis using a measure that reflects the subjective, relative, instead of objective valuation of the chosen option. We computed the Q_{diff}, i.e., the modelled subjective value of the unchosen option subtracted from the value of the chosen option (see Supplementary Analysis S2). This measure thus reflects to what degree the chosen option was perceived as the better/worse option, thereby reflecting intra- and interindividual differences in learning and action-outcome representation (81). Importantly, this analysis yielded a comparable result pattern (see Supplementary Analysis S2).

Discussion

In the present study, healthy young adults learnt stimulus-response-feedback associations while single-pulse TMS (spTMS) was applied to the cerebellum or a control site (vertex) either post-stimulus (i.e., pre-response) or pre-feedback. Response-related ERP components (ERN and Pe) were analysed to investigate whether cerebellar output was necessary for error processing in the forebrain during reinforcement learning. Given that feedback processing during reinforcement learning was compromised in cerebellar dysfunction (23), we expected aberrant error processing for cerebellar TMS. Results in the current study indicate that this is likely the case: Error-correct differentiation in the ERN was blunted by cerebellar TMS, while being intact for vertex TMS. Error-correct differentiation in the Pe, on the other hand, was unexpectedly enhanced for post-stimulus cerebellar TMS.

Consistent with patterns observed in patients with cerebellar damage/dysfunction in a response conflict task (i.e., reduced error-correct differentiation in the ERN, 38–40), we found reduced error-correct differentiation in the ERN under cerebellar spTMS. However, the overall result pattern with *unaffected* reinforcement learning (24,86), *reduced* error-correct differentiation in the ERN, and *increased* error-correct differentiation in the Pe (38) resembled results observed in patients with cerebellar stroke. The consistency in results between reinforcement learning and response conflict tasks suggests that the cerebellum is involved in error processing in both task contexts in a similar way, in line with its proposed function in performance monitoring (26). Of note, long-term compensation and/or functional reorganisation in stroke recovery have been proposed to support preserved task performance for these patients in a response conflict task (38). Such effects were previously not observed in patients with progressive cerebellar degeneration who showed an *altered* ERN,

459 *increased* error rates, but *unchanged* Pe in a response conflict task (39). For the
460 present study, we had expected that cerebellar spTMS disrupts cerebral processing
461 instantaneously (42). Long-term compensation should therefore not be relevant.
462 Instead, increased error-correct differentiation in the Pe in the presence of reduced
463 differentiation in the ERN was observed instantaneously, giving rise to questions on
464 the underlying mechanisms.

465 First, it is debatable whether the observed pattern truly represents a compensatory
466 mechanism, or whether the increased differentiation in the Pe could also be the result
467 of hypermetria. This might be the case in terms of a mismatch in salience which is one
468 parameter that correlates with Pe amplitude (87). Perceived error salience as
469 measured in the Pe might thus be larger than would be appropriate under cerebellar
470 compared to control spTMS. Dysmetria is a common deficit observed in cerebellar
471 disorders (88) and has also been suggested as a deficit in cognitive processes (89).
472 Future studies could test this by using different error severities/saliencies in their study.
473 An interpretation in terms of hypermetria would indicate that TMS affected ERN and
474 Pe separately from each other. While this might be the case, an indirect effect of TMS
475 on the Pe via the ERN is also conceivable. An additional control analysis indicated that
476 effects within the Pe amplitude are at least partially explainable by ERN amplitude. An
477 indirect effect of TMS on Pe via ERN would be more consistent with an interpretation
478 of the pattern in the Pe in terms of compensation. However, indirect effects via
479 propagation of the TMS stimulus to further brain areas within the same network, as
480 shown for repetitive TMS (90), could provide a further possibility.

481 While the ERN is generated mostly by the ACC (91–95,but also see 13), neural
482 generators for the Pe are less clear and appear not to be limited to the ACC (87,93).
483 This wider network might have allowed the Pe to be less or differently affected by

cerebellar spTMS effects, although more conscious error processing as reflected in the Pe may potentially be more effortful and slower. This unexpectedly increased error coding in the Pe might have compensated for deficits in the ERN, allowing unimpeded behavioural performance. Intact behavioural performance was previously not expected due to the instantaneous disruptive effect of spTMS, which in theory does not allow for long-term compensation as seen in stroke patients (38). Conversely, differences in properties of the underlying learning mechanism – potentially caused by the deficits in feedback processing/FRN – might have also resulted in differences in error processing later in the task, resulting in decreased use of systems underlying the ERN and increased reliance on systems underlying the Pe, eventually leading to more Pe-driven error processing. However, these differences in error processing might not always correspond to intact behavioural performance. Relying on later vs. earlier error processing (i.e., on the Pe instead of the ERN) could be unfavourable in everyday tasks that require swift processing, e.g., fast-paced sequences of responses like in sports or music. It is also possible that this potentially compensatory process is not available in all learning contexts, e.g., in more complex tasks. Notably, despite overall preserved learning performance, we did find decreased behavioural flexibility (choice switching; see ref. 23), in line with previous findings (86), which might be related to deficits in the ERN.

Concerning the type of cerebellar output essential for ERN but not Pe, our results do not offer a clear answer. In the present dataset, feedback processing was already shown to be impaired (23). This might have led to impaired adjustments of prediction, resulting in deficits in error processing at the subsequent response stage. However, the effect of cerebellar TMS on ERN and Pe only occurred for post-stimulus TMS (trend-level for ERN), which fits better with a perturbation of information processing

directly at the response stage. This will likely include predictive processes, as the ERN relies on this rapid matching of representations of the desired and the actual response based on internal information (i.e., an efference copy). The interaction between response type and stimulation in ERN was found only late during the experiment, which also supports predictive processes, as these predictions can only form throughout the learning process. Previous studies in healthy adults could show that error processing in ERN is stronger after learning, while before learning, feedback processing is more dominant (4,5,7). Perturbed predictive processes would also be consistent with the finding that stimulation timing did not appear to significantly affect feedback processing (23), as the predictive information is required for updating of predictions at the feedback stage. This mechanism might have affected feedback processing similarly to pre-feedback TMS. ERN and the FRN (96) are thought to share the ACC as neural generator (ERN: 10–12, FRN: 97–99), thus potentially being affected in a similar way. Considering the increased error-correct differentiation in the Pe as a compensatory process, two explanations are possible: The Pe, reflecting more conscious error processing (15,93), might either not rely as strongly on cerebellar information, or might also simply be outside the time window of the disruptive effect of the TMS pulse.

Of note, the Pe in our study is not as pronounced as the positive peaks typically found in response conflict paradigms. However, a distinction between errors and correct responses is visible, and a posterior positivity could also be shown in topographical plots of the difference signal for cerebellar post-stimulus TMS (Supplementary Figure S3). In two previous studies which examined the Pe in feedback learning paradigms, the Pe peak also seemed to be less prominent in the grand averages (100,101), which might be a characteristic of the Pe in reinforcement learning tasks. This might be due

to errors being more ambiguous in feedback learning tasks. However, the Pe is oftentimes not analysed in feedback learning tasks (4,5,7,50).

Finally, subjective perception of action values might differ from the objective classification as error/correct. An additional analysis based on action values (Qdiff; 81) yielded result patterns consistent with the original results for both ERN and Pe, with reduced Q_{diff} differentiation in ERN and increased Q_{diff} differentiation in Pe for cerebellar TMS. This demonstrates that the original findings extend to subjective perception of action value, which might be an interesting measure for future studies.

Limitations

We used an active control site (vertex TMS) instead of sham TMS. While vertex is a common control site in cognitive tasks (e.g., 102–104), at least one study (55) showed that vertex TMS reduced activity in the ACC, the likely generator of the ERN (10,91,92). While we used inverted stimulation which showed considerably less and non-significant ACC deactivation (55), and did not find abnormal ERN patterns during vertex stimulation, we cannot rule out that vertex stimulation affected processing. Unlike Jung et al. (55), we used a more deeply stimulating double cone coil instead of a figure-of-eight coil. Feedback-related ERP components with neural generators within the ACC seemed to be affected by vertex TMS (23). Unfortunately, there currently seems to be no well-tested, better suited site for control stimulation. Sham TMS does not seem ideal as it provides a very different experience regarding vibrations, coil clicks, and magnetic field build (105). Even though we assessed potential side effects of the TMS stimulation and found no significant differences between vertex and cerebellar stimulation (see Figure 3), we cannot exclude that other differences in experience of stimulation between the two sites that were not captured, such as stimulation of the neck muscles, emerged and contributed to the findings described

above. Future studies may want to include several control sites in between-subject designs.

Moreover, we only stimulated the left cerebellum. Given that a learning task was used, it was not feasible to repeat the task several times to incorporate other stimulation sites, as repetition effects would have predominated. Future studies should investigate the effect of spTMS on other cerebellar regions in feedback learning using between-subjects designs.

Last, stimulation was applied either 100 ms post-stimulus or 100 ms pre-feedback. There is currently no established time window of cerebellar-brain inhibition in the cognitive domain as available for the motor domain (106). Given that stimulation was applied 100 ms post-stimulus, it usually occurred several hundred milliseconds before the response. Berlijn et al. (40) varied stimulation timing around the ERN peak in a Go/NoGo flanker task and found that stimulation at or closely after the calculated peak latency, but not shortly before, decreased error-correct differentiation, showcasing time sensitivity of cerebello-cerebral communication in cognition. This might depend on the task at hand, as in the current study, stimulation before responses also led to altered error processing. Future studies need to explore these temporal dynamics in more detail, e.g., by implementing continuous manipulation of stimulation timings.

Conclusions

The present findings show that cerebellar TMS alters cerebral error processing in reinforcement learning. Error processing was decreased by cerebellar TMS in the ERN and increased in the Pe. This pattern closely resembles altered error processing in cerebellar stroke patients as shown in a previous study in a response conflict task. It remains unclear whether the increased Pe in concert with preserved behavioural performance reflects a compensatory process. Processing was affected more strongly

583 by stimulation closer in time to response execution (i.e., post-stimulus/pre-response).
584 Taken together, the present study adds to a growing body of evidence showing that
585 the cerebellum plays an important role in error processing and performance monitoring
586 in general, whereby it directly contributes to reinforcement learning and adaptive
587 control of behaviour.

588

Data and code availability: The experimental protocol was defined prior to experiments and preregistered to the open science framework (OSF, see https://doi.org/10.17605/OSF.IO/A24RG for the TMS study and https://doi.org/10.17605/OSF.IO/RD3XB for the patient study). Raw data used in the analysis is openly available at https://osf.io/9n7yp.

Funding: This work was supported by the German Research Foundation [Deutsche Forschungsgemeinschaft, DFG; grant number: 437661157, 2020] and the Bernd Fink-Foundation.

Disclosure of interest: none.

Ethics approval: The study was conducted in accordance with the ethical principles for medical research involving human subjects outlined in the Declaration of Helsinki and approved by the Ethics Committees at the Faculty of Medicine of Heinrich-Heine-University Düsseldorf (2018-240_1) and the University Hospital Essen (18-8477-BO).

CRediT: **DH**: Conceptualisation, Methodology, Software, Formal Analysis, Investigation, Data Curation, Writing – original draft, Visualisation, Project Administration. **AB**: Conceptualisation, Methodology, Software, Validation, Formal Analysis, Investigation, Data Curation, Writing – Review & Editing, Project Administration. **SG**: Conceptualisation, Methodology, Resources, Writing – Review & Editing, Supervision, Project Administration. **MMit**: Software, Resources, Writing – Review & Editing. **AS**: Resources, Writing – Review & Editing. **CB**: Conceptualisation, Methodology, Validation, Resources, Writing – Review & Editing, Supervision. **MMin**: Conceptualisation, Writing – Review & Editing, Supervision, Funding acquisition. **DT**: Conceptualisation, Resources, Writing – Review & Editing, Supervision, Funding acquisition. **JP**: Conceptualisation, Methodology, Validation, Resources, Writing – Review & Editing, Supervision, Funding acquisition.

614 *Acknowledgements*: We would like to thank Greta Wippich for drawing the
615 Experimental Procedure in Figure 1. We would also like to thank Petyo Nikolov for his
616 help with setting up the TMS and EMG.

617

References

1. Gueguen MC, Schweitzer EM, Konova AB. Computational theory-driven studies of reinforcement learning and decision-making in addiction: what have we learned? Curr Opin Behav Sci. 2021 Apr 1;38:40–8.

2. Chen C, Takahashi T, Nakagawa S, Inoue T, Kusumi I. Reinforcement learning in depression: A review of computational research. Neurosci Biobehav Rev. 2015 Aug 1;55:247–67.

3. Sutton RS, Barto AG. Reinforcement learning: An introduction. MIT press; 2018.

4. Eppinger B, Kray J, Mock B, Mecklinger A. Better or worse than expected? Aging, learning, and the ERN. Neuropsychologia. 2008 Jan 1;46(2):521–39.

5. Bellebaum C, Colosio M. From feedback- to response-based performance monitoring in active and observational learning. J Cogn Neurosci. 2014 Sep 1;26(9):2111–27.

6. Corlett PR, Mollick JA, Kober H. Meta-analysis of human prediction error for incentives, perception, cognition, and action. Neuropsychopharmacology. 2022 Jun 1;47(7):1339–49.

7. Pietschmann M, Simon K, Endrass T, Kathmann N. Changes of performance monitoring with learning in older and younger adults. Psychophysiology. 2008 Jul 1;45(4):559–68.

8. Falkenstein M, Hohnsbein J, Hoormann J, Blanke L. Effects of crossmodal divided attention on late ERP components. II. Error processing in choice reaction tasks. Electroencephalogr Clin Neurophysiol. 1991 Jun 1;78(6):447–55.

9. Gehring WJ, Goss B, Coles MGH, Meyer DE, Donchin E. A neural system for error detection and compensation. Psychol Sci. 1993 Nov 1;4(6):385–90.

10. Dehaene S, Posner MI, Tucker DM. Localization of a neural system for error detection and compensation. Psychol Sci. 1994;5(5):303–5.

11. Miltner WHR, Lemke U, Weiss T, Holroyd C, Scheffers MK, Coles MGH. Implementation of error-processing in the human anterior cingulate cortex: a source analysis of the magnetic equivalent of the error-related negativity. Biol Psychol. 2003 Oct 1;64(1):157–66.

12. Iannaccone R, Hauser TU, Staempfli P, Walitza S, Brandeis D, Brem S. Conflict monitoring and error processing: New insights from simultaneous EEG–fMRI. NeuroImage. 2015 Jan 15;105:395–407.

13. Herrmann MJ, Römmler J, Ehlis AC, Heidrich A, Fallgatter AJ. Source localization (LORETA) of the error-related-negativity (ERN/Ne) and positivity (Pe). Cogn Brain Res. 2004 Jul 1;20(2):294–9.

14. Hester R, Fassbender C, Garavan H. Individual Differences in Error Processing: A Review and Reanalysis of Three Event-related fMRI Studies Using the GO/NOGO Task. Cereb Cortex. 2004 Sep 1;14(9):986–94.

15. Wessel JR. Error awareness and the error-related negativity: Evaluating the first decade of evidence. Front Hum Neurosci. 2012;6:8.

16. Coles MGH, Scheffers MK, Holroyd CB. Why is there an ERN/Ne on correct trials? Response representations, stimulus-related components, and the theory of error-processing. Biol Psychol. 2001 Jun 1;56(3):173–89.

17. Nieuwenhuis S, Ridderinkhof KR, Blom J, Band GPH, Kok A. Error-related brain potentials are differentially related to awareness of response errors: Evidence from an antisaccade task. Psychophysiology. 2001/09/25 ed. 2001;38(5):752–60.

18. Ridderinkhof KR, Ramautar JR, Wijnen JG. To PE or not to PE: A P3-like ERP component reflecting the processing of response errors. Psychophysiology. 2009 May 1;46(3):531–8.

19. Gentsch A, Ullsperger P, Ullsperger M. Dissociable medial frontal negativities from a common monitoring system for self- and externally caused failure of goal achievement. NeuroImage. 2009 Oct 1;47(4):2023–30.

20. Holroyd CB, Coles MGH. The neural basis of human error processing: Reinforcement learning, dopamine, and the error-related negativity. Psychol Rev. 2002;109(4):679–709.

21. Potts GF, Martin LE, Kamp SM, Donchin E. Neural response to action and reward prediction errors: Comparing the error-related negativity to behavioral errors and the feedback-related negativity to reward prediction violations. Psychophysiology. 2011 Feb 1;48(2):218–28.

22. Kostadinov D, Häusser M. Reward signals in the cerebellum: Origins, targets, and functional implications. Neuron. 2022 Apr 20;110(8):1290–303.

23. Huvermann D, Berlijn A, Thieme A, Erdlenbruch F, Groiss SJ, Deistung A, et al. The cerebellum contributes to prediction error coding in reinforcement learning in humans. J Neurosci. 2025;e1972242025.

24. Rustemeier M, Koch B, Schwarz M, Bellebaum C. Processing of positive and negative feedback in patients with cerebellar lesions. The Cerebellum. 2016;15:425–38.

25. Berlijn AM, Huvermann DM, Bechler E, Thieme A, Schnitzler A, Bellebaum C, et al. Impaired reinforcement learning and coding of prediction errors in patients with cerebellar degeneration - a study with EEG and voxel-based morphometry. Cogn Affect Behav Neurosci. 2025;

26. Peterburs J, Desmond JE. The role of the human cerebellum in performance monitoring. Curr Opin Neurobiol. 2016 Oct 1;40:38–44.

27. Popa LS, Ebner TJ. Cerebellum, Predictions and Errors. Front Cell Neurosci. 2019;12:524.

28. Berlijn AM, Huvermann DM, Schneider S, Bellebaum C, Timmann D, Minnerop M, et al. The role of the human cerebellum for learning from and processing of external feedback in non-motor learning: A systematic review. The Cerebellum. 2024;23:1532–51.

29. Sokolov AA, Miall RC, Ivry RB. The Cerebellum: Adaptive Prediction for Movement and Cognition. Trends Cogn Sci. 2017 May 1;21(5):313–32.

30. Wolpert DM, Miall RC, Kawato M. Internal models in the cerebellum. Trends Cogn Sci. 1998;2(9):338–47.

31. Tanaka H, Ishikawa T, Lee J, Kakei S. The Cerebro-Cerebellum as a Locus of Forward Model: A Review. Front Syst Neurosci [Internet]. 2020;Volume 14-2020. Available from: https://www.frontiersin.org/journals/systems-neuroscience/articles/10.3389/fnsys.2020.00019

32. Ramnani N. Frontal lobe and posterior parietal contributions to the cortico-cerebellar system. The Cerebellum. 2012 Jun 1;11(2):366–83.

33. Schmahmann JD, Pandya DN. Anatomic organization of the basilar pontine projections from prefrontal cortices in Rhesus monkey. J Neurosci. 1997 Jan 1;17(1):438.

34. Glickstein M, May III JG, Mercier BE. Corticopontine projection in the macaque: The distribution of labelled cortical cells after large injections of horseradish peroxidase in the pontine nuclei. J Comp Neurol. 1985 May 15;235(3):343–59.

35. Kruithof ES, Klaus J, Schutter DJLG. The human cerebellum in reward anticipation and outcome processing: An activation likelihood estimation meta-analysis. Neurosci Biobehav Rev. 2023 Jun 1;149:105171.

36. Habas C. Functional connectivity of the cognitive cerebellum. Front Syst Neurosci. 2021;15:642225.

37. Bostan AC, Strick PL. The basal ganglia and the cerebellum: Nodes in an integrated network. Nat Rev Neurosci. 2018 Jun 1;19(6):338–50.

38. Peterburs J, Gajda K, Koch B, Schwarz M, Hoffmann KP, Daum I, et al. Cerebellar lesions alter performance monitoring on the antisaccade task—An event-related potentials study. Neuropsychologia. 2012;50(3):379–89.

39. Peterburs J, Thürling M, Rustemeier M, Göricke S, Suchan B, Timmann D, et al. A cerebellar role in performance monitoring–Evidence from EEG and voxel-based morphometry in patients with cerebellar degenerative disease. Neuropsychologia. 2015;68:139–47.

40. Berlijn AM, Huvermann DM, Groiss SJ, Schnitzler A, Mittelstaedt M, Bellebaum C, et al. The effect of cerebellar TMS on error processing: A combined single-pulse TMS and ERP Study. Imaging Neurosci. 2024;2:1–19.

41. Tunc S, Baginski N, Lubs J, Bally JF, Weissbach A, Baaske MK, et al. Predictive coding and adaptive behavior in patients with genetically determined cerebellar ataxia—A neurophysiology study. NeuroImage Clin. 2019 Jan 1;24:102043.

42. Romero MC, Davare M, Armendariz M, Janssen P. Neural effects of transcranial magnetic stimulation at the single-cell level. Nat Commun. 2019;10(1):2642.

43. Shirota Y, Ugawa Y. Transcranial magnetic stimulation. Curr Opin Behav Sci. 2024 Aug 1;58:101396.

44. Luber B, Lisanby SH. Enhancement of human cognitive performance using transcranial magnetic stimulation (TMS). Neuro-Enhanc. 2014 Jan 15;85:961–70.

45. Desmond JE, Chen SHA, Shieh PB. Cerebellar transcranial magnetic stimulation impairs verbal working memory. Ann Neurol. 2005 Oct 1;58(4):553–60.

46. Schutter DJLG, van Honk J. An electrophysiological link between the cerebellum, cognition and emotion: Frontal theta EEG activity to single-pulse cerebellar TMS. NeuroImage. 2006 Dec 1;33(4):1227–31.

47. Viñas-Guasch N, Ng THB, Heng JG, Chan YC, Chew E, Desmond JE, et al. Cerebellar transcranial magnetic stimulation (TMS) impairs visual working memory. The Cerebellum. 2023 Jun 1;22(3):332–47.

48. Du X, Rowland LM, Summerfelt A, Choa FS, Wittenberg GF, Wisner K, et al. Cerebellar-Stimulation Evoked Prefrontal Electrical Synchrony Is Modulated by GABA. The Cerebellum. 2018 Oct 1;17(5):550–63.

49. Fernandez L, Rogasch NC, Do M, Clark G, Major BP, Teo WP, et al. Cerebral cortical activity following non-invasive cerebellar stimulation—A systematic review of combined TMS and EEG studies. The Cerebellum. 2020 Apr 1;19(2):309–35.

50. Herbert M, Eppinger B, Kray J. Younger but not older adults benefit from salient feedback during learning. Front Psychol [Internet]. 2011;2. Available from: https://www.frontiersin.org/journals/psychology/articles/10.3389/fpsyg.2011.00171

51. Oldfield RC. The assessment and analysis of handedness: The Edinburgh inventory. Neuropsychologia. 1971 Mar 1;9(1):97–113.

52. Hardwick RM, Lesage E, Miall RC. Cerebellar Transcranial Magnetic Stimulation: The Role of Coil Geometry and Tissue Depth. Brain Stimulat. 2014 Sep 1;7(5):643–9.

53. Théoret H, Haque J, Pascual-Leone A. Increased variability of paced finger tapping accuracy following repetitive magnetic stimulation of the cerebellum in humans. Neurosci Lett. 2001 Jun 22;306(1):29–32.

54. Torriero S, Oliveri M, Koch G, Caltagirone C, Petrosini L. Interference of Left and Right Cerebellar rTMS with Procedural Learning. J Cogn Neurosci. 2004 Nov 1;16(9):1605–11.

55. Jung J, Bungert A, Bowtell R, Jackson SR. Vertex stimulation as a control site for transcranial magnetic stimulation: A concurrent TMS/fMRI study. Brain Stimulat. 2016 Jan 1;9(1):58–64.

56. Pizem D, Novakova L, Gajdos M, Rektorova I. Is the vertex a good control stimulation site? Theta burst stimulation in healthy controls. J Neural Transm. 2022 Mar 1;129(3):319–29.

57. Stoodley CJ, Schmahmann JD. Functional topography in the human cerebellum: A meta-analysis of neuroimaging studies. NeuroImage. 2009 Jan 15;44(2):489–501.

58. Peterburs J, Hofmann D, Becker MPI, Nitsch AM, Miltner WHR, Straube T. The role of the cerebellum for feedback processing and behavioral switching in a reversal-learning task. Brain Cogn. 2018 Aug 1;125:142–8.

59. Chatrian GE, Lettich E, Nelson PL. Ten percent electrode system for topographic studies of spontaneous and evoked EEG activities. Am J EEG Technol. 1985 Jun 1;25(2):83–92.

60. Wu W, Keller CJ, Rogasch NC, Longwell P, Shpigel E, Rolle CE, et al. ARTIST: A fully automated artifact rejection algorithm for single-pulse TMS-EEG data. Hum Brain Mapp. 2018 Apr 1;39(4):1607–25.

61. Delorme A, Makeig S. EEGLAB: an open-source toolbox for analysis of single-trial EEG dynamics. J Neurosci Methods. 2004;134:9–21.

62. Albrecht C, Bellebaum C. Slip or fallacy? Effects of error severity on own and observed pitch error processing in pianists. Cogn Affect Behav Neurosci. 2023 Aug 1;23(4):1076–94.

63. Meadows CC, Gable PA, Lohse KR, Miller MW. The effects of reward magnitude on reward processing: An averaged and single trial event-related potential study. Biol Psychol. 2016 Jul 1;118:154–60.

64. R Core Team. R: A language and environment for statistical computing [Internet]. Vienna, Austria: R Foundation for Statistical Computation; 2023. Available from: https://www.R-project.org/

65. Posit Team. RStudio: Integrated Development Environment for R [Internet]. Boston, MA: Posit Software, PBC; 2023. Available from: http://www.posit.co/

66. Olvet DM, Hajcak G. The stability of error-related brain activity with increasing trials. Psychophysiology. 2009 Sep 1;46(5):957–61.

67. Pontifex MB, Scudder MR, Brown ML, O'Leary KC, Wu CT, Themanson JR, et al. On the number of trials necessary for stabilization of error-related brain activity across the life span. Psychophysiology. 2010 Jul 1;47(4):767–73.

68. Larson MJ, Baldwin SA, Good DA, Fair JE. Brief reports: Temporal stability of the error-related negativity (ERN) and post-error positivity (Pe): The role of number of trials. Psychophysiology. 2010 Nov 1;47(6):1167–71.

69. Clayson PE, Baldwin SA, Larson MJ. Stability of performance monitoring with prolonged task performance: A study of error-related negativity and error positivity. Psychophysiology. 2025 Feb 1;62(2):e14731.

70. Fischer AG, Klein TA, Ullsperger M. Comparing the error-related negativity across groups: The impact of error- and trial-number differences. Psychophysiology. 2017 Jul 1;54(7):998–1009.

71. Bolker BM. Linear and generalized linear mixed models. Ecol Stat Contemp Theory Appl. 2015;2015:309–33.

72. Krueger C, Tian L. A Comparison of the General Linear Mixed Model and Repeated Measures ANOVA Using a Dataset with Multiple Missing Data Points. Biol Res Nurs. 2004 Oct 1;6(2):151–7.

73. Bates D, Mächler M, Bolker B, Walker S. Fitting linear mixed-effects models using lme4. J Stat Softw. 2015;67(1):1–48.

74. Kuznetsova A, Brockhoff P, Christensen R. lmerTest package: Tests in linear mixed effects models. J Stat Softw. 2017;82(13):1–26.

75. Luke SG. Evaluating significance in linear mixed-effects models in R. Behav Res Methods. 2017 Aug 1;49(4):1494–502.

76. Cook RD. Detection of influential observation in linear regression. Technometrics. 1977 Feb 1;19(1):15–8.

77. Nieuwenhuis R, te Grotenhuis M, Pelzer B. influence.ME: Tools for Detecting Influential Data in Mixed Effects Models. R J. 2012;4(2):38–47.

78. Long JA. interactions: Comprehensive, User-Friendly Toolkit for Probing Interactions [Internet]. 2019. Available from: https://cran.r-project.org/package=interactions

79. McDougle SD, Butcher PA, Parvin DE, Mushtaq F, Niv Y, Ivry RB, et al. Neural signatures of prediction errors in a decision-making task are modulated by action execution failures. Curr Biol. 2019 May 20;29(10):1606-1613.e5.

80. Ichikawa N, Siegle GJ, Dombrovski A, Ohira H. Subjective and model-estimated reward prediction: Association with the feedback-related negativity (FRN) and reward prediction error in a reinforcement learning task. Int J Psychophysiol. 2010 Dec 1;78(3):273–83.

81. Katahira K, Yuki S, Okanoya K. Model-based estimation of subjective values using choice tasks with probabilistic feedback. J Math Psychol. 2017 Aug 1;79:29–43.

82. Cohen J. Statistical Power Analysis for the Behavioral Sciences [Internet]. 2nd ed. New York: Routledge; 1988. Available from: https://doi.org/10.4324/9780203771587

83. Evans JD. Straightforward statistics for the behavioral sciences. Straightforward Stat Behav Sci. 1996;xxii, 600–xxii, 600.

84. Gignac GE, Szodorai ET. Effect size guidelines for individual differences researchers. Personal Individ Differ. 2016 Nov 1;102:74–8.

85. Funder DC, Ozer DJ. Evaluating Effect Size in Psychological Research: Sense and Nonsense. Adv Methods Pract Psychol Sci. 2019 Jun 1;2(2):156–68.

86. Thoma P, Bellebaum C, Koch B, Schwarz M, Daum I. The cerebellum is involved in reward-based reversal learning. The Cerebellum. 2008;7:433–43.

87. Overbeek TJM, Nieuwenhuis S, Ridderinkhof KR. Dissociable components of error processing. J Psychophysiol. 2005 Jan 1;19(4):319–29.

88. Manto MU. Mechanisms of human cerebellar dysmetria: Experimental evidence and current conceptual bases. J NeuroEngineering Rehabil. 2009 Apr 13;6(1):10.

89. Schmahmann JD. Dysmetria of thought: Clinical consequences of cerebellar dysfunction on cognition and affect. Trends Cogn Sci. 1998 Sep 1;2(9):362–71.

90. Hussain SJ, Freedberg MV. Debunking the Myth of Excitatory and Inhibitory Repetitive Transcranial Magnetic Stimulation in Cognitive Neuroscience Research. J Cogn Neurosci. 2025 May 1;37(5):1009–22.

91. Debener S, Ullsperger M, Siegel M, Fiehler K, Von Cramon DY, Engel AK. Trial-by-trial coupling of concurrent electroencephalogram and functional magnetic resonance imaging identifies the dynamics of performance monitoring. J Neurosci. 2005;25(50):11730–7.

92. Ridderinkhof KR, Ullsperger M, Crone EA, Nieuwenhuis S. The Role of the Medial Frontal Cortex in Cognitive Control. Science. 2004 Oct 15;306(5695):443–7.

93. Hester R, Foxe JJ, Molholm S, Shpaner M, Garavan H. Neural mechanisms involved in error processing: A comparison of errors made with and without awareness. NeuroImage. 2005 Sep 1;27(3):602–8.

94. van Veen V, Carter CS. The anterior cingulate as a conflict monitor: fMRI and ERP studies. Physiol Behav. 2002 Dec 1;77(4):477–82.

95. van Boxtel GJM, van der Molen MW, Jennings JR. Differential Involvement of the Anterior Cingulate Cortex in Performance Monitoring During a Stop-Signal Task. J Psychophysiol. 2005 Jan 1;19(1):1–10.

96. Miltner WHR, Braun CH, Coles MGH. Event-related brain potentials following incorrect feedback in a time-estimation task: Evidence for a “generic” neural system for error detection. J Cogn Neurosci. 1997 Nov;9(6):788–98.

97. Foti D, Weinberg A, Bernat EM, Proudfit GH. Anterior cingulate activity to monetary loss and basal ganglia activity to monetary gain uniquely contribute to the feedback negativity. Clin Neurophysiol. 2015 Jul 1;126(7):1338–47.

98. Hauser TU, Iannaccone R, Stämpfli P, Drechsler R, Brandeis D, Walitza S, et al. The feedback-related negativity (FRN) revisited: New insights into the localization, meaning and network organization. NeuroImage. 2014 Jan 1;84:159–68.

99. Nieuwenhuis S, Holroyd CB, Mol N, Coles MGH. Reinforcement-related brain potentials from medial frontal cortex: origins and functional significance. Neurosci Biobehav Rev. 2004 Jul 1;28(4):441–8.

100. Unger K, Heintz S, Kray J. Punishment sensitivity modulates the processing of negative feedback but not error-induced learning. Front Hum Neurosci. 2012;6.

101. Zhuang Q, Zhu S, Yang X, Zhou X, Xu X, Chen Z, et al. Oxytocin-induced facilitation of learning in a probabilistic task is associated with reduced feedback- and error-related negativity potentials. J Psychopharmacol (Oxf). 2021 Jan 1;35(1):40–9.

102. Cao D, Li Y, Tang Y. Functional specificity of the left ventrolateral prefrontal cortex in positive reappraisal: A single-pulse transcranial magnetic stimulation study. Cogn Affect Behav Neurosci. 2021 Aug 1;21(4):793–804.

103. Ciricugno A, Ferrari C, Rusconi ML, Cattaneo Z. The left posterior cerebellum is involved in orienting attention along the mental number line: An online-TMS study. Neuropsychologia. 2020 Jun 1;143:107497.

104. Kalbe E, Schlegel M, Sack AT, Nowak DA, Dafotakis M, Bangard C, et al. Dissociating cognitive from affective theory of mind: A TMS study. Cortex. 2010 Jun 1;46(6):769–80.

105. Duecker F, Sack AT. Rethinking the role of sham TMS. Front Psychol. 2015;6:210.

106. Ugawa Y, Day BL, Rothwell JC, Thompson PD, Merton PA, Marsden CD. Modulation of motor cortical excitability by electrical stimulation over the cerebellum in man. J Physiol. 1991 Sep 1;441(1):57–72.

Imaging Neuroscience
an open access journal

Research Article

The effect of cerebellar TMS on error processing: A combined single-pulse TMS and ERP study

Adam M. Berlijn[a,b,c,*], Dana M. Huvermann[a,d,*], Stefan J. Groiss[c,e], Alfons Schnitzler[c,e], Manfred Mittelstaedt[a], Christian Bellebaum[a], Dagmar Timmann[d], Martina Minnerop[b,c,e], Jutta Peterburs[a,f]

[a]Faculty of Mathematics and Natural Sciences, Heinrich Heine University Düsseldorf, Düsseldorf, Germany

[b]Institute of Neuroscience and Medicine (INM-1), Research Centre Jülich, Jülich, Germany

[c]Department of Neurology, Center for Movement Disorders and Neuromodulation, Medical Faculty, Heinrich-Heine University Düsseldorf, Düsseldorf, Germany

[d]Department of Neurology and Center for Translational and Behavioral Neurosciences (C-TNBS), Essen University Hospital, University of Duisburg-Essen, Essen, Germany

[e]Institute of Clinical Neuroscience and Medical Psychology, Medical Faculty & University Hospital Düsseldorf, Heinrich Heine University Düsseldorf, Düsseldorf, Germany

[f]Institute for Systems Medicine & Department of Human Medicine, MSH Medical School Hamburg, Hamburg, Germany

*Shared first authorship

Corresponding Author: Adam M. Berlijn (berlijn@uni-duesseldorf.de)

ABSTRACT

The present study investigated temporal aspects of cerebellar contributions to the processing of performance errors as indexed by the error-related negativity (ERN) in the response-locked event-related potential (ERP). We co-registered EEG and applied single-pulse transcranial magnetic stimulation (spTMS) to the left posterolateral cerebellum and an extra-cerebellar control region (vertex) while healthy adult volunteers performed a Go/Nogo Flanker Task. In Go trials, TMS pulses were applied at four different time points, with temporal shifts of -100 ms, -50 ms, 0 ms, or +50 ms relative to the individual error latency (IEL, i.e., individual ERN peak latency + median error response time). These stimulation timings were aggregated into early (-100 ms, -50 ms) and late (0 ms, +50 ms) stimulation for the analysis. In Nogo trials, TMS pulses occurred 0 ms, 100 ms, or 300 ms after stimulus onset. Mixed linear model analyses revealed that cerebellar stimulation did not affect error rates overall. No effects were found for response times. As hypothesized, ERN amplitudes were decreased for cerebellar stimulation. No significant differences were found for the error positivity (Pe). Similar to TMS application to probe cerebellar-brain inhibition in the motor domain, the inhibitory tone of the cerebellar cortex may have been disrupted by the pulses. Reduced inhibitory output of the cerebellar cortex may have facilitated the processing of error information for response selection, which is reflected in a decreased ERN.

Keywords: Error processing, cerebellum, cognitive control, EEG, single pulse TMS, performance monitoring, executive functions

1. INTRODUCTION

The cerebellum is assumed to be strongly involved in making predictions, processing error information, and adjusting behavior not only in the motor but also in the cognitive domain (King et al., 2019; Sokolov et al., 2017). Specifically, it has been suggested to generate internal models of movement and thought that are crucial for efficiency and precision in adaptive control (Ito, 2008; Koziol et al., 2014; Wolpert et al., 1998). These internal models reflect the process of error detection and correction in

Received: 3 August 2023 Revision: 24 November 2023 Accepted: 29 December 2023 Available Online: 16 January 2024

which the cerebellum functions as a comparator, comparing the actual and predicted outcomes of actions and adjusting the predictions accordingly. Along these lines, performance monitoring, which includes error and feedback processing, has been proposed to be an overarching function of the cerebellum (Peterburs & Desmond, 2016).

Performance monitoring can be indexed by the error-related negativity (ERN) in the event-related potential (ERP) in the electroencephalogram (EEG). The ERN, a relative negativity that typically peaks within 100 ms after an erroneous response, is interpreted to reflect processes related to the detection of errors (Falkenstein et al., 1991; Gehring et al., 1993) or response conflict (Botvinick et al., 2001; Yeung et al., 2004). The ERN has a symmetric, frontocentral scalp distribution, and its neural generator is likely in the anterior cingulate cortex (ACC) or supplementary motor area (Dehaene et al., 1994; Herrmann et al., 2004). It has been proposed that the ACC is critical for detecting conflict and conveying conflict-related information to other brain regions such as the lateral prefrontal cortex (Cohen et al., 2000). The ACC is also a key structure for evaluating actions and their outcomes, thus playing a critical role for reinforcement learning (Holroyd & Yeung, 2011).

Findings from studies in patients with cerebellar diseases suggest that the cerebellum contributes to the processing of errors and response conflict. Specifically, the ERN was shown to be reduced in patients with focal post-acute vascular lesions of the cerebellum (Peterburs et al., 2012) and cerebellar degenerative disease (Peterburs et al., 2015). The latter patient group also exhibited increased error rates, and the ERN reduction and behavioral impairment were linked to gray matter volume loss in posterolateral cerebellar regions (Peterburs et al., 2015). In contrast, patients with post-acute cerebellar lesions did not show altered behavior. However, another ERP component related to error processing, the error positivity (Pe), a relative positivity occurring 200–400 ms post-response that has been linked to more conscious aspects of error processing (Falkenstein et al., 1995), was increased (Peterburs et al., 2012). Interestingly, the Pe was unaffected in patients with progressive cerebellar degeneration (Peterburs et al., 2015). This result pattern could be indicative of a compensatory mechanism that may help maintain behavioral performance in patients with longstanding lesions but is absent in patients with cerebellar degenerative disease. In contrast, Tunc et al. (2019) investigated error processing in patients with different types of spinocerebellar ataxia (SCA) and failed to find behavioral impairments beyond a slowing of response times. However, they did report a trend-level reduction of the ERN in patients compared with healthy controls, which conforms to previous findings (Peterburs et al., 2015). The less pronounced neurophysiological differences and discrepancy in behavioral results compared with the study by Peterburs et al. (2015) may be attributed to sample differences (e.g., SCA subtypes with extra-cerebellar degeneration included in the study by Tunc et al., differences in extent and location of cerebellar degeneration). Cerebellar degeneration in Crus I, Crus II, and the deep cerebellar nuclei may cause stronger effects on error processing than the degeneration of other, more motor control related regions of the cerebellum, such as the anterior regions (see King et al., 2019 for a detailed overview on different cognitive functions reflected in different regions of the cerebellum).

While these patient studies provided strong evidence for a role of the cerebellum in error processing, testing patients is not the only option to probe such cerebellar involvement. An alternative approach that offers the possibility of direct manipulations of brain activity is to use non-invasive stimulation of the cerebellum. Transcranial magnetic stimulation (TMS) is a widely used non-invasive brain stimulation technique that can be applied to a variety of brain regions (for a review, see Grimaldi et al., 2014) to establish causal links to behavior (see Vaidya et al., 2019). Single-pulse TMS (spTMS) is assumed to be useful for both facilitation (Shirota et al., 2012) and disruption of neuronal processes (Pascual-Leone, 1999) and can be used in fast-paced task designs (Verleger et al., 2009). A number of studies have targeted the cerebellum with TMS, among other techniques, to investigate cerebellar-brain inhibition (Ugawa et al., 1995; Fernandez et al., 2018). For instance, Ugawa et al. (1995) demonstrated that the motor cortex could be influenced by stimulating the cerebellum. The cerebellar cortex inhibits the deep cerebellar nuclei, which are the only output source of cerebellar projections to higher cortical regions via the thalamus (Palesi et al., 2017). The TMS pulse triggers activity of the cerebellar cortex that suppresses motor cortical excitability in M1 via increased inhibition of the cerebellar nuclei. Notably, effects of cerebellar TMS have also been reported in the non-motor domain. Stimulation of the right superior cerebellum led to increased response times in a verbal working memory task (Desmond et al., 2005) and disrupted phonological prediction (Sheu et al., 2019). We, thus, assume the influence of spTMS on the cerebellum to be similarly disruptive for other cognitive domains like the processing of performance errors.

Mannarelli et al. (2020) used cathodal transcranial direct current stimulation (tDCS) to the cerebellum before healthy participants performed a Go/Nogo task. In contrast to the facilitating effects of anodal tDCS, cathodal tDCS causes a hyperpolarization of neurons, making upcoming action potentials harder to trigger. After cerebellar tDCS compared with sham stimulation, the Nogo-N2, a negative ERP component peaking around 250–300 ms post stimulus onset (Folstein & van Petten, 2008), was reduced. The N2 has been linked to response inhibition and cognitive control, with decreased amplitudes indicating improved performance monitoring in terms of cognitive flexibility (Larson & Clayson, 2011). In addition, false alarm rates were increased. These results provide the first evidence that cerebellar neuromodulation alters behavioral and ERP indices of performance monitoring and cognitive control. In particular, it has been suggested that the stimulus-locked N2 and the response-locked ERN may reflect activity of the same underlying error monitoring system (Ferdinand et al., 2008; Folstein & van Petten, 2008; van Veen & Carter, 2002). Hence, perturbing cerebellar function by non-invasive brain stimulation should also affect error processing and the ERN, and this is what the present study aimed to demonstrate. However, it must be noted that findings on effects of cerebellar tDCS on cognition and motor behavior have been rather heterogeneous and inconsistent (Jalali et al., 2017), and the exact mechanisms on the cell or network level are still unclear (van Dun et al., 2017). TMS, on the other hand, allows for a more focal and controlled stimulation that can reach deeper regions in the brain by generating pulses in a time resolution of less than 1 ms (Koponen et al., 2018). Therefore, the present study made use of cerebellar spTMS (and stimulation of vertex as a control site) in a Go/Nogo Flanker Task (Voegler et al., 2018) to investigate effects on error processing. Guided by the previous patient studies (Peterburs et al., 2012, 2015), our main focus was on the response-locked ERP components ERN and Pe. The stimulus-locked ERP components Nogo-N2 and Nogo-P3 investigated in the previous tDCS study in healthy subjects (Mannarelli et al., 2020) were not the focus of the present work, so data on and analyses of these components are only provided as Supplementary Material. For a more comprehensive neurophysiological account, we have also exploratively analyzed induced theta power in the time-frequency domain as an index of cognitive control (e.g., Cavanagh & Frank, 2014). Information on preprocessing, results, and discussion with respect to these dependent variables is provided in the Supplementary Material (see Figs. S11–S14).

We selected the left lateral cerebellum for stimulation with a double cone TMS coil because of several studies pointing towards the significance of posterolateral cerebellar regions for executive functions, which also encompass error processing (King et al., 2019; Sheu et al., 2019; Stoodley & Schmahmann, 2009). The experiment was conducted on two different days resulting in a fully within-subject design (each participant underwent both cerebellum and vertex stimulation). We followed the study design by Verleger et al. (2009) in which an spTMS pulse was delivered in each trial of a Flanker Task. As outlined above, spTMS has a high temporal resolution, and it can thus help elucidate causal links between brain and behavior. Thus, spTMS can also help elucidate temporal aspects of cerebellar contributions to error processing. Verleger et al. (2009) temporally shifted the pulses depending on an individually estimated peak latency of the lateralized readiness potential, a potential reflecting motor cortex activity leading up to voluntary movements, which was measured before the TMS blocks. In the present study, pulses were delivered at four different time points relative to the individual error latency (IEL, i.e., individual ERN peak latency + median error response time) in Go trials, and at three different time points relative to stimulus onset in Nogo trials.

Similar to deficits found in patients with cerebellar degeneration (Peterburs et al., 2015), we expected increased error rates in Go trials for cerebellar TMS compared to vertex TMS, but only when pulses were delivered before the responses, due to disturbance of the internal forward-model generated within the cerebellum (see Ramnani, 2006). Concerning the ERN, patients with cerebellar damage showed reduced negativity in the error-correct difference signal in the typical ERN time window (Peterburs et al., 2012, 2015). Consequently, we expected a reduced ERN for cerebellar TMS compared to vertex for pulses that were applied 100 ms and 50 ms before the IEL, since these time points should precede the onset of error processing. Since the Pe in patients with cerebellar lesions was interpreted to be the result of long-term compensatory processes of the brain (Peterburs et al., 2012), we did not expect effects of cerebellar spTMS on the Pe. Further, more exploratory hypotheses regarding response inhibition in Nogo trials as reflected in Nogo-N2 and Nogo-P3 and an additional analysis on the induced theta power are provided and discussed in the Supplementary Material.

2. METHODS

2.1. Sample

Twenty-five young and healthy participants were recruited through newspaper advertisements and postings at Heinrich-Heine-University Düsseldorf. Data from nine participants had to be excluded from the analyses: two participants attended only the first appointments necessary for study completion, further two participants complained of mild headaches during the task and dropped out, a miscalculated TMS onset value was used in another two participants, two participants made too few errors in the main task, and another misunderstood the task. Concerning the pre-task, which was used to determine the individual error latency (IEL, see below), we aimed to repeat the Go/Nogo Flanker until participants who committed at least six errors in all conditions, because at least six error trials are needed to reliably measure the ERN (see Olvet & Hajcak, 2009; Pontifex et al., 2010). For one participant we only discovered post hoc, after trial inspection and removing double responses, that only five error trials in one condition remained (see Table S1 in the Supplementary Material). As the ERN was clearly visible after averaging the five error trials, we decided to include the participant in further data analysis. The final sample thus consisted of 16 participants. The required sample size was estimated based on studies which used cerebellar spTMS in a different task (n = 17, Desmond et al., 2005; n = 10, Panouillères et al., 2012; n = 23, Sheu et al., 2019), or spTMS at another location in a Flanker task (n = 20, Danielmeier et al., 2009; n = 21, Klein et al., 2014; n = 8, Soto et al., 2009; n = 12, Verleger et al., 2009). Participants were healthy adults (age range 19–32 years, M = 24.00 years, SD = 3.70, n = 13 females, n = 12 right-handed and n = 1 ambidextrous; for more details, see Table S1 in the Supplementary Material). As TMS uses electromagnetic pulses, exclusion criteria were metal parts within the body (e.g., implants, pacemakers, shards of metal, pumps for medication), spinal fractures, acute heart attacks, or pregnancy. Further exclusion criteria were current psychiatric disorders, neurological disorders, alcohol or substance abuse, and intake of medication affecting the central nervous system. Participants were paid 40 Euros for participating in the two appointments. All participants gave written informed consent. The study was preregistered on the Open Science Framework (OSF: https://osf.io/6v9pa) and was approved by the Ethics Committee at the Faculty of Medicine of Heinrich Heine University Düsseldorf in accordance with the Declaration of Helsinki.

2.2. Questionnaires

Participants had to fill in a demographic questionnaire as well as the "Mehrfachwahl-Wortschatz-Intelligenztest" (IQ: M = 98.75, SD = 10.88; Lehrl et al., 1977), a multiple-choice vocabulary intelligence test.

2.3. Go/Nogo Flanker task

Participants completed a modified Go/Nogo Flanker task coded in the software *Presentation* (version 20.0, Build 02.20.17, Neurobehavioral Systems, Inc.). Figure 1 provides a schematic illustration of the time course and sequence of stimulus presentation in each trial. The main task consisted of 600 trials in four blocks. Go trials made up 80 % of all trials (480 trials), while Nogo trials made up 20 % of all trials (120 trials). In 80 % of Go Trials (384 trials), the flanker arrows aligned with the central target arrow (congruent trials), while in the other 20 % of Go trials (96 trials), the flankers pointed in the opposite direction (incongruent). Each trial started with the onset of arrow flankers positioned above and below a fixation cross for 200 ms. During Go trials, the fixation cross was replaced by the central target arrow to which participants had to respond by pressing the corresponding (left or right) button on a response pad with the index or middle finger of their right hand, respectively. Participants were instructed to respond as fast and as accurately as possible. If participants did not press one of the two buttons within the response time window of 350 ms (alternatively 400 ms, when the miss rate was too high in the flanker pre-task), a reminder to respond faster was displayed. No feedback was provided concerning the correctness of the response. During Nogo trials, the fixation cross was replaced by a filled circle, to which participants should suppress their response and not press a button. As in Go trials, the flankers together with the circle were displayed in the response time window for 350/400 ms. Thereafter, a fixation cross without flankers was displayed for 500 ms. During the subsequent inter-trial interval, the fixation cross was presented for a further 900–1300 ms (jittered).

Since the aim of the present study was to disturb error processing on a trial-by-trial basis using TMS pulses applied to the cerebellum and to elucidate temporal aspects of cerebellar involvement in error processing, it was critical to determine the time point at which cerebellar input was needed for error processing. More specifically, cerebellar input could be needed at the very onset of error processing or a bit later when error processing is already underway. To temporally approximate the onset of error processing individually for each participant, we

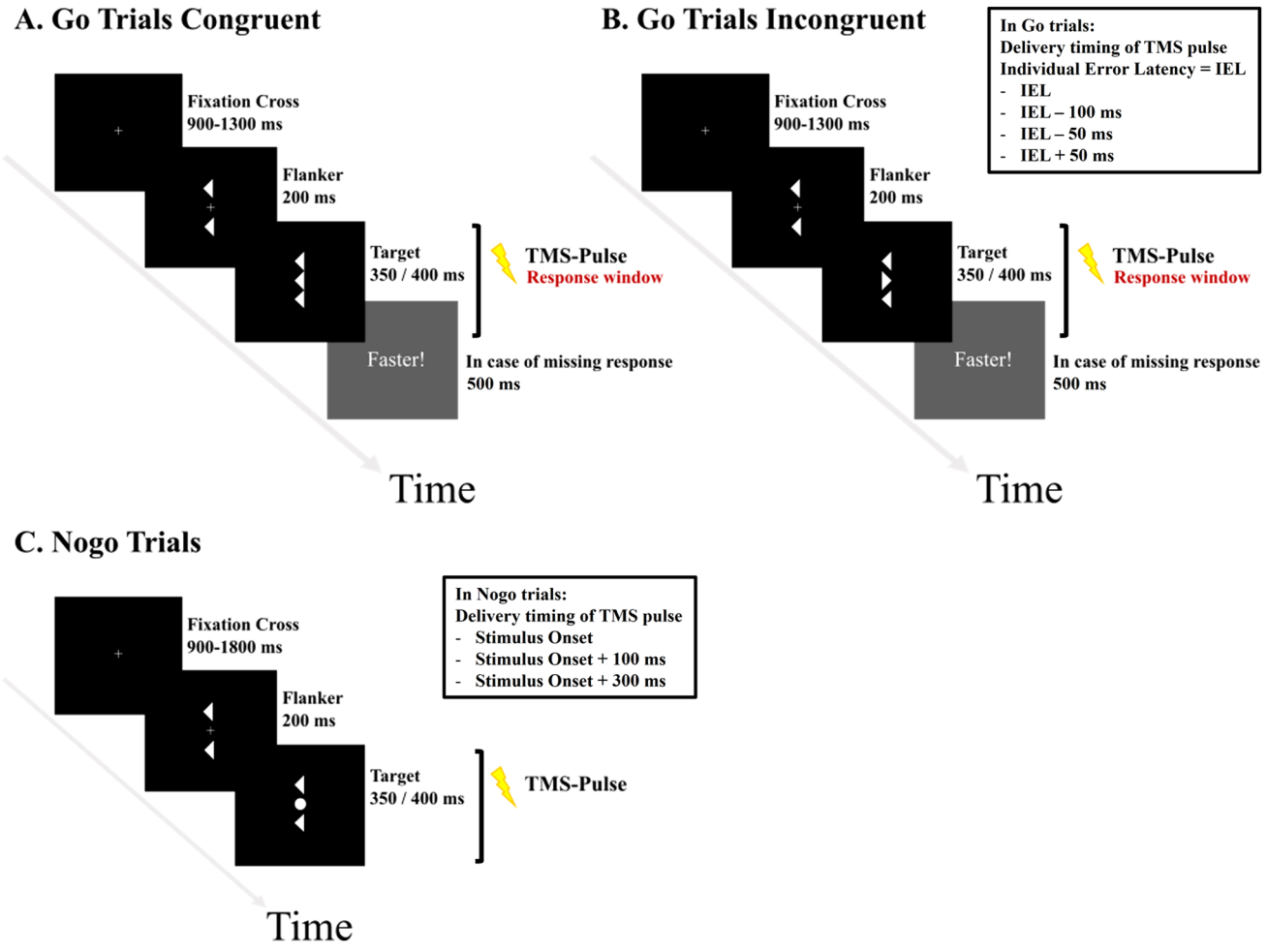

Fig. 1. Schematic illustration of time course and sequence of stimulus presentation in a trial of the Go/Nogo Flanker Task. Go trials with congruent flankers (A) and with incongruent flankers (B) relative to the target arrow in the center. Only one single pulse was applied in each trial. TMS pulses were delivered for Go trials shortly before the IEL (-100 ms, -50 ms), at the IEL, or shortly after the IEL (+50 ms). (C) In Nogo Trials, the target stimulus indicating the need to inhibit the response was a circle. TMS pulses were delivered at stimulus onset or shortly after target onset (+100 ms or +300 ms).

determined the IEL using a Flanker pre-task without pulses. This Flanker pre-task consisted of the same ratio of Go and Nogo Trials as the main task (120 trials in total, 80 Go and 40 Nogo trials). The IEL was calculated by adding the median error response time to the latency of the ERN in the response-locked ERP. If a participant was unable to respond within the standard response time window of 350 ms in more than 25 % of trials in the pre-task, the task was repeated with an increased response time window of 400 ms. This was done to ensure that enough valid trials were recorded. In total, three participants required the longer response time window.

Throughout the Flanker main task, monophasic single TMS pulses were applied within each trial. The time points at which TMS was applied differed for Go and Nogo trials. In Go trials, TMS pulses were delivered at the IEL (0 ms) as well as 100 ms before (-100 ms), 50 ms before (-50 ms), and 50 ms after (+50 ms). In Nogo trials, TMS pulses were delivered at fixed time points, that is, at stimulus onset as well as 100 ms and 300 ms after stimulus onset (+100 ms and +300 ms, respectively). Pulse timings relative to the IEL in Go and relative to stimulus onset in Nogo trials were randomized throughout the task but occurred an equal number of times per trial type and block.

2.4. Procedure

Upon arriving at the laboratory, the participants were seated in a brightly lit room in front of a laptop (DELL®

Precision M4800, 15.4 inch with a resolution of 1920 × 1080 pixels and a refresh rate of 60 Hz) with a response box (Cedrus RB-740, Science Plus Group, Groningen, NL) positioned before it. The distance between response box and laptop was kept constant. Only two keys were relevant for the task and had to be pressed with the index (left key) and middle finger (right key) of the right hand. A third key was used to navigate through pauses and instruction slides. After positioning the participants and putting earplugs in their ears, the EEG cap was aligned on the head, and the scalp electrodes were prepared. The electrodes on the cap were further covered with a plastic wrap to avoid any direct contact between electrodes and the TMS coil which could cause artifacts (Hernandez-Pavon et al., 2023). EMG electrodes were attached to the left hand, and the TMS stimulators were started and triggered via the laptop so that pulses were sent for the determination of the individual motor threshold (IMT). After IMT determination, the coil was firmly aligned and fixed with a custom mounting structure. Thereafter, the Flanker pre-task was started, in which no pulses occurred. Subsequently, another experimental task with spTMS was completed, which is not part of this manuscript. While participants were completing this task, we calculated the individual ERN peak latency and median response time for errors as described above. Subsequently, the IEL was calculated and used as an input value for the Flanker main task. Afterwards, the Flanker main task was performed. Participants underwent cerebellar and vertex stimulation in separate appointments. They were aware that both sessions included stimulation, but they were not explicitly informed about the specifics of the two stimulation sites. They were also naïve to the study's intent. The two appointments took place with a temporal gap of at least 48 hours (M = 82.13 days, SD = 143.36 days, range from 2 to 373 days). Due to a defect in the TMS stimulators, the second measurement had to be postponed for a long time, resulting in time gaps of 362 to 373 days for 3 subjects. Correcting for the delay of these subjects, the time interval between the two appointments was on average only 16.00 days (SD = 20.52 days, range from 2 to 74 days). The order of the stimulation sites was counterbalanced.

2.5. TMS-EEG-EMG interface

2.5.1. EEG system

A TMS compatible amplifier (BrainAmp MR plus, BrainProducts GmbH, Munich, Germany) was used with a cap containing 32 flat multitrodes. The flat electrodes minimize the distance between the coil and the skull surface. The following electrode sites were used: Fp1, Fp2, Fz, F3, F4, F7, F8, FCz, FC1, FC2, FC5, FC6, Cz, C3, C4, CPz, CP1, CP2, CP5, CP6, T7, T8, Pz, P3, P4, P7, P8, Oz, O1, and O2. BrainVision Recorder software, version 1.21 (BrainProducts, Munich, Germany) was used for recording. Impedances were kept below 5 kΩ. Data were sampled at 1000 Hz.

2.5.2. EMG system

Two surface EMG Ag/AgCl-electrodes (20 × 15 mm, Ambu, Ballerup, Denmark) were placed on the left M. abductor pollicis brevis in resting condition to record the muscle activity in terms of motor evoked potentials (MEPs) that reflect the corticospinal excitability throughout the estimation period of the IMT. This also allowed us to check that no MEPs would be triggered by the TMS pulses during the tasks. The signal was amplified with a Digitimer D360 (Digitimer Ltd, Hertfordshire, UK). The frequency band of the filter was 100–5000 Hz and digitized at a sampling rate of 5 kHz (Signal version 6.02, Cambridge Electronic Design Ltd., Cambridge, UK).

2.5.3. TMS system

We estimated the IMT with a custom script in *Presentation* that sent a code to a single TMS stimulator (Magstim® 200²) every 10 seconds to elicit a pulse. The double cone coil was aligned so that we could stimulate the right motor cortex (region M1). After an MEP was detected in the EMG signal using the independent trigger mode in the software *Signal*, 5 consecutive trials (out of 10) were counted to determine whether the position also clearly stimulated the motor cortex. The output power of the device was then reduced until only 5 out of 10 trials elicited an MEP. The estimated IMT with additional 20 % power (corresponding to 120 % motor threshold) was used as the output power for the TMS system for both appointments. Nevertheless, we measured the motor-threshold on both appointments to see if there was any variability. Checking the IMT revealed no significant difference between the first (M = 38.20 %, SD = 7.84 %) and second appointment (M = 37.68 %, SD = 7.97 %), $t(37)$ = 0.20, p = .840, and no significant difference between the cerebellar (M = 37.80 %, SD = 8.15 %) and vertex (M = 38.11 %, SD = 7.64 %) stimulation appointments $t(37)$ = -0.12, p = .905. The TMS coil was either placed at the level of the left lateral cerebellum (3 cm left and 1 cm inferior to the inion; Hardwick et al., 2014) or at

the vertex position which corresponds to electrode position Cz of the international 10–20 system (Pizem et al., 2022, see Fig. 2 for an illustration, and Figs. S15 and S16 for real photographs in the Supplementary Material) with the voltage flow in the inferior direction. After the coil was correctly aligned, it was fixed with a custom stand so that the same position was maintained over the course of the session. In addition, we used a fabric elastic band to ensure that the coil-to-head distance was kept constant (forehead for the cerebellar TMS or chin for the vertex TMS). The distance of the coil to the head surface was observed during the task and adjusted during the pause between the individual, since even small changes lead to a decrease in the induced magnetic field strength (Hernandez-Pavon et al., 2023).

The BiStim TMS stimulators were manually charged before the first trial, and the independent trigger mode was selected in Signal for the subsequent tasks to trigger the stimulators. Then, the single-pulses were observed in the EMG-signal to ensure that no MEPs were evoked, particularly when stimulating the cerebellum. If MEPs had occurred, the session would have been interrupted, and the coil would be realigned, in order to avoid co-stimulating the brainstem. However, this did not occur during our study. Additionally, the coil position was constantly monitored and readjusted between the blocks and tasks if substantial movement had occurred to ensure that the distance between coil and scalp was consistent. Since the recharge period of a single Magstim® 200² stimulator exceeded the duration of a single trial, we alternated activation of two BiStim stimulators. Unfortunately, due to overheating of the stimulators, trials were lost in 3 participants towards the end of the task, for the TMS system no longer sent any pulses while the task and EEG measurements were still running. The time of termination was checked in the EEG signal, so that all trials without TMS pulses were excluded from analysis. The heat development in the stimulators was related to both

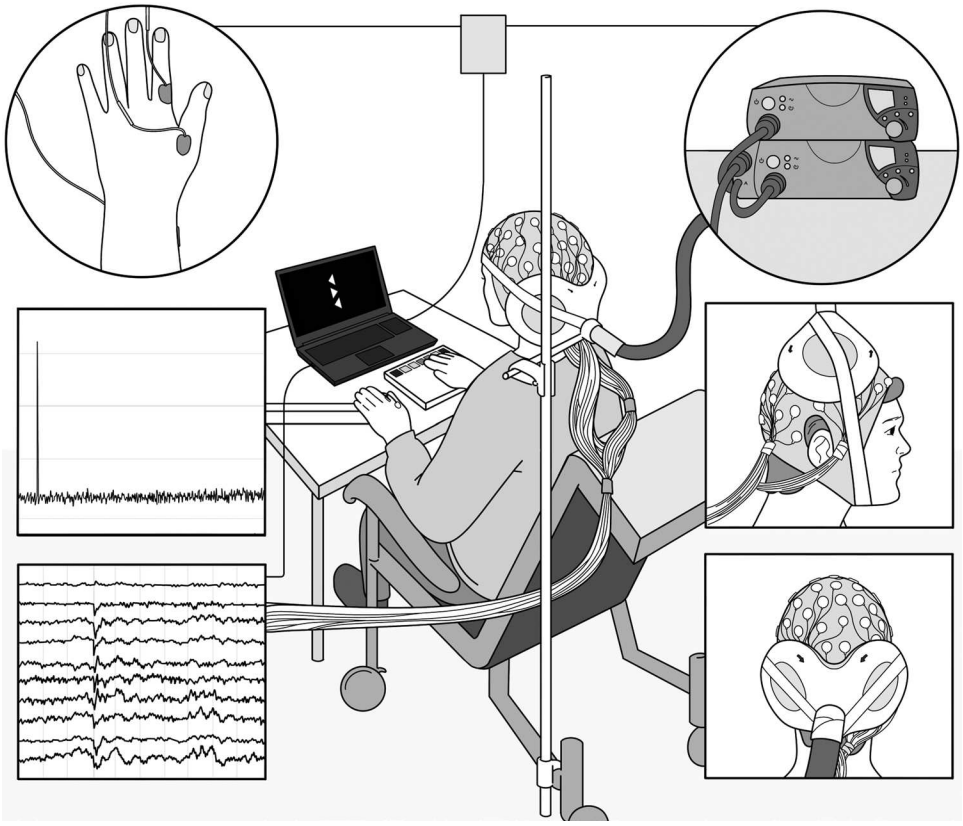

Fig. 2. Illustration of the TMS-EEG Setup for cerebellar and vertex stimulation. Top left circle shows the placement of the electrodes for recording of the EMG signal. Below, the TMS pulse is shown in the EMG signal. Bottom left, continuous measures of the EEG signal. Top right, TMS generators are shown. Below, the TMS coil orientation for vertex stimulation is shown and, in the bottom, right, the coil alignment for the cerebellar stimulation is presented. The voltage flow indicated by the arrows is aligned inferiorly. A double-cone coil was used for stimulation.

the high number of single pulses and the output power which varied greatly among the participants (see Table S1 in the Supplementary Material).

In case of a port conflict due to close proximity of two marker codes sent by the presentation laptop to the EEG system (i.e., codes sent within 5 ms), which may be the case for the response codes and matching TMS pulse codes, the later code was delayed until the port conflict no longer arose. The respective code timings were corrected in the EEG marker file using a custom script in MATLAB. Time points were not changed for the TMS pulse codes because the timing in the marker file always fitted the timing of the real TMS pulse. Instead, trials with a TMS pulse differently timed than the planned onset due to marker code delay were excluded.

2.6. Individual error latency estimation based on the flanker pre-task

ERN latency was determined by peak detection performed in BrainVision Analyzer software, version 2.1 (BrainProducts, Munich, Germany). All trials containing two or more responses were removed beforehand. Preprocessing for peak detection was performed as follows: First, data were re-referenced to the average signal of all electrodes, and the signal at FCz was re-established. Next, a DC detrend was performed, followed by low-pass filtering with a cut-off of 30 Hz and a slope of 12 dB/oct, high-pass filtering with a cut-off of 0.1 Hz and a slope of 12 dB/oct, and a notch filter set to 50 Hz. Subsequently, automatic ocular correction ICA was performed, and data were segmented into epochs of 600 ms, starting 200 ms before and ending 400 ms after erroneous responses. The baseline-corrected data (with the 200 ms period preceding response onset as baseline) underwent artifact rejection (only 3 trials were rejected across all participants and sessions) with the following settings: maximum difference of values over 100 µV or activity lower than 0.1 µV within an interval of 100 ms, voltage steps exceeding 50 µV/ms, or values above 100 µV or below -100 µV. Segments were then averaged, and peak detection was performed on a time window of 100 ms after the response, searching for a negative peak at site FCz.

2.7. Dependent variables

Behavioral outcome variables were error rates and response times in Go trials. For the EEG data, we analyzed the ERN for Go Trials in the response-locked ERP. In an exploratory analysis, the Pe (Go trials) was also analyzed. The ERN was defined as the local maximal negative peak in the error-correct difference signal within a time window of 100 ms post-response at site FCz (see Hajcak & Foti, 2008). The Pe was defined as the maximum positive peak in the difference signal within the time window between 200 and 400 ms post-response at Pz (see Larson et al., 2010). Follow-up analyses with the original waveforms were conducted to further elucidate if effects were specifically driven by altered ERP amplitudes for errors or correct responses. In addition, analyses of false alarm rates and Nogo-N2 and Nogo-P3 ERP components as well as analyses of induced theta power in the time-frequency domain are provided in the Supplementary Material.

2.8. Preprocessing of the TMS-EEG data

Preprocessing of the spTMS-EEG co-registered EEG raw data was conducted using the EEGLAB Toolbox (version 2021.1) in MATLAB (version R2021a) (MathWorks, Natick, Massachusetts, USA) and the Automated aRTIfact rejection for Single-pulse TMS-EEG Data (ARTIST) algorithm created by Wu et al. (2018). This algorithm provides an efficient and objective approach to preprocess raw EEG data and has proven to be superior to manual artifact rejection by experts and other algorithms such as TESA (Rogasch et al., 2017; Wu et al., 2018). Some of the default settings were adapted because the signal at electrode FCz, which had been used as online reference during EEG recording, needed to be re-established. In addition, the high pass filter of 1 Hz was kept, and the low pass filter was changed from 100 Hz to 30 Hz. The notch filter was changed from 60 Hz to 50 Hz. Electrode Iz was removed before applying the ARTIST algorithm because of low signal quality. The ARTIST algorithm creates segments around a given code which marks the onset of the TMS pulse. Here, segments were created with a length of 2500 ms, spanning 1000 ms before and 1500 ms after TMS pulse onset. Next, response onsets were checked by a custom script using MATLAB to ensure that only valid trials were included into the analysis (see above, some responses and therefore the respective response codes had overlapped with other codes within trials and were therefore delayed). In addition, we manually rejected trials without a TMS pulse (due to overheating or close proximity of two TMS pulses, see above) before re-referencing and segmenting the data. Following this, the ARTIST algorithm preprocessed the data in three distinct stages. In the first stage, large-amplitude artifacts were removed by applying DC drift correction, the removal and

interpolation of the TMS pulse artifact (15 ms prior to the TMS marker code onset until 5 ms after), downsampling of the data, and the removal of the TMS decay artifacts in a first ICA run. In the second stage, the AC line noise was removed, and the band-pass filter was applied. Then, the signal was segmented around the TMS pulse onset, and segments that exceeded the default thresholds were removed. The final step within the second stage was the removal and interpolation of poor channels. ARTIST interpolated on average 1.13 channels (*SD* = 1.13) per participant and stimulation site. In addition, on average, 44.13 trials (*SD* = 50.93) were rejected, including both trials which were manually rejected due to overheating (*M* = 29.25, *SD* = 39.67, range = 5–169) and trials which ARTIST rejected (*M* = 14.88, *SD* = 14.72, range = 1–63), with slightly more excluded trials in total for cerebellar (*M* = 47.56, *SD* = 54.69) compared to vertex (*M* = 40.69, *SD* = 48.41) stimulation (*N* = 16). In the third stage, poor independent components were removed in a second ICA run. The data average was referenced, and the baseline was corrected. The output data were imported into BrainVision Analyzer 2.1, and further segmentation was performed according to trial type (Go/Nogo). For Go trials, segmentation was done for response and stimulus onset separately for error and correct trials. The adapted scripts and raw data can be found in the following OSF folder: https://osf.io/jwfn9/

2.9. Statistical models

We deviated from our preregistration and ran mixed linear model (MLMs) analyses in R (R Core Team, version 4.0.3) using RStudio Team (2020: version 1.3.959) and the lme4 package (version: 1.1.25, Bates et al., 2014) in place of traditional repeated-measures ANOVA. This enabled us to analyze factors with missing values and use the participant as a random factor to further explain variance in the data. Meteyard and Davies (2020) proposed in their best practice guidelines for MLMs that the maximum model should be chosen, including all within-subject main and interaction effects as random effects. The maximum model should be only chosen if no errors in the model fit, in terms of converging errors or singular fits, appear, which would cause an overfitting of the model. To avoid this, the models were checked using an iterative process in which the within-subject highest order interaction was first included as random factor and the random slopes rejected subsequently in case of model fit errors. All our models included stimulation site and stimulation timing as fixed effects, but for some models, these factors were additionally included as random slopes depending on the model fit. In addition, Cooks distance (Cook, 1977) was calculated to identify potential outlier subjects before running the MLM analysis using the influence.ME package (version 0.9–9; Nieuwenhuis et al., 2012).

Before setting up our models for ERP analysis in Go trials, we grouped the four stimulation timings into a two-level factor, resulting in "early" and "late" stimulation. For this purpose, the -100 ms and -50 ms trials were combined into "early" and the 0 ms (at IEL) and +50 ms trials into "late." This allowed us to pool more error trials together, to better take into account the variability of the IEL within and across participants, and to compare the effect of stimulation timing on error processing over a broader time period.

To check for baseline performance differences between the two sessions in the Flanker pre-task, we calculated Linear models (LMs) comparing error rates (Go trials) and ERN amplitude between the cerebellar stimulation and vertex stimulation session (see Fig. S1 and Table S3 in the Supplementary Material).

To analyze behavioral performance in the Flanker main task for Go trials, we set up an MLMs for error rates including stimulation site (cerebellum, vertex), stimulation timing (early, late), and the interaction between these factors as fixed effects and added stimulation site and the interaction with stimulation site and stimulation timing as random slopes and participant as random effect in the model.

$$\text{Error rate} \sim \text{site} * \text{timing} + (1 + \text{site} + \text{site} : \text{timing} \mid \text{participant})$$

For response times, we included all responses to see whether there was a difference in response times between correct and error trials. In the final model, we included trial type (correct trials, error trials) as fixed effect and as random slope into the model equation.

$$\text{Response time} \sim \text{site} * \text{timing} * \text{trial type} + (1 + \text{site} * \text{trial type} \mid \text{participant})$$

In a third MLM, we analyzed error responses by their timing relative to TMS onset to identify a possible influence of the pulse itself on the error rates independent of the trial type. Here, the model was specified using the error rates as the dependent variable, stimulation site (cerebellum, vertex) and TMS timing (response preTMS, response postTMS) as fixed effects and random slopes:

$$\text{Error rate} \sim \text{site} * \text{TMStiming} + (1 + \text{site} + \text{site} : \text{TMS timing} \mid \text{participant})$$

For ERP analyses for Go trials, we analyzed the ERN and Pe peak amplitudes obtained from the difference wave as the dependent variables.

$$\text{ERN\_diff}\,(\text{amp}) \sim \text{site} * \text{timing} + (1 + \text{site} + \text{timing} \mid \text{participant})$$

$$\text{Pe\_diff}\,(\text{amp}) \sim \text{site} * \text{timing} + (1 + \text{site} \mid \text{participant})$$

In addition, we analyzed the original waveforms, entering the amplitudes at the time points corresponding to the ERN latency in the difference signal. We added fixed effects of stimulation site (cerebellum, vertex) and timing (early, late) and trial type (correct trials, error trials) for the analysis as well as the interaction between the fixed effects as well as the three factors as random slopes and participant as a random effect. In addition, the optimizer was changed from the default to Nelder-mead to cope with an occurring convergence error as suggested by the best practice guideline by Meteyard and Davies (2020).

The final, maximum model specification was as follows:

$$\text{ERN}\,(\text{amp}) \sim \text{site} * \text{timing} * \text{trial type} + (1 + \text{site} + \text{timing} + \text{trial type} + \text{site} : \text{timing} \mid \text{participant})$$

We simple-coded the categorical predictors stimulation site (0.5 = cerebellum, –0.5 = vertex), stimulation timing (0.5 = early, –0.5 = late), and trial type (0.5 = correct, –0.5 = error). Also, TMS-timing (response pre-TMS = 0.5, response post-TMS = –0.5) was simple-coded for the additional analysis of the error rate. We used the lmerTest package (version: 3.1.3, Kuznetsova et al., 2017) in R using Satterthwaite's method to estimate the degrees of freedom and to generate *p*-values for MLMs. We considered *p*-values below .05 as statistically significant. Statistical models for the analyses of false alarms, Nogo-N2, and Nogo-P3 are provided in the Supplementary Material.

3. RESULTS

3.1. Error rates

MLM analysis revealed no significant effects of stimulation site or timing on error rates (all $p \geq .384$, $n = 15$, see Fig. 3A). However, exploring the influence of TMS timing relative to response execution (i.e., whether a pulse had occurred prior to a response on a given trial or after the response) revealed a highly significant main effect of TMS timing ($\beta = 5.02$, $t(15.00) = 13.30$, $p < .001$, see Fig. 3B). Error rates were higher in trials in which pulses had occurred after the response (i.e., response pre-TMS: $M = 13.69$ %, $SD = 4.47$ %) compared to trials in which pulses had occurred prior to the response (i.e., response post-TMS: $M = 8.66$ %, $SD = 4.59$ %), irrespective of stimulation site. The main effect of stimulation site was only marginally significant ($\beta = –1.11$, $t(15.00) = –2.03$, $p = .061$). The interaction between stimulation site and TMS timing relative to response was not significant ($\beta = –0.79$, $t(15.00) = –0.80$, $p = .437$ $N = 16$, see Fig. 3B).

3.2. Response times

For response times, there was a significant main effect of trial type ($\beta = 25.66$, $t(14) = 10.05$, $p < .001$). Overall, responses were faster in error trials ($M = 239.40$ ms, $SD = 19.53$ ms) compared to correct trials ($M = 265.07$ ms, $SD = 18.41$ ms). The main effects of site and stimulation timing as well as the interaction between these factors were not significant (all *p*-values $\geq .119$, $n = 15$, see Fig. 3C).

3.3. EEG results

3.3.1. ERN based on the difference wave (ERN-diff)

Figure 4A provides response-locked grand-average ERP difference waves (error minus correct) at electrode FCz according to stimulation site (cerebellum, vertex) and stimulation timing (early, late), along with scalp topographies for the time points of maximum negativity in the ERN time window. Figure 4B displays corresponding response-locked grand-average ERPs for errors and correct responses.

There was a significant main effect of stimulation site ($\beta = 0.93$, $t(13.00) = 2.82$, $p = .015$). The ERN was less negative for cerebellar ($M = –5.56$ µV, $SD = 2.81$ µV) compared to vertex stimulation ($M = –6.49$ µV, $SD = 2.98$ µV). The main effect of timing was non-significant ($\beta = –0.02$, $t(13.00) = –0.05$, $p = .962$). The interaction of stimulation site and timing was significant ($\beta = –1.36$, $t(12.99) = –2.52$, $p = .026$). Simple slope analyses of the stimulation site for early and late stimulation timing yielded a significant slope (see Fig. S4 in the Supplementary Material) for late stimulation ($\beta = 1.61$, $t = 3.78$, $p < .001$). For early stimulation, the slope was non-significant ($\beta = 0.25$, $t = 0.59$, $p = .563$). The interaction between site and timing seemed to be driven by the late stimulation: for cerebellar TMS, the negativity was reduced for late ($M = –5.21$ µV, $SD = 2.72$ µV) compared to early stimulation ($M = –5.90$ µV,

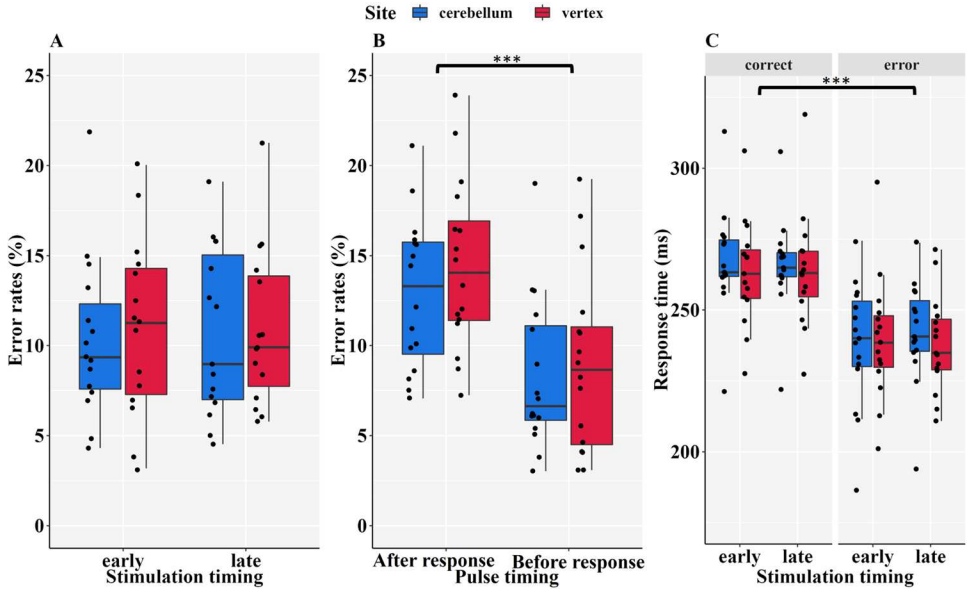

Fig. 3. (A) Mean error rates in Go trials according to stimulation site and stimulation timing. The analysis did not yield any significant effects of stimulation site or stimulation timing on error rates. (B) Mean error rates in Go trials according to stimulation site and pulse timing relative to response onset (i.e., whether a pulse had occurred prior to a response on a given trial or after the response). Asterisks indicate the significant main effect of pulse timing relative to response onset: error rates were higher in trials in which pulses had occurred after the response compared to trials in which pulses had occurred prior to response. (C) Mean response times in Go trials according to stimulation site and stimulation timing. Asterisks indicate the significant main effect of trial type: response times were shorter for errors compared to correct responses. The dots were jittered horizontally, the central line reflects the median and the whisker the first and third quartiles (the 25th and 75th percentiles) in all plots.

SD = 2.97 μV), and in contrast, vertex stimulation led to increased negativity for late (*M* = –6.82 μV, *SD* = 2.85 μV) compared to early stimulation (*M* = –6.16 μV, *SD* = 3.17 μV; see Fig. 5A for the boxplots of the ERN amplitudes as well as Fig. S4 for the interaction plot in the Supplementary Material).

3.3.2. *ERN in the original waveforms*

To elucidate whether the decreased negativity in the difference waves for cerebellar compared to vertex stimulation was specifically driven by altered neural responses to errors or correct responses, the original waveforms were analyzed (see Fig. 6). We found a significant main effect of trial type (β = 6.01, *t*(12.99) = 8.18, *p* > .001), with increased negativity for errors (*M* = –5.46 μV, *SD* = 3.98 μV) compared to correct responses (*M* = 0.55 μV, *SD* = 3.30 μV). All other main effects were non-significant (all $p \geq .079$). The interaction between trial type, and site was significant (β = –0.93, *t*(38.99) = –2.95, *p* = .005). Crucially, the three-way interaction between site, timing, and trial type was also significant (β = 1.36, *t*(38.99) = 2.16, *p* = .037). To resolve this interaction, we performed simple slope analysis. Results showed only a marginal significant slope for error trials on the stimulation sites and during late stimulation (β = 0.98, *t* = 2.06, *p* = .052). The slope was positive, indicating that the ERN was more negative in vertex (*M* = –5.78 μV, *SD* = 4.23 μV) compared to cerebellar stimulation (*M* = –5.13 μV, *SD* = 3.76 μV).

All other simple slopes for trial type, stimulation site, and stimulation timing were not significant (all $p \geq .200$).

3.3.3. *Pe-diff*

Analysis of the Pe in the difference waves did not yield any significant effects (all $p \geq .198$; see Fig. 5B for the boxplots of the Pe amplitudes).

4. DISCUSSION

This study investigated the role of the cerebellum in error processing using spTMS to stimulate the cerebellum while co-registering EEG. With the help of a Flanker pretask, we estimated individual ERN peak latencies and

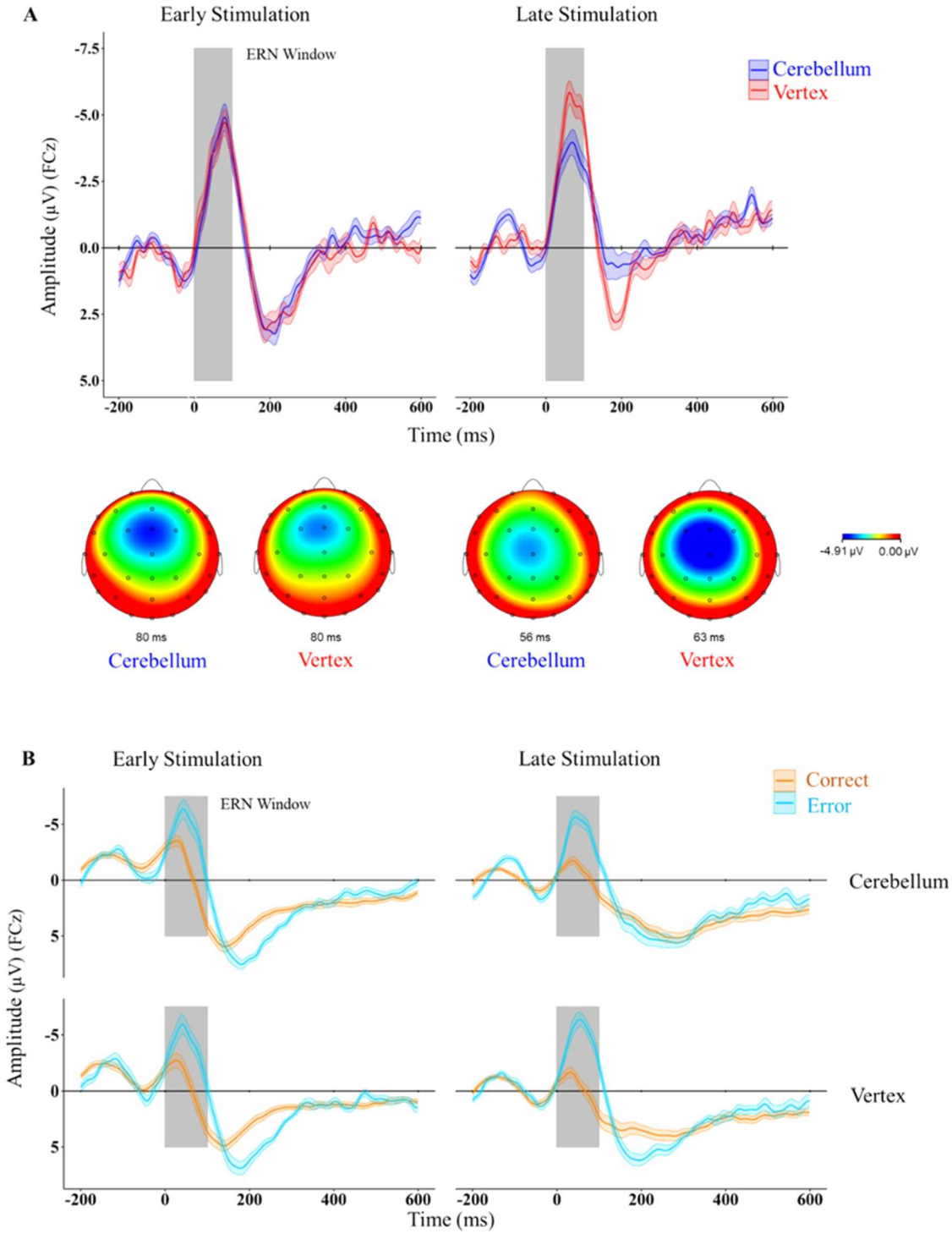

Fig. 4. (A) Response-locked grand-average ERP difference wave (error minus correct) at electrode FCz according to stimulation site (cerebellum, vertex) and stimulation timing (early, late), along with scalp topographies for the time points of maximum negativity in the ERN time window. (B) Response-locked grand-average ERPs for errors and correct responses at electrode FCz according to stimulation site (cerebellum, vertex) and stimulation timing (early, late) and trial type (correct, error). Smoothing around the lines in panel (A) and (B) indicate the standard error. The shaded area indicates time window for ERN quantification (0–100 ms post-response).

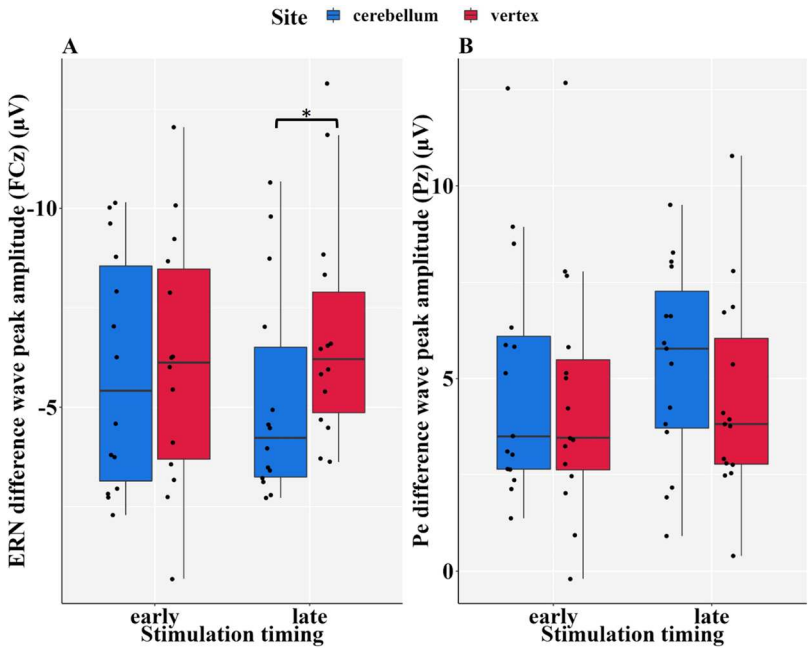

Fig. 5. (A) ERN peak amplitudes in the difference wave (error – correct) at electrode FCz as a function of stimulation site (cerebellum/vertex) and stimulation timing (early/late). Asterisks indicate the significant interaction effect between site and stimulation timing with the highly significant slope for late stimulation timing only. (B) Pe peak amplitudes in the difference wave (error – correct) at electrode Pz as a function of stimulation site (cerebellum/vertex) and stimulation timing (early/late). The dots were jittered horizontally. The central line reflects the median and the whisker the first and third quartiles (the 25th and 75th percentiles).

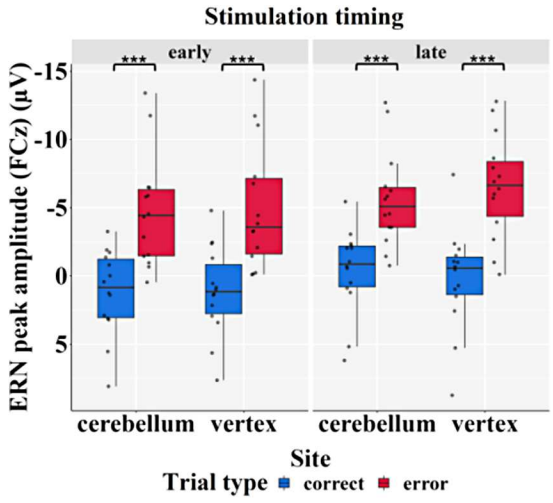

Fig. 6. ERN peak amplitudes as derived from the original waveforms at electrode FCz as a function of trial type (correct, error), stimulation site (cerebellum, vertex), and timing (early, late). Asterisks indicate significant main effects of trial type in both, cerebellar and vertex stimulation. All dots were jittered horizontally. The central line reflects the median and the whisker the first and third quartiles (the 25th and 75th percentiles).

median error response times to calculate the Individual Error Latency (IEL) as an approximation of the onset of error processing for each study participant. TMS pulses were then applied at different time points around the IEL in each trial of the subsequent Flanker main task. We expected to observe differences in error rates as well as in response-locked ERP components (specifically ERN, Pe) for cerebellar compared to vertex stimulation.

In line with our predictions, analysis of the ERP difference waves revealed that the ERN was reduced for cerebellar compared to vertex stimulation. This difference was also modulated by the timing of stimulation, with blunting particularly present for late compared to early stimulation. Analysis of the original ERP waveforms to determine whether the reduced negativity in the difference signal was particularly driven by altered neural responses to either errors or correct responses revealed that this effect was not specific to either response type.

Importantly, ERN magnitude in the Flanker pre-task was comparable between the day of cerebellar (M = –6.37 μV, SD = 2.09 μV) and vertex stimulation (M = –5.97 μV, SD = 2.18 μV, see Table S3 in the Supplementary Material). While we cannot exclude that active vertex stimulation

slightly increased the ERN (M = –6.49 μV, SD = 2.98 μV), ERN magnitude was substantially reduced for cerebellar stimulation (M = –5.56 μV, SD = 2.81 μV). Thus, the reduction of the ERN magnitude appeared to be driven mostly by spTMS applied to the cerebellum and not the vertex region, although vertex contributions cannot be fully excluded.

In general, the observed effect of stimulation site may indicate that monophasic single-pulse TMS disrupted inhibitory functions of the cerebellar cortex towards the deep cerebellar nuclei. This may have caused disinhibition, thereby facilitating information exchange with higher cortical structures through the cerebello-thalamo-cortical loop (Palesi et al., 2017). Here, the anterior cingulate cortex (ACC, Rubia et al., 2007), which is highly involved in the generation of the ERN (Dehaene et al., 1994; Holroyd & Coles, 2002), may be of particular interest. According to the reinforcement learning theory (Holroyd & Coles, 2002), the ERN is generated when a reduction of dopaminergic input from the VTA, possibly reflecting prediction errors, disinhibits deep cingulate cortical neurons. Recent findings show that the cerebellum may contribute to the generation of prediction errors. For instance, electrophysiological findings in mammals show that different cerebellar cell populations are sensitive to reward predictions and prediction violations (Heffley et al., 2018; Hull, 2020), and by the presence of direct cerebellar projections to the VTA that can modulate dopamine release in the striatum (Yoshida et al., 2022). Regarding the present results, with facilitated cerebello-cerebral information exchange, less phasic dopaminergic input towards the ACC may have reduced the cognitive demand for error processing (Holroyd & Coles, 2002).

In the conflict-monitoring theory (Botvinick et al., 2001, 2004), the ACC is seen as a monitoring system detecting conflicts (such as between opposing response options) and signaling the need for cognitive control. Here, facilitated cerebello-cerebral information exchange may have promoted conflict detection, leading to a reduced need for cognitive control that could be reflected in a reduced ERN. Adjustments in cognitive control related to conflict adaptation have previously been associated with increased functional interaction between prefrontal regions, superior temporal regions, and the anterior cerebellum (Egner & Hirsch, 2005). In addition, right cerebellar activation along with frontal and parietal activations were observed in the presence of persistent conflict leading to the interpretation that the cerebellum is involved in visuospatial attention processes during conflict to maintain high activation (Casey et al., 2000). However, somewhat contrary to both interpretations, error rates in the present study were not affected by cerebellar spTMS, and it could be argued that reduced cognitive demand or facilitated conflict detection should have led to increased accuracy/decreased error rates.

By taking advantage of the temporal resolution of spTMS, the present study addressed the question *when* cerebellar input is used during error processing. Our results show that late TMS pulses, that is, pulses that were applied to the cerebellum at IEL onset or shortly after, were more effective in that they were associated with a decrease in ERN magnitude in the error-correct difference signal. Early pulses, that is, pulses applied within 100 ms prior to IEL onset, left the ERN unaffected. A possible explanation for this pattern could be that the cerebellum receives information about the action through sensory input pathways and compares the actual information with the predicted outcome as stated in the forward model (Sokolov et al., 2017). Along these lines, cerebellar input for error processing is needed as this process is already underway. The peak of the ERN might correspond with the reconciliation of the predicted and actual action representation, that is., the use of the cerebellar input. Cerebellar spTMS may facilitate continuous information exchange with frontal regions by disinhibiting the cerebellar output signal. Thus, ERN generation would depend on this interplay of multiple regions, extending the existing framework (Falkenstein et al., 1991; Gehring et al., 1993) towards involvement of the cerebellum.

Analysis of the Pe in the difference signal did not reveal any significant effects of stimulation site or timing, which is in line with our hypothesis (see Fig. S5 of the grand averages in the Supplementary Material). The Pe likely reflects the conscious detection of an error (Endrass et al., 2007; Orr & Carrasco, 2011), and it is conceivable that error awareness might have been low due to the lack of feedback information in our rapid Go/Nogo Flanker task. Unfortunately, we did not implement any assessment of error awareness in the present study, so this notion remains speculative. Regardless of this, Pe alterations in the context of cerebellar damage were found in one previous study (Peterburs et al., 2012) in which patients with chronic cerebellar lesions were investigated. Here, an increase in Pe amplitudes—in concert with decreased ERN and preserved performance accuracy—was interpreted to reflect a compensatory mechanism. Importantly, spTMS to the cerebellum elicits a temporary effect while a stroke is associated with permanent tissue damage. Therefore, we can only roughly compare spTMS-induced "virtual lesions" of the cerebellum with degenerative or focal cerebellar diseases (Çan et al., 2018).

Analysis of the behavioral data showed no significant effects of site or timing. The lack of a site effect was unexpected, given that we had hypothesized an increase in error rates for cerebellar stimulation based on results observed in patients with cerebellar degeneration in an antisaccade task (Peterburs et al., 2015). However, another previous study also failed to find altered error rates in patients with cerebellar degeneration using a more comparable flanker task (Tunc et al., 2019). The present findings also resemble to some extent results obtained in patients with basal ganglia lesions, in whom the ERN was reduced in the absence of behavioral deficits in a flanker task (Ullsperger & von Cramon, 2006). In general, altered neural responses despite preserved behavior therefore are not particularly unusual. Interestingly, such a pattern of results has also been reported for feedback-based learning (Rustemeier et al., 2016) and in the acquisition phase of learning stimulus related contingencies in cerebellar lesion patients (Thoma et al., 2008), However, impaired learning performance in these patients was present when the task required reversal of learned stimulus-response-outcome contingencies (Thoma et al., 2008). Based on these observations, it could be speculated that the simple Flanker task used in the present study may not have been sensitive enough to detect more subtle performance differences as a function of stimulation site. It is conceivable that impaired cerebellar function may specifically affect behavioral flexibility, as suggested by findings of impaired feedback-based learning in cerebellar lesion patients only when the task involved reversal learning (Thoma et al., 2008). Behavioral flexibility is not tested in the Flanker task. Future studies could therefore investigate feedback-based learning and/or reversal learning in the context of cerebellar TMS.

When analyzing error rates according to TMS timing relative to response execution, we observed increased error rates in trials in which pulses had occurred after the response compared to trials in which pulses had occurred prior to response, irrespective of stimulation site. Thus, this effect is not informative about cerebellar contributions to error processing. Given that there were no baseline differences in error rates (based on flanker pre-task runs, see Fig. S1), this effect cannot be attributed to differences in baseline performance. It could, however, be speculated that the pulses themselves (regardless of where they were delivered) may have elicited a small startle response that could have slowed down subsequent responses. Along these lines, decreased error rates for trials in which pulses had occurred prior to the response could reflect a speed-accuracy trade-off, if increased accuracy after pre-response pulses coincided with increased response times. Unfortunately, response times could not be meaningfully analyzed according to TMS timing relative to response onset because stimulation timing was determined based on the IEL.

4.1. Limitations

This complex and technically advanced procedure led to some unique challenges and limitations that are relevant when interpreting the present results.

To begin, stimulation location was based on anatomical landmarks and not neuro-navigated. Moreover, the pulses were generated using two Magstim 200² in the Bistim configuration to overcome the challenge of the recharge period of the individual stimulators that is determined by the used output power, which varied greatly across the participants (see Table S1 in the Supplementary Material). Nevertheless, individual trials still had to be removed before analysis because no pulse had occurred. This was mostly due to the development of heat in the coil which caused the system to shut down so that the task was still running, and EEG was still recorded but no pulses were delivered. Here, the number of trials and breaks between the blocks need to be considered when planning a similarly fast-paced task in which monophasic single pulses are delivered across several hundreds of trials. Monophasic pulses are more likely to cause overheating due to the higher electrical charge compared to biphasic pulses (see Klomjai et al., 2015). Here, an external cooling system could help reduce heating issues.

Furthermore, the stimulation sites were the cerebellum and the vertex region, but we cannot exclude the possibility that stimulation also affected other brain regions. The direction of the magnetic field lines of the double cone coil are well-established to target deeper brain layers (Çan et al., 2018), but at the expense of a less focal stimulation in comparison to a figure-of-eight coil. Therefore, it may have caused stimulation of other, adjacent regions. This has been shown to be especially critical for vertex stimulation, which caused decreases in the BOLD signal in the default-mode network (see Jung et al., 2016). Regardless, we expected vertex stimulation to be a better control condition than sham because of a more comparable experience for participants regarding vibrations, coil click sounds, magnetic field build (Duecker & Sack, 2015), and discomfort. Some of the participants told us that they experienced the stimulation as uncomfortable, and that focusing on the task was

difficult because of the frequency of the pulses. Two participants dropped out in the cerebellar stimulation condition after the first block because they found the stimulation very unpleasant. The short trial period and jitter as well as the total number of trials might have contributed to this. Nevertheless, no systematic differences in ratings of these side effects were present between the two sessions, demonstrating that TMS pulses were perceived as similar for the stimulation sites (see Table S2 in the Supplementary Material).

In addition, Nogo trials and the analysis of response inhibition related ERP components were not the main focus of this work. This was partially due to the unexpectedly strong impact of TMS-induced EEG artifacts that hampered data analysis and result interpretation. In the grand-average ERPs for Nogo trials, the TMS induced artifacts did not completely disappear after preprocessing (see Fig. S7 in the Supplementary Material), and ERP components of interest, especially the Nogo-N2, occurred in close temporal proximity to pulses. We were able to identify the Nogo-N2 and Nogo-P3 to a certain degree, with grand-average patterns resembling those described in the literature (e.g., Rietdijk et al., 2014). The pulse artifact itself was cut out of the segment by the ARTIST algorithm, but there was still noise present that was likely caused by aftereffects (e.g., decay artifact) superimposed on the signal. Visual inspection of the grand-averages showed that the artifact was temporally shifted depending on pulse timing and more visible for vertex compared to cerebellar TMS, likely due to spatial proximity to analyzed electrode sites. Nevertheless, the grand-averages were also very similar to those obtained in the Go/Nogo pre-task without TMS pulses (see Fig. S2 for Go and Fig. S3 for Nogo ERPs in the Supplementary Material).

5. CONCLUSION

The present study investigated the role of the cerebellum for error processing using spTMS to stimulate the cerebellum while co-registering EEG. Applying cerebellar TMS caused a blunting of the ERN, directly supporting cerebellar involvement in performance monitoring. Of note, this effect was not specific to erroneous responses but generalized also to correct responses. Most importantly, our study also provides a first glimpse into temporal aspects of cerebellar contributions to error processing. The effect of cerebellar TMS on the ERN depended on pulse timing and was evident only when stimulation occurred around the onset of the IEL or shortly after. Finally, Pe as an index of late, more cognitive, awareness-related aspects of error processing, was not affected by cerebellar TMS.

In general, the present study adds to a growing body of research supporting cerebellar involvement in error processing and performance monitoring. More studies applying brain stimulation techniques are needed to further develop this line of research and investigate other aspects of performance monitoring such as feedback processing and feedback-based learning to better understand the role of the cerebellum for adaptive control of (non-motor) behavior.

DATA AND CODE AVAILABILITY

The data and code are openly available through the Open Science Framework at https://osf.io/jwfn9/

AUTHOR CONTRIBUTIONS

A.M.B., D.M.H., S.J.G., M.M., and J.P. planned the study. A.M.B. programmed the task. A.M.B. and D.M.H. set up the experiment, collected data, created the preprocessing pipeline, and analyzed the data. M.M. constructed the interface between the TMS and EEG system. J.P. supervised the project. A.M.B. and D.M.H. wrote the first draft of the manuscript. All authors contributed to results discussion and interpretation, and manuscript revision, and read and approved the submitted version.

FUNDING

This work was supported by the Deutsche Forschungsgemeinschaft (DFG) - Project number 437661157 awarded to J.P., M.M., and D.T.

DECLARATION OF COMPETING INTEREST

The study protocol was defined prior to the experiment and preregistered on osf.org (osf.io/6v9pa).

ACKNOWLEDGEMENT

We thank Greta Wippich for the illustration of the technical setup.

SUPPLEMENTARY MATERIAL

Supplementary material for this article is available with the online version here: https://doi.org/10.1162/imag_a_00080

REFERENCES

Bates, D., Mächler, M., Bolker, B., & Walker, S. (2014). Fitting linear mixed-effects models using lme4. *arXiv preprint* arXiv:1406.5823.

Botvinick, M. M., Braver, T. S., Barch, D. M., Carter, C. S., & Cohen, J. D. (2001). Conflict monitoring and cognitive control. *Psychological Review*, *108*(3), 624. https://psycnet.apa.org/doi/10.1037/0033-295X.108.3.624

Botvinick, M. M., Cohen, J. D., & Carter, C. S. (2004). Conflict monitoring and anterior cingulate cortex: An update. *Trends in Cognitive Sciences*, *8*(12), 539–546. https://doi.org/10.1016/j.tics.2004.10.003

Çan, M. K., Laakso, I., Nieminen, J. O., Murakami, T., & Ugawa, Y. (2018). Coil model comparison for cerebellar transcranial magnetic stimulation. *Biomedical Physics & Engineering Express*, *5*(1), 015020. https://doi.org/10.1088/2057-1976/aaee5b

Casey, B. J., Thomas, K. M., Welsh, T. F., Badgaiyan, R. D., Eccard, C. H., Jennings, J. R., & Crone, E. A. (2000). Dissociation of response conflict, attentional selection, and expectancy with functional magnetic resonance imaging. *Proceedings of the National Academy of Sciences*, *97*(15), 8728–8733. https://doi.org/10.1073/pnas.97.15.8728

Cavanagh, J. F., & Frank, M. J. (2014). Frontal theta as a mechanism for cognitive control. *Trends in Cognitive Sciences*, *18*(8), 414–421. https://doi.org/10.1016/j.tics.2014.04.012

Cohen, J. D., Botvinick, M., & Carter, C. S. (2000). Anterior cingulate and prefrontal cortex: Who's in control?. *Nature Neuroscience*, *3*(5), 421–423. https://doi.org/10.1038/74783

Cook, R. D. (1977). Detection of influential observation in linear regression. *Technometrics*, *19*(1), 15–18. https://doi.org/10.1080/00401706.1977.10489493

Danielmeier, C., Wessel, J. R., Steinhauser, M., & Ullsperger, M. (2009). Modulation of the error-related negativity by response conflict. *Psychophysiology*, *46*(6), 1288–1298. https://doi.org/10.1111/j.1469-8986.2009.00860.x

Dehaene, S., Posner, M. I., & Tucker, D. M. (1994). Localization of a neural system for error detection and compensation. *Psychological Science*, *5*(5), 303–305. https://doi.org/10.1111/j.1467-9280.1994.tb00630.x

Desmond, J. E., Chen, S. A., & Shieh, P. B. (2005). Cerebellar transcranial magnetic stimulation impairs verbal working memory. *Annals of Neurology*, *58*(4), 553–560. https://doi.org/10.1002/ana.20604

Duecker, F., & Sack, A. T. (2015). Rethinking the role of sham TMS. *Frontiers in Psychology*, *6*, 210. https://doi.org/10.3389/fpsyg.2015.00210

van Dun, K., Bodranghien, F., Manto, M., & Marien, P. (2017). Targeting the cerebellum by noninvasive neurostimulation: A review. *The Cerebellum*, *16*, 695–741. https://doi.org/10.1007/s12311-016-0840-7

Egner, T., & Hirsch, J. (2005). The neural correlates and functional integration of cognitive control in a Stroop task. *NeuroImage*, *24*(2), 539–547. https://doi.org/10.1016/j.neuroimage.2004.09.007

Endrass, T., Reuter, B., & Kathmann, N. (2007). ERP correlates of conscious error recognition: Aware and unaware errors in an antisaccade task. *European Journal of Neuroscience*, *26*(6), 1714–1720. https://doi.org/10.1111/j.1460-9568.2007.05785.x

Falkenstein, M., Hohnsbein, J., & Hoormann, J. (1995). Event-related potential correlates of errors in reaction tasks. *Electroencephalography and Clinical Neurophysiology*, *44*, 287–296. In G. Karmos, M. Molnar, V. Csepe, I. Czigler, & J. E. Desmedt (Eds.), *Perspectives of event-related potentials research* (EEG Journal Supplement 44) (pp. 280–286). Amsterdam: Elsevier.

Falkenstein, M., Hohnsbein, J., Hoormann, J., & Blanke, L. (1991). Effects of crossmodal divided attention on late ERP components. II. Error processing in choice reaction tasks. *Electroencephalography and Clinical Neurophysiology*, *78*, 447–455. https://doi.org/10.1016/0013-4694(91)90062-9

Ferdinand, N. K., Mecklinger, A., & Kray, J. (2008). Error and deviance processing in implicit and explicit sequence learning. *Journal of Cognitive Neuroscience*, *20*(4), 629–642. https://doi.org/10.1162/jocn.2008.20046

Fernandez, L., Major, B. P., Teo, W. P., Byrne, L. K., & Enticott, P. G. (2018). Assessing cerebellar brain inhibition (CBI) via transcranial magnetic stimulation (TMS): a systematic review. *Neuroscience & Biobehavioral Reviews*, *86*, 176–206. https://doi.org/10.1016/j.neubiorev.2017.11.018

Folstein, J. R., & Van Petten, C. (2008). Influence of cognitive control and mismatch on the N2 component of the ERP: A review. *Psychophysiology*, *45*(1), 152–170. https://doi.org/10.1111/j.1469-8986.2007.00602.x

Gehring, W. J., Goss, B., Coles, M. G., Meyer, D. E., & Donchin, E. (1993). A neural system for error detection and compensation. *Psychological Science*, *4*, 385–390. https://doi.org/10.1111/j.1467-9280.1993.tb00586.x

Grimaldi, G., Argyropoulos, G. P., Boehringer, A., Celnik, P., Edwards, M. J., Ferrucci, R., Galea, J. M., Groiss, S. J., Hiraoka, K., Kassavetis, P., Lesage, E., Manto, M., Miall, R. C., Priori, A., Sadnicka, A., Ugawa, Y., & Ziemann, U. (2014). Non-invasive cerebellar stimulation—A consensus paper. *The Cerebellum*, *13*, 121–138. https://doi.org/10.1007/s12311-013-0514-7

Hajcak, G., & Foti, D. (2008). Errors are aversive: Defensive motivation and the error-related negativity. *Psychological Science*, *19*(2), 103–108. https://doi.org/10.1111/j.1467-9280.2008.02053.x

Hardwick, R. M., Lesage, E., & Miall, R. C. (2014). Cerebellar transcranial magnetic stimulation: The role of coil geometry and tissue depth. *Brain Stimulation*, *7*(5), 643–649. https://doi.org/10.1016/j.brs.2014.04.009

Heffley, W., Song, E. Y., Xu, Z., Taylor, B. N., Hughes, M. A., McKinney, A., Joshua, M., & Hull, C. (2018). Coordinated cerebellar climbing fiber activity signals learned sensorimotor predictions. *Nature Neuroscience*, *21*(10), 1431–1441. https://doi.org/10.1038/s41593-018-0228-8

Hernandez-Pavon, J. C., Veniero, D., Bergmann, T. O., Belardinelli, P., Bortoletto, M., Casarotto, S., Casula, E. P., Farzan, F., Fecchio, M., Julkunen, P., Kallioniemi, E., Lioumis, P., Metsomaa, J., Miniussi, C., Mutanen, T. P., Rocchi, L., Rogasch, N. C., Shafi, M. M., Siebner, H. R., … Ilmoniemi, R. J. (2023). TMS combined with EEG: Recommendations and open issues for data collection and analysis. *Brain Stimulation*, *16*(2), 567–593. https://doi.org/10.1016/j.brs.2023.02.009

Herrmann, M. J., Römmler, J., Ehlis, A. C., Heidrich, A., & Fallgatter, A. J. (2004). Source localization (LORETA) of the error-related-negativity (ERN/Ne) and positivity (Pe). *Cognitive Brain Research*, *20*(2), 294–299. https://doi.org/10.1016/j.cogbrainres.2004.02.013

Holroyd, C. B., & Coles, M. G. (2002). The neural basis of human error processing: Reinforcement learning,

dopamine, and the error-related negativity. *Psychological Review*, *109*(4), 679. https://doi.org/10.1037/0033-295X.109.4.679

Holroyd, C. B., & Yeung, N. (2011). An integrative theory of anterior cingulate cortex function: Option selection in hierarchical reinforcement learning. *Neural Basis of Motivational and Cognitive Control*, *16*, 333–349. https://doi.org/10.7551/mitpress/9780262016438.003.0018

Hull, C. (2020). Prediction signals in the cerebellum: Beyond supervised motor learning. *elife*, *9*, e54073. https://doi.org/10.7554/eLife.54073

Ito, M. (2008). Control of mental activities by internal models in the cerebellum. *Nature Reviews Neuroscience*, *9*(4), 304–313. https://doi.org/10.1038/nrn2332

Jalali, R., Miall, R. C., & Galea, J. M. (2017). No consistent effect of cerebellar transcranial direct current stimulation on visuomotor adaptation. *Journal of Neurophysiology*, *118*(2), 655–665. https://doi.org/10.1152/jn.00896.2016

Jung, J., Bungert, A., Bowtell, R., & Jackson, S. R. (2016). Vertex stimulation as a control site for transcranial magnetic stimulation: A concurrent TMS/fMRI study. *Brain Stimulation*, *9*(1), 58–64. https://doi.org/10.1016/j.brs.2015.09.008

King, M., Hernandez-Castillo, C. R., Poldrack, R. A., Ivry, R. B., & Diedrichsen, J. (2019). Functional boundaries in the human cerebellum revealed by a multi-domain task battery. *Nature Neuroscience*, *22*(8), 1371–1378. https://doi.org/10.1038/s41593-019-0436-x

Klein, P. A., Petitjean, C., Olivier, E., & Duque, J. (2014). Top-down suppression of incompatible motor activations during response selection under conflict. *NeuroImage*, *86*, 138–149. https://doi.org/10.1016/j.neuroimage.2013.08.005

Klomjai, W., Katz, R., & Lackmy-Vallée, A. (2015). Basic principles of transcranial magnetic stimulation (TMS) and repetitive TMS (rTMS). *Annals of Physical and Rehabilitation Medicine*, *58*(4), 208–213. https://doi.org/10.1016/j.rehab.2015.05.005

Koponen, L. M., Nieminen, J. O., Mutanen, T. P., & Ilmoniemi, R. J. (2018). Noninvasive extraction of microsecond-scale dynamics from human motor cortex. *Human Brain Mapping*, *39*(6), 2405–2411. https://doi.org/10.1002/hbm.24010

Koziol, L. F., Budding, D., Andreasen, N., D'Arrigo, S., Bulgheroni, S., Imamizu, H., Ito, M., Manto, M., Marvel, C., Parker, K., Pezzulo, G., Ramnani, N., Riva, D., Schmahmann, J., Vandervert, L., & Yamazaki, T. (2014). Consensus paper: The cerebellum's role in movement and cognition. *The Cerebellum*, *13*, 151–177. https://doi.org/10.1007/s12311-013-0511-x

Kuznetsova, A., Brockhoff, P. B., & Christensen, R. H. (2017). lmerTest package: Tests in linear mixed effects models. *Journal of Statistical Software*, *82*, 1–26. https://doi.org/10.18637/jss.v082.i13

Larson, M. J., Baldwin, S. A., Good, D. A., & Fair, J. E. (2010). Temporal stability of the error-related negativity (ERN) and post-error positivity (Pe): The role of number of trials. *Psychophysiology*, *47*(6), 1167–1171. https://doi.org/10.1111/j.1469-8986.2010.01022.x

Larson, M. J., & Clayson, P. E. (2011). The relationship between cognitive performance and electrophysiological indices of performance monitoring. *Cognitive, Affective, & Behavioral Neuroscience*, *11*, 159–171. https://doi.org/10.3758/s13415-010-0018-6

Lehrl, S., Merz, J., & Burkhard, G. F. S. (1977). *Mehrfachwahl-Wortschatz-Test (MWT-B)*. Erlangen: Straube.

Mannarelli, D., Pauletti, C., Petritis, A., Delle Chiaie, R., Currà, A., Trompetto, C., & Fattapposta, F. (2020). Effects of cerebellar tDCS on inhibitory control: Evidence from a Go/NoGo task. *The Cerebellum*, *19*, 788–798. https://doi.org/10.1007/s12311-020-01165-z

Meteyard, L., & Davies, R. A. (2020). Best practice guidance for linear mixed-effects models in psychological science. *Journal of Memory and Language*, *112*, 104092. https://doi.org/10.1016/j.jml.2020.104092

Nieuwenhuis, R., te Grotenhuis, M., & Pelzer, B. (2012). Influence.ME: Tools for detecting influential data in mixed effects models. *R Journal*, *4*(2), 38–47. https://doi.org/10.32614/rj-2012-011

Olvet, D. M., & Hajcak, G. (2009). The stability of error-related brain activity with increasing trials. *Psychophysiology*, *46*(5), 957–961. https://doi.org/10.1111/j.1469-8986.2009.00848.x

Orr, J. M., & Carrasco, M. (2011). The role of the error positivity in the conscious perception of errors. *Journal of Neuroscience*, *31*(16), 5891–5892. https://doi.org/10.1523/JNEUROSCI.0279-11.2011

Palesi, F., Rinaldis, A. de, Castellazzi, G., Calamante, F., Muhlert, N., Chard, D., Tournier, J. D., Magenes, G., D'Angelo, E., & Gandini Wheeler-Kingshott, C. A. M. (2017). Contralateral cortico-ponto-cerebellar pathways reconstruction in humans in vivo: Implications for reciprocal cerebro-cerebellar structural connectivity in motor and non-motor areas. *Scientific Reports*, *7*(1), 12841. https://doi.org/10.1038/s41598-017-13079-8

Panouillères, M., Neggers, S. F., Gutteling, T. P., Salemme, R., Stigchel, S. V. D., van der Geest, J. N., … & Pelisson, D. (2012). Transcranial magnetic stimulation and motor plasticity in human lateral cerebellum: Dual effect on saccadic adaptation. *Human Brain Mapping*, *33*(7), 1512–1525. https://doi.org/10.1002/hbm.21301

Pascual-Leone, A. (1999). Transcranial magnetic stimulation: Studying the brain–behaviour relationship by induction of 'virtual lesions'. *Philosophical Transactions of the Royal Society of London. Series B: Biological Sciences*, *354*(1387), 1229–1238. https://doi.org/10.1098/rstb.1999.0476

Peterburs, J., & Desmond, J. E. (2016). The role of the human cerebellum in performance monitoring. *Current Opinion in Neurobiology*, *40*, 38–44. https://doi.org/10.1016/j.conb.2016.06.011

Peterburs, J., Gajda, K., Koch, B., Schwarz, M., Hoffmann, K. P., Daum, I., & Bellebaum, C. (2012). Cerebellar lesions alter performance monitoring on the antisaccade task—An event-related potentials study. *Neuropsychologia*, *50*(3), 379–389. https://doi.org/10.1016/j.neuropsychologia.2011.12.009

Peterburs, J., Thürling, M., Rustemeier, M., Göricke, S., Suchan, B., Timmann, D., & Bellebaum, C. (2015). A cerebellar role in performance monitoring–Evidence from EEG and voxel-based morphometry in patients with cerebellar degenerative disease. *Neuropsychologia*, *68*, 139–147. https://doi.org/10.1016/j.neuropsychologia.2015.01.017

Pizem, D., Novakova, L., Gajdos, M., & Rektorova, I. (2022). Is the vertex a good control stimulation site? Theta burst stimulation in healthy controls. *Journal of Neural Transmission*, *129*(3), 319–329. https://doi.org/10.1007/s00702-022-02466-9

Pontifex, M. B., Scudder, M. R., Brown, M. L., O'Leary, K. C., Wu, C. T., Themanson, J. R., & Hillman, C. H.

(2010). On the number of trials necessary for stabilization of error-related brain activity across the life span. *Psychophysiology*, *47*(4), 767–773. https://doi.org/10.1111/j.1469-8986.2010.00974.x

Ramnani, N. (2006). The primate cortico-cerebellar system: Anatomy and function. *Nature Reviews Neuroscience*, *7*(7), 511–522. https://doi.org/10.1038/nrn1953

Rietdijk, W. J., Franken, I. H., & Thurik, A. R. (2014). Internal consistency of event-related potentials associated with cognitive control: N2/P3 and ERN/Pe. *PloS One*, *9*(7), e102672. https://doi.org/10.1371/journal.pone.0102672

Rogasch, N. C., Sullivan, C., Thomson, R. H., Rose, N. S., Bailey, N. W., Fitzgerald, P. B., Farzan, F., & Hernandez-Pavon, J. C. (2017). Analysing concurrent transcranial magnetic stimulation and electroencephalographic data: A review and introduction to the open-source TESA software. *NeuroImage*, *147*, 934–951. https://doi.org/10.1016/j.neuroimage.2016.10.031

RStudio Team. (2020). *RStudio: Integrated Development for R*. Boston, MA: RStudio, PBC, http://www.rstudio.com/

Rubia, K., Smith, A. B., Taylor, E., & Brammer, M. (2007). Linear age-correlated functional development of right inferior fronto-striato-cerebellar networks during response inhibition and anterior cingulate during error-related processes. *Human Brain Mapping*, *28*(11), 1163–1177. https://doi.org/10.1002/hbm.20347

Rustemeier, M., Koch, B., Schwarz, M., & Bellebaum, C. (2016). Processing of positive and negative feedback in patients with cerebellar lesions. *The Cerebellum*, *15*(4), 425–438. https://doi.org/10.1007/s12311-015-0702-8

Sheu, Y. S., Liang, Y., & Desmond, J. E. (2019). Disruption of cerebellar prediction in verbal working memory. *Frontiers in Human Neuroscience*, *13*, 61. https://doi.org/10.3389/fnhum.2019.00061

Shirota, Y., Hamada, M., Terao, Y., Ohminami, S., Tsutsumi, R., Ugawa, Y., & Hanajima, R. (2012). Increased primary motor cortical excitability by a single-pulse transcranial magnetic stimulation over the supplementary motor area. *Experimental Brain Research*, *219*, 339–349. https://doi.org/10.1007/s00221-012-3095-7

Sokolov, A. A., Miall, R. C., & Ivry, R. B. (2017). The cerebellum: Adaptive prediction for movement and cognition. *Trends in Cognitive Sciences*, *21*(5), 313–332. https://doi.org/10.1016/j.tics.2017.02.005

Soto, D., Montoro, P. R., & Humphreys, G. W. (2009). Transcranial magnetic stimulation of the primary motor cortex modulates response interference in a flanker task. *Neuroscience Letters*, *451*(3), 261–265. https://doi.org/10.1016/j.neulet.2008.12.052

Stoodley, C. J., & Schmahmann, J. D. (2009). Functional topography in the human cerebellum: A meta-analysis of neuroimaging studies. *NeuroImage*, *44*(2), 489–501. https://doi.org/10.1016/j.neuroimage.2008.08.039

Thoma, P., Bellebaum, C., Koch, B., Schwarz, M., & Daum, I. (2008). The cerebellum is involved in reward-based reversal learning. *The Cerebellum*, *7*, 433–443. https://doi.org/10.1007/s12311-008-0046-8

Tunc, S., Baginski, N., Lubs, J., Bally, J. F., Weissbach, A., Baaske, M. K., Tadic, V., Brüggemann, N., Bäumer, T., Beste, C., & Münchau, A. (2019). Predictive coding and adaptive behavior in patients with genetically determined cerebellar ataxia—A neurophysiology study. *NeuroImage: Clinical*, *24*, 102043. https://doi.org/10.1016/j.nicl.2019.102043

Ugawa, Y., Uesaka, Y., Terao, Y., Hanajima, R., & Kanazawa, I. (1995). Magnetic stimulation over the cerebellum in humans. *Annals of Neurology*, *37*(6), 703–713. https://doi.org/10.1002/ana.410370603

Ullsperger, M., & von Cramon, D. Y. (2006). The role of intact frontostriatal circuits in error processing. *Journal of Cognitive Neuroscience*, *18*(4), 651–664. https://doi.org/10.1162/jocn.2006.18.4.651

Vaidya, A. R., Pujara, M. S., Petrides, M., Murray, E. A., & Fellows, L. K. (2019). Lesion studies in contemporary neuroscience. *Trends in Cognitive Sciences*, *23*(8), 653–671. https://doi.org/10.1016/j.tics.2019.05.009

Van Veen, V., & Carter, C. S. (2002). The anterior cingulate as a conflict monitor: fMRI and ERP studies. *Physiology & Behavior*, *77*(4–5), 477–482. https://doi.org/10.1016/S0031-9384(02)00930-7

Verleger, R., Kuniecki, M., Möller, F., Fritzmannova, M., & Siebner, H. R. (2009). On how the motor cortices resolve an inter-hemispheric response conflict: An event-related EEG potential-guided TMS study of the flankers task. *European Journal of Neuroscience*, *30*(2), 318–326. https://doi.org/10.1111/j.1460-9568.2009.06817.x

Voegler, R., Peterburs, J., Lemke, H., Ocklenburg, S., Liepelt, R., & Straube, T. (2018). Electrophysiological correlates of performance monitoring under social observation in patients with social anxiety disorder and healthy controls. *Biological Psychology*, *132*, 71–80. https://doi.org/10.1016/j.biopsycho.2017.11.003

Wolpert, D. M., Miall, R. C., & Kawato, M. (1998). Internal models in the cerebellum. *Trends in cognitive Sciences*, *2*(9), 338–347. https://doi.org/10.1016/S1364-6613(98)01221-2

Wu, W., Keller, C. J., Rogasch, N. C., Longwell, P., Shpigel, E., Rolle, C. E., & Etkin, A. (2018). ARTIST: A fully automated artifact rejection algorithm for single-pulse TMS-EEG data. *Human Brain Mapping*, *39*(4), 1607–1625. https://doi.org/10.1002/hbm.23938

Yeung, N., Botvinick, M. M., & Cohen, J. D. (2004). The neural basis of error detection: Conflict monitoring and the error-related negativity. *Psychological Review*, *111*(4), 931–959. https://doi.org/10.1037/0033-295X.111.4.931

Yoshida, J., Oñate, M., Khatami, L., Vera, J., Nadim, F., & Khodakhah, K. (2022). Cerebellar contributions to the basal ganglia influence motor coordination, reward processing, and movement vigor. *Journal of Neuroscience*, *42*(45), 8406–8415. https://doi.org/10.1523/JNEUROSCI.1535-22.2022